Repulsive signaling from the *Drosophila* midline requires *slit* function: Repellent signaling through Robo1 requires the Slit LRR

BY

ROBIN ANTONY BATTYE, B.Sc.(Hon.), M.Sc.

A Thesis

Submitted to the School of Graduate Studies

in Partial Fulfillment of the Requirements

for the Degree

Doctor of Philosophy

McMaster University

DOCTOR OF PHILOSOPHY (2000) McMaster University

(Biology) Hamilton, Ontario

TITLE: Repulsive signaling from the *Drosophila* midline requires *slit* function:

Repellent signaling through Robo1 requires the Slit LRR

AUTHOR: Robin Antony Battye, B.Sc.(Hon.)(Brock University), M.Sc.

(Ottawa/Carleton University)

SUPERVISOR: Professor J.R. Jacobs

NUMBER OF PAGES: 259

Abstract

To establish the bilateral symmetry present in the midline of the *Drosophila* CNS the midline cells must generate a repulsive barrier that divides both halves of the embryo. Here we report the identification and characterization of the midline repellent ligand Slit. Slit is expressed and secreted from the MG where it signals to growth cones pathfinding along the lateral border of the midline. In embryos of severe *slit* mutants all CNS axons fuse at the midline. *slit* transgenes expressed at the midline functionally rescue the *slit* mutant phenotype. Furthermore, ectopic expression of *slit* transgenes repels CNS axons away from regions of transgene expression.

Analysis of point mutations in the *slit* locus suggest that the LRR motifs found in Slit protein are required for Slit's repulsive function in the midline cells. Additionally, *in vivo* expression of truncated *slit* transgenes containing only the LRR was sufficient to partially restore Slit repellent signaling to the midline and generate ectopic signaling phenotypes. *slit* transgenes lacking the LRR domains have no repellent activity. Embryos transheterozygous for *slit* and *robo1* have pathfinding errors that are not observed in embryos heterozygous for either allele, a classic indication of a genetic interaction between two genes. Additionally, *in vitro* binding assays demonstrate that Slit binds Robo1 and more specifically that this binding requires the complete Slit LRR domain. These data show that Slit is midline ligand that binds the repellent receptor Robo1 in order to establish the midline barrier formed between opposite halves of the *Drosophila* embryo.

ACKNOWLEDGEMENTS

I would like to thank Dr. J. Roger Jacobs for his contributions to my doctoral studies and for his support during my education. I also thank the members of my committee, Dr. Ana Campos, Dr. Michael Rudnicki, Dr. Margaret Fahnestock, and Dr. Juliet Daniel for their time and advice.

My wife Dorothy DeSousa has been patient and supportive throughout this project and deserves a great deal of credit for the completion of this dissertation. I only hope I can be as helpful and as understanding as she finishes her Ph.D..

The members of my lab have been a great source of support and ammusement for me during the times I required help and needed to releive stress. I would like to thank Adrienne Stevens, Brad Lanoue, Chris Stemerdink, Rong Dong, Allison MacMullin, Amanda Hawley, Michael Gordon, Christian Smith, Rena G., Maria Guanieri, and Rob Perry.

Finally I would like to thank my family Rosamund, David, Jeremy Battye and Maddy and Peter Kingham for sticking by me. Their unconditional love and understanding during both the ups and downs have been a real comfort to me.

TABLE OF CONTENTS

LIST OF FIGURES

LIST OF ABBREVIATIONS

A/P-anterior to posterior

aCC-anterior corner cell

ALPS-Agrin, Laminin, Perlecan, Slit

BNDF-brain derived neurotrophic factor

CAMs-cell adhesion molecules

CNS-Central Nervous System

DAB-3,3-Diaminobenzidine Tetra hydrochloride

DER-*Drosophila* EGF-receptor

DUM-dorsal unpaired median neurons

DVD-Digital Video Disk

D/V-dorsal to ventral

ECM-extracellular matrix

EGF-epidermal growth factor

EM-electron microscopy

EMS-Ethylmethanesulfonate

FGF-fibroblast growth factor

G-domain-globular domain

GAL-4-galactosidase transgene with 4 binding sites

GMC-ganglion mother cells

GOF-gain of function

GPI-glycosylphosphatidylinositol

HRP-horseradish peroxidase

Ig-Immunoglobulin

LG-longitudinal glia

LRR-Leucine rich repeats

MB-mega byte

MCR-multiple cloning region

MEC-mesectodermal cell

MG-midline glia

MGM-middle midline glia

MGP-posterior midline glia

MGA-anterior midline glia

MNB-median neuroblasts

MP1- midline progenitor 1 neurons

vMP2- ventral midline progenitor 2 neurons

NB-neuroblasts

NCAM-neural cell adhesion molecule

NGF-nerve growth factor

PAGE-polyacrylamide gel electrophoresis

PBS-phosphate buffered saline

PCR-polymerase chain reaction

pCC-posterior corner cell

PEG-Polyethylene glycol

RAM-read(random) accessible memory

RGC-retinal ganglion cells

RPTK-receptor protein tyrosine kinases

RPTP-receptor protein tyrosine phosphatases

SDS-Sodium Dodecyl Sulfate

SC-superior colliculus

TAG-transiently expressed axonal glycoproteins

UMI-unpaired median interneuron

UTR-untranslated region

VL-ventral longitudinal

VO-ventral oblique

VUM-ventral unpaired median neurons

INTRODUCTION

As a person reaches down to tie a shoelace or sits at a desk to write a letter they witness the use of two symmetrical hands that allow them to perform intricate and complex tasks. How is it that animals have developed two body hemispheres that are mirrored at a central axis? Furthermore, how is the circuitry of the central nervous system (CNS) organized to coordinate and manage both of these hemispheres such that two hands can cooperate to perform such complex tasks as tying a shoelace or writing a letter? Bilateral symmetry first developed in the Bilatera metazoans marked by the advent of gastrulation that resulted in the formation of three germ layers, the endoderm, ectoderm, and mesoderm. This divergence very early in evolution meant that many different species today exhibit bilateral properties. Similarly, as deuterostomes (anus first) and protosomes (mouth first) diverged in this phylogenetic branch many other aspects of development remain conserved in species as divergent as homo sapiens (humans) and Plathyelminthes (flatworms) (Gilbert *et al*, 1996). Neurogenesis - the process by which neurons are formed - proceeds remarkably similarly in different phyla including *Drosophila melanogaster* and mice (Arendt & Nubler-Jung, 1999). Furthermore, parallels drawn between vertebrate and invertebrate development in particular, are drawing ever closer as our understanding of the gene function and developing cells increases (Holland & Holland, 1999). The tools available to genetically manipulate *Drosophila* in general and specifically the *Drosophila* midline have developed such that we are now able to generate specific mutations in genes, study their resultant phenotypes, and finally dissect genetic function at a molecular level (for a review of *Drosophila* protocols refer to (Sullivan *et al*, 2000)). This level of access

applied to the developing *Drosophila* nervous system provides the ideal system in which to investigate the processes of neuronal guidance and signaling necessary to understand the kind of neuronal complexity described above.

The *Drosophila* CNS is also bilateral and develops as a characteristic ladder-like axon scaffold that forms early in neurogenesis and persists throughout larval development as neurons pathfind along its foundation (Goodman *et al*, 1986). This ladder-like structure consists of two sets of longitudinal axon tracts that develop in parallel to the ventral midline and then run anterior and posterior along it. The ventral midline contains few other axons with the exception of two commissural axon tracts. The anterior and posterior commissures cross the midline within each segment connecting the left and right halves of the embryo and then turn to project along the contralateral longitudinal tracts or project peripherally (Jacobs & Goodman, 1989a;Jacobs & Goodman, 1989b). The symmetrical and repeated pattern of the *Drosophila* CNS raises many questions as to the mechanisms that are responsible for establishing such a regulated and stereotypical structure. For example, how do two dimensional sheet of neuroepithelial cells give rise to a three dimensional nervous system consisting of diverse sets of neurons and glial cells? Additionally, what mechanisms are responsible for maintaining the barrier that divides left and right domains such that specific commissural axons may cross, but similar longitudinal axons may not? We intend to address the last of these two questions by first characterizing mutations associated with establishing the midline barrier in the *Drosophila* midline and secondly to understand the mechanisms by which these associated genes act to form this barrier.

Early in the study of *Drosophila melanogaster,* large scale saturation mutageneses were performed in order to provide libraries of mutations resulting from lethal changes in a wide range of *Drosophila* genes. The classical studies of Nüsslein-Volhard and Wieschaus in the early 80's focused on the collection of observable mutant phenotypes in order to deduce the genes and principles involved in early pattern formation. Vast numbers of male flies fed Ethylmethanesulfonate (EMS) characteristically developed single base pair changes within their genomic DNA that were subsequently inherited by their progeny. Progeny from these crosses carrying lethal changes could be stabilized over balancer chromosomes, which consist of a number of genomic inversions that prevent selective recombination(Nusslein-Volhard & Wieschaus, 1980) (Nusslein-Volhard *et al*, 1985;Seeger *et al*, 1993). Lethal mutations resulting from EMS mutagenesis were then stored and selectively screened for phenotype, mutation localization, and genetic complementation with known genes.

Because of the well defined and relatively simple structure of the *Drosophila* midline, screens for mutations resulting in perturbances in CNS structure were fairly easy to identify. Furthermore, the generation of a number of monoclonal antibodies to CNS specific structures (BP102, FasciclinII, and 22C10) along with cell specific enhancer traps, accelerated this process, uncovering a number of genes apparently required for CNS development. Among the most prominent of these was the mutation in *single minded* (*sim*) that resulted in a total collapse of all CNS axons onto the midline. The characterization of this gene revealed that *sim*, which codes for a bHLH family transcription factor, functions as a master regulatory gene that determines the mesectodermal cell (MEC) lineages. Not surprisingly these MECs are the founders of the

midline cells (Crews *et al*, 1988;Crews, 1998;Crews & Fan, 1999). In embryos with mutations affecting *sim* function, the midline barrier fails to differentiate and hence removes any inductive or signaling mechanisms provided by the ventral midline. As in the vertebrate floor plate these set of cells function to regulate patterning during early embryonic development (Arendt & Nubler-Jung, 1999), hence the removal of midline cells perturbs CNS development. The vertebrate floor plate consists of a small group of cells that are located at the ventral midline of the neural tube and perform a critical role in the patterning of the vertebrate CNS (Jessell & Dodd, 1990). A great deal of controversy surrounds the exact inductive event that regulates development of the floor plate (see (Le Douarin & Halpern, 2000) and (Placzek *et al*, 2000) for arguments); however, there is little dispute that the secreted protein Sonic hedgehog (Shh) is necessary for inducing the differentiation of cells in the midline neural plate overlying the dorsal Notochord (Ohyama, 1999). This process is similar to the induction of *sim* expression in the formation of the *Drosophila* mesectoderm. Other genes that reduce or remove the MEC lineages such as the *Egfr* pathway (*Star, rhomboid, spitz,* and *vein*) and early cell polarity mechanisms such as *Notch, patched,* and *wingless* also produce CNS mutant phenotypes where affected axons collapse towards the midline of the embryo (Menne *et al*, 1997;Menne & Klambt, 1994;Sonnenfeld & Jacobs, 1994;Lanoue & Jacobs, 1999;Stemerdink & Jacobs, 1997;Lanoue *et al*, 2000). Therefore, it is clear that the MEC lineages and their derivatives are vital for the signaling events necessary for establishing the separation of the midline axon fascicles. It is not clear however, precisely which properties of the MECs are responsible for different aspects of midline development and commissural separation.

The severity of CNS phenotype observed in *sim* mutant embryos highlights the importance of the MECs in midline development; however, the complete collapse of all CNS axons in *sim* -like mutants overshadows the finer aspects of axon pathfinding. In order to identify midline cell contributions to axon guidance the examination of other genes involved in later states of MEC development proved more fruitful. Some genes that are active in early MEC development include *slit,* the *netrins*, *wrapper*, and *Dichaete* to name a few (Jacobs, 2000). Mutations in the *slit* locus produced a similar CNS phenotype to that of *sim* (Seeger *et al*, 1993;Rothberg *et al*, 1988). *slit* cDNA was originally isolated in a screen for EGF-like genes that function in neurogenic development. Utilizing probes from the *Notch* EGF locus, EGF-like repeats were identified in a number of *Drosophila* genes including *slit* which mapped to polytene chromosome band 52D (Rothberg *et al*, 1988). The temporal and spatial expression of Slit protein and RNA in the MG suggested a possible role for *slit* in the development of the CNS. Furthermore, mutations in this locus identified during the Nüslein-Volhard screens (Nusslein-Volhard *et al*, 1985) result in the collapse of the regular axon suggesting that *slit* may function in a similar manner to *sim* in the control of MEC cell lineages (Rothberg *et al*, 1990). Later studies have shown however, that MEC lineages develop appropriately in *slit* mutants suggesting that *slit* has another yet undiscovered function in midline development (Sonnenfeld & Jacobs, 1994) (Jacobs, J.R. personal communication). This observation speaks to the fact that genetic analysis of midline development must be approached from two perspectives: the study of genes that affect cell fate and those that regulate cell communication. The similar patterns of early expression and mutant phenotypes observed in both *slit* and *sim* mutant embryos suggests

that where mutations in *sim* remove the source of midline signaling, mutations in *slit* remove the midline signal. When this project began, *slit* was relatively uncharacterized and its role in axon guidance had yet to be determined. The focus of our investigation was the identification of mechanisms responsible for establishing the bilaterally symmetric midline. The *slit* phenotype strongly suggested that Slit was central to this function.

As we stated earlier, the total collapse of CNS axons onto the midline, as is observed in *slit* mutant embryos obscures other aspects of midline guidance under the tangle of fused axon tracts. Fortunately, these were not the only types of CNS phenotypes identified in the early mutant screens. Mutations in *comm.* resulted in the disappearance of all commissural axons leaving two isolated tracts of longitudinal axons. (Tear *et al*, 1996). Mutations in *robo* caused axons that did not normally cross the midline to make projections across it and axons that normally only crossed once instead of repeatedly recrossing the midline (Kidd *et al*, 1998a). Additional variations in these types of phenotypes, such as mutations in *karussell* that result in cross overs between commissures (Hummel *et al*, 1999a) and *schizo* and *weniger* that appear to disrupt commissural projection mechanisms (Van Vactor *et al*, 1998;Hummel *et al*, 1999a) suggest that a great many genes contribute to the refinement of the axon scaffold. We will revisit these genes and more as we discuss guidance mechanisms in detail; however, a short overview of midline development is in order to set the stage for introducing these mechanisms and their functions.

Origin of the *Drosophila* midline

The neurogenic regions that sandwich the ventral midline originally develop from adjacent domains in the early cellular blastoderm (Leptin, 1999). Expression of three genes in the ventral-most blastoderm establishes the boundary of three prominent tissues that include the mesoderm (forms germ layer for somatic structures such as musculature, fat bodies, and heart), mesectoderm (develops the midline lineages), and the neurogenic regions (origin of neuroblasts) (Leptin, 1995). The activity of the *dorsal* group genes establishes the dorsal/ventral axis of the blastoderm. Consequently, sufficient levels of Dorsal in the nucleus activates the expression of *twist* and *snail* forming two overlapping gradients along the ventral edge of the blastoderm. *twist* expression forms a gradient within the boundary of Dorsal expression, whereas the pattern of *sna* expression has sharp boundaries that stops several cells medial to the limit of *twist* expression. At the lateral limit of *snail* expression, a bilateral boundary is formed, marked by the expression of the *sim* gene (Leptin, 1991;Seeger *et al*, 1993). This boundary represents the cells of the mesectoderm that separate the medial mesoderm from the more lateral neurogenic regions. During gastrulation, the MECs unite at the midline to found the cells of the ventral midline.

During gastrulation the mesoderm invaginates, bringing the two rows of mesectodermal boundary cells together at the ventral midline where they pair and prepare to delaminate from the ventral ectoderm. These midline precursors delaminate before the neuroblasts (NB) emerge from the ventral ectoderm. The NBs then invaginate following the establishment of the midline cells and proceed to make repeated asymmetrical divisions, generating a series of ganglion mother cells (GMCs) on either side of the

midline precursors. These cells divide once and create a pair of post-mitotic neurons contributing to the expanding nerve cord (Doe, 1996). The order of asymmetric divisions and staggered delamination of NBs from the neurogenic tissues establishes an ancestry of neurons, the earliest of which are responsible along with intermingled glia cells for the development of the early axon scaffold (Jacobs & Goodman, 1989a;Jacobs & Goodman, 1989b).

sim function is essential in the determination of midline identities (Nambu *et al*, 1991) and acts in a manner similar to 'master regulatory' genes in the regulation of MEC cell identity. In embryos lacking *sim* function, cells at the *twist/snail* border remain ectodermal or initiate apoptosis, but either way the absence of the MECs results in a fusion of adjacent ventral structures removing the definition of medial lateral boundaries associated with the ventral midline (Zhou *et al*, 1997). Perhaps of greater significance in our investigations is that the elimination of MEC identities results in the medial fusion of developing neuronal processes in ventral nervous system (Seeger *et al*, 1993). Clearly, elimination of the MECs results in a removal of normal midline function that is responsible for establishing the structure and medial to lateral organization of the ventral nerve cord. Additional investigations into the role of MEC lineages in midline patterning have identified 5 specific cell lineages that are dependent upon *sim* expression that we will outline below (Jacobs & Goodman, 1989a).

After gastrulation the two rows of MEC cells invaginate at the midline and unite into a single row of cells that run anterior to posterior (A/P) along the ventral midline. Under the regulation of pair rule and segment polarity genes (see below) these cells acquire 5 identities that are recapitulated in 11 segments (for a review see Jacobs, 2000).

The midline glia (MG), referred to as the posterior (MGP), middle (MGM), and the anterior (MGA) respectively comprise the first three cells. The fourth midline progenitor I cell (MP1) together with another adjacent neuroblast (vMP2) forms the first anteriorly projecting axon tracts, while the Unpaired Median Interneurons (UMI) and the next two ventral unpaired median (VUM) progenitors form interneurons and bilaterally projecting motor neurons respectively (Jacobs, 2000). Finally the median unpaired neuroblast (MNB) divide as a stem cell giving rise to Dorsal Unpaired Median neurons (DUM) that project bifurcating axons to a variety of muscle cells and interneurons (Schmid *et al*, 1999). Limited evidence suggests that all the unpaired neurons are in fact early progeny of the MNBs based on similar patterns of axon projections and gene expression; however this does not alter the overall architecture of the midline (Schmid *et al*, 1999). MECs, with the exception of the MNB, divide once producing a pair of each cell type and proceed to organize and develop within each respective segment creating and anterior region of glia cells and a posterior region of neurons. The relatively simple nature and accessibility of the *Drosophila* nerve cord thus provides an excellent resource for the investigation of midline neuronal development.

Segmentation of the *Drosophila* midline

As specific groups of genes are necessary for defining dorsal/ventral and medial patterning in the blastoderm; similarly, groups of segmentation genes are responsible for the anterior to posterior (A/P) division of the blastoderm. Division of the ventral midline into anterior to posterior segments generates regions in which further subdivisions can be defined in order to specify particular groups of cells that are required in a repeated pattern along the A/P axis. This segmentation is obvious in the repeated pattern of anterior and

posterior commissures that is observed in each of 11 segments that form the ventral nerve cord (see (von Dassow *et al*, 2000) for review). Polarity within these segments in part defines the fate the MEC will retain as they differentiate into MG or Neurons. Basically, the anterior of each midline segment under the regulation of *Wingless* signaling is fated for glia cell development; whereas, the absence of *Wingless* signaling in the posterior of the segment leads the MEC to the default neuronal fate (Richter *et al*, 1998;Bhat *et al*, 2000). Mutations in *hedgehog* (*hdg*) result in a dramatic increase in the number of glia cells in the midline of embryos (Patel *et al*, 1989a;Martinez, 1998;Martinez, 1994) whereas *patched* mutant embryos have a complimentary phenotype demonstrating a lack of glial cells and an increase in the number of neurons (Patel *et al*, 1989b). *hedgehog* normally represses the negative action of *patched* on the expression of *Wingless* in the anterior of each segment releasing *Wingless* signaling to direct anterior cells to a glial fate. *hedgehog* expression which precedes that of *patched* and *wingless* is restricted to the anterior of each segment by the activity of other segment polarity genes whose introduction is beyond the scope of this review. The graded and overlapping expression of different segmentation genes is therefore responsible for generating a specific anterior region within each repeated segment that directs MEC to differentiate as glia. The significance of the position and role of these particular glia will become evident as we introduce the known guidance mechanisms that establish the anterior and posterior commissures.

Glial scaffold supports the pioneering CNS

The CNS is comprised of many cell types, the two most prominent of which are the neurons and the glia. Both these cell types appear at the earliest stages of

neurogenesis and develop alongside each other as the CNS is established. Neurons have received a great deal of attention for their role in CNS function, but the glia have an equally important supporting role in the CNS as scavengers, guidance cues, sources of axonal ensheathment and in the formation of the blood brain barrier (for a review see Jacobs (Jacobs, 2000)). There are a great many sub-types of glia; however the best studied and most relevant in our investigations are the glia that comprise the *Drosophila* ventral CNS and midline consisting of the longitudinal (LG), exit root glia, and the MG alluded to above.

The longitudinal glia derive from the neurogenic regions surrounding the midline and are specified by the master regulatory gene *glial cells missing* (*gcm*) (Jones *et al*, 1995;Giesen *et al*, 1997). As *Notch* and other neurogenic genes limit the number of neuroblasts in the neuroepithelium similarly *gcm* expressing glioblasts will develop into the glia that surround and support these developing neurons (Hosoya *et al*, 1995;Jones *et al*, 1995). Clusters of longitudinal glia migrate with and support the pioneering axon tracts, while at the same time other glia migrate to opposite sides of the midline and form tracts that run parallel to it. Early in axonogenesis, the pioneering growth cones of most neurons do not need the glia to survive, but coordinate with the glia to lay down the rudimentary axon pathways. Later in development, the follower axons are dependent on these substrata for survival and pathfinding (Hidalgo & Booth, 2000;Booth *et al*, 2000). These rows of longitudinal glia that form alongside the midline support and guide the initial axon pioneers from both the neuroepithelium and midline neurons. The bilateral set of longitudinal axons that develop will eventually provide the framework or scaffold that will support future generations of axons called followers (Hummel *et al*, 1997). Part

of this support comes by localizing or providing both contact dependent and secreted signaling molecules that guide and regulate the growth of other glia and axons that form the longitudinal axon tracts. These roles will be introduced shortly.

In addition to the LG that run along either side of the midline the Exit and Nerve Root glia establish positions at the future intersegmental nerve roots. Here they will provide guidance cues and support for specific subsets of neurons (mainly motor neurons) that will innervate the segmental muscles and other tissues. Similar to the LG, the Exit and Nerve Root glia do not dictate the pathway of the pioneering nerve root ganglion, but will prove essential in the refinement of its peripheral projections (Auld, 1999;Hidalgo & Booth, 2000). With both the LG and other non-midline glia, early pioneering events appear to be coordinated slightly in advance of the axon growth cones. Selected ablation or perturbance of glial cell function does not dramatically affect axogenesis and early pathfinding; however, later pathfinding events show significant problems associated with these deficits (Klambt *et al*, 1999). Non-midline glia described here are specified early in development and establish the axon scaffold as demonstrated in studies by the Goodman lab (Jacobs & Goodman, 1989a;Jacobs & Goodman, 1989b;Jacobs *et al*, 1989;Klambt & Goodman, 1991a). The most significant functions of these cells can be summarized in terms of glia to glia and glia to neuron contact, growth cone attraction or repulsion, defasciculation and also fasciculation (Hidalgo & Booth, 2000;Goodman, 1996). We will reintroduce these issues in the outline of axon guidance mechanisms.

Unlike the LG or Nerve Root and Exit glia, the MG are the only glial cells to originate from the MEC lineages and consequently are regulated by slightly different

molecular mechanisms. Whereas the peripheral glia are established by the expression of *gcm*, no similar master gene has yet been identified in the MG with the exception of *sim* which acts in concert with Fish-hook (Fsh), a SOX HMG domain protein, and Drifter (Dfr), a POU domain protein to coordinate midline gene expression (Ma *et al*, 2000). The early expression of *sim* and *slit* in all MECs is rapidly restricted to the MG as the MEC acquire their identities, yet in *slit* mutant embryos the MC still retain glial characteristics (Rothberg *et al*, 1990;Jacobs, 1993). A number of factors have become evident that regulate the specification of different midline lineages, one of which is the Hedgehog gradient. In the midline, posterior lineages become neuronal and anterior lineages become glia. Mutations in *hedgehog* result in an overall anterior polarity where all MEC take on a glial fate. *hedgehog* is responsible for repressing the negative action of *patched* on the expression of *wingless,* indicating that in part *wingless* under the control of *hedgehog* specifies a glia fate to the anterior cells in each segment.

Additional mechanisms that control MG fate include neuronal Tramtrack69 that represses differentiation and conversely Pointed that promotes differentiation in both the peripheral and midline glia. Both these proteins are found exclusively in non-neuronal cells (Giesen *et al*, 1997). *Ttk* mutant embryos develop a reduced number of CNS glia; however, remaining glia appear normal, a fact that when considered with other data was interpreted to mean that *ttk* expression is necessary to repress the natural default tendency of glia to revert to their neuronal fate (Badenhorst *et al*, 1996;Giesen *et al*, 1997). Consequently, mutations in *ttk* also cause a partial fusion of segmental commissures further implying the importance of the MG during midline development (Giesen *et al*, 1997;Kwiatkowska & Kwiatkowska-Korczak, 1999). Pointed on the other hand is

required for the differentiation of a number of tissues during embryogenesis, including the ventral ectoderm, certain muscle fibers, the tracheal system, and some CNS cells including the MG (Scholz *et al*, 1993). In embryos mutant for *pointed* the anterior and posterior commissures do not become separated and appear fused as a result of improper differentiation of the glial cells (Klambt, 1993) (Klaes *et al*, 1994). The expression of Pointed is dependent on high levels of DER (the *Drosophila* EGF receptor) activity (Gabay *et al*, 1996). Therefore, where Pointed expression is necessary to induce MEC to differentiate as glia, *Ttk* is required for them to retain their acquired glial identity. The role of DER however, does not end in the differentiation of the MG but is also responsible for their survival later in development. In early midline development (stage12), the MEC produce 10-12 MG precursors that participate in commissure establishment and signaling. These cells are subsequently reduced to 3 in later stages of embryonic development as their roles diminish to simply commissure ensheathment and support (for a complete review see (Jacobs, 2000)). We will focus on the early signaling properties of the MG seeing that development of the bilateral CNS is established with the very first pioneering axons and continues prior to the reduction in MG.

Differentiation of the MEC to MG is necessary for the formation of the anterior and posterior commissures and absence of these cells in *sim* mutant embryos results in the fusion of the midline CNS. In mutations such as *netrin, comm.*, and *slit* that disrupt gene expression in the MG, but do not significantly alter MG morphology or unrelated functions, we still observe severe perturbances in CNS development that imply signaling provided by the MGs is as important as their presence.

Axon guidance

Neurogenesis initiates the production of nerve cells throughout the developing embryo that must ultimately interconnect neurons over both short (adjacent cells) and long (projections of motor neurons from CNS) distances to establish a central communication system. Our understanding of the mechanisms and molecules involved in organizing this complex network of cells has been rapidly expanding along with the tools and resources that are being applied in this research. A brief outline of current findings will provide a foundation for our studies on the axon guidance functions of *slit*. First we will address some of the mechanisms by which axon growth cones pathfind through their environment and then describe some of the molecules involved in mediating pathfinding.

Mechanisms of Axon Guidance

Large numbers of CNS neurons, approximately 90% of which are interneurons project axons across the midline to the contralateral side. Once these axons cross, mechanisms are in place at the midline that will not permit them to cross again. For axons to establish the symmetric structure of the ladder-like scaffold, they must receive and respond to many specific cellular and environmental signals. Axons read their environment by extending a growth cone into a complex array of environmental signals (Zallen *et al*, 1999;Knobel *et al*, 1999). Conserved receptor/ligand systems found at the leading edge of each growth cone transduce mechanical and molecular signals that alter the behaviour of the growth cone accordingly. The growth cone response is mediated by at least four types of mechanisms: chemoattraction, chemorepulsion, contact attraction, and contact repulsion that function in a coordinated and synchronized manner to direct axon elongation (Tessier-Lavigne & Goodman, 1996) (for a complete review on growth

cone mechanisms see (Song & Poo, 1999) and (Pawson & Nash, 2000)). The complexity of pathfinding can be simplified by subdividing difficult trajectories into choice points that function as intermediate growth cone targets and serve as the launch point for the next leg of the journey (Klambt *et al*, 1991;Auld, 1999). The journey of an axon can therefore be broken down into two basic steps, the simple linear growth from one choice point or target tissue to the next, and the careful evaluation of the extracellular environment followed by a directional decision made at each choice point (Stoeckli & Landmesser, 1998;Cook *et al*, 1998).

So how do axons make their directional decisions? All axons grow along a physical substrate that is both adhesive and permissive for growth. This substrate provided by the ECM and local cells is the primary source of the short range contact dependent signals (Crair, 1999). Graded distribution of attractive and repulsive cues along this substrate form channels through which the axon extends while evaluating its environment for countermanding signals. As more pathways are developed, the network of pathways become more complex and often axons fasciculate along similar or selectively tagged pathways, a process referred to as selective fasciculation (Lin *et al*, 1994). This process simplifies later development by encouraging the growth of follower axons towards choice points without the need to continually sample their environment. At choice points, where axons diverge to different target tissues, follower axons defasciculate from the axon bundle and acquire new directional guidance cues from the surrounding tissue. As suggested, short range contact dependent signaling is not the only guiding force in growth cone pathfinding.

Long range chemorepulsive and chemoattractive signaling molecules are generated by target tissues and diffuse away from their source (Bagnard *et al*, 2000). These molecules create a diffusible gradient or directly signal to distant growth cones repelling axons from or attracting them towards the source of the signal. In combination with short range signals these mechanisms of axon guidance direct growth cones to synapse with their target tissue with a very low frequency of error. For a complete review of axon guidance refer to (Tessier-Lavigne & Goodman, 1996).

Molecular Biology of Axon Guidance

The growth cones of neurons use many signals and receptors to precisely reach and contact their targets. The molecules that are present either on or around the developing neurons have the ability to direct neuronal growth such that very precise and accurate connections can be made between adjacent cells or target tissues great distances from the neuronal origin (Tessier-Lavigne & Goodman, 1996). Accumulating evidence of the conservation between receptor and ligand orthologs in different species suggests that the mechanisms and molecular substrates involved in axon guidance are stereotyped and conserved (Arendt & Nubler-Jung, 1999). Therefore, we may assume that mechanisms identified in the *Drosophila* may be extrapolated to more complex vertebrate systems and vice versa (Goodman, 1994).

The range of molecules identified as agents in axon guidance appear to retain multiple roles that allow them to function diversely in different tissues. For example, vertebrate Netrins and one of their invertebrate homologues (C-elegans UNC-6) are required in similar processes of axon guidance. In chickens, netrins are involved in the guidance of commissural axons towards and away from the floor plate in the neural tube

(Colamarino & Tessier-Lavigne, 1995) and in C-elegans UNC-6 is involved in a similar process regulating circumferential migration in the nerve ring (Zallen *et al*, 1999). We will review here a number of different molecules that have identified roles in axon guidance and relate them to the development of the *Drosophila* midline. During this review it will become readily apparent that our understanding of mechanisms that mediate the midline barrier is still unclear.

CAMS

The two large families of cell adhesion molecules (CAMs), the immunoglobulin (Ig) and cadherin superfamilies were some of the first characterized neuronal signaling proteins to be discovered. Roles of the CAMs in axon development were found to include functions as ligands and/or as receptors during axon pathfinding. The structure of CAMs -typically consisting of multiple immunoglobulin domains and Fibronectin III related repeats- is highly conserved between species and in function (Elkins *et al*, 1990). Few Ig CAMS have intracellular domains; however, most still appear to function as extracellular signaling mechanisms either by the binding of neurons to neurons (homophilic) or of neurons to other cell types (heterophilic)(Doherty & Walsh, 1994;Walsh *et al*, 1994) a process that is still unclear. The Ig CAMs have been well documented for their role in axon guidance and fasciculation of a variety of pathways where they mediate cell-cell adhesion providing a positive substrate for cell growth (Tear, 1998).

The neural cell adhesion molecule (NCAM) subtypes are anchored to the membranes of neuronal and support tissues where they guide axonal growth and development. Removal of NCAM function results in improper axon outgrowth and

defasciculation events that cause aberrant axon targeting (Yin *et al*, 1995). Similarly, L1 CAMS another of the Ig CAM are detected in cells that promote axon outgrowth at choice points of axon guidance in mice, in particular on the longitudinal axons on the midline. The presence of the NCAMS or L1 CAMS actively promotes axon outgrowth and fasciculation to target tissues. One Ig CAM that is prominent in *Drosophila* development is Fasciclin II (Fas II), found on subsets of axons that form the three sets of longitudinal axon pathways on either side of the *Drosophila* midline (Lin *et al*, 1994). Loss of function observed in FasII mutant embryos results in a failure of these axons to fasciculate, whereas ectopic expression of FasII on specific sets of axons that normally defasciculated prevents defasciculation and causes normally separate pathways to remain together (Grenningloh *et al*, 1991). Additionally, transiently expressed axonal glycoproteins (TAG) expressed on vertebrate commissural axons while they are migrating across the commissures are down regulated upon reaching the contralateral longitudinal tracts. The down regulation of TAG-1 causes axons to defasciculate and then refasciculate along the longitudinal tracts, a process mediated by the L1 CAMs (Warren, Jr. *et al*, 1999;Matise *et al*, 1999). Hence, CAMS are one of the molecules that mediate the 'selective fasciculation' events described earlier that simplify axon guidance over distances.

Specific signaling mechanisms attributed to the CAM family of proteins are illustrated by the roles of Deleted in Colorectal Cancer (DCC) and Neogenin in axon guidance at the midline. DCC binds Netrin-1, an ECM protein secreted by the midline cells that functions as an attractive guidance cue to commissural axons (Mitchell *et al*, 1996). The expression pattern of DCC on the commissural axons of the spinal cord along

with data from genetic and selective blocking experiments has shown that DCC (homologue of *Drosophila frazzled*) in part mediates the attractive guidance function of Netrin-1 at the midline (Keino-Masu *et al*, 1996). Furthermore, *neogenin*, which has a similar molecular structure to DCC (50%)(Meyerhardt *et al*, 1997) is also believed to function in Netrin guidance at the midline and in the eye (Keeling *et al*, 1997;Gad *et al*, 1997;Gad *et al*, 2000). The close protein structure and binding affinities of DCC and Neogenin suggest that they may function together in a complex when interacting with Netrin-1 (Gad *et al*, 2000;Shu *et al*, 2000). The role of CAMs or CAM complexes in axon guidance then is important in promoting the outgrowth of axons and guiding their fasciculation to target tissue. We have introduced Netrin, a well know axon guidance molecule that is incorporated into the CAM complex, DCC/Neogenin described above. In this complex, Netrin-1 acts as an attractive cue to commissural axons exploring the midline. Do the CAMs act as receptors to the Netrins in these situations, or do they simply localize the attractive Netrin signal to another attractive receptor?

Netrins

The Netrins comprise a small phylogenetically conserved family of guidance cues important for routing particular axonal growth cones to their targets (Muller *et al*, 1996). Netrins are secreted and soluble molecules found in both vertebrates (Netrins 1-3) and invertebrates (Netrin A & B in *Drosophila*, UNC-6 in *C.elegans*) and are detected in the developing CNS and different subsets of neurons, muscles, and epidermal patches (Mitchell *et al*, 1996;Guthrie, 1997). We have introduced two of the receptors by which the Netrins affect guidance, DCC and Neogenin; however, Netrins also have important

chemorepulsive roles in axon guidance as demonstrated in *C.elegan* nerve ring (Chan *et al*, 1996).

First, we will address the attractive mechanisms in the *Drosophila* midline that involve both Netrin A & B (apparently redundant proteins see (Winberg *et al*, 1998a) and (Seeger & Beattie, 1999) for discussion on alternate mechanisms) and are mediated by the DCC *Drosophila* homologue *frazzled* (Kolodziej *et al*, 1996). In *netrin A&B* or *frazzled* mutant embryos axon guidance is defective in the CNS and motor axon pathways. In these mutant pathways, subsets of axons fail to make appropriate commissural projections or innervate specified groups of muscle (Mitchell *et al*, 1996;Tear, 1998). The mutant phenotype of either *netrin* or *frazzled* is subtle and occurs only in subsets of axons suggesting that Netrins are not the only attractive mechanism in the midline. Additionally, ectopic *frazzled* expression produces no visible phenotypic changes whereas the ectopic expression of *netrin* results in axon pathfinding errors in the surrounding tissue (Kolodziej *et al*, 1996). This would suggest that *frazzled* has an extremely localized function, and possibly *netrin* is capable of functioning through other receptors. Recent studies however, have suggested that *frazzled* does not act as a receptor for the Netrins, but instead captures them and localizes them to the dorso-lateral receptor mechanisms in the CNS that correlate with the pattern of *frazzled* expression (personal communications with Hiramoto *et al.*, 2000). This would appear more consistent with the properties of the CAM that lack intercellular signaling mechanisms, but provide a prominent substrate for cell and protein localization. By capturing attractive signals such as Netrins and localizing them to precise areas of activity, CAMs would appear to act as signaling mechanisms themselves (Hiramoto *et al*, 2000). For this reason, it will be very

important to carefully identify the patterns of *Slit* mRNA and protein expression in the midline to determine its true area of activity.

The controlled localization of Netrins in the midline as suggested above has further ramifications for the second role of Netrins, chemorepulsion. In the *C.elegans* nerve ring and the mouse cerebellum, UNC-5 (Hedgecock *et al*, 1990), its mammalian homologues RCM (Ackerman *et al*, 1997;Ackerman & Knowles, 1998) and UNC5H3 (Przyborski *et al*, 1998;Hong *et al*, 1999) respectively have been attributed to mediating the repulsive signaling properties of Netrin (Colavita & Culotti, 1998). Mice that lack Unc5h3 lack the chemorepulsive events that are required for proper formation of the rostral cerebellar boundary (Przyborski *et al*, 1998). Similarly, the expression of UNC5 proteins in *Xenopus* neurons converts the native attraction response of their growth cones to Netrin-1 into repulsive ones (Hong *et al*, 1999). Additionally, misexpression of *unc*-5 in axons that are not normally dependent on *unc-6* can repel these axons from their normal pathways suggesting that UNC-5 misexpression can convert an attractive netrin response to a repulsive one. The bifunctional role of netrin therefore seems dependent on the role of specific netrin receptors. Whereas the CAMs, DCC and Frazzled do not contain intracellular domains associated with cellular signaling, the UNC-5 family of repulsive Netrin receptors have a conserved intracellular Death Domain and DB or *zonula occludens-like* domain (ZU-5) that have proved vital to repulsive signaling (Hong *et al*, 1999). Furthermore, the recent implication that DCC (UNC-40) and the UNC-5 family of proteins both function in repulsion now appears logical (Przyborski *et al*, 1998;Hong *et al*, 1999). If the CAMs are responsible for localizing netrin signaling, it is reasonable to assume that DCC and any netrin receptor can be found in a complex. Other

repulsive signals have been found to mediate signaling through their cytoplasmic domains including Eph, Plexins, and Robo receptors; however, no homologues have yet been identified between these domains (Bashaw & Goodman, 1999). Bashaw and Goodman (1999) found that the cytoplasmic domain of the receptor determines the function of the receptor/ligand complex, therefore the CAMs likely function to localize Netrin signaling. This would mean that the distribution of netrin receptors is related to their function and that a specific attractive receptor for netrin has yet to be identified. The bifunctional role of Netrins in axon guidance is clear, however the mechanisms by which Netrins perform these roles now seem more complex. Recent studies would suggest that secreted Netrins are captured rather than being allowed to diffuse and transported via a CAM to create a precise Netrin distribution in order to signal to other axons. Obviously, many of the Netrin and other signaling mechanisms in the midline remain to be uncovered. Netrin itself only attracts a subset of axons towards the midline and only at the segmental commissures (Serafini *et al*, 1996). The uncharacterized genes *schizo* and *weniger* act synergistically with Netrin, suggesting that there are multiple attractive mechanisms in the midline providing guidance cues for pioneering growth cones (Hummel *et al*, 1999b). Still, these molecules only appear to provide attractive signals to axons competent to cross the midline and only at commissural choice points. Furthermore, one of the largest unexplored and possibly most important mechanisms of axon guidance as indicated above is the process of cytoplasmic signaling (Seeger & Beattie, 1999) an aspect of axon guidance that has been given little attention.

Semaphorins

The Semaphorins are a very large family of both secreted and transmembrane molecules that can be found throughout the animal kingdom. They are characterized by a conserved 500 amino acid N-terminal domain (Kolodkin *et al*, 1993) which acts as their key signaling element. Semaphorins appear to function in axon guidance by influencing steering decisions, as diffusible chemo repellents, inhibiting formation of synaptic arbors and inhibiting axon branching (Kolodkin *et al*, 1993). The family of Semaphorins are divided into classes based on whether they are transmembrane (I-II in invertebrates & IV-VI in vertebrates) or secreted (SEMIII in vertebrates) and primarily function in highly localized, contact mediated events. One additional class of SEMVII molecules exists in viruses acting via the Plexin family receptor VESPR; however we will not consider this class in our review (Winberg *et al*, 1998b). Neuropilin-1 (NP-1), a transmembrane protein with strong SEMIII binding properties is most likely to function as the SEMIII receptor or mediate formation of a functional receptor complex. The concept of SEMIII in a receptor complex is supported by the identification of an additional Neuropilin (II) with equal SEM binding affinity as Neuropilin I. This is reminiscent of the CAM (UNC5) complex introduced above. Both Neuropilins, which lack functional cytoplasmic domains, can function as homo or heterodimers in conferring responsivity to SEMIIIs, still this complex likely requires other receptor components as suggested by the *in vitro* data (Chen *et al*, 1997;Takahashi *et al*, 1999a). One of these additional components is from the family of Plexin receptors that bind the remaining SEMs. Plexin 1 does not bind SEMIII directly, but by binding to NP1, plexins can increase the affinity of the NP1 for SEMIII (Takahashi *et al*, 1999a) thus mediating axon repulsion indirectly. Tyrosine in the cytoplasmic domain of Plexin can be phosphorylated, suggesting that the

Plexins signal via a tyrosine kinase (Glass *et al*, 1997;Glass *et al*, 1996). In *Drosophila*, only class 1 and II semaphorins have been identified to date and both appear to function through a plexin receptor (Winberg *et al*, 1998b). SemI and PlexinA mutant embryos both exhibit specific defects in motor and CNS axon guidance that are similar to transheterozygous combinations of both genes. Both SemI and PlexinA are expressed on a majority of the motor axons where they are believed to establish basal levels of axon-axon repulsion. Shifts in basal level signals, such as a drop in FASII or a release of Beat (Fambrough & Goodman, 1996) at specific choice points removes higher levels of attractive signaling and releases the repulsive signaling provided by SEM1/PlexinA to promote rapid axon defasciculation (Winberg *et al*, 1998b). Therefore we can see that the role of Semaphorins in axon guidance both in vertebrates and invertebrates is to establish a basal level of axon repulsion through the activity of tyrosine kinase transduced by the plexin receptors. Basal levels of repulsion in the motor and CNS axons that can be easily overcome by other attractive cues generates a sensitivity in these networks to changes in signaling that permits them to make rapid defasciculation at key choice points. Other repulsive mechanisms such as the receptor protein tyrosine kinases (RPTKs) that mediate inhibitory influences are discussed below.

Eph/Ephrins

The Eph family of receptors is a subfamily of the Receptor protein tyrosine kinases (RPTKs) that also include the fibroblast growth factor (FGF) and the Trk family of neurotrophin receptors; nerve growth factor (NGF), brain-derived neurotrophic factor (BNDF), neurotrophin-3 (NT-3), and neurotrophin-4/5 (NT-4/5) (Hallbook, 1999). These RPTKs are involved in the regulation of neuronal differentiation, survival, neurite

growth, and plasticity - the Eph family in particular are known to mediate axon growth and target tissue invasion (Pasquale, 1997). The Ephs are all membrane-anchored via a phospholipid or a transmembrane domain and are widely expressed in the developing nervous system (Drescher *et al*, 1995;Ciossek *et al*, 1998;Tessier-Lavigne, 1995). There are many individual Eph receptors that have been identified in different species and for unification they have been divided into two groups, EphA receptors that preferentially interact with glycosylphosphatidylinositol (GPI)-linked ligands and the EphB group that preferentially interacts with the transmembrane ligands (1997). Activation of Eph receptors via a variety of Ephrin class ligands results in the autophosphorylation on tyrosine residues and the activation of the Eph kinase activity - linked to the repulsive activity of the receptor. The Ephrins have been best characterized for their role in generating topographic maps for projecting retinal ganglion cells (RGCs) in the optic tectum (mammalian superior colliculus (SC)) see (O'Leary & Wilkinson, 1999).

As indicated above Ephrins are also grouped into two classes, the GPI-linked EphrinA ligands and the transmembrane EphrinB ligands. The graded distribution of Eph and Ephrins in the developing retinotectal systems is crucial for establishing appropriate A/P and D/V projections in the tectum. In general, gradients of EphrinA ligands established from the anterior to posterior poles of the tectum repel EphA expressing RGC axons from higher posterior concentration gradients to lower anterior gradients depending on the EphA/EphrinA molecules involved. Similarly, gradients of EphrinB ligands establish connectivity of the EphB expressing axons from low ventral concentrations to increasing dorsal repellent levels (O'Leary & Wilkinson, 1999). In addition, exceedingly high levels of Ephrin expression in the underlying tissues such as

the Inferior colliculus, establish a negative boundary across which no axons pass encapsulating RGC projections within the tectum. Taken together, we can see that the expression of different Eph receptor and Ephrin ligands in specific tissues can establish gradient barriers or clearly defined barriers of repulsive signals that funnel axons towards permissive attractive cues provided by target tissues (Pasquale, 1997). This type of regulation is much what we would expect to find in the definition of *Drosophila* midline barrier; however very little evidence of Eph or Ephrin activity in the CNS or floor plate has been revealed to date.

Identification of a murine ephrin-B3 that is expressed prominently at the dorsal and ventral midline of the neural tube and in particular the floor plate was one of the first indication that Ephrins may mediate patterning activities in the midline (Bergemann *et al*, 1998). More recently, all three Eph family transmembrane ligands, ephrinB1, ephrinB2, and ephrinB3 have been detected in the floor plate region of the spinal cord (Imondi *et al*, 2000). What is more interesting in this model is that commissural axons that cross the midline do not express a receptor for these ligands until they are across the midline, thus creating an environment in which they will not be permitted to cross again. Furthermore, strong evidence points to the fact that EphB receptors are expressed by axons projecting in the A/P axis. Consequently, with the down regulation of TAG-1 and the concomitant up regulation of L1 on crossing commissural axons, crossing the midline promotes the co localization of EphB and L1 on commissural axons that would restrict entrance to the midline (Imondi *et al*, 2000). The EphB receptors are acquired as commissural axons probe the contralateral longitudinal tracks. Binding of EphrinB3 to EphB repels commissural axons away from the midline where they fasciculate with the contralateral

longitudinal axon bundles or project to peripheral targets. Once across the midline, these axons never cross back again likely under the regulation of RPTK repulsion (Hummel *et al*, 1997;Hummel *et al*, 1999b;Hummel *et al*, 1999a). A second relatively uncharacterized protein that is involved in repulsive signaling pathways is coded by *karussell*. In *karussell* mutant embryos' commissures appear thicker and subsets of commissural axons turn inappropriately to cross the midline again instead of turning to grow along the contralateral longitudinal tracts (Hummel *et al*, 1999a). Similarly, with characterization of Dek in *Drosophila*, an Eph RPTK , data now suggests that this subfamily of RTKs does exist in *Drosophila*. However, limited research has been carried out in this area. Dek is expressed in the interneurons and photoreceptors of developing embryos that would indicate that Dek may function in a similar manner to the vertebrate EphBs, yet further analysis is required before any conclusions may be drawn. Evidence described above suggests that in the CNS midline, the Eph/Ephrin families provide the mechanism that restricts commissural axons from recrossing the midline but do not prevent pioneering growth cones from making their first projections into the midline. This role likely involves other midline mechanisms such as Slit.

RPTP

Signaling mediated by the RPTKs is dependent on the control of tyrosine phosphorylation in the growth cone as alluded to above. Receptor protein tyrosine phosphatases, which reverse the reactions catalyzed by tyrosine kinases provide another means by which to regulate tyrosine phosphorylation in growth cones (Goodman, 1996). RPTPs that are predominately located in the invertebrate and vertebrate CNS axons control specific pathfinding events by regulating growth cone repulsion from the CNS

(Menon & Zinn, 1998). In *Drosophila* embryos, four neuronal RPTPs have been characterized DLAR, DPTP69D, DPTP99A, and most recently DPTP10D. A complex involving all four RPTPs is required to prevent longitudinal axons that express receptors to attractive forces from crossing the midline (Sun *et al*, 2000). With mutations that remove DPTP10D and DPTP69D function, embryos develop a robo-like CNS phenotype; furthermore, when all four RPTPs are eliminated most longitudinal pathways convert to commissural pathways. One interpretation is that RPTPs regulate tyrosine phosphorylation to modify how growth cones respond to midline signals (Sun *et al*, 2000). Genetic interactions found between DPTP10D and DPTP69D with Robo, Slit, and Comm. also suggest that the RPTPs are positive regulators of the Robo signaling pathway (Sun *et al*, 2000). One possibility is that Robo's become phosphorylated on tyrosines after binding a midline repellent and that the RPTPs are then recruited into this complex by their interactions with the phosphotyrosine motifs.

Twice now we have introduced evidence that points towards *robo* in the regulation of midline repulsion but have not identified the key mechanism(s) necessary for providing repulsive signaling at the midline. Another class of molecules, the extracellular matrix (ECM) molecules to which Slit and Netrin are members include many other molecules that are expected to play roles in axon guidance.

ECM

The extracellular environment is in part responsible for providing and localizing signals mediating lineage decisions, triggering differentiative events, and decisions affecting cell behaviour (Streuli & Edwards, 1998). ECM molecules include members such as the Laminins, Tenascins, Collagens, the Thrombospondins, Fibronectins,

Vitronectins, and types of proteoglycans all of which have been shown to regulate neurite outgrowth and extension *in vitro* (Tessier-Lavigne & Goodman, 1996). ECM molecules are all glycoproteins. This classification encompasses a range of proteins with one or more covalently linked oligosacharide chains and includes most secreted proteins and those proteins exposed to the outer surface of the plasma membrane such as Comm and Robo. Many ECM molecules are expected to play roles in axon guidance; however, little attention has been paid to the role of these molecules *in vivo* (Tessier-Lavigne & Goodman, 1996). We will focus on one such ECM protein Slit, that is secreted from the MG in *Drosophila* and is localized to the commissural and longitudinal axons of the *Drosophila* midline (Rothberg *et al*, 1988). Mutations in the *slit* locus result in a total collapse of all developing axon tracts onto the midline were they remain fused along the A/P axis (Takahashi *et al*, 1999b;Rothberg *et al*, 1990). Slit is a large glycoprotein with four distinct protein motifs that include: 4 Leucine Rich Repeats (LRR) flanked on either side by conserved amino and carboxy regions; 7 EGF-like repeats separated between the 6^{th} and 7^{th} repeat by a G-domain sharing homologues with similar domains in Agrin, Laminin and Perlecan; and finally a cysteine rich conserved carboxy-terminus (Rothberg & Artavanis-Tsakonas, 1992). The expression pattern and nature of Slit suggest that it is an excellent candidate to provide a mechanism of signaling in the *Drosophila* midline as we have indicated above.

The discovery of both *robo* and *comm* genes shed new light onto the events that occur at the commissural choice points which expose axons to the attractive factors being expressed at the midline. The characterization of the *robo* family of receptors, an evolutionarily conserved immunoglobulin super family, revealed that growth cone

receptors can mediate the repulsive function at the midline. In *robo1* mutants, too many axons cross and recross the midline (Kidd *et al*, 1998a;Kidd *et al*, 1998b) and when both *robo1* and *robo2* are removed in double mutant embryos, the CNS phenotype resembles that of *slit* mutants (Dickson *et al*, 2000). Growth cones expressing Robo from early in development are repelled from the midline, and when Robo is dysfunctional, axons enter the midline freely suggesting that Robo is the midline repellent receptor (Kidd *et al*, 1998c). The distribution of Robo found on the pioneering growth cones is regulated by *commissureless* (*comm.*) that is expressed by the MG at the anterior and posterior commissure. Robo expressing growth cones that contact Comm. while exploring the midline down regulate *robo* expression and cross the midline (Tear *et al*, 1996;Kidd *et al*, 1998c). In *comm.* mutant embryos, no commissural axons are formed indicating that Comm. is necessary in order to down regulate Robo permitting commissural axons to enter the midline. We propose that Slit, a secreted extracellular matrix protein expressed by the MG provides the repellent signal that binds the Robo receptor and establishes the repulsive barrier at the *Drosophila* midline.

Objectives

Experiments designed to address this hypothesis were divided into four stages shown in each of four chapters. Chapter one focuses on the detailed characterization of the *slit* gene and Slit expression in order to address concerns regarding published gene sequences and patterns of protein expression. Slit expression in the MG and on longitudinal axon tracts was re-evaluated, along with the time course and pattern of Slit expression in the heart. The previously uncharacterized pattern of Slit expression in the muscle apodemes has been investigated along with the time course of Slit expression

throughout development. In order to facilitate a functional analysis of *slit* structure, the complete genomic and cDNA sequences were generated and the published protein structure was assessed against modern databases. Finally, based on data derived from the genomic structure of *slit*, we were able to accurately sequence coding regions from within the genomic sequence of a single fly, thus facilitating the genomic sequencing and analysis of mutant *slit* alleles.

Chapter two characterizes several *slit* mutations to identify mutations in different domains of the Slit protein that might lead to a better understanding of *slit* function. A series of hypomorphic *slit* alleles were analyzed for variations in mutant phenotype in tissues where Slit expression was characterized. The penetrance of the *slit* phenotypes were assessed and ranked in order of severity ranging from mild to severe. Hypomorphic mutations in the *slit* locus were then sequenced in order to correlate domain specific mutations with the characterization of each respective mutant phenotype.

Chapter three describes the investigation of *in vivo* Slit function using complete and truncated transgenic *slit* genes designed based on domain functions revealed in Chapter 2. We determined whether transgenic *slit* expression in the MG was sufficient to rescue the *slit* phenotype and which domains of Slit were vital to this role. Additionally, the proposed role of Slit as a repulsive ligand was investigated in both overexpression and ectopic expression experiments using complete and truncated forms of the *slit* transgene. Data from chapters two and three were then compiled in order to evaluate domain specific functions attributable to Slit expression in the *Drosophila* midline and the potential role of *slit* in other tissues.

Finally, chapter four investigates the genetic interaction of *slit* with *robo* and introduces molecular evidence demonstrating Robo binding to specific domains in Slit. Questions that were addressed included: does *slit* interact with *robo* genetically; do *slit* hypomorphs interact with *robo*; do *slit* hypomorphs interact with *robo* outside of the midline CNS; what domain of *slit* genetically interacts with *robo*; and finally what domain of Slit binds Robo? The results of these experiments are discussed in terms of what does this tell us about axon guidance and the development of the bilaterally symmetric nervous system.

slit, an extracellular matrix protein, is expressed in the midline glia, on commissural axon pathways, cardioblasts, and muscle apodemes

CHAPTER 1

In this chapter we will characterized the pattern of Slit expression throughout embryonic development and establish the time course of expression from embryos into adult flies. A complete cDNA of *slit* will be presented alongside the genomic sequence identifying the intron and exon boundaries for the purpose of generating sequencing and vector primers for later experiments. Finally, we will demonstrate and verify the PCR amplification and sequencing of genomic exons from single larval and fly preparations.

MATERIALS AND METHODS 1

Fly Maintenance

All fly stocks were maintained in a common room at a temperature of 21 ± 2°C, changed on a 2 week cycle and treated with tedion (2,4,5,4' –tetrochloro-diphenyl sulphone) soaked filter paper (2% in acetone) bi annually. The room was maintained on a natural light dark cycle and trays (Fisher, 14-809-24; 14-809-30) of fly vials (Fisher, AS519) were stored individually on shelves treated quarterly with a 50% solution of Benzyl benzoate in ethanol and plugged with rayon rope (Fisher, APS205). The flies were raised on a basic agar medium supplemented with (final concentrations) 10% sucrose, 0.8% Potassium Sodium Tartrate, 0.1% Potassium dibasic salt, 0.05% of each NaCl, CaCl, MgCl, and Ferric Sulfate, then autoclaved and combined with a 2.5% autoclaved solution of dry Yeast in H_2O. Food was partially cooled (54°C) and treated with 0.4% Tegosept (10 % in ethanol) and 0.25% Acid Mix (42 % Proprionic Acid & 4% Phosphoric Acid).

Genetic Stocks

Fly stocks used for wild-type characterization of *slit* were screened for endogenous P-elements and derived from the Canton S. (Caltech Stock Center, 1) *Drosophila* stock.

Genomic clones and cDNA

Chromosome *in situs* of slit DNA obtained from clones generated by Rothberg et al. ((Rothberg *et al*, 1988)) show that *slit* maps to region 52D on the 2nd chromosome. A series of cosmids containing a total of 45 genomic fragments from region 52D were screened by PCR for 5' and 3' domains of the slit DNA (5'for-5'

ACTCGAGCGACTGGACATCT 3', 5'rev 5' GTCGTCGAAAGCTGGAGAAC 3', 3'for 5' GCACAGCAGGCATACAAGAA 3', & 3'rev 5' AGCAATTGGGTAGTCGCATC 3'). Three of the smallest genomic clones (cosmids 60E2, 113E7, & 118G10) that contained both 5' and 3' slit cDNA were isolated and purified for the complete genomic sequencing of *slit* by primer walking (Voss et al., 1993). Primers for genomic sequencing were designed from different regions of the *slit* cDNA and amplified from the three different genomic templates for sequencing on an Applied Biosystems 373-A Stretch XL Sequencer with Big Dye Terminator Chemistry. Results of sequencing were aligned using DNAStar MegAlign version 3.18 and intron/exon boundaries were assessed based on the slit cDNA and Mount et. al. (1992) and Talerico and Berget (1994) Drosophila defined splicing criteria.

A total cDNA of *slit* was constructed based on fragments of clones provided by Rothberg et al. ((Rothberg *et al*, 1988)) and PCR generated bridges from the genomic cosmids (118G10 & 60E2). Primers were designed that overlaid known restriction sites and also generated a 5 'HindIII (5' CATA**AAGCTT**CCACAATGGCCGCGCC 3') and a 3' SpeI (5' CATCGTGCGCAAGTGCGGA**ACTAG**TAACAA 3') restriction site for rapid sub cloning into Strategene pBS KSII +. All products were completely sequenced and verified against the published and genomic sequence. Discrepancies in cDNA sequence were documented and verified by further sequencing.

DNA obtained from bacterial transformations, stock plasmid, PCR, transgenic constructs and agarose gels was extracted by Qiagen Plasmid Mini (Qiagen-tip 20, 12129), Midi (Qiagen-tip 100, 12243), PCR purification (28104), Mega endofree

(Qiagen-tip 2500, 12381), and QIAquick gel (28304) respectively. Genomic preparations were obtained from cosmids or tissue.

Cosmids were prepared by PEG precipitation using 500ml LB/kan inoculated from an overnight culture ((Sambrook *et al*, 1989)). Broth was spun down at 4K(4°C) for 15 minutes and bacteria were resuspended in 30 mls STE (0.1M NaCl, 10mM Tris-HCl [pH 8.0], 1mM EDTA [pH 8.0]), transferred to a fresh centrifuge tube and spun down again 4K(4°C) for 15 minutes. Bacteria were then carefully resuspended in 10 mls of ice-cold Solution I (50mM glucose, 24 mM Tris-HCl [pH 8.0], 10mM EDTA [pH8.0]) before being lysed with fresh Solution II (0.2 M NaOH, 1% SDS) mixed 8-10 times and incubated for 4-5 minutes on ice. The lysed solution was neutralized with 10 mls of ice cold SolutionIII (3M potassium acetate, 5M glacial acetic acid in ddH_2O) with progressively vigorous shaking over 10 seconds and then incubated on ice for 10 minutes. The supernatant was filtered through sterile cheesecloth into a fresh centrifuge tube and precipitated at -20°C for at least 20 minutes with 0.6 volumes of isopropanol and careful shaking. The precipitate was spun down 4K(4°C) for 15 minutes and resuspended in 4mls of 2.5M LiCl for incubation at 4°C for 15 minutes. After centrifugation at 4K(4°C) for 10 minutes the supernatant was removed and diluted with 2 volumes of 100% ethanol and precipitated for 20 minutes at -20°C. The precipitate was spun down again at 4K(4°C) for 10 minutes and then the pellets was dissolved in 2 mls $sddH_2O$ with 5 µl of 10mg/ml RNAse and incubated at 37°C for 15 minutes. One volume of PEG solution (1.6M NaCl, 13% PEG8000) was added and the mixture was left on ice for at least 30 minutes before being spun down 4K(4°C) for 10 minutes and washed twice with 70%

EtOH. The genomic DNA was stored in an appropriate volume of buffer TE [0.1M, pH 8.0], quantified by spectrophotometry, and analyzed by gel electrophoresis.

Genomic DNA extraction from embryo, larva or fly tissues was adapted from Ashburner ((Ashburner, 1989)). Wild-type flies (~50) were collected under CO_2 and then combined with 1000 µl of Solution A (0.1M Tris HCl [pH 9.0], 0.1 M EDTA, 1% SDS, 100ul of 1mg/ml Proteinase K) and crushed in a 1.5 ml Dounce Homogenizer with 4 strokes of an A Pestle. The extraction was incubated at 70°C for 30 minutes and then 140µl of 8M potassium acetate was added and the mixture was incubated another 30 minutes on ice. The supernatant was collected twice into clean tubes with two spins of 12000rpm (4°C) for 20 minutes and then precipitated with 0.5 volumes of isopropanol at -20°C for 1 hour. DNA was collected and washed twice with 70% EtOH before being dissolved in 100 µl of TE [pH 8.0]. Prepared DNA was cleaned with 1-2 µl of DNAse free RNAse at 37° for 1 hour, phenol/chloroform extracted and then precipitated with 1/10 volume 3 M sodium acetate and 2.5 volumes of 100% chilled ethanol. The washed and dried DNA was dissolved in 100µl of TE [pH 8.0], quantified and tested on a 0.8% agarose gel.

Genomic Sequence Analysis

Sequencing of the cosmids provided the template from which to define the complete genomic sequence of *slit* and this was confirmed by alignments to AC005556 of the Berkeley *Drosophila* Genome Project. Primer pairs were designed to flank each of the 19 exons found and tested by PCR with cosmid, wild type genomic, and the *slit* deficiency *WMG* DNA. The format of these primers is presented in Appendix A.

PCR for sequencing was performed using Perkin Elmers ULTma DNA Polymerase (N808-0117) with GeneAmp dNTPs (N808-0007) which provided 3'-5' exonuclease proofreading activity with a $2*10^{-6}$ misincorporation rate of 0.982 under these conditions. Reagent mix was prepared for 100 µl reactions in 0.2 ml thin walled GenAmp reaction tubes (N801-0612) consisting of 1X UlTma Buffer, 1.0 mM $MgCl_2$, 40µM dNTP mix, 0.25 µM forward and 0.25µM reverse primers, 1.0U polymerase per reaction, and the volume was completed with purified ddH_2O (Gibco-BRL, 15230-170). The standard format for these reactions was 5 mins. at 97°C, an 85°C hold at which point Taq polymerase was added, followed by 35 cycles of 1.0 min at 95°C, 1.0min at 58.0°C, and 2.0-3.0 minutes at 72°C. PCR products were then stored at 4°C prior to purification by Qiagen PCR kit. Reactions were repeated 2-3 times and independent products were prepared for sequencing and agarose gel analysis. Sequencing products were aligned and documented for comparison to sequenced mutant exons and cDNA templates.

Slit antibody generation

Two hybridoma lines (4C.1 and 6D.4) generated during the original characterization of *slit* by Rothberg et al. (1988) were donated by S. Artavanis-Tsakonas and re-established in RPMI Medium 1640 (Gibco-BRL, 11875-093) supplemented with 10 % fetal calf serum (Gibco-BRL, 16010-159) and Penicillin Streptomycin (Gibco-BRL, 15070-063). In order to improve the low titer observed in these hybridoma supernatants, both cell lines were diluted to single cell cultures and individual cell lines were generated and tested. Five sub colonies of mAb 6D.4 showed dramatically improved Slit staining patterns in both Western and *in* vivo preparations. These colonies were expanded and sera was purified on Protein G Sepharose 4 Fast Flow beads (Pharmacia Biotech, 71-

7083-00) and stored in 0.95μg/μl aliquots at -20°C. Molecular characterization of the purified Slit mAb suggests that this antibody binds to a region of *in vitro* translated Slit between EGF-2 and EGF-6 on a Western blot.

Western blot analysis of native Slit expression

Expression of Slit protein during development was investigated using purified and unpurified tissue lysate. Tissue was collected from 0-4, 4-9, 9-13, 13-19, 19-24 hour embryos, larva, and adult flies which was then homogenized in RIPA lysis buffer (150 mM NaCl, 1.0% NP-40, 0.5% DOC, 0.1% SDS, 50 mM Tris-HCl [pH8.0], Protease Inhibitor Cocktail Tablets 1/10 ml (Roche Complete, mini, EDTA-free, 1836170)), incubated on ice for 10 minutes, centrifuged 5 minutes at 12000g and then the supernatant was collected. All procedures were carefully carried out on ice and samples were stored at -80°C.

Raw samples were defrosted and 15 μl of each sample was mixed with 5μl of 4x Laemli buffer (2% SDS, 10% glycerol, 100mM DTT, 60mM Tris [pH8.0], 0.01% Bromophenol Blue) and heated for 5 minutes at 80°C. Samples were loaded onto a 7.5 % gel for PAGE and then transferred to a PVDF membrane. The membrane was washed and blocked prior to incubation in 1:10000 mAb Slit blocking solution and then tagged with GαM HRP. The membrane was washed again 5*15 minutes in 1xTTE and then reacted with 2mls of ECL (Amersham Pharmacia Biotech, RPN 2106) chemiluminescence for detection of HRP bound primary antibody on Kodak X-OMAT AR (XAR) Film.

Slit was purified from tissue lysate on a Protein G Sepharose 4 Fast Flow substrate (Pharmacia Biotech, 71-7083-00) bound to mAb Slit. Raw samples were

defrosted and 250 µl was removed and incubated for 2 hours with 2 µl of mAb slit while being rotated at 4°C. The Sepharose was mixed thoroughly and 25 µl was added to each sample before being incubated a further 15-20 hours on the rotator at 4°C. Samples were collected by centrifugation and washed 5 times with chilled RIPA buffer. The Sepharose pellet was suspended with 50 µl of 1x Laemli buffer and heated to 80°C for 5 minutes. Samples were loaded onto a 7.5 % gel for PAGE and then transferred to a PVDF membrane. The membrane was washed and blocked prior to incubation in 1:10000 mAb slit blocking solution and then tagged with GαM HRP. The membrane was washed again 5*15 minutes in 1xTTE and then reacted with 2mls of ECL (Amersham Pharmacia Biotech, RPN 2106) chemiluminescence for detection of HRP bound primary antibody on Kodak X-OMAT AR (XAR) Film.

Tissue *in situ* hybridization

cDNA templates for *in situ* hybridization probes were transformed into pBS KSII+ with a 5' orientation at the T3 sense and T7 anti-sense promoter producing RNA transcripts. RNA labeling by *in vitro* transcription was performed with a DIG RNA labeling Kit (Roche, 1175025), detected by anti-digoxigen Fab Fragments conjugated to Alkaline Phosphatase (Roche, 1093274) and catalyzed with a 0.75:1 solution of 5-Bromo-4-chloro-3-indolyl-phosphate (BCIP Roche, 1383221) and 4-Nitroblue tetrazolium chloride (NBT Roche, 1383213).

Drosophila embryos were collected on apple juice agar plates and aged from 24-30 hours at 22°C. Fixation was carried out as described in Tautz et al. (1992) and the embryos were dehydrated in ethanol and stored at -20°C. Hybridization of *Drosophila* whole embryos was performed at 70°C overnight using an adaptation of Jowett (1997)

and reacted in the dark until background was apparent. Embryos were then post fixed in 4% formaldehyde overnight, dehydrated in ethanol, and cleared in methyl salicylate for whole mounting in DPX (Sigma 31761-6). Mounted embryos were observed under a Zeiss Axiophot microscope at 63X oil objective and documented on Kodak T-64 ecktachrome colour slide film.

Immunocytochemistry

Drosophila embryos were collected on apple juice agar plates and aged from 16-30 hours at 22°C. Fixation and immunocytochemistry was adapted from Patel (1994). mAb slit (1:200) and α β-gal (Cappel, 55976) were diluted in phosphate-buffered saline (PBS) containing 0.5% Triton X-100 and incubated at room temperature for 4-6 hours. Embryos were washed repeatedly for 2 hours and then incubated for 2 hours in biotinylated secondary antibodies (Vector Laboratories, mouse IgG PK-6102, Rabbit IgG PK-6101, Rat IgG, PK-6104) followed by a 1 hour incubation in Vector Laboratories Elite ABC (PK-6100). In cases of double labeling where mAb slit, α-sim, α-β-gal, & α-wrapper were used as the first label, reactions where performed in the presence of 0.03% nickel/cobalt chloride. Second or single labels were reduced with 3,3-Diaminobenzidine Tetra hydrochloride (DAB) (Gibco-BRL, 15972-011) to a brown precipitate and then dehydrated into methyl salicylate (Sigma M6752). Nerve cords were dissected or embryos were mounted whole and visualized on a Zeiss Axiophot microscope at 63X oil objective and documented on Kodak T-64 ecktachrome colour slide film.

Data presentation

Kodak T-64 ecktachrome colour slide film used to document light microscope work was developed commercially, and mounted in Gepe glassless slide mounts.

Selected montages were scanned into an Intel Pentium III 450 using a Minolta Dimâge Scan Dual colour slide scanner at 2400 dpi creating an Adobe PhotoShop 5.5 image file 24 MB in size. Images were stored on either individual CD-R (Hewlett Packard, C4437A) disks created on a Plexwriter CD Burner (Plextor, RW4/2/20) or Panasonic DVD-RAM (LM-DA52) disks created on a Panasonic DVD-RAM (LF-D101). Kodak X-OMAT AR (XAR) Film was scanned on a UMAX Astra 1220S Flatbed scanner at 600 dpi into Adobe Photoshop and saved as a 43 MB Raster image and confocal images were directly imported into Photoshop as TIFF graphic files. Images and figure plates were prepared using Adobe Photoshop 5.5 and maintained as multilevel image files 50-100 MB in size at 600 dpi. Plates were printed on an Epson Stylus 740 at 1440 dpi on Epson Photo Paper (S041141).

RESULTS 1

slit

Drosophila slit has been characterized as a large extracellular matrix (ECM) protein containing a peptide signal sequence and four distinct protein motifs consisting of: four Leucine Rich Repeats (LRR), 7 EGF-like repeats, an Agrin-Laminin-Perlecan-Slit (ALPS) like motif and a Cysteine-Rich Carboxy terminus (Rothberg & Artavanis-Tsakonas, 1992). A cursory analysis of RNA and protein expression shows that Slit is expressed in the midline glia (MG) and the cardioblast cells of the dorsal vessel, along with light protein staining on the longitudinal and commissural axons of the nerve cord (Rothberg *et al*, 1990). Our preliminary analysis suggested that cDNA clones available from the original study (Rothberg *et al*, 1988) represented only a portion of the entire *slit* cDNA, and that antibodies used to characterize Slit expression had degenerated. In order to revive the investigation of *slit*, we have completed and revised the sequence and structure of *slit* cDNA, re-established a working antibody, characterized the time course and patterns of Slit expression, and refined a genomic map of *slit* from which exon specific PCR sequencing primers were designed.

slit cDNA

Sequence data analyzed from the original *slit* cDNA clones indicated that *slit* had an ORF of 4443 b.p. coding for 1480 a.a. ((Rothberg *et al*, 1990)). Based on sequencing of PCR products generated from genomic cosmids and new cDNA clones an additional 72 b.p. of *slit* cDNA was identified in the region of the 1st LRR. Additionally, a number of sequencing errors were identified and the revised sequence with the sequenced changes indicated in red were summarized in Figure 1.1. Coding and nucleotide

corrections identified by PCR of cosmid genomic DNA were verified against later genomic and cDNA accessions published on GeneBank (AC005556). Using PCR amplified DNA from genomic clones that was engineered to correct the coding errors in the older cDNA clones, a regenerated complete *slit* cDNA was created consisting of 4515 b.p. coding for 1504 a.a. (Battye *et al*, 1999).

Based on motifs defined by Rothberg (Rothberg *et al*, 1990;Rothberg & Artavanis-Tsakonas, 1992) we have reanalyzed the Slit structure. The predicted initiating methionine is followed by an amino acid sequence containing regions characteristic of a secretory signal sequence (pink). Hydropathy plots have not indicated any transmembrane domains within the Slit protein, suggesting that the *slit* locus encodes a secreted extracellular protein (Protean, DNAStar). Analysis of the remaining amino acids reveals four notable protein motifs.

The first motif consists of four Leucine Rich Regions (LRRs, yellow in Fig. 1.1) each containing 4 or 5 24 amino acid Leucine Rich Repeats (LRR, xxxxFxxLxxLxxLxLxxNxLxxL, where x is any a.a.). These regions are each flanked by a conserved amino- (CPxxCxC.....xGxxVDCxxxGLx..xαPxxαPxDTTx) and carboxy- (PWxCDCxα.....WLxxxxxxxxxxxxx.....RCxxPxxxxxxxαxxαxxxxFx..CP) region (orange) that creates a defined flank-LRR-flank pattern shown in Figure 1.2 (B). An additional sequence of 72 nucleotides that codes for proteins characteristic of another Leucine Rich Region was identified (red, LxLxxNxLxxI xxxxFxx xx) in the first LRR that was not originally characterized by Rothberg *et al.* (1990). These changes do

Figure 1.1 The *slit* nucleotide coding sequence

A regenerated *slit* cDNA has nucleotide and coding changes from Rothberg's original sequence (1990) indicated in red, and encodes a number of protein domains (butting domains are demarked with a black bar and labeled as either Leucine (L#) or EGF (E#)). The putative signal sequence (pink) is followed by four blocks of Leucine Rich Repeats (LRRs, yellow) flanked by characteristic amino- and carboxy- regions shown in orange. A series of EGF-like repeats (blue) are separated between the 6th and 7th repeat by a globular domain (G-domain, gray) and the carboxy-terminal domain is characterized by a Cysteine-Rich region referred to as a Cysteine Knot (green). The potential N-linked glycosylation sites are noted by an open black bar and the β-hydroxylation sequence in the 3rd and 5th EGF repeats are marked by a green tab. The proposed cleavage site TSPCQNHE identified by Brose *et al.* (1990) is defined by a purple box at the beginning of the 6th EGF-like repeat.

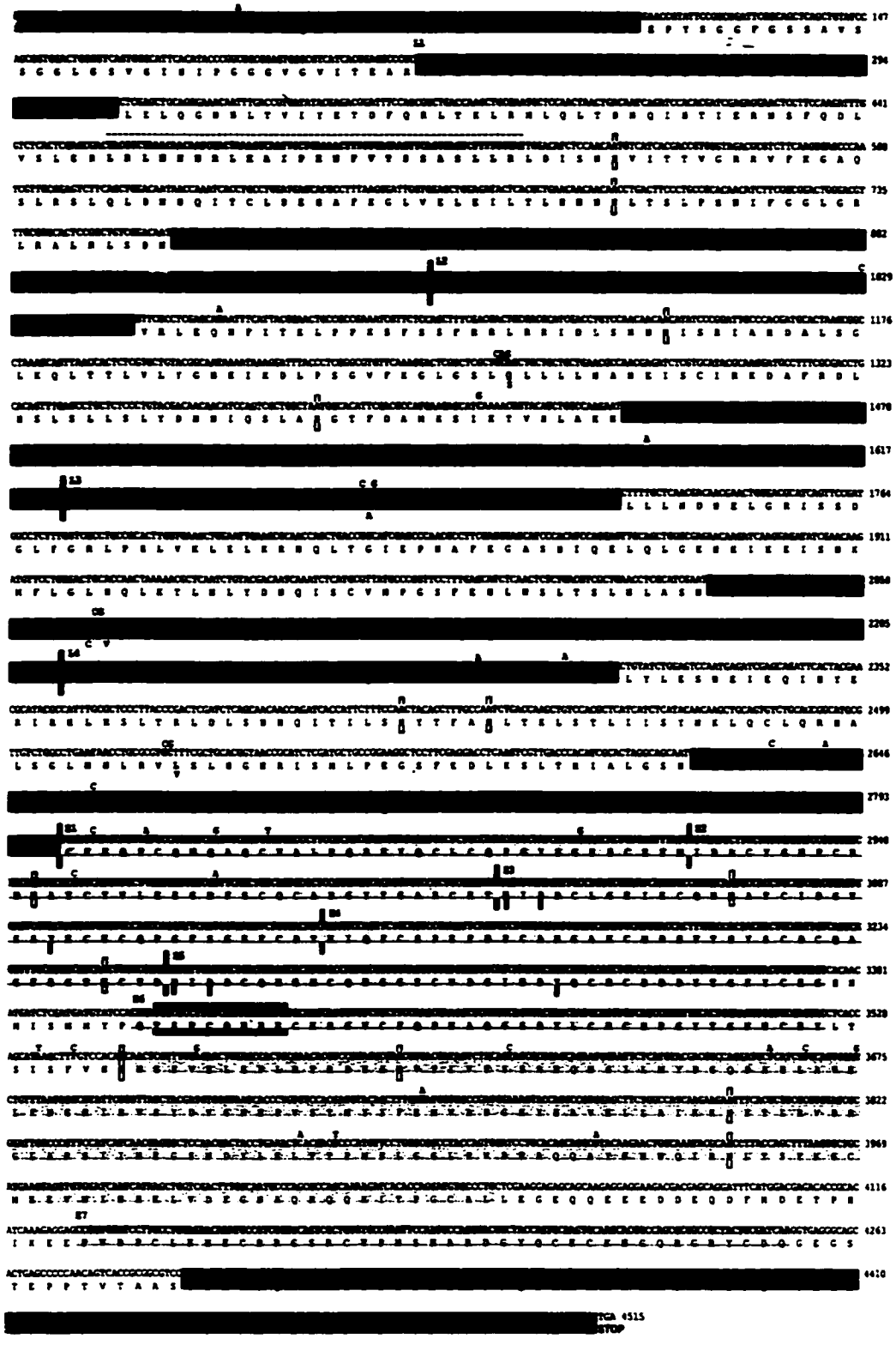
putative signal sequence
EGF-like repeats
Leucine Rich Regions
G-Domain (formally agrin, laminin, perlecan)
amino and carboxy flanking regions
cystine knot
clevage site

Figure 1.2 Slit protein distribution in the nerve cord showing schematic of antibody design.

A polyclonal antibody that was raised against the 6th EGF-like repeat and a portion (550 bp, EcoR1 2632-4182) of the G-domain (also known as the ALPS domain) labels *slit* protein in the midline glial cells (A, arrowhead) and on fascicles of the longitudinal axon tracts (A, arrow). A schematic representation of the *slit* protein shows the arrangement of the protein domains (B). The circle indicates the domain used for antibody generation by Rothberg *et al.* (1988).

NH2
COOH
B

not appear to change the originally proposed conformation of the protein (Bland, personal communication). The flank-LRR-flank repeats represent more than half of the total protein and are followed by a smaller series of 40 amino acid EGF-like repeats (blue, xCxxxxxxCx xxxCxxxxxxxxxxxCxxCxxGxxGxxCx –variant residues are gray), which form the second significant protein motif. The first six EGF repeats are separated from the final seventh EGF repeat by a globular domain (gray). The globular domain is characteristic of similar regions in Agrin, Perlecan, and Laminin (xSxxxxxxLxxxxxxxxxxxxFxxx G L xGxxxx--
x xx xxG. xxxx xG xx- x xxxxxxGx x xx xx x xLx xx------
xxxxxxx. x xx -. x x-x. GGx---
x xx xxxxxxxxxxxx xGCx xxx xxx xxxxx xxxxx xx-) forming the third Slit motif (G-domain, previously the ALPs motif, Figure 1.2, B). The final EGF repeat is followed by a conserved carboxy-terminal cysteine-rich motif (green, xCxxxxxxxxxxxxxxxCx xxx xxxx xxxxxx CCx xx xxxx xxxCxx xxxx xxxx x xCxXxxx-Cxxx-Cxxx xxxxxxx--xxxxxxxxx) characterized as a cysteine knot. Thirteen sites that are believed to be potential N-linked glycosylation sites are identified by an open box suggesting that Slit is a heavily glycosylated protein. The consensus sequences for β-hydroxylation in the third and fifth EGF repeats are marked with a green tab and the possible β-hydroxy derivative (GEGSTEPPTVT) is located between the last EGF repeat and the cysteine knot. Based on Western analysis and micro sequencing of *in vitro* expressed recombinant human Slit, *myc* tagged at both the C and N-terminus, Brose *et al.* (Brose *et al*, 1999) identified a putative cleavage site (TSPCDNFD). The homologous *Drosophila* sequence (TSPCQNHE in purple, Fig 1.1) is the proposed target site of one

or more Slit-cleaving proteases which process *Drosophila* Slit into a ~190 kDa and ~55-60 kDa bands on a Western blot of *Drosophila* extracts (Fig. 1.5B, black arrow)

Slit expression patterns

In the initial characterization of Slit expression Rothberg, *et al.* (1988; 1990) generated a polyclonal (Figure 1.2 A, arrowhead) and monoclonal antibody based on a 550 b.p. EcoRI fragment localized to the 6th EGF-like motif, along with a tissue *in situ* probe based on the same fragment (Figure 1.2 B, circle). Attempts to reproduce this antibody and other antibodies based on Slit domains have repeatedly failed in a number of Laboratories. Inquiries into the availability of the original antibodies revealed that the polyclonal antibody was extinct, and that the monoclonal cell lines were badly degenerated and/or polluted. After obtaining two samples from the original monoclonal cell lines (6D.1 & 4B.1, Artavanis-Tsakonas) we decided to attempt to regenerate a high titer Slit monoclonal antibody by sub cloning and screening individual cells from each original stock (with the assistance of Rob Perry from the McMaster Rudnicki Lab). The regenerated Slit antibody and a tissue *in situ* probe based on the entire *slit* cDNA were then used to reassess the pattern of Slit protein and RNA expression.

Slit expression has been shown in the MG, in the cardioblasts that form the heart and the polyclonal antibody lightly labels the longitudinal and commissural axons of the nerve cord (Rothberg *et al*, 1990). Using the regenerated mAb to Slit and the complete RNA probe we identified other tissues from a pool of wild type embryos that expressed Slit protein and confirmed the specificity and quality of the new antibody in already identified patterns of expression (Figure 1.3). Slit mAb and RNA labeling was identified

Figure 1.3 Expression pattern of Slit

Wild type embryos (stage 16) were stained with a mAb to Slit (A, C, E, G) and an *in situ* probe made against the complete *slit* cDNA (B,D,F,H,). Slit is expressed in the midline glial cells (MG) within each neuromere (A, B arrow) shown in this sagittal plane. From a ventral perspective Slit is observed in the midline (C, D arrow), but only protein is detected at the points of muscle insertion (C, arrowhead). Both Slit protein and RNA are expressed in the cardioblast cells that form the heart (E, F black arrow). Looking directly at the segmental muscles, Slit is detected only at the intersegmental boundaries (arrowhead) where these muscle insert into the ectoderm (G). Strongly over-reacted *in situ* staining that produces background artifact, shown in this frontal plane (H, black arrowhead), indicates no *slit* RNA expression at the points of muscle insertion.

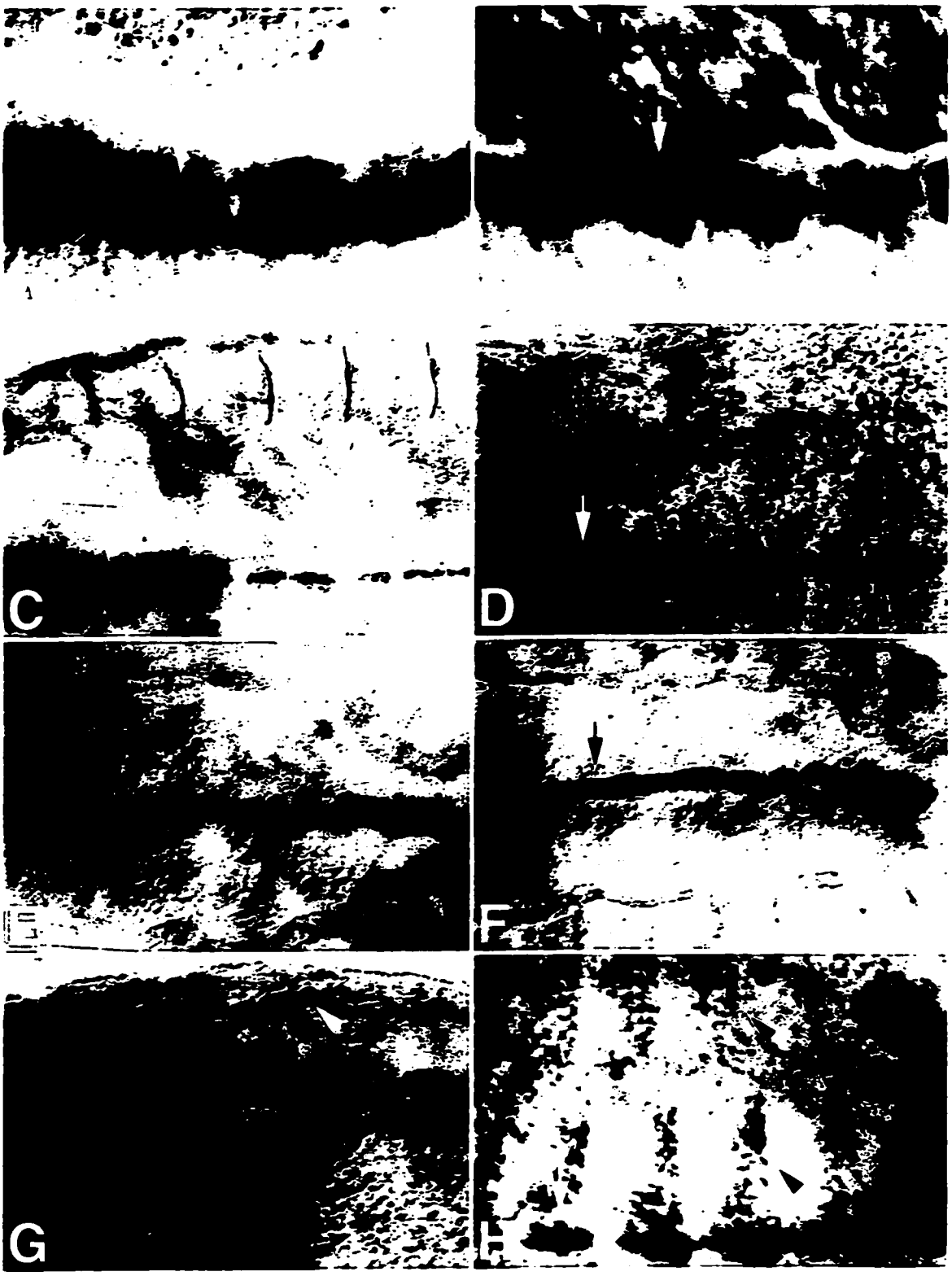
C
D
F
G
H

in the midline glia (MG) within each neuromere (white arrow) (A,B) but was not detected on the longitudinal fascicles (C). Bands of antibody labeling were found at the intersegmental boundaries (white arrowhead), but RNA was not detected in corresponding tissue (D). On closer inspection, the antibody labeling at the intersegmental boundaries is localized to the point at which the dorsal oblique muscles insert at the intersegmental boundary (E, white arrowhead). In overreacted RNA tissue *in situs* that produced background labeling in each segment (F, black arrowhead), no *slit* RNA labeling was found at the intersegmental boundaries. Both protein and RNA were found in the cardioblast cells of the dorsal vessel (black arrow E,F). A previously unidentified pattern of Slit labeling was observed in the nuclei of presyncytial embryos. Early stage 2-5 embryos show a punctate pattern of Slit labeling that is distributed at first (Fig. 1.4 A, arrowhead) and becomes more regular and uniform as the embryo develops (B-E). As the syncytial blastoderm begins to cellularize (F-H), Slit labeling is observed to localize to the surface of the embryo (F) and later (G-H) within the cell membrane of each cell. In all, analysis of the regenerated Slit antibody was validated by observed expression in the MG and cardioblast cells, and additionally localized Slit protein to the muscle apodemes and the early presyncytial blastoderm.

Time course of Slit expression

Protein localization in previous studies has been described only in older embryos and developed tissues (Rothberg *et al*, 1990). The observed patterns of Slit expression in muscle apodemes and the presyncytial blastoderm suggest that a more careful analysis of the time course of Slit expression was warranted. *Drosophila* tissues collected at different times in development were analyzed for the expression of Slit. Whole cell

Figure 1.4 Early embryonic Slit expression

A mAb to Slit shows a punctate pattern of Slit expression (arrowhead) in early embryos (A-F) prior to cellularization. As the embryos develop Slit labeling increases and appears to localize to the surface of the embryo (F). As cellularization begins Slit antibody labeling appears localized within the newly formed cells (H). The time course of Slit antibody labeling during embryogenesis is shown schematically at the bottom.

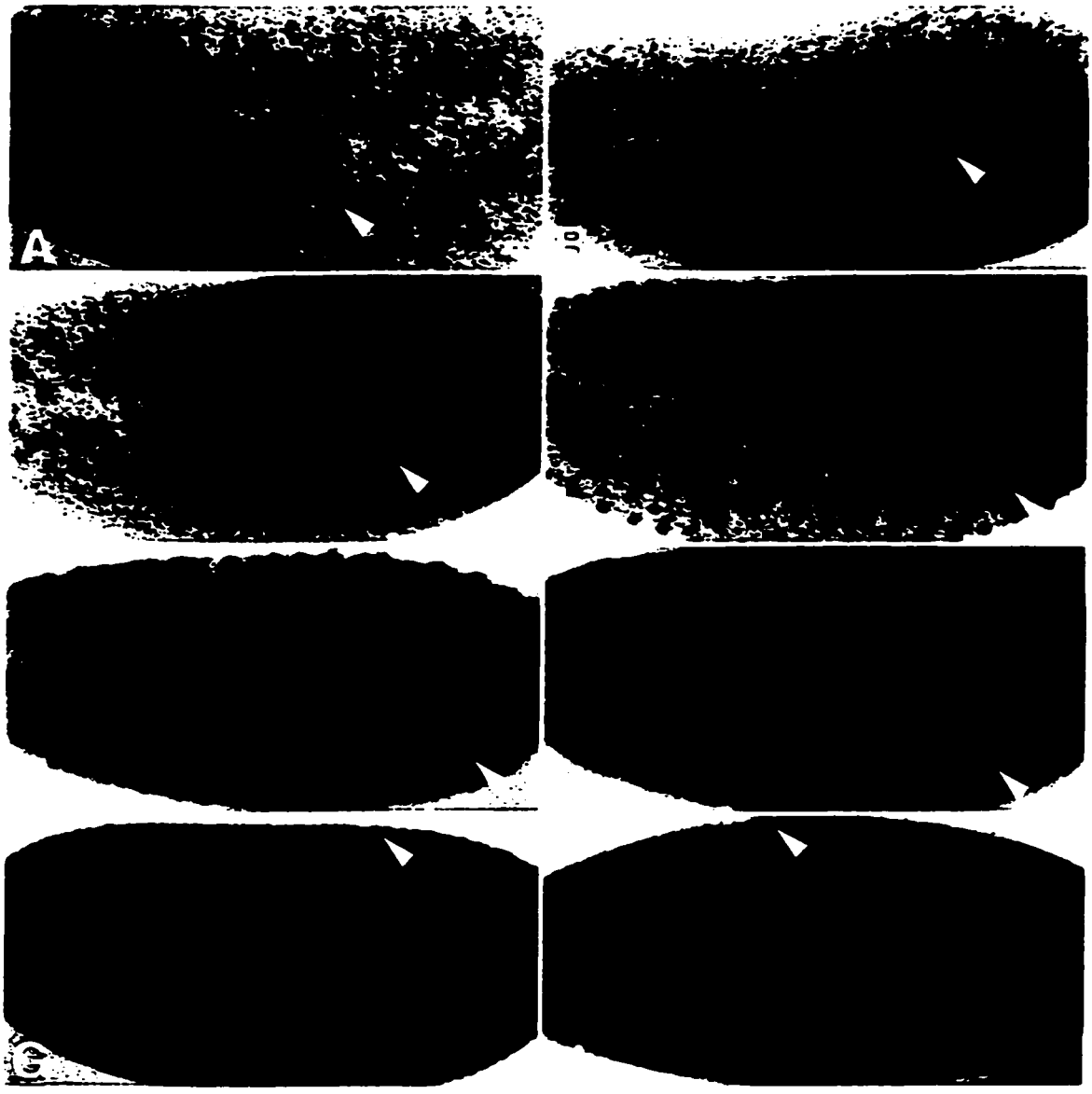
A
G

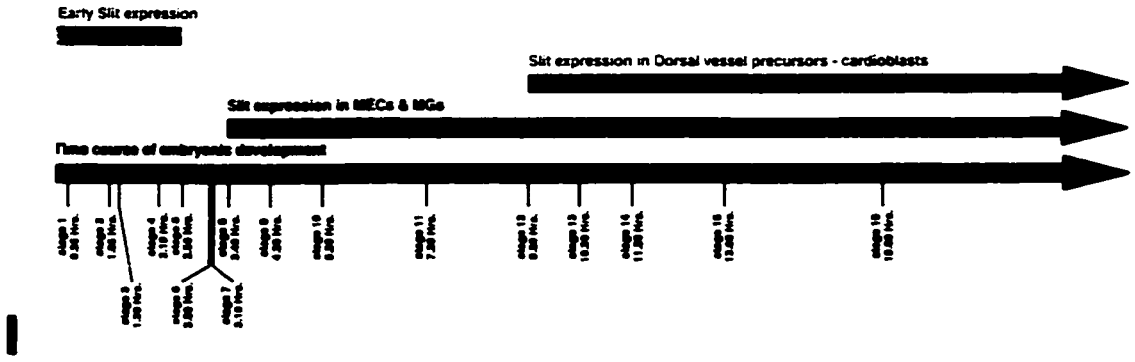
Early Slit expression
Slit expression in Dorsal vessel precursors - cardioblasts
Slit expression in MECs & MGs
Time course of embryonic development

lysate extracted from *Drosophila* tissues aged for 0-4 hours (stages 1-8), 4-9 (stages 9-12), 9-13 (stages 12-15), 13-19 (stages 15-17), 19-24 (hatching-larva), and adults was separated on a 10% non-denaturing PAGE (Fig. 1.5, A), immunoblotted on PVDF membrane and analyzed for Slit expression (B). The predicted size of Slit protein is approximately 168.6 kD and Slit was detected in a band at >205 kD in all tissues except stages 1-8 (B, white arrowhead). Protein bands at ~13 kD in stage 1-8 embryos were detected by the *slit* mAb (B, white arrow) that corresponds to the time course of presyncytial protein labeling that was observed previously (Fig. 1.4). Other protein bands in adult tissue at ~50 kD (B, black arrow) also did not correspond to the predicted size of Slit, but were the predicted size of cleaved Slit proposed by Brose *et al.* (1999). Tissue lysate that was purified on a mAb Slit column pulled down a single species of ~190 kD (C, black arrowhead). An immunoblot of the immunopurified extract indicated that the isolated proteins were detected by an antibody to Slit at ~190 kD in all tissues sampled (D).

Embryos collected from a series of stages in development were analyzed for Slit protein and RNA expression in the MG and cardioblast cells. Slit expression in the mesectodermal cells and MG (Figure 1.6; white arrow-protein, black arrow-RNA) was detected in stage 8 embryos (A,B) through to stage 17 (Q,R) and remained localized to the dorsal surface of the ventral nerve cord. The precursors of the dorsal vessel began to express Slit at stage 12 (Fig. 1.6 sagittal I, white arrowhead-protein; J, black arrowhead-RNA; Fig.1.7 dorsal A, B). As the precursors of the dorsal vessel differentiated into cardioblast cells (Fig. 1.6 K,L; Fig. 1.7 C, D), and then began to migrate dorsally (Fig. 1.6 M-R; Fig1.7 E-H) Slit expression remained localized to these cells. During closure of the dorsal vessel, Slit expression remained consistent (E-H) and as the cardioblast cells

Figure 1.5 Expression of Slit protein during development detected by Western blot. Tissue extracts from *Drosophila* at different points in development were either analyzed as whole cell lysate (A,B) or purified on Slit antibody column (C,D). Whole cell lysate from 0-4, 4-9, 9-13, 13-19, 19-24 hour egg collections along with adult tissue was run on a 10 % PAGE (A) and then blotted onto PVDF membrane for immunolabelling with mAb *slit* (B). Slit protein (white arrowhead) was detected as a greater than 205 kD complex in all tissue samples with the exception of 0-4 hour embryos where a smaller, ~ 14 kD protein was detected (white arrow). A second complex (black arrow) was observed in the adult cell lysate that was ~ 60 kD that likely represents cleaved Slit (Brose, *et al.*, 1999). Whole cell lysate purified against *slit* mAb on a G-Sepharose column pulled down a single ~ 170 kD protein (black arrowhead) from 4-9, 9-13, 13-19, 19-24 hour embryos and adults (C). A Western blot immunolabelled for Slit shows that the isolated protein detected by the mAb for Slit is 170kD at all stages sampled (D, black arrowhead).

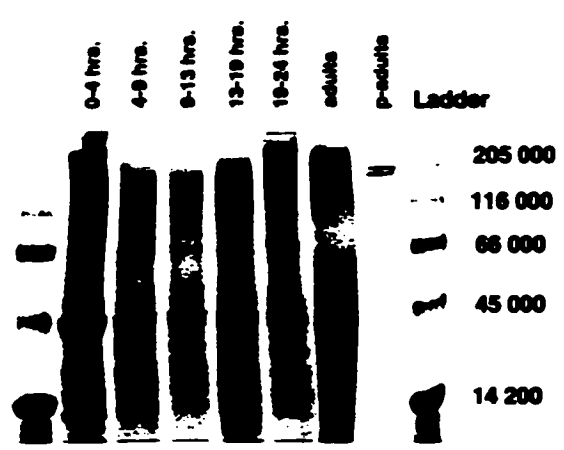
0-4 hrs.
4-8 hrs.
8-13 hrs.
13-18 hrs.
18-24 hrs.
adults
p-adults
Ladder
205 000
116 000
66 000
45 000
14 200

A

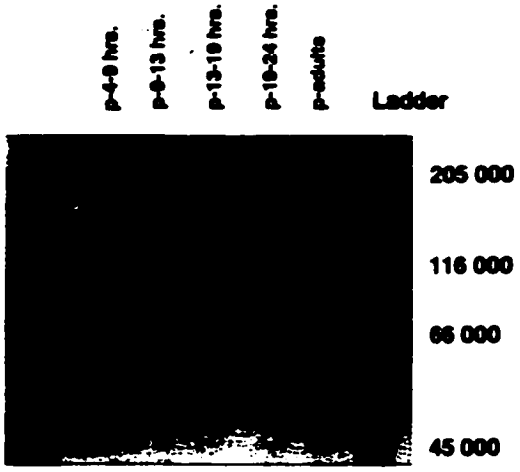
p-4-8 hrs.
p-8-13 hrs.
p-13-18 hrs.
p-18-24 hrs.
p-adults
Ladder
205 000
116 000
66 000
45 000

C


0-4 hrs.
4-8 hrs.
8-13 hrs.
13-18 hrs.
18-24 hrs.
adults
p-adults

B

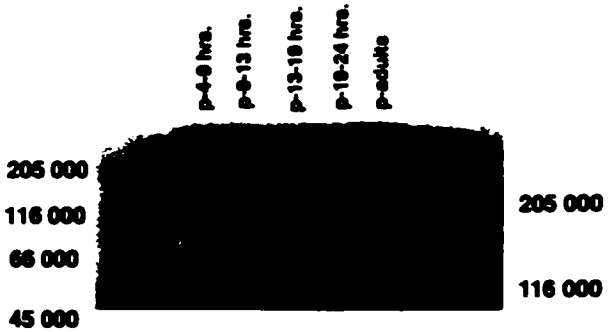
p-4-8 hrs.
p-8-13 hrs.
p-13-18 hrs.
p-18-24 hrs.
p-adults
205 000
116 000
66 000
45 000
14 200
205 000
116 000

D

Figure 1.6 Expression pattern of *slit* during embryonic development.

The expression pattern of *slit* (A/B-stage 8, C/D-stage 9, E/F-stage10, G/H- stage 12/5, I/J-stage 12/0, K/L-stage 13, M/N-stage 14, O/P-stage 15, Q/R-stage 16) during development is shown for both protein (A, C, E, G, I, K, M, O, Q) and RNA (B, D, F, H, J, L, N, P, R). Slit expression is observed in mesectodermal cells from stage 8 to stage 16 (protein white arrow, RNA black arrow), and is localized to the midline of the ventral nerve cord. From stage 12 on both protein (white arrowhead) and RNA (black arrowhead) are detected in the precursor cells of the dorsal vessel. As these cells differentiate the pattern of *slit* expression is localized to the cardioblasts that eventually form the heart.

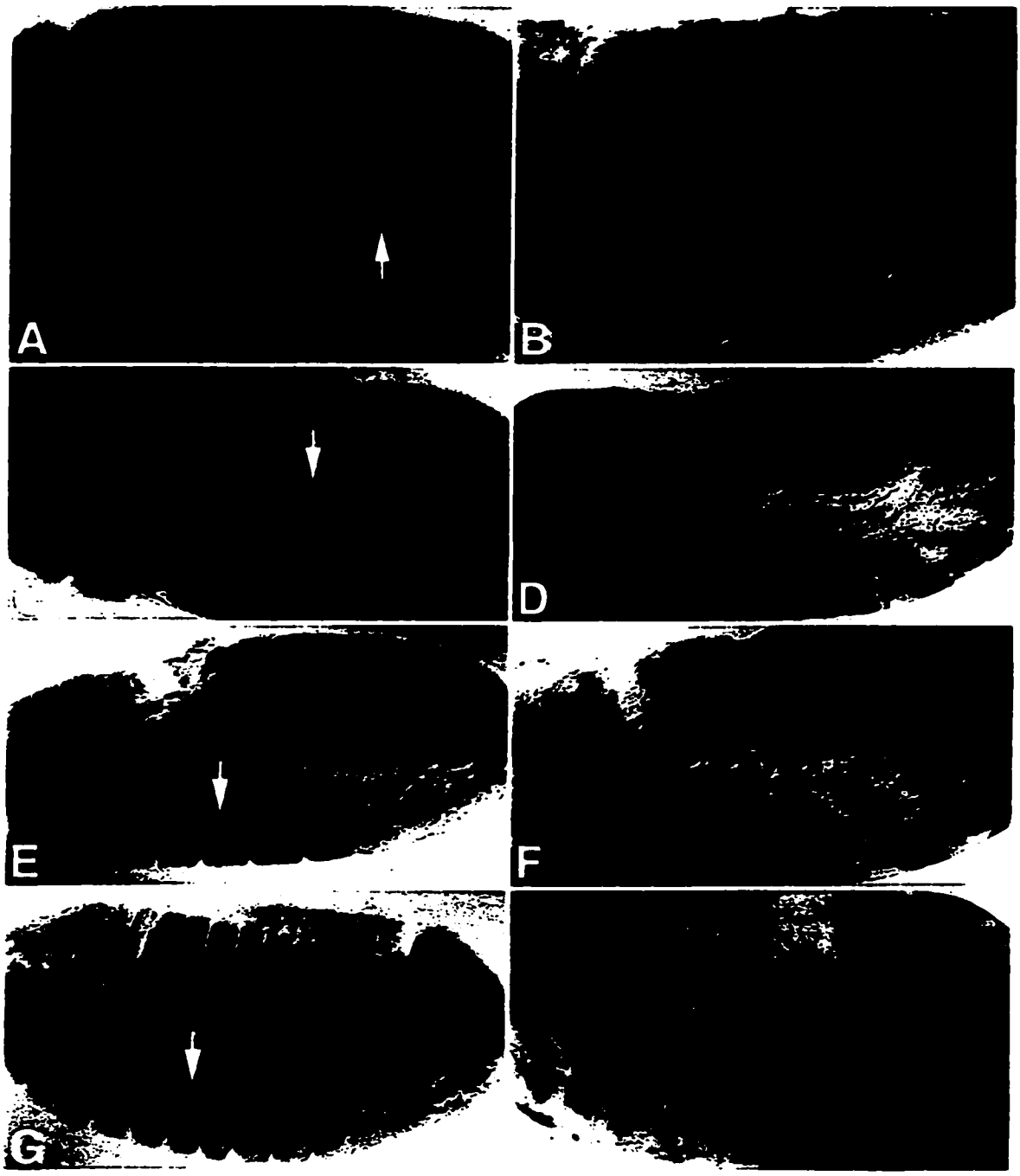
A
B
D
E
F
G

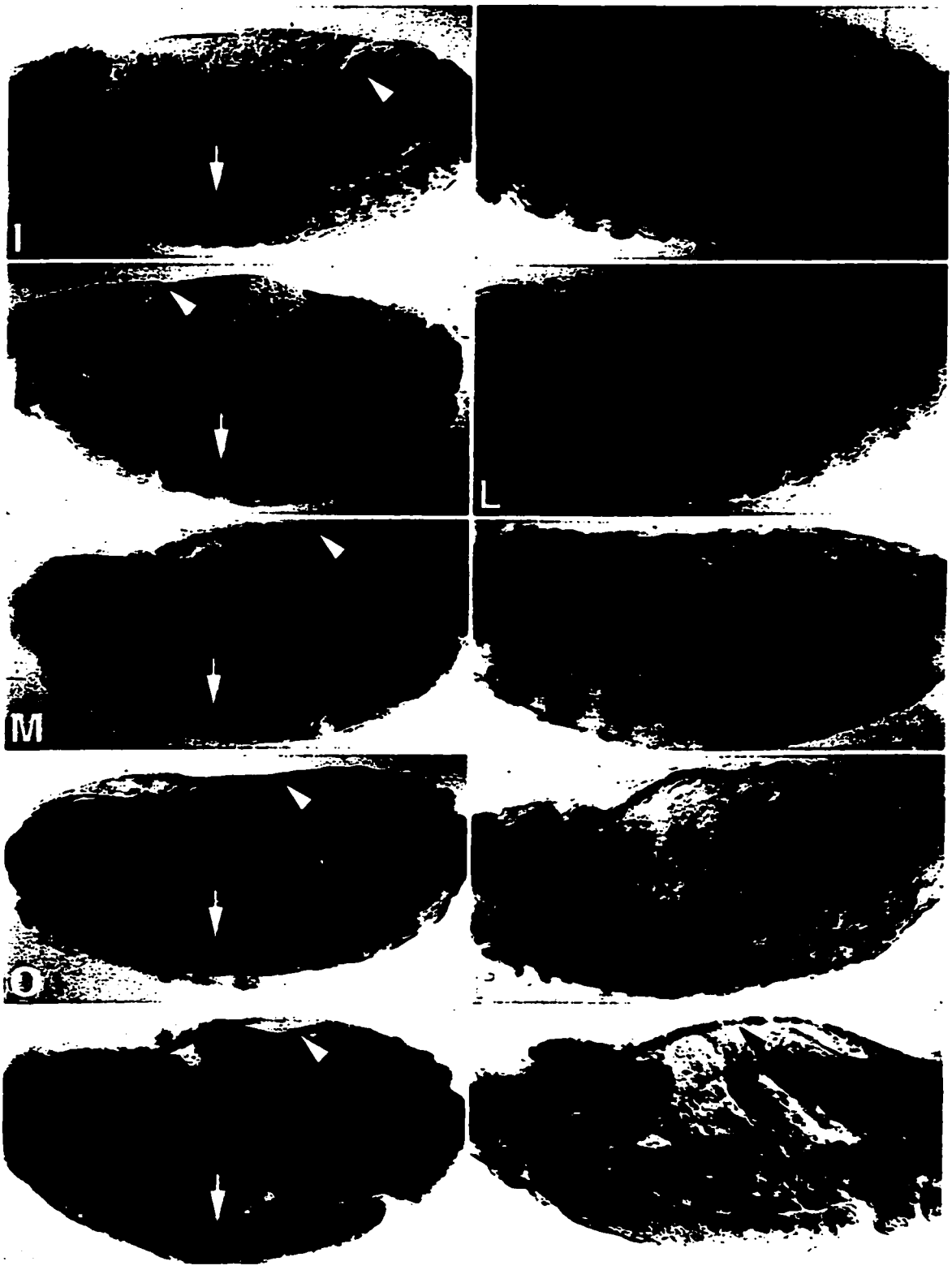
I
L
M
O

Figure 1.7 Expression pattern of Slit in the heart during development.

Slit protein (A, C, E, G, I, white arrowheads) and RNA (B, D, F, H, J, black arrowheads) is detected in the hindgut (hg) in the lateral part of the mesoderm (A, B). In stage 13 (C, D), Slit expression is observed in the early cardioblasts and as these cells move dorsally (E, F –stage 14; G, H –stage 15) to meet during dorsal closure. Slit expression remains restricted in these cells (I, J –stage 17). At dorsal closure a higher concentration of Slit labeling is observed at the leading edge of the cardioblasts (white and black arrows).

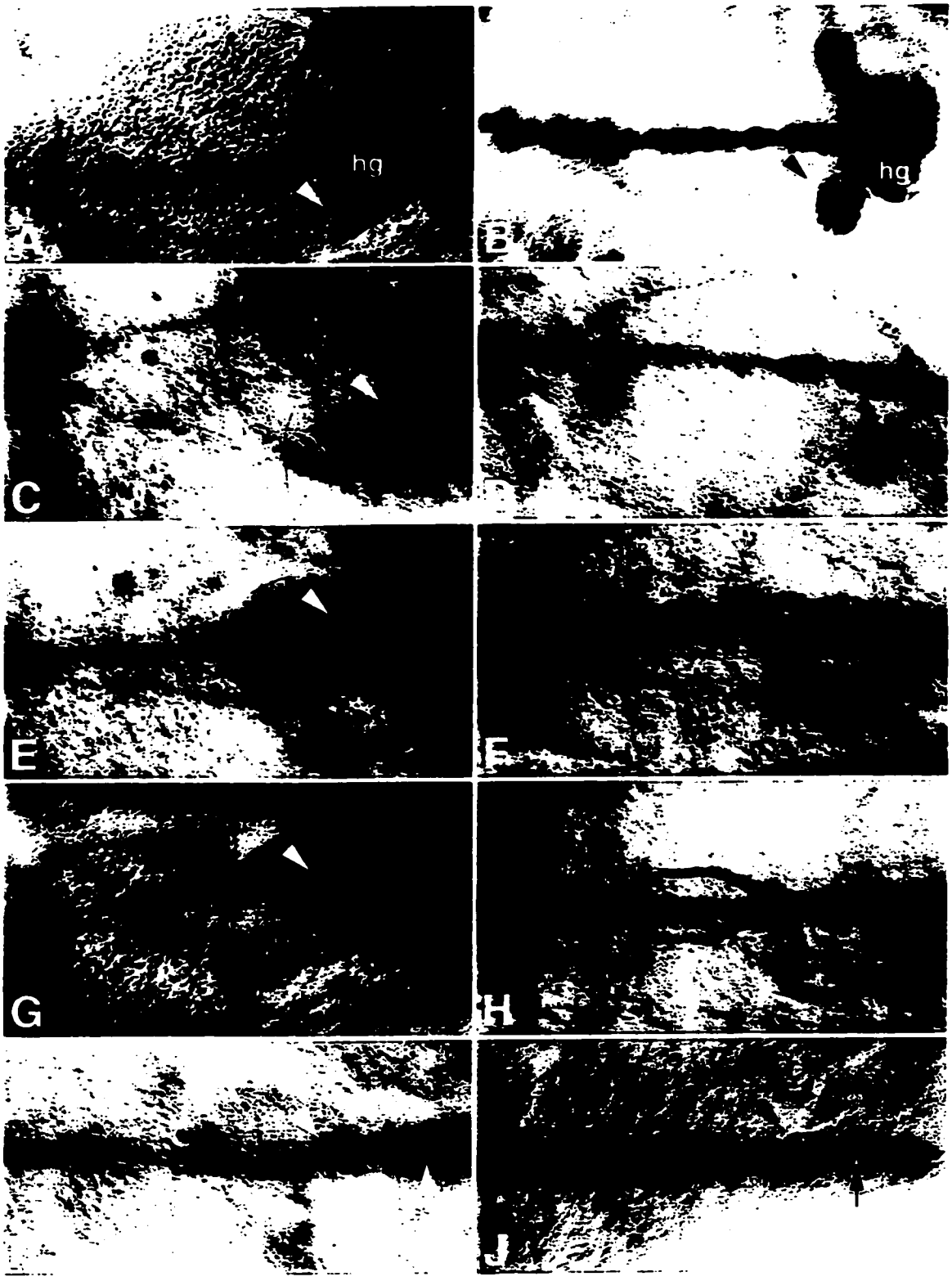
hg
A
hg
B
C
E
F
G
H
J

paired at the dorsal midline (I,J) the concentration of Slit at points of contact between cells appeared to increase (white arrow-protein, black arrow-RNA). A schematic of the time course of Slit expression (Figure 1.7, I), shows the development of Slit expression in relation to embryonic development. Western and *in vivo* analysis of Slit expression, showed that Slit is present during all stages of development. Patterns of Slit expression have also been shown to vary in different tissues dependent on the stage of embryonic development.

***slit* genomic DNA**

slit has been mapped to region 52D of the second chromosome in *Drosophila.* Early analysis of southern blots proposed that *slit* cDNA spans a genomic region of ~20 k.b. and described 8 known intron/exon boundaries (Rothberg *et al*, 1990). With hopes of later sequencing *slit* coding regions in embryos mutant for *slit*, it became necessary to properly define the genomic sequence of *slit* along with precise intron/exon boundary definitions. Based on this analysis we expected to design PCR primers capable of amplifying the entire *slit* coding region from genomic DNA.

Analysis of *Drosophila* genomic cosmids using PCR primers specific to the 5' and 3' termini of *slit* cDNA confirmed 3 cosmids from region 52D of the second chromosome that contained the complete *slit* locus. The genomic sequencing of *slit* using cosmid primers (cos) designed based on *slit* cDNA, revealed a genomic locus covering 17264 bp and defined 19 exons encoding *slit* cDNA (Figure 1.8). The nucleotide sequence was confirmed against P1 sequence from region 52D provided by the Berkeley Genome Sequencing Project (AC005556). Based on the size and grouping of *slit* exons, PCR primers were designed that flanked each *slit* exon and were used to amplify, wild-

Figure 1.8 Schematic representation of *slit* genomic sequences and mutant sequencing primers.

Green bars representing *slit* exons are shown in relation to the entire 17264 bps of genomic sequence incorporating *slit*. Introns (red) define the intron/exon boundaries that are labeled with their respective size and position. PCR primers designed to flank exon boundaries are for sequencing purposes are represented below the genomic map and defined by forward and reverse arrows. The primers used to sequence the genomic cosmids (cosf & cosr) are indicated in relation to the DNA from which they were designed.

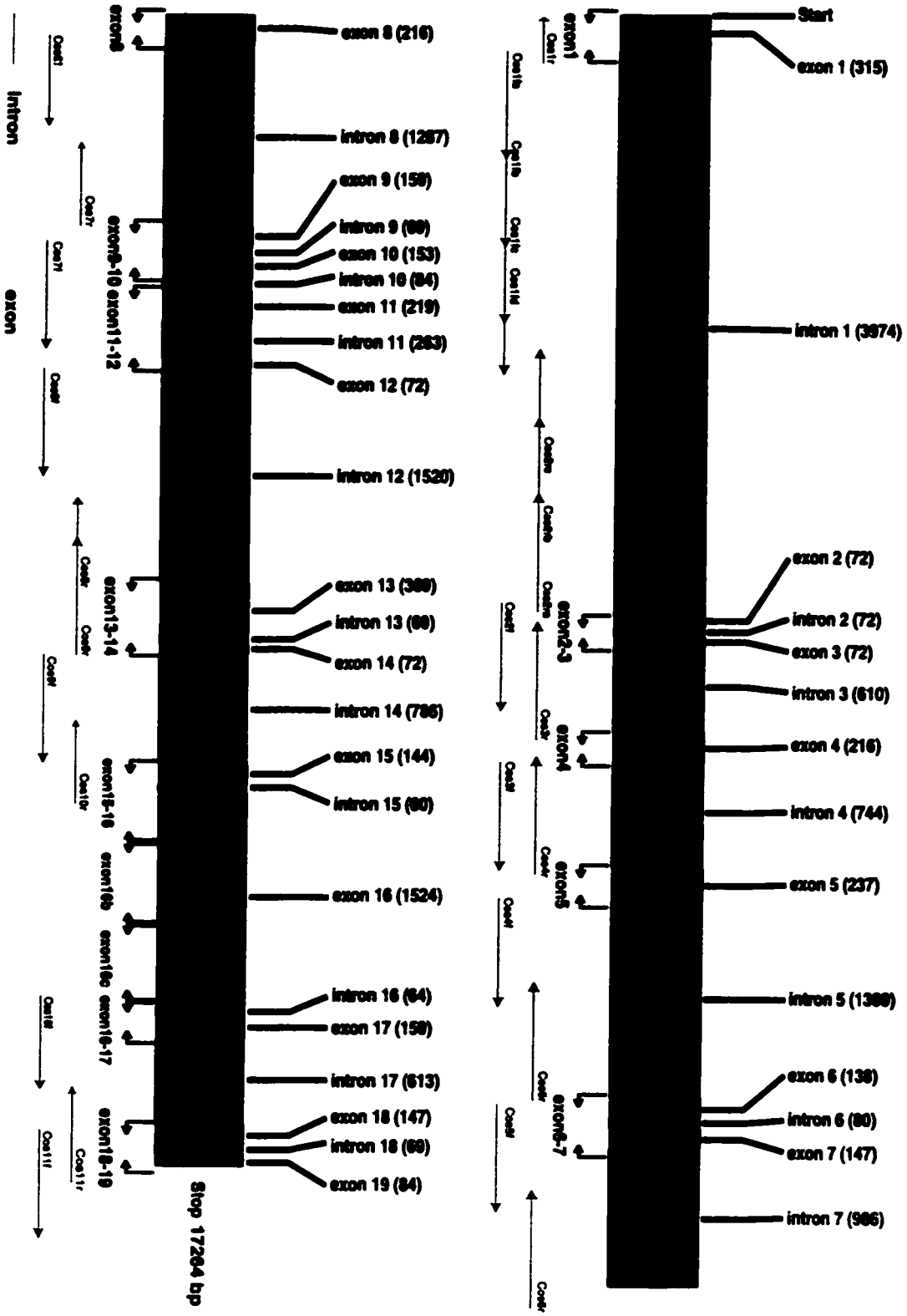
Intron
exon
Start
exon 1 (315)
intron 1 (3974)
exon 2 (72)
intron 2 (72)
exon 3 (72)
intron 3 (610)
exon 4 (216)
intron 4 (744)
exon 5 (237)
intron 5 (1389)
exon 6 (138)
intron 6 (80)
exon 7 (147)
intron 7 (986)
exon 8 (216)
intron 8 (1287)
exon 9 (159)
intron 9 (89)
exon 10 (153)
intron 10 (84)
exon 11 (219)
intron 11 (263)
exon 12 (72)
intron 12 (1520)
exon 13 (369)
intron 13 (89)
exon 14 (72)
intron 14 (786)
exon 15 (144)
intron 15 (80)
exon 16 (1524)
intron 16 (84)
exon 17 (159)
intron 17 (613)
exon 18 (147)
intron 18 (89)
exon 19 (84)
Stop 17264 bp

type *Drosophila* genomic, cosmid genomic, and genomic DNA from flies carrying a deficiency for *slit* (*Df(2R)WMG*). The amplification of exons from wild-type and cosmid DNA confirmed that these primer pairs were adequate to sequence *slit* exons from a genomic source (Figure 1.9 A,B). The *slit* primers did not amplify DNA from a stock deficient for *slit* (*Df(2R)WMG*), suggesting that the primers were specific to *slit* exons. Sequencing of these PCR products confirmed the accuracy of the primers used (data not shown). Small PCR products (Fig. 1.9 C, arrow) could not be sequenced and based on sizes of ~ 72 bp were assumed to be primer concatamers.

Figure 1.9 PCR amplification of genomic DNA

Genomic DNA prepared from cosmids (A), wild-type flies (B), and a stock deficient for *slit* (Df(2R)WMG) (C) was PCR amplified using primers designed to amplify *slit* exons defined in Figure 1.3 and analyzed on a 2.0% agarose gel. All *slit* primers produced PCR products that corresponded in size to each respective exon using cosmid (A) and wild-type genomic DNA (B). Genomic DNA prepared from a stock deficient for *slit* (C) failed to produce a detectable PCR product using any of the *slit* sequencing primers (data not shown). The only distinct PCR bands (indicated with arrows) shown at the leading edge of the control gel (C) are likely primer concatamers and background amplification due to the fact that these products would not sequence.

mutx1
mutx2-3
mutx4
mutx5
mutx6-7
mutx8
mutx9-10
mutx11-12
mutx13-14
mutx15-16
mutx16b
mutx16c
mutx16-17
mutx18-19
506 bp
396 bp
344 bp
298 bp
220 bp
A
mutx1
mutx2-3
mutx4
mutx5
mutx6-7
mutx8
mutx9-10
mutx11-12
mutx13-14
mutx15-16
mutx16b
mutx16c
mutx16-17
mutx18-19
506 bp
396 bp
344 bp
298 bp
220 bp
B
298 bp
220 bp
201 bp
154 bp
75 bp
C

DISCUSSION 1

Molecular characterization of *slit*

Slit protein is synthesized and excreted from the MG cells where it becomes associated with the surfaces of axons that traverse them (Rothberg *et al*, 1990). Slit is also found tightly localized with the sites of muscle attachment and sites of contact between adjacent pairs of cardioblast cells as they meet to form the lumen of the larval heart. Embryos homozygous for chromosomal deletions uncovering the *slit* locus show a medial collapse of the ladder-like arrangement of the midline axon tracts. The expression pattern and published sequence of *slit* is consistent with its proposed role in axonal scaffold development and midline patterning (Rothberg *et al*, 1988;Rothberg *et al*, 1990). In order to further examine this role we needed to engineer a complete *slit* cDNA for sequencing and protein analysis, generate an antibody to Slit, and establish the intron/exon boundaries of the genomic sequence to facilitate sequencing of nine *slit* mutant alleles.

slit was cloned during an attempt to isolate Notch EGF-like proteins in *Drosophila* using probes based on the Notch EGF-like repeats. As a result, a number of clones were isolated that represented polytene chromosome region 52D, labeled *slit* during the Nüsslein-Volhard mutant screen in 1984 (Nusslein-Volhard, 1984;Rothberg *et al*, 1988). Later analysis and compilation of these clones revealed four distinct protein motifs containing: four LRR, 7 EGF-like repeats separated between the sixth and seventh repeat by the ALPS (Agrin, Laminin, Perlecan, Slit) motif that we will refer to as the G-Domain, and a cysteine rich region at the carboxy terminus(Rothberg & Artavanis-Tsakonas, 1992). The *slit* cDNA sequence extrapolated from these clones came into

question when attempts to PCR amplify genomic DNA revealed uncharacterized coding sequences that were not included in the published sequence. These anomalies were confirmed upon communication with the Hartley and Goodman Labs who were also pursuing investigations into Slit function.

Genomic sequencing undertaken by our lab and later confirmed by completion of the *Drosophila* genome project has now finalized the complete *slit* cDNA and genomic sequence. *slit* cDNA is represented by 4515 b.p.'s. that codes for a 1504 a.a. protein originating from a genomic locus of 17264 b.p. in region 52D of the 2nd chromosome (Battye *et al*, 1999). The overall structure of the predicted protein did not change with the exception of an additional LRR in the first Leucine array, the elimination of the proposed alternate splice variant, and a series of redundant b.p. changes throughout the cDNA. The revised sequence and protein structure is encapsulated in Figures 1.1 and 1.2. Slit contains a unique combination of extracellular matrix (ECM) and protein-protein interaction motifs that have independently been associated with cell growth, signaling, and guidance properties (Zallen *et al*, 1998). Represented in combination as a large secreted glycoprotein, the individual functional nature of the Slit motifs suggest that *slit* has a multifunctional role in CNS development.

The pattern of Slit expression, previously characterized using an antibody specific to the 6th EGF repeat and an small portion of the G-Domain has been described in the literature a number of times(Rothberg *et al*, 1988;Rothberg *et al*, 1990;Rothberg & Artavanis-Tsakonas, 1992). Attempts to create new polyclonal and monoclonal antibodies to different regions within Slit or with the original EcoRI construct have met with repeated failures in our Lab and others. The original Slit polyclonal antibody was

raised against a 550 bp EcoRI fragment that was homologous to the probe that isolated the *slit* cDNA and was subsequently used to generate a series of monoclonal cell lines. The necessity for a working Slit antibody required us to regenerate and characterize a number of old monoclonal cell lines created during the original investigation of *slit* (Rothberg *et al*, 1990). This afforded us the opportunity to carefully analyze the time course and pattern of Slit expression and protein distribution.

Cell lines that were found to yield high titers of antibody proved to emulate the pattern of Slit expression reported by Rothberg in 1988 (Rothberg *et al*, 1988). Protein labeling in the MG, cardioblast cells, and at the points of muscle insertion were readily detectable; however deposition of Slit on CNS axon tracts was not apparent in most preparations. We suspect that long term storage, and media changes involved with restoring the original cell lines has decreased the sensitivity of the Rothberg antibody. It is clear from both light level and transmission electron microscopy (Fleming & Kwak, 1986) that one form of Slit is present on and transported by the CNS axons that traverse the midline. It will be necessary to generate a new antibody to different regions of Slit in order to determine in what form Slit becomes localized to these axon tracts. New cell media such as Invitrogens DES (*Drosophila* Expression System, Q500-01) developed to yield natively processed insect proteins may hold the answer for generating correctly processed Slit products that will elicit an antigenic response.

***slit* protein distribution**

Midline

The MG derive from the MEC that invaginate during gastrulation at 3 hours of development (stage 7) and pair to define what will eventually become the ventral midline

boundary. Slit expression is first observed in the MEC at approximately 3.5 hours of development (stage 8) as the MEC meet to form a bilaterally symmetric column of cells along the A/P axis shortly following the expression of *sim* (*single minded*) (Crews *et al*, 1988) and the *achaete-scute complex* (AS-C) (Nambu *et al*, 1993). Slit expression, both RNA and protein becomes localized to a specific subset of midline glia, the posterior (MGP), middle (MGM), and anterior (MGA), as the embryo develops. By 20 + hours of development (stage 17) three MG remain localized to the anterior half of each hemisegment that continue to express Slit. The specific localization of Slit to the MG that remain closely associated with the formation of both anterior and posterior commissures (Jacobs & Goodman, 1989a;Jacobs & Goodman, 1989b), exposes Slit expression to all axons that may potentially cross the midline. Consistent with our proposition that Slit functions as an extracellular signaling molecule in the midline, the temporal and spatial distribution of Slit describes the ideal candidate molecule to regulate midline boundary signals.

Cardioblasts

During development and in particular the organization of the dorsal vessel, the cardioblasts move along the surface of the epidermis until their leading edges meet at the dorsal midline. These cells are present in segments *t1* to *a7* and become organized into pairs with their counterparts from the adjacent side as dorsal closure completes. Once contact occurs, interdigitations appear on their ventral surface in order to increase the area of contact between cardioblasts (Campos-Ortega & Hartenstein, 1997). Slit expression can be detected early in the precursors of cardioblast cells before they separate from the mesoderm. Slit expression continues as the cardioblasts migrate dorsally and

upon closure of the dorsal vessel strong Slit labeling is observed in the areas of contact between adjacent cardioblasts. Protein expression in the cardioblast cells corresponds directly with observed RNA expression, suggesting that *slit* expression is native to these cells. Formation of the dorsal vessel and cardioblast morphology has not been previously investigated in a *slit* background and therefore it is difficult to attribute a function to Slit in these cells. Whereas Slit appears to have a vital role in maintaining the axon scaffold in the CNS, a parallel function in the cardioblasts is not obvious.

Muscles

Slit protein observed at the muscle apodemes becomes apparent as muscle fibers attach to the epidermis beginning at stage 15. Localized RNA expression was not readily detectable here suggesting that Slit is being transported to the sites of muscle insertion by diffusion or exported along the ECM. The progenitors of the somatic musculature exist superficially in the mesoderm where they segregate to become the muscle founder cells. The founder cells fuse into muscle precursors in a pattern similar to the mature muscle fibers where they attach themselves to the epidermis(Campos-Ortega & Hartenstein, 1997). The role Slit may play in this muscle patterning has not previously been addressed; however, as with neurons, muscle cells produce growth cones that explore their environment looking for cues or instructions that determine their fate (Chiba *et al*, 1993;Keshishian *et al*, 1996). Similar to the role Slit plays in the development of the midline CNS axon scaffold, muscle growth cones may require a Slit signal to establish appropriate patterning.

Western

The sensitivity of the antibody observed *in vivo* did not limit our ability to detect Slit expression in protein extracts from all stages of development. Western analysis of whole tissue lysates show that Slit can be identified in a >200 kDa complex consistently beginning from 4 hours of development. Additionally, a ~50 kDa species in adult tissues and a smaller ~13 kDa species found in extracts from 0-4 hour embryos were found to label with the Slit mAb. Interestingly, the smaller protein complex was found to correspond with antibody labeling in embryos fixed in the same time range, an observation that has not been previously reported. The punctate pattern of expression appears localized to the nuclei prior to cellularization of the syncytial blastoderm and is not detectable shortly thereafter. Prior to isolation and analysis of this apparently autonomous species, we have not been able to identify a relationship if any that this pattern of protein expression has with Slit. It is very likely that the EGF-like nature of the antigen used here is able to detect growth factors with homologous domains that are present during early development.

The larger 50 kDa species was detected in addition to the >200 kDa complex in adult tissues. Recent identification and analysis of *slit* homologs in humans (Takke & Campos-Ortega, 1999;Campos-Ortega, 1997;Chien, 1998), rats (Li *et al*, 1999;Marlin *et al*, 1991), mouse (Takke *et al*, 1999;Kunisch *et al*, 1994), and *Xenopus* (Roth *et al*, 1989;Wu *et al*, 1999) have revealed a number of insights into the nature of Slit processing *in vitro*. Perhaps most significant here is the proteolytic cleavage of human Slit2 from COS cells into ~190 kDa and ~55-60 kDa bands that can be detected by both myc-tagged hSlit2 antibody and the *Drosophila* Slit mAb. Additionally, purification and

micro sequencing of cleaved recombinant hSlit2-C (Nambu *et al*, 1990) has identified a highly conserved cleavage site (**TSPCDNFD**) at the beginning of the 6th EGF-like repeat that is present in most *slit* homologues in a similar location. The 55-60 kDa band reported by Brose, *et al.* (1999) closely corresponds to the 50 kDa species that we have isolated in our adult tissue extracts. Cleavage of Slit, separating the G-Domain and cysteine rich region from the LRR and disrupting the EGF repeated motif, could essentially define three functional forms of Slit or the modification of one Slit with two different roles.

Slit domains

LRR

The nature of the LRR as found in Slit includes *slit* in a large and growing family of LRR proteins which include Trk (Windisch *et al*, 1995), Decorin, Biblycan, Keratocan, Fibromodulin, Lumican, and Chondroadherin that share one unifying function which is the mediation of protein-protein interactions such as receptor and ligand binding (Hocking *et al*, 1998;Krishnan *et al*, 1999). Similarly, the G-Domain which is found in α-Laminin chains, Perlecan, and Agrin (DGC) (Noonan *et al*, 1988;Noonan *et al*, 1991;Gesemann *et al*, 1995;Gesemann *et al*, 1996;Gesemann *et al*, 1998) where it confers binding to heparins (Andac *et al*, 1999), Integrins (Sasaki *et al*, 1998), and the α-Dystrophin-glycoprotein complex (Sasaki *et al*, 1988) mediates other protein-protein interactions in the ECM. Here the Laminin G-domain, in particular the site containing CSRARKQAAS**IKVAV**SADR that shares a >30% similarity with *Drosophila slit* has been attributed with functions involving cell adhesion (Sasaki *et al*, 1988;Brown *et al*, 1997), spreading, migration (Sasaki *et al*, 1998), and neurite outgrowth (Sephel *et al*, 1989). The EGF-like repeats that separate the LRR and G-domains are often associated

with very large glycoproteins such as complete *slit* (>1000 amino acid residues), and this size is believed to be a physical consequence for carrying out their biological function (Nakayama *et al*, 1998).

EGF & G-domains

EGF-like domains play a critical role in extracellular events some of which include cell adhesion and receptor ligand interactions (Campbell & Bork, 1993). The role of EGF in Slit likely involves localizing the secreted signaling domains of LRR and the G-domain to the extracellular matrix within the CNS where Slit may interact with pioneering growth cones that approach the midline. The detection of Slit at points of muscle insertion where no *Slit* expression is observed, suggest that some form of Slit is being transported or is diffusing to where it may interact with the ECM at the muscle apodemes. Consequently, it is important to note that the Integrin rich environment at the muscle apodemes (Bunch *et al*, 1998) could be an ideal substrate for the Laminin-like G-domain in Slit (Gotwals *et al*, 1994) and that this portion of Slit retains epitopes to the functional antibody.

The cleavage of Slit into a LRR protein retaining 5 EGF-like repeats at the carboxy terminus (Brose *et al*, 1999) and an independent G-domain product that is flanked by two EGF-like repeats similar to the Agrins and Perlecans (Gesemann *et al*, 1995;Gesemann *et al*, 1996) suggests that this proteolytic processing could reveal two separate independently functional proteins. One of these proteins would maintain LRR signaling by remaining bound to the extracellular matrix via its EGF tail, and the second would become a diffusible signal that could interact with Integrin at the muscle apodemes. Purification of Slit from tissue lysates under denaturing conditions results in a

single immunodetectable species from 4 hours of development onwards suggesting that Slit *in vivo* remains associated with a larger protein complex. Until specific antibodies to these cleaved Slit products can be generated and investigated *in vivo* it will be difficult to separate the function and pattern of activity associated with truncated and complete forms of Slit.

Two additional methods for establishing the function of Slit and its domains *in vivo* that can proceed without the generation of domain specific antibodies include the analysis of point mutations in different Slit coding domains and the use of transgenic Slit constructs to examine both native and ectopic *slit* function. Using the complete *slit* cDNA that has been characterized above to generate a series of complete and truncated Slit transgenic proteins we will be able to study the role of various *slit* transgenes using transgenic flies and various tissue specific GAL-4 drivers. Additionally, the generation of 9 specific point mutations in the *slit* locus during the Seeger (1993) mutagenesis, provides us with a possible range of mutations in Slit that may uncover domain specific phenotypes. In order to characterize these mutations it will be necessary to catalogue the mutant phenotypes within each tissue in which Slit expression has been detected and then correlate these phenotypes with identified mutations in each allele of *slit*.

As we have observed the *slit* locus includes 17264 b.p. within region 52D of the second chromosome in *Drosophila*. This represents an enormous task in the identification of 9 individual point mutations within alleles of *slit*. To facilitate sequencing of these alleles it was necessary to identify and precisely define the boundaries of the 19 exons that compose the *slit* coding region and design PCR primers that flank each of these exons. Amplification of the exons from genomic DNA prepared

from single larval samples produced clearly defined products that when sequenced precisely annotated the entire *slit* coding region. By using this method of sequencing mutant cDNA it should be possible to identify mutations resulting in each *slit* allele.

By establishing the pattern of Slit expression, cDNA clones, genomic sequence, and a method for sequencing *slit* mutant alleles we have managed to reassemble the tools necessary to continue our investigation of *slit* function.

Axon guidance in the midline of the *Drosophila* CNS requires *slit* function

CHAPTER 2

Chapter two will describe the characterization of different mutant alleles of *slit*. Morphology of the CNS, cardioblasts, muscles and MG will be compared along with the viability of each mutant allele in order to classify a range of *slit* mutant phenotypes. We will assess the penetrance of the *slit* phenotypes and then attempt to determine the molecular sequence changes associated with each allele in order to develop an understanding of *slit* function.

MATERIAL AND METHODS 2

Fly Maintenance

Refer to Methods Section 1

Genetic stocks

Most *slit* alleles were isolated on a background deficient for Fasciclin III and Fasciclin I as reported in Seeger (Seeger *et al.*, 1993). $slit^{JG107}$ was isolated by Nüsslein-Volhard (Nüsslein-Volhard, 1984), $slit^{E158}$ by Bellen *et al.* (1989), $slit^{F81}$, and $slit^{F119}$ by Bier *et al.* (1989). The B2-3-20 and AA142 enhancer lines were provided by Bodmer and Klambt respectively. All alleles and fly stocks were restored to a wild-type background prior to study and analyzed based on a *CyO-P{eng-lacZ}* marked balancer. Alleles used for viability testing and mutant sequencing were transferred to a *CyO-P{y⁺)* balancer and all *slit* stocks were backcrossed to a stock deficient for *slit* (*Df(2R)WMG*) in order to verify the lack of complementation.

Tissue *in situ* hybridization

Refer to Methods Section 1.

Immunocytochemistry

Drosophila embryos were collected on apple juice agar plates and aged from 16-30 hours at 22°C. Fixation and immunocytochemistry was adapted from Patel (1994). BP102 (1:2), mAb 1D4 (1:4), mAb slit (1:200), mAb C1.427 (1:4), α-sim (1:4), α-wrapper (1:4), α-Tiggrin, and α β-gal (Cappel, 55976) (N. Patel, C. Goodman, G. Tear, R. White, S. Crews, J. Noordermeer, & Martin-Bermundo respectively) were diluted as indicated and processed as per method section 1.

Fluorescence microscopy

Manually devitellinised embryos were dissected on glass in PBS and fixed for 10 min in 4% paraformaldehyde. The dissections were washed in buffer and incubated for 30 minutes in Rhodamine-labeled Phalloidin (Verheyen & Cooley, 1994) (Molecular Probes R415) and mounted in glycerol with p-phenylene d-amine (Sigma P-6001) as an anti-bleaching agent. Projections made from confocal images were collected with a Zeiss 310.

Electron microscopy

Dechorionated embryos were fixed in heptane equilibrated with 25% glutaraldehyde (Fluka) in 0.1 M sodium cacodylate (pH 7.2). Embryos were manually devitellinised in 4% paraformaldehyde and 2.5% glutaraldehyde in cacodylate buffer, post-fixed in 1% osmium tetroxide and stained before embedding in uranyl acetate (Jacobs and Goodman, 1989). Lead stained 0.1 μm sections were examined on a JEOL 1200EXII microscope.

Genomic clones and cDNA

Refer to Methods Section1.

Genomic Sequence Analysis

Refer to Methods Section 1.

Mutant viability

Viability of each *slit* mutant was assessed using the *CyO{y+}* balanced stocks as a late embryonic and larval marker, as each of the mutant lines was previously determined as adult lethal ((Rothberg *et al*, 1988)& (Seeger *et al*, 1993)). Embryo viability was calculated by arranging 10 lines of 100 embryos on plates of apple juice agar that were incubated at 22°C and observed at 6 hour intervals. Following 48 hours of incubation

unhatched embryos were dissected and counts were taken from infertile, balanced, and mutant embryos lacking the *CyO{y⁺}*. Embryo viability was calculated as the percent of fertile embryos that hatched without a *{y⁺}* marker. Larva were collected from the same embryo collections of mutant lines above and based on absence of the *CyO{y⁺}* balancer. Larva were aged at 22°C and observed until pupation or death. A record denoting the furthest stage of development was collected from a qualitative sample of larva collected under these conditions.

Heteroallelic combinations of each mutant were screened for adult viability and the percent of unbalanced progeny was calculated based on five F1 generations. In addition, heteroallelic combinations of the Slit receptor *robo* (Kidd *et al*, 1999)with each mutant allele were tested for viability. These were assessed as a percentage of unbalanced *CyO{y⁺}* adult flies from three F1 generations.

Midline axon tract structure

Analysis of the *slit* mutant CNS was based on the staining pattern of mAb 1D4 (α FasII) and BP102. mAb 1D4 was used to determine the effect of each *slit* mutant on the formation of the three FasII labeled longitudinal axon fascicles which extend along each side of the nerve cord at the later stages of development and the route of the early anterior projections of the posterior corner cells (pCC). BP102 was used to assess the formation of the commissural axons and the separation of the two longitudinal tracts, and also used to assess the length of the stage 16 nerve cord in each *slit* allele.

Nerve cord length

Embryos of each *slit* stock were collected, aged to optimize for stage17, and fixed for staining with BP102. Homozygous *slit* mutants were collected based on lac-Z

balancer staining and mounted for measurement under camera Lucida at 250X projection. Embryo length and nerve cord length were marked on data sheets and the respective differences between marks were recorded in millimeters. The proportion of nerve cord length to whole embryo length was determined for a sample of each mutation and the means with standard deviations were compared to wild type and heterozygous mutant alleles.

Mesectodermal cell position

The position and number of *slit* expressing and associated cells were determined using the enhancer AA142 pattern, α-Sim, and α-Wrapper patterning, along with the native Slit expression pattern. Both early stage 12 and late stage 16 embryos were immunolabelled and analyzed for MG placement, number, and their ability to ensheath (α Wrapper) local axons in both wild-type and *slit* mutant embryos.

Heart morphology

The enhancer trap B2-3-20 was used to follow the development of the cardioblast cells in which the mAb Slit has previously been shown to express.

Muscle morphology

The pattern of muscle insertions in wild-type and *slit* mutant embryos was followed using an antibody for Tiggrin a novel extracellular matrix ligand for the *Drosophila* PS2 Integrins (Bunch *et al*, 1998), Rhodamine-labeled Phalloidin and mAb slit 6D.

Single Fly PCR

Control DNA collected from single samples was prepared and PCR amplified using the genomic exon primers in order to test the reliability and accuracy of the

sequencing strategy. Single flies from each of the mutant *slit* stocks were immobilized with CO_2 and placed in a 0.5 ml tube containing 50 µl of homogenization buffer (10 mM Tris-HCl [pH8.2], 1 mM EDTA, 25 mM NaCl, and 200 µg/ml Proteinase K, fresh), carefully crushed for 5-10 seconds with a pipette tip and then incubated at 37°C for 30 minutes. The digested extract was inactivated by heating to 95°C for 1-2 minutes and then 1µl was removed for PCR amplification as described above.

Mutant sequence analysis

Mutant genomic DNA was obtained from single homozygous embryos or larva not carrying a *CyO[y⁺]* balancer in a *yw⁻* genetic background. Samples were collected from balanced populations housed on apple juice agar plates that were aged for 48 hours and then screened for mutant embryos or larva. Individual mutant samples were washed in sddH_2O (sterile deionized and distilled water) and transferred to a 0.2 ml thin walled PCR tube containing 83 µl of PCR buffered sddH_2O where they were crushed and then the remaining PCR reagents were added. PCR was conducted as described above; however, the prehybridization phase was extended to 10 minutes. One tenth of each PCR product was analyzed on a 2% agarose gel with Ethidium Bromide in order to verify presence and purity of the product. Pure single banded products were isolated with the Qiagen PCR purification kit (28104) for each sample and sequenced with both relevant forward and reverse primers. At least three independently sequenced products were generated for each primer pair and genetically mutant allele. A database of wild type and mutant sequences were compiled and analyzed using DNASTAR's EditSeq and MegAlign software package. Aligned sequences were manually screened and sequence discrepancies were verified against sequencing traces generated during sequencing at the

MOBIX Facility. Consistent discrepancies were investigated, and results were recorded relative to the position and allele in which the error was detected (Fig. 1.1).

Data presentation

Refer to Methods Section 1.

RESULTS 2

During screens for mutations that affect CNS axon tract development, a number of mutant alleles have been isolated that map to the *slit* locus in region 52D (Seeger *et al*, 1993). After selecting alleles that failed to complement a stock deficient for *slit* (*Df(2R)WMG*) we identified and characterized the mutant phenotypes associated with each allele. Tissues in which wild-type Slit protein expression had been localized were analyzed for each allele and a gradient of phenotypes was established. Sequence changes for each allele were determined and mapped to the affected structural domain and then correlated to the respective mutant phenotype in an attempt to link structure with function.

slit alleles

Alleles of *slit* were obtained from the Nüsslein-Volhard (1984) and Seeger mutagenesis ((Seeger *et al*, 1993)). Each *slit* allele was tested against *Drosophila* deficient for *slit* (*Df(2R)WMG*) and transheterozygous embryos (*slit/Df(2R)WMG*) were labeled with BP102 and compared to the midline phenotype of embryos homozygous for the *slit* deficiency (Fig 2.1 B). Alleles were grouped by the degree of midline fusion (arrowhead) and the loss of intersegmental longitudinal axons (Fig. 2.1 A, arrow). Midline axon fusion observed in *slit /Df(2R)WMG* embryos ranged from total fusion within each neuromere (C-J) to partial separation of longitudinal axon tracts revealing both anterior and posterior commissures (K-O). More intersegmental longitudinal axons remain in embryos that exhibit some degree of midline separation (K-O), but all the *slit* alleles appear to have more intersegmental axons than the embryos deficient for *slit* (Appendix B, shows FasII labeling in deficiencies).

Figure 2.1 BP102 phenotype of *slit* hypomorphs and deficiencies.

The wild type BP102 labeling in *Drosophila* embryos (A) shows the axon scaffold of the ventral nerve cord defined by commissural axons (arrowhead) and the longitudinal axons (arrow). Homozygous embryos that are deficient for *slit* (Df(2R)WMG) have fused commissures and the intersegmental longitudinal fascicles cannot be detected (B). Embryos transheterozygous for *slit* and a Deficiency uncovering *slit*, (C, $slit^{JG107}$/+) produce a wild type midline architecture. Embryo heterozygous for $slit^{JG107}$/(*Df(2R)WMG*) (D), $slit^{GA20}$/(*Df(2R)WMG*) (E), $slit^{GA178}$/(*Df(2R)WMG*) (F), $slit^{GA945}$/(*Df(2R)WMG*) (G), $slit^{3149}$/(*Df(2R)WMG*) (H), $slit^{1912}$/(*Df(2R)WMG*) (I), and $slit^{550}$/(*Df(2R)WMG*) (J) have fused midline axons that do not produce any intersegmental axons. Evidence of separation of the longitudinal fascicles and the development of intersegmental projections was observed in embryos heterozygous for $slit^{532}$/(*Df(2R)WMG*) (K), $slit^{2990}$/(*Df(2R)WMG*) (L), $slit^{F81}$/(*Df(2R)WMG*) (M), $slit^{F119}$/(*Df(2R)WMG*) (N), and $slit^{E158}$/(*Df(2R)WMG*) (O).

F
J
C
B
G
K
A
E
I
D
H
L

The degree of midline fusion observed in embryos mutant for severe alleles of *slit* (Fig. 2.1, D-J) makes it difficult to determine whether the longitudinal and commissural axon projections are developing using standard immunohistochemistry. By studying the ultra structure of one neuromere using an EM micrograph of a cross section through a wild type neuromere (Fig. 2.2 A) the longitudinal axon tracts could clearly be distinguished and commissural axons were also observed projecting across the midline glia (MG). In embryos that are mutant for a severe *slit* allele ($slit^{IG107}$, B), the number of longitudinal axons were reduced and the remaining axons were fused at the midline. Commissural projections across the midline were prominent and the MG remained associated with commissure formation at the midline. The presence of commissural axons observed in milder *slit* phenotypes (Fig. 2.1, K-O) indicated that the axon commissures formed appropriately in *slit* mutants and that the severity of each *slit* hypomorph was relative to the degree of fusion of longitudinal fascicles at the midline.

Development of Longitudinal axon fascicles varies in Slit hypomorphs

The midline of the *Drosophila* nervous system is composed of three regions, the left and right neurogenic regions that generate a majority of the neurons and a midline region that separates the two neurogenic regions. The midline region is derived from MEC cells that generate a small number of neurons and the glial cells in which Slit is expressed. These cells demark the midline boundary of each neuromere and define the bilateral symmetry present in each hemisegment. As embryonic axons develop from the neurogenic regions they enroll in specific functions that include peripheral muscle innervation, intercommunication between other CNS neurons, and some neurosecretory functions (Goodman & Doe, 1984). Of these neurons, most are capable of making

Figure 2.2 Midline fusion of commissural and longitudinal axons in embryos mutant for *slit*.

A cross section of a wild-type nerve cord at the posterior limit of the anterior commissure of an abdominal segment at stage16 (A) outlines the normal architecture of the commissural axons (comm) that traverse the midline, here in association with the midline glia (MG). Longitudinal tract axons (long) dominate the dorsal aspect of the lateral neuropil. A cross-section at an equivalent location of a homozygous *slit2* mutant nerve cord (B) demonstrates the dorsal midline fusion of the longitudinal tract, overlying a bundle of medially compacted commissurally projecting axons. Scale bar, 5μm. (electron micrographs produced by J.R. Jacobs)

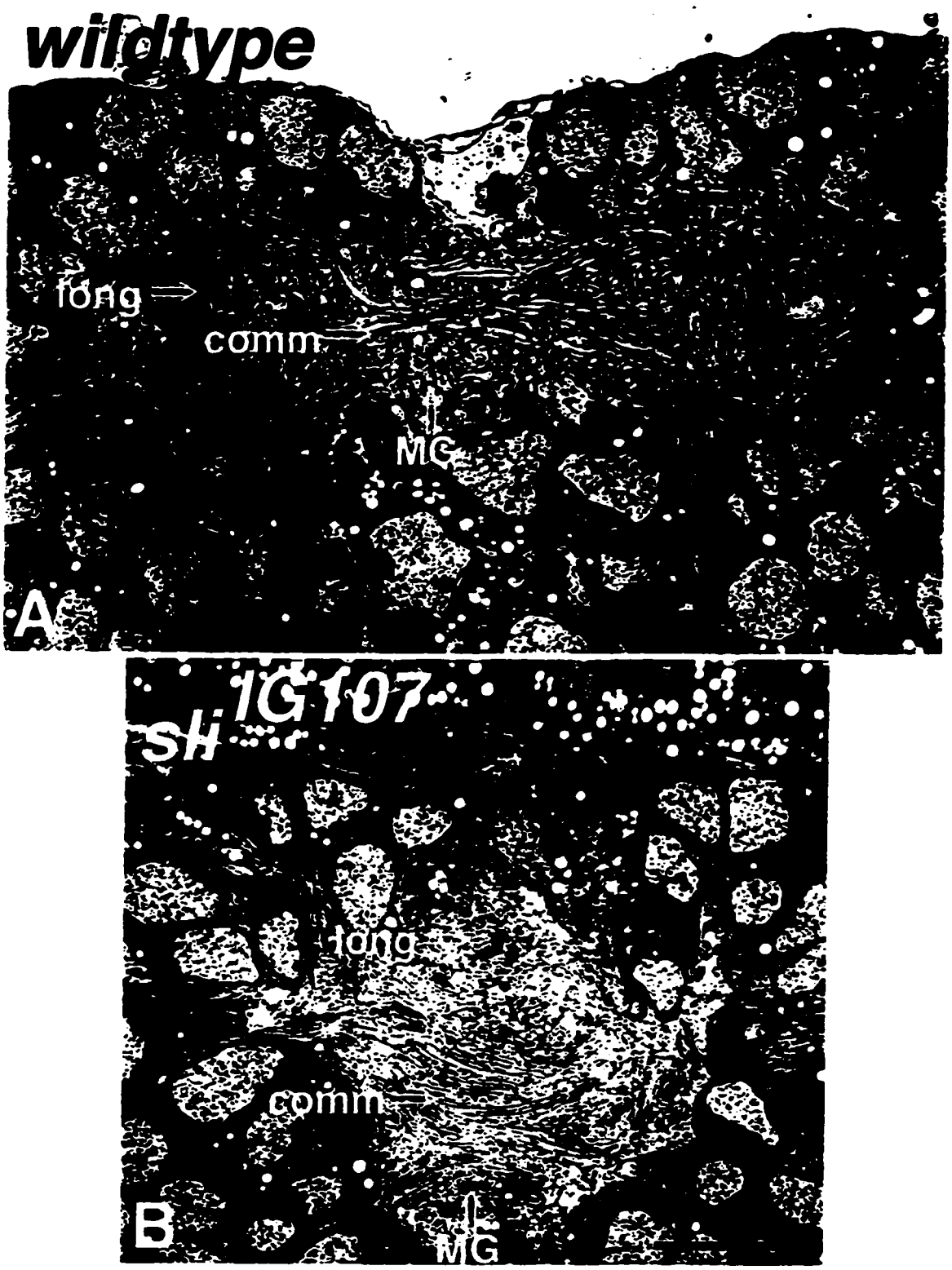
wildtype
long
comm
MC
A
SH
1G107
long
comm
B
MG

contralateral projections across the midline and once they have crossed, they change or are altered such that they may never cross again. Other CNS axons that develop in the neurogenic regions maintain an established distance from the midline and form the longitudinal axons tracts that run on each side of the midline. When mesectodermal derived cells are removed early in development by mutations in the *single-minded* gene, all axons collapse into the midline region (Nambu *et al*, 1993). Similarly, when MEC are removed early in development by expressing toxic transgenes in specific midline cells, a collapse of embryonic neurons in that region is observed (Jacobs, 2000). One plausible explanation for the observed collapse of CNS neurons upon the removal of midline cells is the disruption of a signaling mechanism necessary for maintaining a gradient of repulsive signaling from the midline region. When *slit* function is absent in embryos deficient for *slit* (*Df(2R)*WMG) a similar mutant CNS phenotype to that of *single minded* mutants is observed. We hypothesized that *slit* is required for maintaining the repulsion of longitudinal neurons from the midline. Here we have characterized a range of *slit* mutants to determine whether their phenotypes reflected *slits* function as a midline repellent signal.

Using the mAb BP102 that labels commissural axons and a subset of longitudinal axons together with an antibody to Fasciclin II that labels a subset of the longitudinal axon fascicles, we examined the affect of different *slit* mutations on CNS development in embryos and larva. Slit is expressed in the MG that are positioned where commissural axons make contralateral projections across the midline (Figure 2.3 A, arrowhead). A range of CNS phenotypes was observed in embryos mutant for different *slit* alleles (Fig. 2.3, D-O). This range was defined by the magnitude of longitudinal axon fusion

Figure 2.3 Axon commissures collapse and longitudinal fascicle are thinner in embryos homozygous for hypomorphic alleles of *slit*.

Wild type embryos showing the localization of Slit expression (A, black) and embryos heterozygous for $slit^{JG107}$ (B) and $slit^{2990}$ that are labeled with BP102 (B, C) show a normal ladder-like axon scaffold. Arrows indicate the placement of longitudinal axon fascicles between segments and arrowheads identify where anterior and posterior commissures separate. Embryos that are homozygous for a range of *slit* hypomorphic alleles show a general thinning of longitudinal axons (D-O), but varying degrees of midline collapse. Axon commissures cannot be identified in embryos where the longitudinal axons appear fused at the midline (D, $slit^{JG107}$; E, $slit^{GA20}$; F, $slit^{GA178}$; G, $slit^{GA945}$; H, $slit^{3149}$). In other nerve cords where BP102 labeling indicates a partial separation of longitudinal axon fascicles, the anterior and posterior commissures can be identified (I, $slit^{1912}$; J, $slit^{550}$; K, $slit^{532}$) suggesting a moderate *slit* CNS phenotype. In *slit* hypomorphs that show very mild CNS phenotypes (L, $slit^{2990}$; M, $slit^{F81}$; N, $slit^{F119}$; O, $slit^{E158}$) the axon commissures are clearly defined and the ventral nerve cord has a narrowed appearance with weak labeling of the longitudinal fascicles between segments.

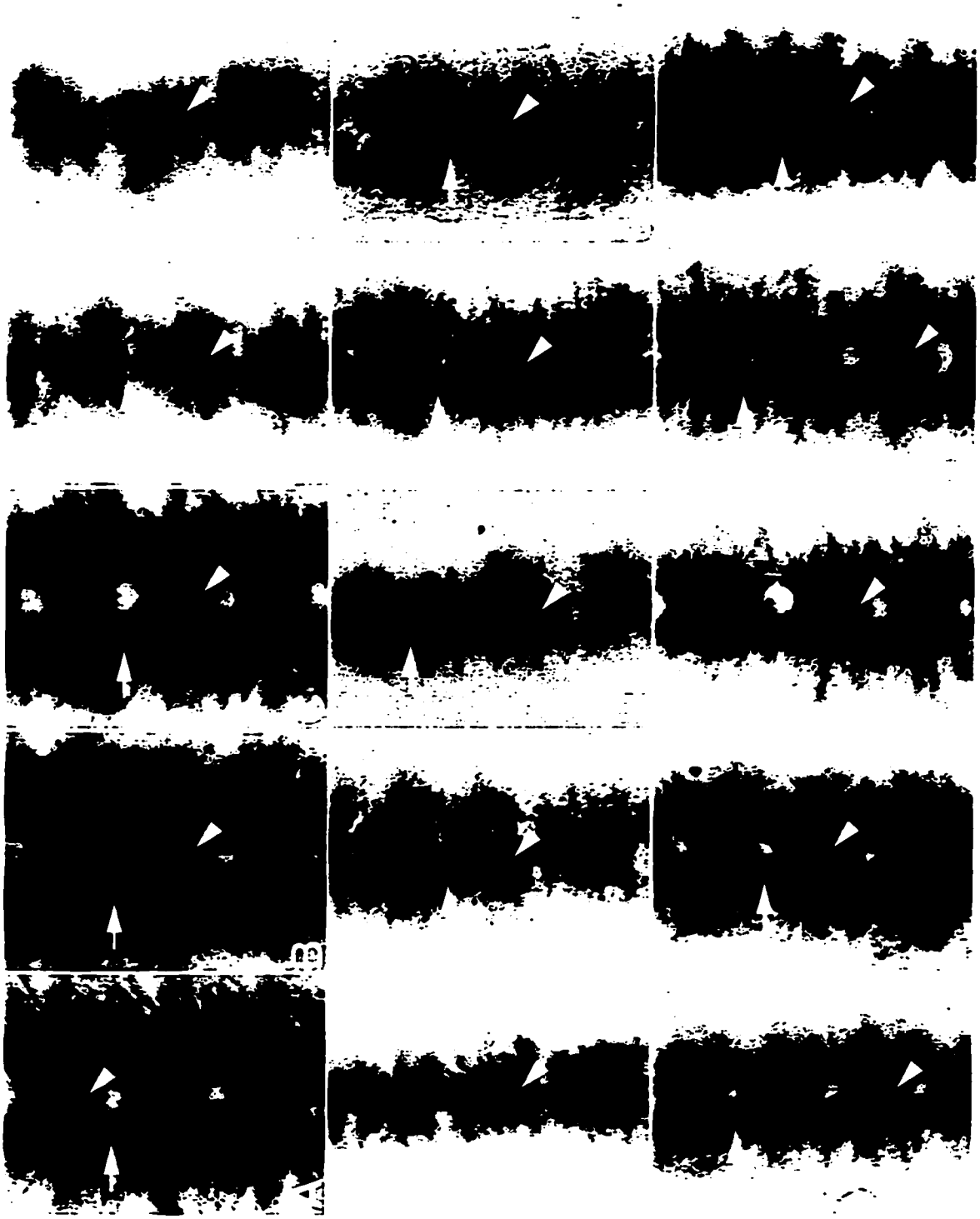

observed at the midline. Severe *slit* phenotypes were those that resulted in a complete fusion of the midline axons, where breaks were observed in the intersegmental longitudinal axons and no commissures were detected (D, $slit^{JG107}$; E, $slit^{GA20}$; F, $slit^{GA178}$; G, $slit^{GA945}$; H, $slit^{3149}$). The CNS phenotype was considered moderate when axon commissures were detectable as a result of partial separation of the longitudinal axons from the midline. However, in most examples the intersegmental longitudinal axons (arrows) were absent or thin (I, $slit^{1912}$; J, $slit^{550}$; K, $slit^{532}$). Mild *slit* phenotypes described embryos that exhibited a substantial separation of the longitudinal axon tracts, sufficient to distinguish both the anterior and posterior commissures (L, $slit^{2990}$; M, $slit^{F81}$; N, $slit^{F119}$; O, $slit^{E158}$). These embryos typically developed more intersegmental longitudinal axons and wider midlines, but still notably different from wild type.

Where BP102 labeling defined a subset of the longitudinal axons including those that made contralateral projections across the midline, FasII labeling identified a subset of the longitudinal axons, none of which made projections across the midline. Fasciclin II is detectable early in development on the pioneering growth cones of posterior corner cells (pCC), midline precursors 1 (MP1), and midline precursors 2 (MP2) neurons. These cells establish the first longitudinal axon tracts that form alongside the midline glia where Slit expression is observed. The pCC and the ventral midline precursors 2 (vMP2) make anterior projections that eventually form the most medial longitudinal axon fascicle while the dorsal midline precursors (dMP2) and MP1s make posterior projections that will later develop into the lateral longitudinal fascicles (Campos-Ortega & Hartenstein, 1997). Early Fas II expression, labeled the pioneering projections of the MP (Fig. 2.4 A, arrow) and pCC (arrowhead) neurons that project between neuromeres in stage 12/3 wild-type

Figure 2.4 Early medial axon projections in *slit* hypomorphs collapse towards the midline.

The first anterior projections of the pCC neurons in wild type embryos (A, arrowhead) form the most medial longitudinal axon fascicles that express FasII. The posterior projections of the MPs join to eventually form the second longitudinal axon fascicle (A, arrow) that represents the middle FasII labeled fascicle in stage 16 NC (Figure 2.4, A). In *slit* hypomorphs where the MPs and MPs axon projections are displaced towards the midline (B, $slit^{JG107}$; C, $slit^{GA20}$; D, $slit^{GA178}$; E, $slit^{GA945}$) we also observe pCC projections that cross and/or fuse at the midline. Embryos that are hypomorphic for moderate alleles of *slit* (F, $slit^{1912}$; G, $slit^{550}$; H, $slit^{532}$) develop distinct axonal projections that eventually fuse at the midline as they develop between segments. When MPs and their posterior projections in mild *slit* hypomorphs appear normal (I, black arrow-$slit^{2990}$), the projections of the pCC neurons still fuse (white arrowhead) or cross (black arrowhead) at the midline and cells are displaced medially.

embryos (Fig. 2.4, arrow). Projections across the midline (arrow head) in wild type embryos were not observed. In severe *slit* hypomorphs (Fig. 2.4 B, $slit^{IG107}$; C, $slit^{GA20}$; D, $slit^{GA178}$; $slit^{GA945}$) the axonal and neuronal somas of the MPs were medially displaced by stage 12/3 and the developing growth cones had fused at the midline region. Anterior projections of the pCC neurons that appeared displaced towards the midline remain there and became obscured within the posterior projections of the MP neurons. The neuronal somas in moderate *slit* hypomorphs (Fig. 2.4 F, $slit^{1912}$; G, $slit^{550}$; H, $slit^{532}$) were less significantly displaced towards the midline and early axon projections were individually distinct. However, as the projections of the MPs reached the posterior segment they were observed to cross over the midline inappropriately, and anterior axonal projections towards the points of crossover were concurrently assimilated. The early nerve cord of a mild *slit* hypomorph (Fig. 2.4 I, $slit^{2990}$) developed distinct longitudinal fascicles, yet sporadic examples of midline fusion still occurred (Fig. 2.4 I, arrowhead). Although, neuronal cells were still partially displaced at the midline causing the ventral nerve cord to narrow, a proportion of the MP and pCC neurons still made appropriate connections (Fig. 2.4 I, arrow). Despite evidence that the more lateral fascicles of the MP axons were established (Fig. 2.4 I, black arrow), anterior medial projections of the pCC neurons were still observed to cross the midline (black arrowhead). Variations in *slit* mutant phenotypes early in development, suggested that *slit* had a role in CNS development beginning with the first projections of early neuronal pioneers.

As embryonic development proceeds the Fasciclin II axons separate into three distinct fascicles that migrate to separate tracts within each neurogenic region (Fig. 2.5 A, black arrowhead). When Slit signaling was absent in embryos deficient for *slit*, all Fas II

Figure 2.5 Longitudinal axon fascicles make erroneous projections in embryos homozygous for hypomorphic alleles of *slit*.

Wild type embryos develop three well defined FasII expressing axons fascicles that project longitudinally on each side of the midline (A). Slit expression, labeled in black with a mAb to Slit, shows the position of the MG within each neuromere relative to the axon fascicles. Arrows show the longitudinal axon fascicles and arrowheads define the midline boundary. In embryos heterozygous for $slit^{JG107}$ (B) and $slit^{2990}$ (C), axons maintain three well defined fascicles and no axon labeling at the midline. In *slit* hypomorphs that have fused longitudinal fascicles at the midline (D, $slit^{JG107}$; E, $slit^{GA20}$; F, $slit^{GA178}$; G, $slit^{GA945}$) we observe some longitudinal fascicles that are still present between segments. Embryos homozygous for other hypomorphic alleles of *slit* that have a separation of fascicles from the midline (H, $slit^{3149}$; I, $slit^{1912}$; J, $slit^{550}$; K, $slit^{532}$) one also observes longitudinal fascicles that make erroneous contralateral projections back and forth across the midline. This is more apparent in *slit* hypomorphs where the longitudinal fascicles are individually defined and only the most medial fascicles are observed to deviate across the midline (L, $slit^{2990}$; M, $slit^{F81}$; N, $slit^{F119}$; O, $slit^{E158}$).

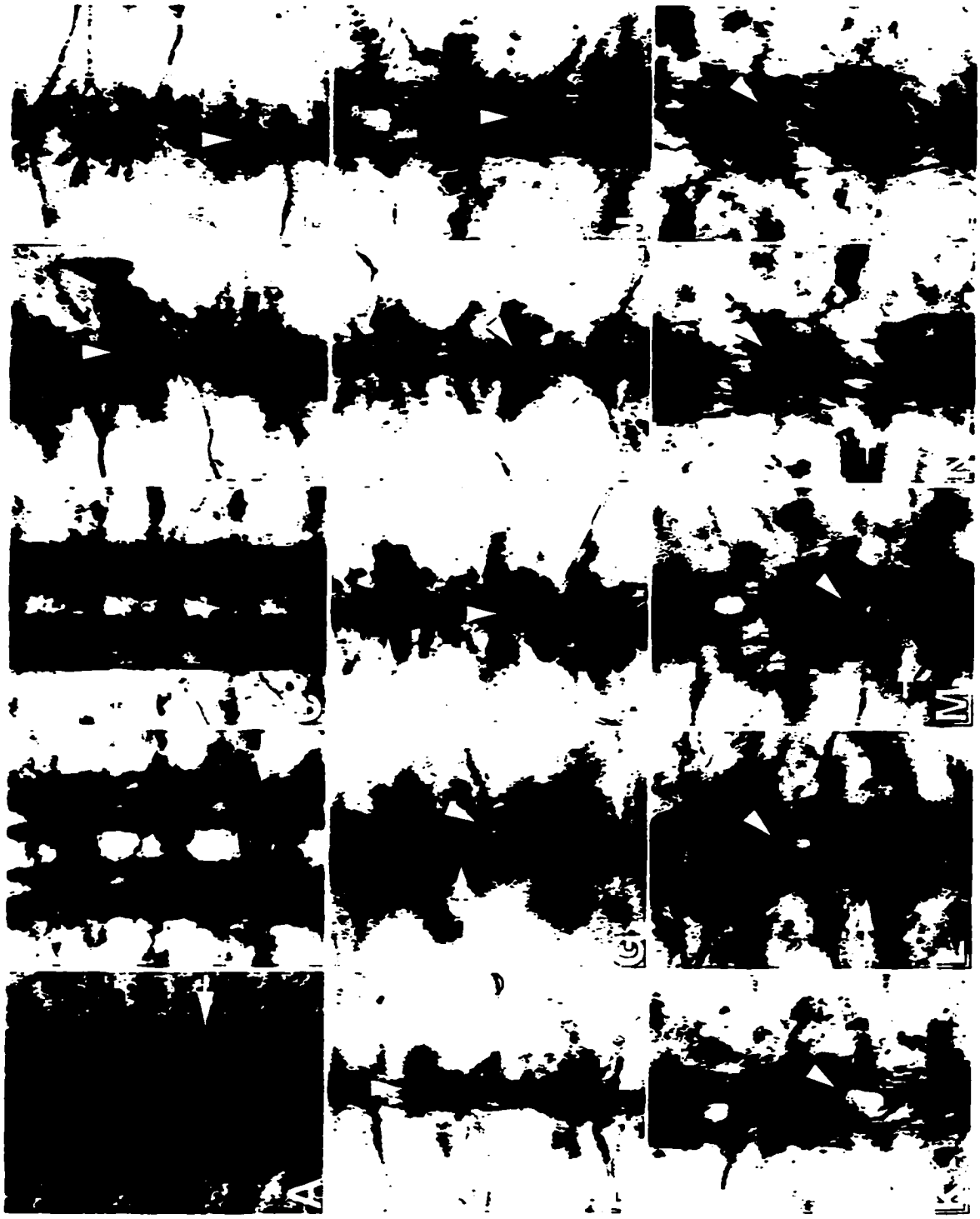

labeled axons were observed to collapse onto the midline (Appendix B), suggesting that all these axons respond to Slit. However, with each individual axon fascicle migrating to a different distance from the midline region separate axons must respond differently to Slit. By studying the development of Fas II axons in the range of *slit* mutants, we hoped to identify properties of Slit that differentially affect axon repulsion from the midline region.

Severe *slit* mutations result in a complete collapse of longitudinal axons onto the midline (Fig. 2.5, D-H) making it impossible to distinguish individual FasII labeled axon fascicles. Individual fascicles are detectable in moderate *slit* phenotypes (J-K) with the exception of embryos mutant for $slit^{1912}$. The separation of BP102 labeled longitudinal axons (Fig. 2.3 I) was not readily detectable in FasII labeled $slit^{1912}$ embryos. Embryos of moderate *slit* mutations also revealed that FasII labeled longitudinal axons not only fused at the midline, they appeared to make contralateral projections back and forth across it (white arrowhead). This aberrant crossing of longitudinal axon fascicles across the midline was clearly evident in mild *slit* phenotypes (L-O). In mild *slit* mutations, we observed that the most medially axon fascicles were more likely to cross the midline than the more lateral adjacent fascicles (arrow). Thus, the severity of the *slit* phenotype not only depended on the degree of midline fusion, but also reflected the number of FasII labeled axons fascicles that were involved in deviant projections across the midline. Medial Fas II axon tracts appeared more sensitive to changes in Slit signaling, which suggested that the lateral axon fascicles do indeed respond to Slit signaling differently. Whether these differences are due to changes in levels of Slit expression or mutations in different regions of the protein, remains to be revealed with sequencing of the mutants.

Slit expression has been detected throughout *Drosophila* development (Fig. 1.5). We have observed that with mild *slit* hypomorphs, embryos hatched and in some instances survived through to adulthood (see below). Larval development and pupation bring about large changes in CNS organization that include continued development of the midline CNS (Fig. 2.6 A, arrow). The mild *slit* CNS phenotype observed in mutant embryos (Fig. 2.5 L) was present in late stage 17 embryos prior to hatching. In order to determine whether this CNS phenotype persisted through to larval development we prepared larval nerve cords from moderate *slit* hypomorphs and labeled axons with an antibody to FasII. The medial longitudinal axon fascicles in $slit^{532}$ mutant larva (Fig. 2.6, C) continued to demonstrate a tangle (white arrowhead) of misguided axon fascicles that weaved across the ventral midline. When the midline glia were removed late in embryogenesis using a dominant-negative DER transgene expressed in the MG (*P{slit1.0-GAL4}*), the most medial FasII labeled axons were observed to make deviant projections across the midline (Fig. 2.6 C, white arrowhead). Thus, it appears that guidance errors due to abnormalities in *slit* signaling carry over through different stages of development.

Cardioblast cells of the dorsal vessel develop inappropriately in *slit* hypomorphs

Slit expression in the cardioblast cells that form the heart was observed in the early precursors of the dorsal vessel through to larval heart development. In order to study the role of Slit in heart morphogenesis we followed the development of the cardioblast cells using an enhancer trap (B2-3-20) that expressed a Lac-Z fusion protein in early cardioblast precursors and cardioblast cells in both severe and mild alleles of *slit*. Wild type heart development (Fig. 2.7 A, D, G, J) followed with a mAb to the pericardial

Figure 2.6 FasII labeled axons in *slit* mutant Larva make aberrant projections across the midline.

FasII expression in the nerve cord of second instar larva appears on the longitudinal axons that run in parallel on each side of the midline (A, arrow). The MG (shown with an antibody to Wrapper, black arrowhead) demark the boundary of the midline. In wild type nerve cords no FasII labeled axons are observed to cross this boundary (white arrowhead). When these MG are reduced in number by expressing a Dominant Negative DER transgene in the MG (*P{slit1.0-GAL4}*), longitudinal fascicles are observed to make aberrant projections across the midline (white arrowhead, B). A larva that is mutant for $slit^{532}$ and immunolabelled with an antibody to FasII (C, arrow) shows that aberrant projections made in embryo longitudinal axons persist in L1 or LII larva.

A
B
C
D
E

Figure 2.7 Cardioblast cells fail to pair appropriately at the dorsal midline in *slit* hypomorphs.

During formation of the dorsal vessel, the cardioblast cells monitored with the enhancer trap B2-3-20 in black (A, white arrow-stage 13) and the extracellular pericardium labeled with MAB3 in brown (A, black arrowhead) migrate towards the dorsal midline as two single rows of cells (D, stage 14). As the primordium of the dorsal vessel migrates with the overlying ectoderm the cardioblasts remain aligned (G, stage 15) and pair uniformly with the adjacent cardioblast cells as dorsal closure completes at stage 5-16 (J). The cardioblast cells of embryos mutant for ^{slitlG107} (B) do not remain aligned as dorsal closure begins (E, white arrowhead). Clusters of cardioblast cells meet at the dorsal midline (H, white arrowhead) and as the dorsal vessel closes, cells remain unpaired (K, black arrow) and cause distortion in the dorsal vessel proper. *slit*^{2990} hypomorphic alleles result in minor distortion in mutant embryos early in development (C, stage 13) that cause clusters of cells (F, white arrowhead) to migrate towards the midline resulting in small distortions as dorsal closure continues (I). *slit*^{2990} hypomorphs have minor distortion in the dorsal vessel (L, black arrow), but cardioblast cells still pair at the dorsal midline.

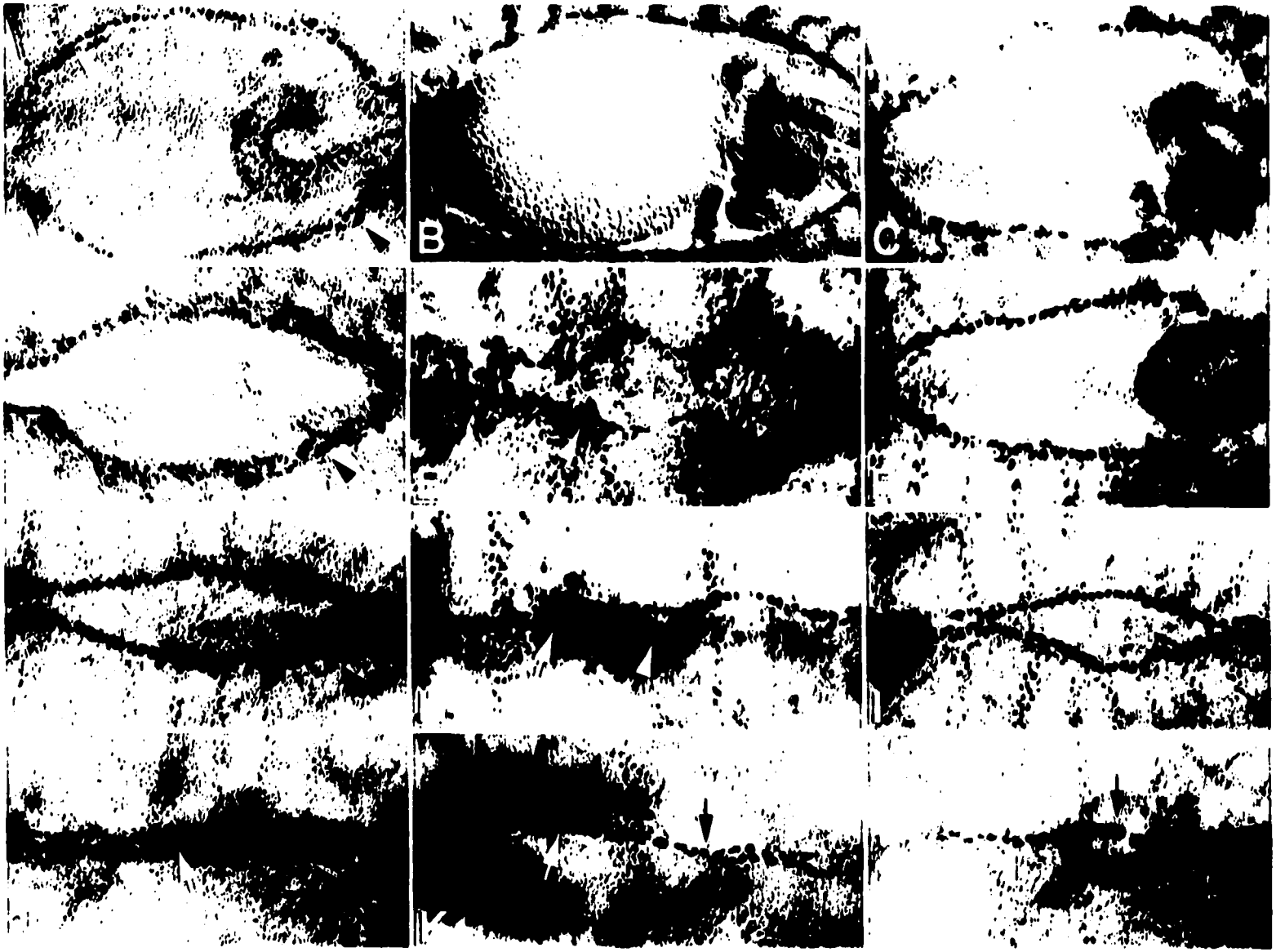
B
C

cells that surround the heart (black arrowhead) and B2-3-20 expression (white arrow) showed that cardioblast cells at the rim of the dorsal vessel migrated in single row of cells towards the dorsal midline (A, stage 13; D, stage 14; G, stage 16). As the cardioblast cells reached the dorsal midline, each cell paired with its contralateral partner and formed a uniform tube as the aminoserosa internalized. Early in development the cardioblasts of both severe (Fig. 2.7 *slit*^{JG107} B, E, H, K white arrow) and mild (*slit*^{2990} C, F, I, L white arrow) *slit* mutants migrated sporadically, and quickly begin to cluster or separate (E, F white arrowhead). As the migrating cells closed towards the dorsal midline (H) defects in severe *slit* mutants often seemed more pronounced, but as dorsal closure completed defects and unpaired cells were observed in both classes of *slit* alleles (Fig. 2.7 K, L black arrow).

Muscles fail to appropriately insert at muscle apodemes in *slit* hypomorphs

Developing muscles form attachments at muscle apodemes that are maintained by the interaction of PS_2 Integrins and their ligand Tiggrin in the ECM (Fogerty *et al*, 1994;Bunch *et al*, 1998). The observation of Slit expression at the muscle apodemes, suggested that *slit* may perform a role in the ECM at points of muscle attachment also maintained by Tiggrin. Tiggrin labeled muscle inserts (Fig. 2.8, white arrows) in wild type embryos appeared uniform at the intersegmental boundaries adjacent to the ventral midline (A). From a sagittal perspective the Tiggrin antibody labeled muscle attachments along the intersegmental borders in a similar pattern (B). In severe *slit* mutants (Fig. 2.8 C-D, *slit*^{JG107}) the sites of muscle attachment labeled with the Tiggrin antibody were reduced (white arrowhead) or even absent in some segments (black arrow) along the

Figure 2.8 Muscle apodemes are deformed or missing in severe *slit* hypomorphs.

Immunostaining with antibodies to Tiggrin label the muscle apodemes observed in wild type ventral (A, arrow) and sagittal (B, arrow) planes. Embryos that are mutant for $slit^{IG107}$ fail to develop the stereotypic pattern of Tiggrin labeling (C-D, black arrow) and labeled muscle apodemes at the ventral midline are deformed (white arrowhead). $slit^{532}$ hypomorphs (E,F) develop muscle patterning that is comparable to wild type.

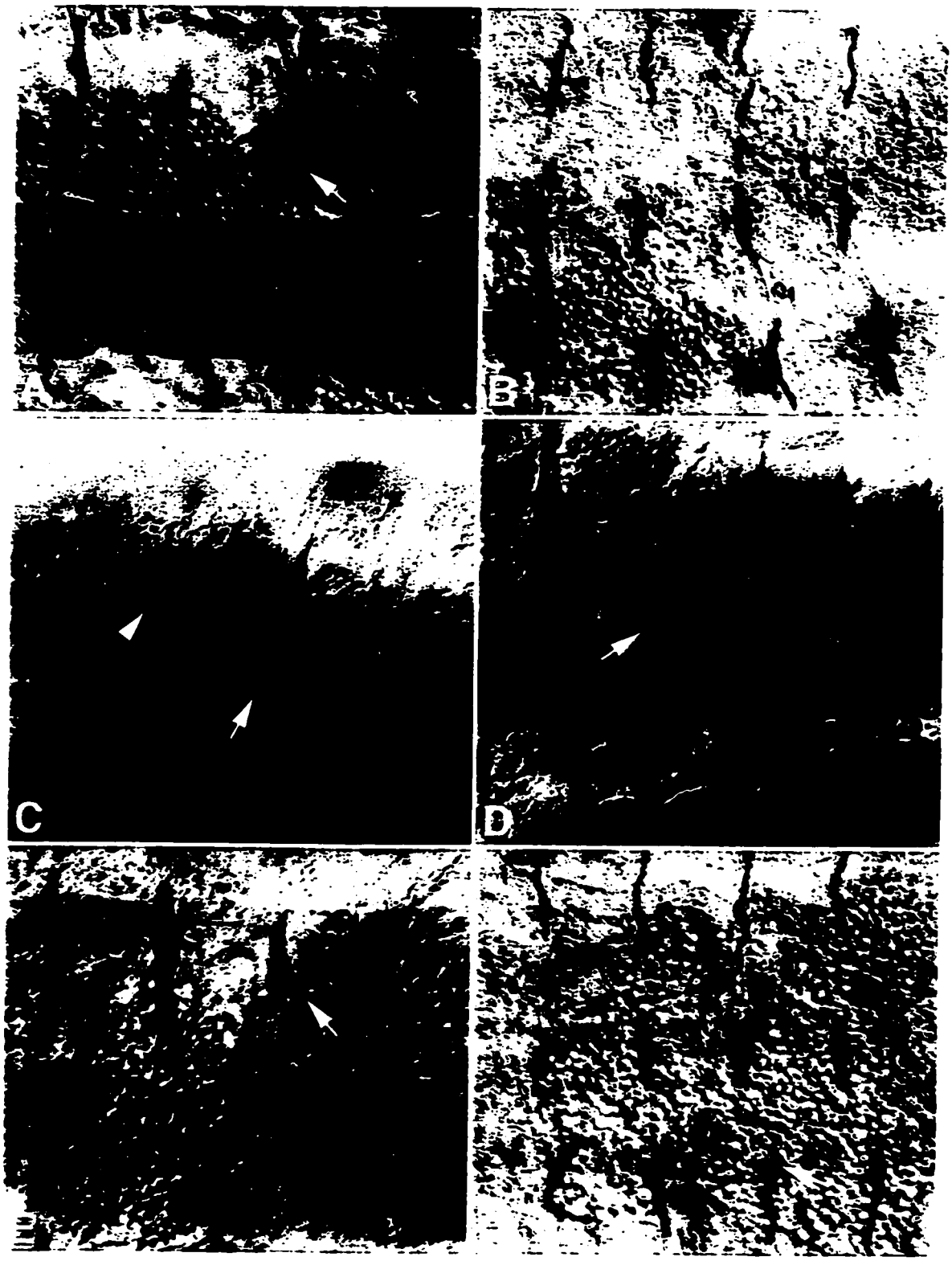
B
C
D

midline (C). The lateral Tiggrin labeling at the peripheral muscle inserts was also inconsistent and in some cases absent (D, black arrow). Moderate alleles of *slit* (Fig. 2.8 E-F, $slit^{532}$) did not appear to significantly affect the pattern of muscle insertions that correspond with Tiggrin labeling adjacent to the midline (E) or in the periphery (F).

Severe mutations in *slit* were observed to cause abnormalities in Tiggrin labeling at the intersegmental boundaries adjacent to the midline. These abnormalities are likely to correspond with morphological changes at the sites of muscle attachment. To investigate this we studied two groups of muscle that insert at the intersegmental boundaries adjacent to the midline, the ventral longitudinal (VL) and the ventral oblique (VO) both of which can be visualized with Rhodamine labeled Phalloidin. In wild type embryos, Phalloidin labeling at the intersegmental boundaries was distinct (Fig. 2.9 A, white arrow). The VL muscles of wild type embryos attached between the intersegmental boundaries (A, black arrow) while the VO muscles project towards the midline and insert in the epidermis adjacent to the midline without crossing the midline (arrowhead). Additionally, VO muscles that were observed to project from abnormal muscle apodemes failed to insert in the local epidermis and aberrantly crossed the midline and attached inappropriately in the contralateral hemisegment (arrowhead). As was found in severe *slit* mutations, embryos homozygous for a moderate allele of *slit* (Fig. 2.9 C, $slit^{1912}$) developed deformations in VL muscles (white arrow), and the muscle apodemes appeared distorted (black arrow). The VO muscles consistently failed to make appropriate insertions in the epidermis and regularly projected across the midline (C, arrowhead). Similar deviations in the VO muscles were observed in embryos mutant for $slit^{532}$ (D, arrowhead), but midline crossovers were far less frequent. The formation of

Figure 2.9 Morphology of ventral oblique muscles in embryos mutant for *slit*.

Confocal images of Rhodamine labeled Phalloidin embryos shows the ventral oblique muscle inserts ipsilateral to the ventral nerve cord (A, arrowhead) in wild type embryos. In embryos homozygous for $slit^{JG107}$ (B), the ventral oblique muscles project dorsally over the ventral nerve cord and insert inappropriately contralateral to their origin. Similar misprojections are observed in embryos mutant for $slit^{1912}$ (C) and $slit^{2990}$ (D), however the number of muscle cells that transverse the midline decrease respectively in each mutant.

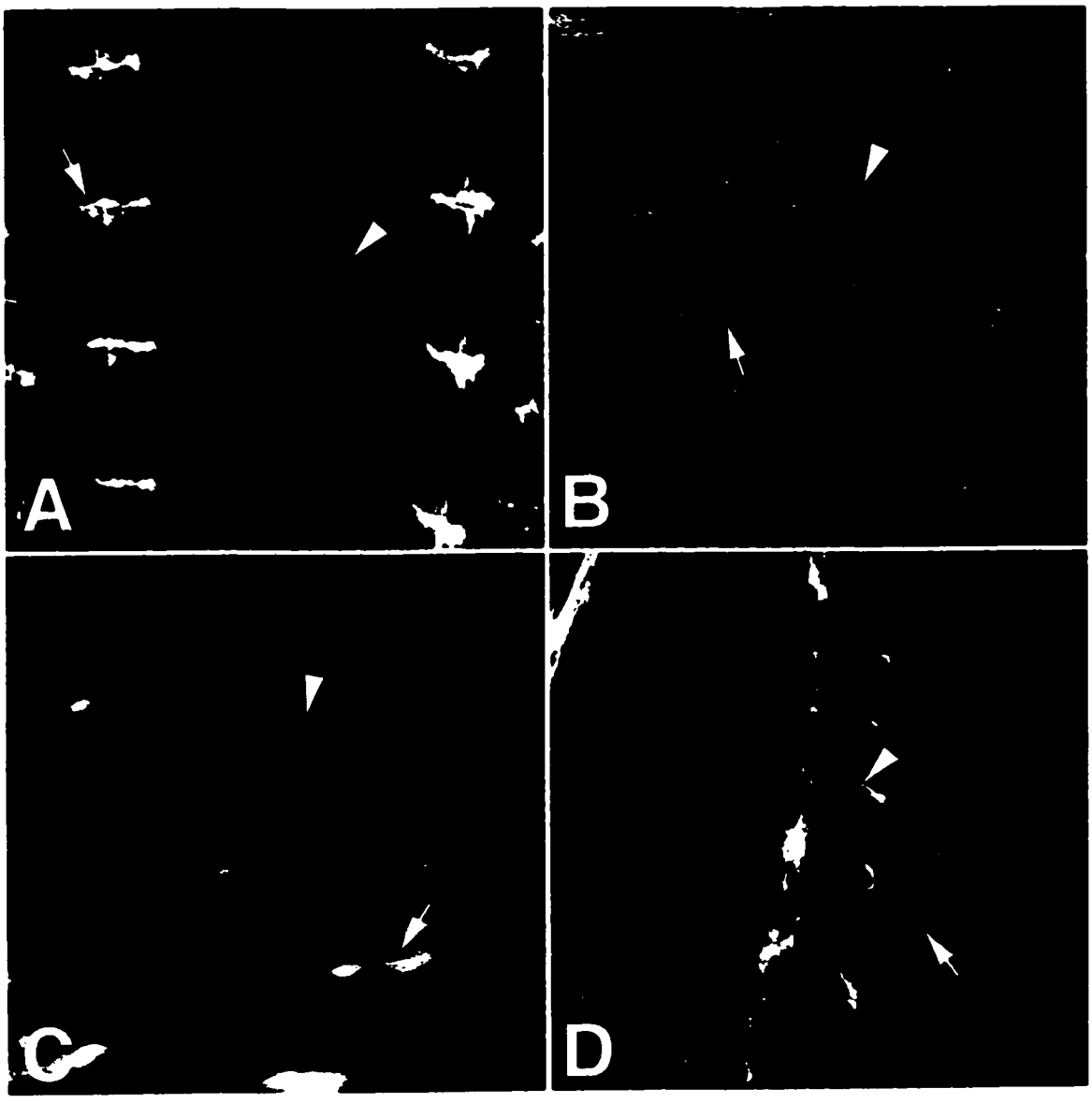
A
B
C
D

muscle apodemes and VL muscle development appeared normal which was consistent with Tiggrin labeling at the muscle apodemes (Fig. 2.8, E). The VL muscles and muscle apodemes appear distorted in *slit* mutant embryos in which a large proportion of the VO muscles misproject across the midline; however, in less severe *slit* mutations where fewer abnormalities are observed, the VL muscles and muscle apodemes appear normal.

Midline Glia are ventrally displaced in *slit* hypomorphs

The MG that express Slit derive from the mesectodermal cells that meet at the midline furrow during gastrulation and differentiate to define the ventral midline(Nambu *et al*, 1990;Lee *et al*, 1999). MG arise in the anterior portion of each neuromere at the dorsal boundary of the midline (Fig. 2.10 A, arrow stage 12/3). They can be visualized with an antibody to Wrapper that labels the cell surface of the MG. As these cells develop they migrate to ensheath both the anterior and posterior commissural axons (B, arrowhead stage16) but remain distinct within each neuromere at the dorsal midline boundary. In embryos that are mutant for a severe allele of *slit* (IG107 C, D) the MG appear ventrally displaced and Wrapper labeling was reduced early in development (C). By stage 17 (D), the processes of the MG were observed at the dorsal surface of the midline, but Wrapper labeling was distinctly reduced. Wrapper labeling in embryos mutant for moderate alleles of *slit* (Fig. 2.10 1912 E, F) was stronger, but the MG were still inappropriately positioned in stage 12/3 embryos (E). Later in development, the ventralized MG extended processes towards the anterior commissure (F, arrowhead), yet Wrapper labeling in the posterior segment was absent. As with moderate *slit* phenotypes, mild *slit* hypomorphs developed ventralized MG that appeared only to ensheath axons in

Figure 2.10 Midline Glial cells are ventrally displaced in *slit* hypomorphs

The midline glial develop in the anterior quadrant of each neuromere (arrow) to wrap around to ensheath both commissural axons as the commissures develop (arrowhead). The MG in wild type embryos (A-stage 12, B-stage 16) labeled with an antibody to Wrapper, show that in early embryos, glial cells are concentrated in the anterior-dorsal quadrant of each neuromere (A). By stage 16 (B) the MG ensheath both axon commissures in the anterior and posterior dorsal quadrants of each neuromere. The MG in embryos that are mutant for $slit^{IG107}$ are ventrally displaced at stage12 (C). At stage 16 the Wrapper labeling in the MG of $slit^{IG107}$ hypomorphs is reduced and appears ventralized and isolated to the anterior boundary of the neuromere in some segments. The MG in $slit^{1912}$ hypomorphs are ventrally displaced (E) at stage 12 and Wrapper labeling is also reduced in stage 16 embryos (F). $slit^{2990}$ mutant embryos show a slight displacement of the MG at stage 12 (G), but by stage 16 (H) the MG cells are still displaced ventrally.

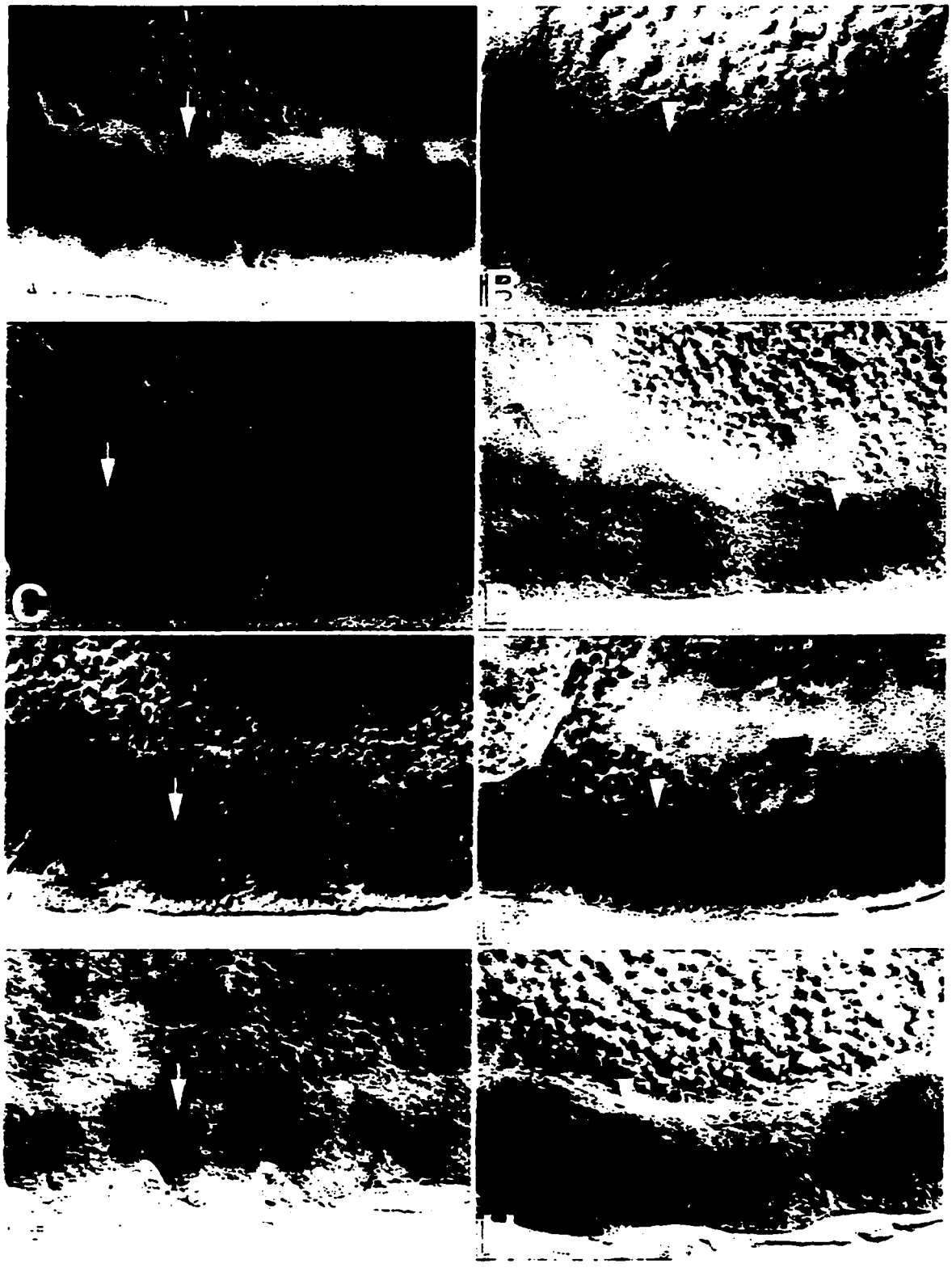
C

the anterior portion of each neuromere (*slit*^{2990}, G, H). Early Wrapper labeling in stage 12/3 MG of *slit* mutants indicates that these cells are ventrally displaced prior to axonogenesis of the midline neurons. As the midline commissures develop, the MG appropriately extended processes to ensheath adjacent axons in the anterior commissures, but remained ventral to the nerve cord. The mechanism resulting in the ventral displacement of the MG was unclear.

Wrapper labeling on the processes of the MG suggested that the cells were ventrally displaced in severe *slit* mutants and that ensheathing processes were localized in the anterior portion of each neuromere. Using an enhancer trap line that expressed a Lac-Z fusion protein specifically around the nucleus of the MG (AA142) we investigated the position and distribution of MG nuclei in the same range of *slit* hypomorphs.

The MG in stage 16 embryos were localized to the anterior (Fig. 2.11, white arrow) and posterior (black arrow) commissure of a BP102 labeled nerve cord (Fig. 2.11, A) shown in this ventral perspective. From a sagittal plane, 3.28±0.46 MG (n=32 neuromeres) are observed distributed in an 'L' shaped pattern (white arrowhead) over the anterior and posterior commissure within each neuromere. The number of MG in severe *slit*^{IG107} mutant embryos (D, 2.41±0.76, n=32 $p<0.05$) was significantly reduced in each neuromere and the remaining cells were ventrally displaced from the posterior commissure (C, D). Embryos mutant for moderate (*slit*^{1912} E, F) and mild (*slit*^{2990} G, H) alleles of *slit* developed a wild-type number of MG; however, MG in moderate *slit* hypomorphs were more severely displaced than mild phenotypes. Moderate *slit* phenotypes described MG that were only observed at the anterior commissure (E, F white

Figure 2.11 MG in *slit* hypomorphs are displaced from the commissures and in severe mutations are reduced in number

The enhancer trap line AA142 marks the position of MG cells by driving nucleus targeted β-galacotosidase expression in these cells. From a ventral perspective the midline glia, labeled with an antibody to α β-gal, are localized at the anterior (white arrow) and posterior (black arrow) commissures (BP102) in stage 16 wild type embryos (A). MG cell bodies in embryos mutant for $slit^{IG107}$;*AA142* (C) are displaced from where the anterior and posterior commissures fuse. The numbers of MG are reduced from an average of 3.28 ± 0.46, n=32 cells per segment in stage 16 wild type embryos (B, arrowhead) to 2.41 ± 0.76, n=32 in $slit^{IG107}$ mutants (D) and from a sagittal plane the MG appear to be displaced from the posterior commissure. Embryos homozygous for the $slit^{1912}$ allele, have a normal number of MG (3.12 ± 0.56), however the MG are displaced ventrally from the posterior commissure (F), but remain at the midline (E). MG are slightly displaced in the segments that appear more tightly fused in embryos homozygous for $slit^{2990}$ (G). In a sagittal plane, a few segments have ventrally displaced MG (H), however the number of MG is the same as wild type (3.28 ± 0.46).

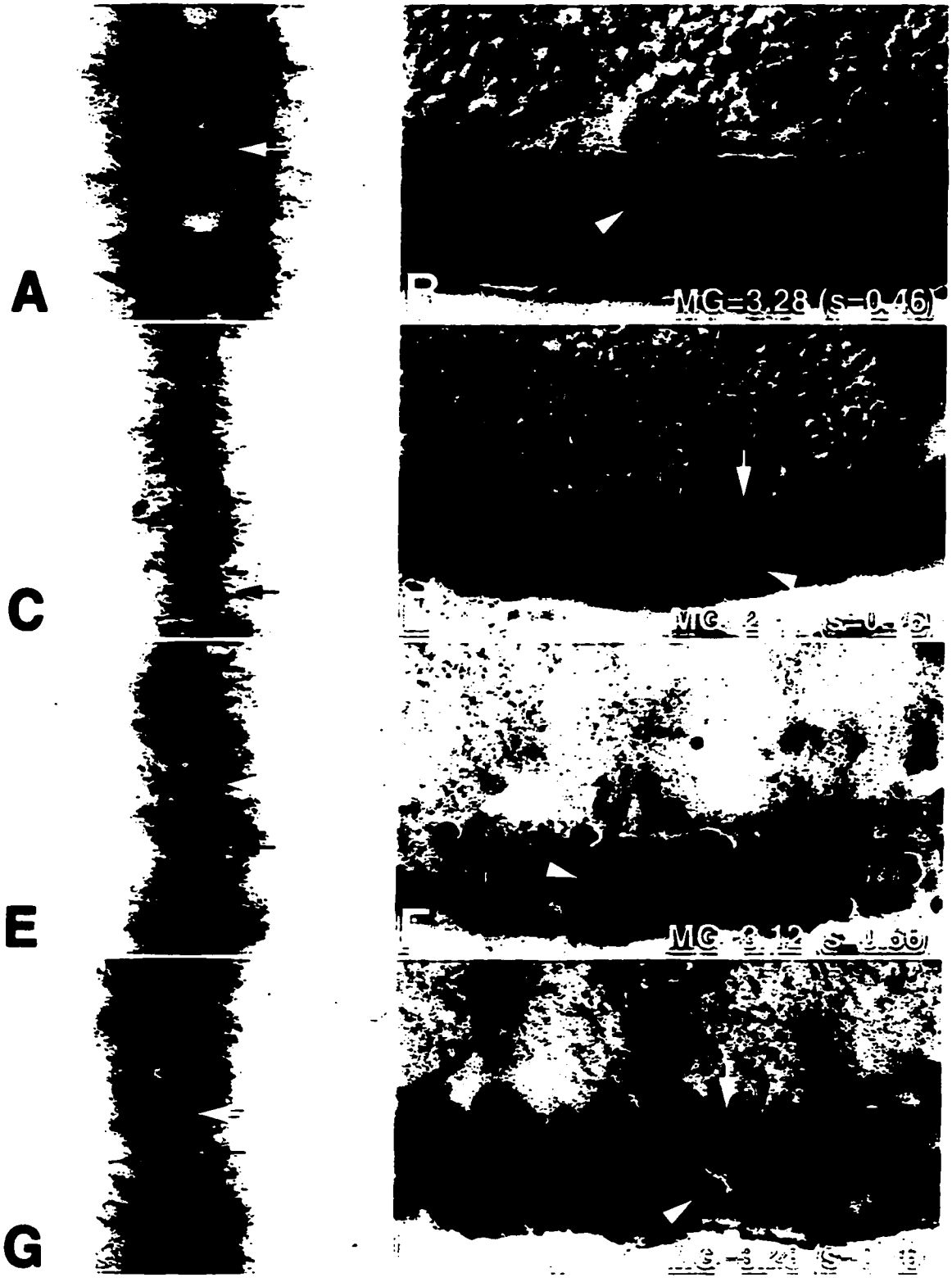
A
C
E
G
MG=3.28 (s=0.46)

arrow), while the remaining glial cells were ventrally displaced (F, arrowhead) leaving no glial cells directly adjacent to the posterior commissure (E, F black arrow). In mild *slit* mutants, few MG failed to migrate to their appropriate position, yet the midline architecture was not organized as uniformly as was observed in wild type embryos. The MG in *slit* mutants were only reduced in number in severe *slit* mutations. All *slit* mutants demonstrated a general ventral displacement of MG from the posterior commissure that varied in degree to the respective severity of the *slit* CNS phenotype.

Protein and RNA expression in *slit* alleles

The MG in *slit* mutants maintain an active role in supporting and ensheathing the commissural axons, despite the disruption of Slit function. Furthermore, the MG remain associated with the commissural axons in embryos mutant for *slit*, suggesting that the production of *Slit* mRNA and protein observed in the MG of wild type embryos is either absent or not functional in *slit* mutant embryos. Using a tissue *in situ* probe generated from full length *slit* cDNA it was observed that embryos homozygous for the selected alleles of *slit* all produced a detectable *Slit* transcript (Fig. 2.12, C-N). Additionally, detectable levels of Slit protein were found in most mutant embryos, with the exception of $slit^{IG107}$, $slit^{GA20}$, and $slit^{1912}$ mutants using an antibody developed from the 6th EGF repeat and beginning of the G-domain (Fig. 2.13, C,D,H). The level of Slit protein expression suggested that the density of immunolabelling was higher in mild *slit* hypomorphs (I-K); however, P-element induced mutations that are believed to reduce levels of *slit* expression (L, $slit^{F81}$ & M, $slit^{F119}$) had Slit labeling comparable to severe *slit* hypomorphs. Data from tissue *in situs* using the entire *Slit* RNA (Fig. 2.12) and smaller fragments of *Slit* RNA (data not shown) suggest that a complete Slit transcript is

Figure 2.12 ***Slit*** **RNA expression in** ***slit*** **hypomorphs**

Slit mRNA is detectable in the midline glia (arrow) and cardioblast cells (arrowhead) of wild type (A) and $slit^{IG107}$ (B) heterozygous embryos. An mRNA probe based on the complete *slit* cDNA, labeled cardioblast (not shown in all panels) and MG in all *slit* hypomorphs. C, $slit^{IG107}$; D, $slit^{GA20}$ E, $slit^{GA178}$ F, $slit^{GA945}$ G, $slit^{3149}$ H, $slit^{1912}$ I, $slit^{550}$ J, $slit^{532}$ K, $slit^{2990}$ L, $slit^{F81}$ M, $slit^{F119}$ N, $slit^{E158}$. Some embryos show mRNA labeling localized to muscle apodemes in the periphery (black arrowhead E, H, K, M), however this was not consistent within or between samples.

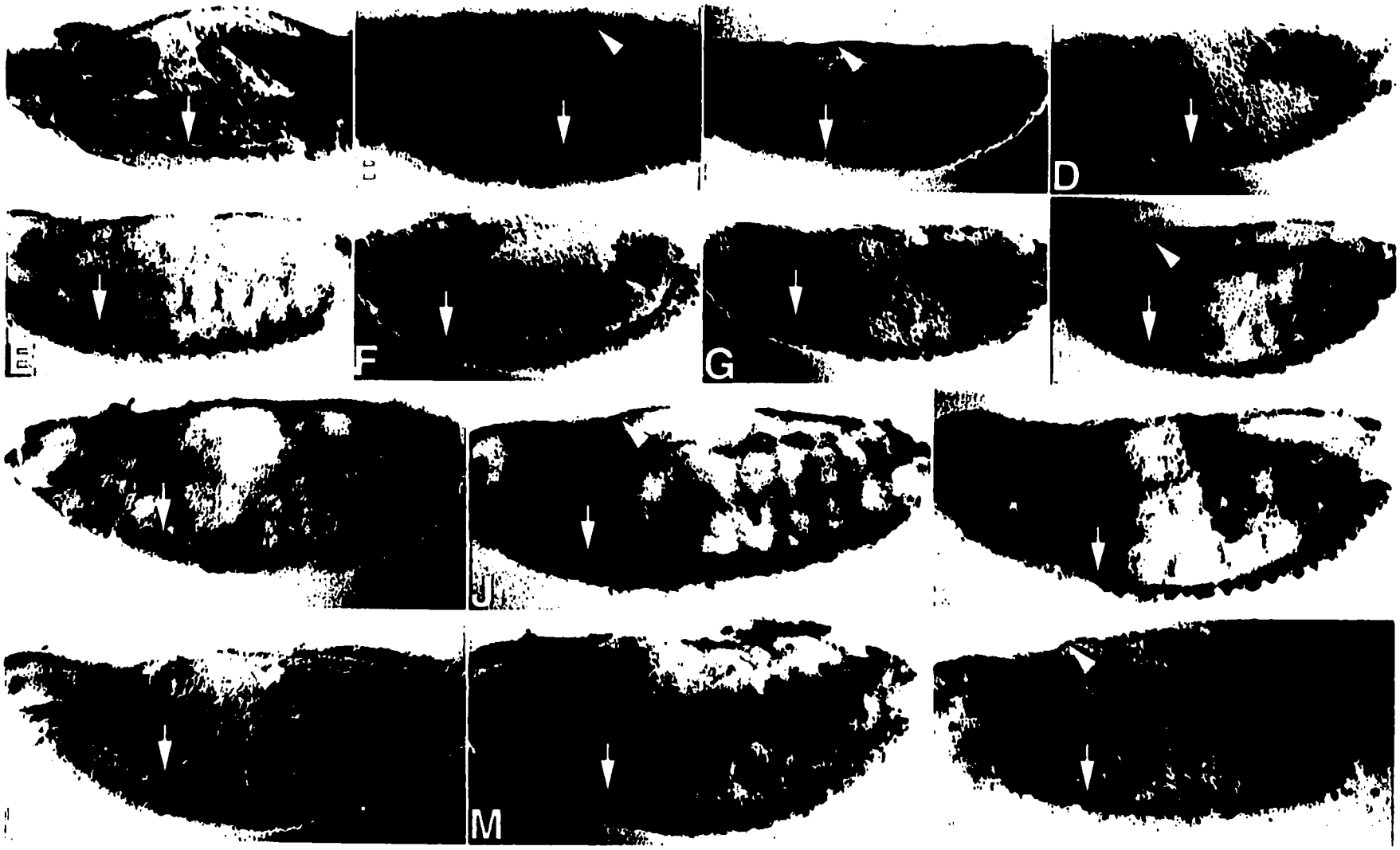
D
F
G
J
M

Figure 2.13 Slit expression in *slit* hypomorphs

Using a mAb specific to on a 550bp EcoRI fragment of *slit* cDNA from the 6th EGF-like repeat, Slit protein is readily detectable in the midline glia (arrow) and cardioblast cells (arrowhead) of +/*CyOP{eng-lacZ}* (A) and heterozygous $slit^{JG107}$ embryos (B). Embryos homozygous for hypomorphic alleles of *slit* were selected using a marked balancer (A-black arrowhead) and assessed for Slit expression. $slit^{JG107}$, $slit^{GA20}$, and $slit^{1912}$ show no Slit expression (C, D, H) and the levels of expression in $slit^{GA178}$, $slit^{GA945}$, and $slit^{3149}$ were barely detectable (E-G, respectively). Slit expression is clear in embryos homozygous for $slit^{550}$, $slit^{532}$, & $slit^{2990}$ (I-K, respectively), however the level of expression in $slit^{F81}$, $slit^{F119}$, & $slit^{E158}$ hypomorphs appears dramatically reduced.

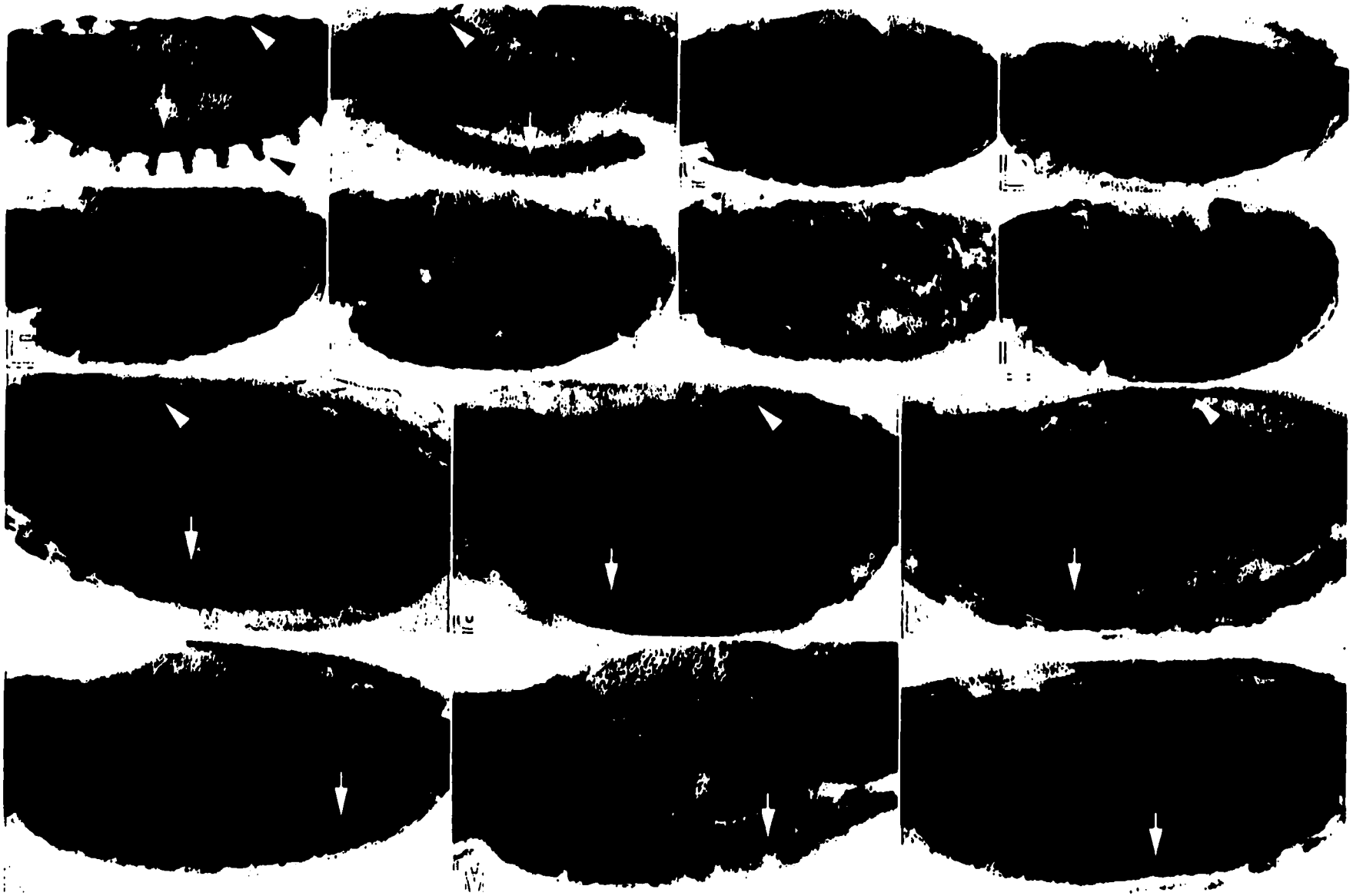

produced in each mutant. The three alleles of *slit* that appeared to be protein null, did not behave genetically as protein null upon investigation of the CNS phenotypes (Fig. 2.1, 2.3, 2.5, & Appendix B). It is likely that mutations in these alleles affect protein translation upstream of the antibody epitope, but do not completely disrupt *slit* function.

Alleles of *slit* differentially affect larval viability

Alleles of *slit* were maintained over either an embryonic (*CyO-P{eng-lacZ}*) or larval (*CyO-P{y+}*) marked balancer to identify homozygous mutant progeny. All *slit* alleles were embryonic lethal when heterozygous with a deficiency for *slit* (*Df(2R)WMG*) (Fig. 2.14). *slit* alleles $slit^{532}$, $slit^{2990}$, $slit^{F81}$, and $slit^{F119}$ produced homozygous viable adults at a low frequency (Table 2.1). Transheterozygous combinations of *slit* alleles shown in Figure 2.14 demonstrate that a percentage of the expected transheterozygous progeny from specific combinations survived to adulthood while the remainder were larval lethal. The moderate and mild CNS phenotypes observed in embryos mutant for $slit^{550}$, $slit^{532}$, $slit^{2990}$, $slit^{F81}$, $slit^{F119}$, and $slit^{E158}$ correlated with combinations of different *slit* alleles that produced viable offspring.

Classification of *slit* mutant phenotypes

Alleles of *slit* have been grouped into severe, moderate, and mild phenotypes (Table 2.1). Embryos with severe *slit* mutant phenotypes were observed to develop completely fused BP102 and FasII labeled axon tracts that projected axons across the midline but intersegmental longitudinal tracts were significantly diminished. The MG were ventrally displaced early in development and failed to appropriately migrate towards the posterior commissure. Latter in embryonic development, fewer MG were

Figure 2.14 Homozygous and transheterozygous crosses of specific *slit* alleles produce viable mutant offspring.

The viability of progeny resulting from both female/male and male/female pair wise mateings of balanced alleles of *slit* was investigated. Homozygous progeny from $slit^{532}$, $slit^{2990}$, $slit^{F81}$, & $slit^{F119}$ alleles produced a small percentage of viable adults. Transheterozygous combinations of these alleles indicated in green resulted in a general but small increase in the observed viability . Two exceptions $♀slit^{2990}/♂slit^{532}$, and $♀slit^{F119}/♂slit^{F81}$ were noted. Heterozygous allelic combinations of $slit^{E158}$ with $slit^{532}$, $slit^{2990}$, $slit^{F81}$, & $slit^{F119}$ produced viable progeny, despite homozygous $slit^{E158}$ embryos being lethal. Embryos homozygous for $slit^{550}$ were lethal, and only male $slit^{550}$ flies produced viable adults with $slit^{532}$, $slit^{F81}$, $slit^{F119}$, & $slit^{E158}$.

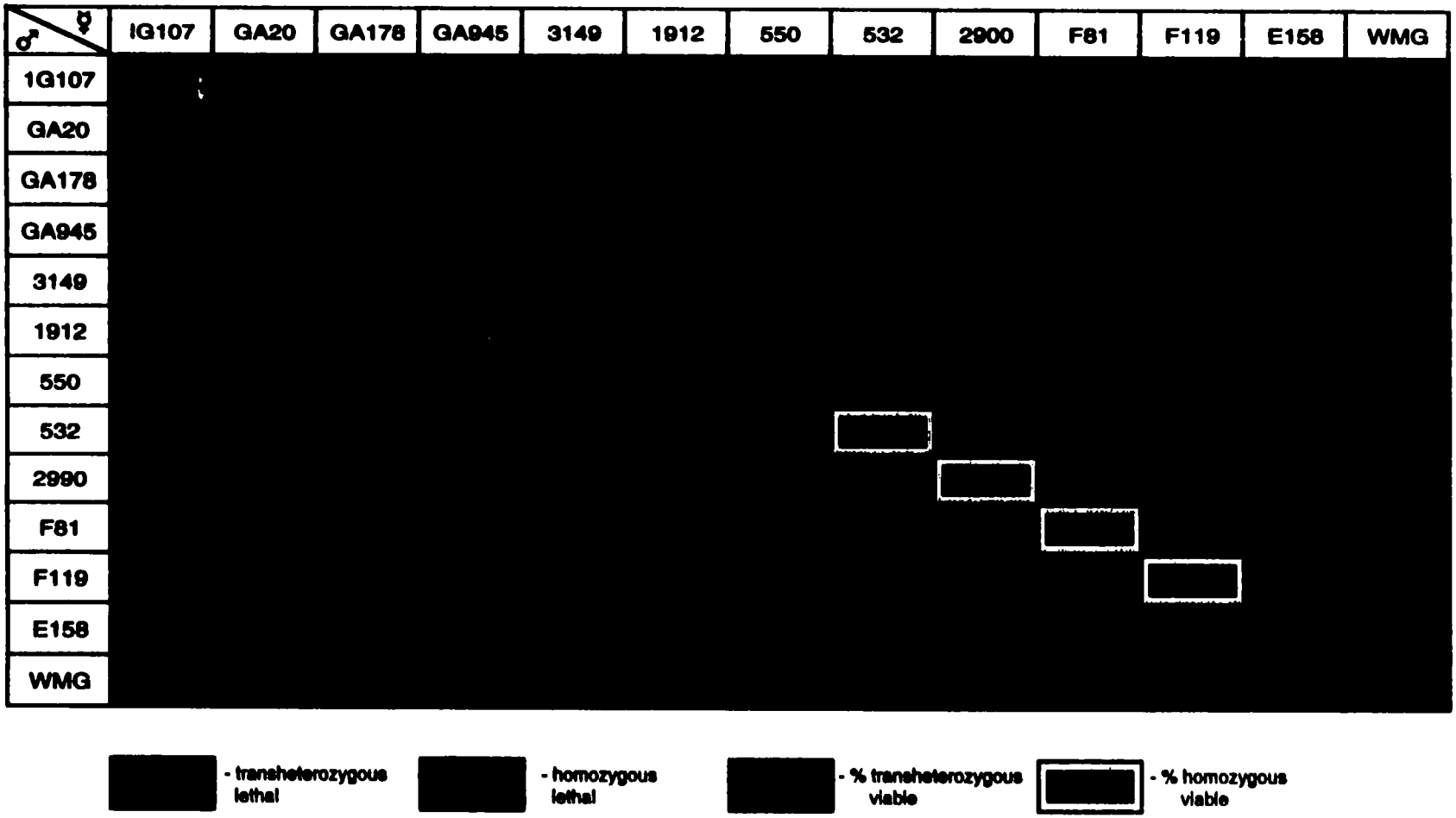
♀
♂
1G107
GA20
GA178
GA945
3149
1912
550
532
2900
F81
F119
E158
WMG
- transheterozygous lethal
- homozygous lethal
- % transheterozygous viable
- % homozygous viable

Table 2.1 Summary of slit phenotypes

Slit Allele	Embryonic [1] Lethality	Mutant Larval Viable (25% expected)	Latest Observed Stage	Adult Viable	Proportion Nerve [2] Cord Length	Classification [3] of alleles
yw^-	2.0% (429)	98%	Adult	94%	0.73 ±0.04	Normal
$slit^2$	31% (978)	1.0 %	L1	0	0.88 ±0.06	Severe*
$slit^{GA20}$	25% (956)	1.9%	L1	0	0.90 ±0.02	Severe
$slit^{GA178}$	27% (914)	13%	L1	0	0.91 ±0.03	Severe
$slit^{GA945}$	27% (475)	2.3%	L1	0	0.88 ±0.02	Severe
$slit^{3149}$	25% (473)	5.1%	L2	0	0.94 ±0.02	Severe
$slit^{1912}$	28% (484)	7.4%	Pupa	0	0.92 ±0.02	Moderate
$slit^{550}$	28% (924)	0.5%	L1	0	0.89 ±0.03	Moderate
$slit^{532}$	25% (971)	7.1%	Adult	0.5%	0.76 ±0.05	Moderate
$slit^{2990}$	32% (438)	2.0%	Adult	0.2%	0.85 ±0.04	Mild
$slit^{F81}$	19% (970)	11%	Adult	1.5%	0.82 ±0.06	Mild*
$slit^{F119}$	13% (943)	17%	Adult	2.1%	0.80 ±0.07	Mild*
$slit^{E158}$	19% (953)	3.1%	Pupa	0	0.82 ±0.04	Mild*

[1] the percentage of fertile mutant embryos that failed to hatch were recorded from the total embryonic sample shown in brackets
[2] based on BP102 staining of *slit* mutant nerve cords, the length of the nerve cord was measured as a proportion of the entire embryo length
[3] alleles of *slit* were classified into one of three groups based on their mutant phenotype as described in the text
* *slit* mutants were also analyzed with a polyclonal antibody ({Rothberg, Hartley, et al. 1988 125 /id})

observed than in wild type embryos, but existing cells projected processes to ensheath local axon tracts. Additionally, muscle apodemes at the peripheral hemisegments and adjacent to the midline were distorted or absent. The projections of the ventral oblique muscles fail to insert appropriately in the epidermis adjacent to the midline, instead making projections across the midline to insert in the contralateral epidermis. Mutant phenotypes observed in the heart development were consistent across all alleles of *slit*. The embryonic heart developed irregularly, the cardioblast cells migrated unevenly, resulting in unpaired cardioblast cells within the dorsal vessel that formed an incomplete dorsal tube.

Moderate *slit* CNS phenotypes were also described as fused longitudinal axon tracts; however, the fused axon tracts were typically broader and developed thicker intersegmental longitudinal axon. Occasionally, longitudinal axons were observed to separate from each other revealing both posterior and anterior commissures. The MG were ventrally displaced early in development and failed to migrate towards the posterior commissure, yet in contrast to severe *slit* phenotypes no reduction in glia number was observed in older embryos. As was observed in severe *slit* mutants, muscle apodemes adjacent to the ventral nerve cord became distorted but were not absent. The ventral oblique muscle made fewer projections across the midline, but still made sufficient insertion errors to distort the ventral midline.

The mild *slit* CNS phenotype was remarkable due to the distinct separation of the longitudinal axon fascicles that revealed complete anterior and posterior commissures in most midline segments. The intersegmental longitudinal axons were clearly developed

and FasII labeling revealed that the more lateral axons fascicles were less severely disrupted in contrast to the medial axon tracts that continued to make inappropriate projections across the midline. The MG in mild *slit* mutants developed normally, and only occasional disruption of MG migration were observed. Neuromeres that contained such ventral displacement errors often corresponded to localized collapse of axon commissures within that region. The muscles apodemes in both the peripheral and medial hemisegments appeared normal, yet ventral oblique muscles consistently made misguided projections across the ventral nerve cord. Mild *slit* mutants were occasionally observed to survive through to adulthood whereas other *slit* mutants died early in larval development. A notable increase in length of the ventral nerve cord in relation to the size of embryo was observed in all *slit* mutants; however, this difference was less dramatic with mild *slit* alleles.

Characterization of EMS mutations

Nine of the selected *slit* alleles were generated by EMS mutagenesis that typically alters single nucleotides in the genomic DNA. In order to determine the lesion that resulted in the observed *slit* phenotypes we PCR amplified and then sequenced all the *slit* coding regions in each of these alleles. During this process we identified 19 consistent polymorphisms between groups of *slit* alleles indicated in red on Table 2.2 that did not alter protein coding with one exception. At cDNA 2660 a thymine to adenine change results in an Isoleucine becoming an Asparagine. Since this change occurs consistently in 4 or the 9 sequenced alleles, and other more significant mutations were attributed to phenotypes observed in embryos mutant for these alleles we assumed the changes were not deleterious. Investigations into the history of each of these alleles did not reveal a

common ancestry that would explain consistencies in the polymorphism observed in these alleles. Furthermore, patterns of polymorphisms established between alleles in the 5' half of the cDNA did not carry over to patterns established in the 3' portion of the cDNA. Although attempts to define a clear pattern of these polymorphisms in the generation of these mutants failed, further details outlining the history of these mutant alleles may shed light onto their genetic background.

We successfully identified point mutations in seven of the nine *slit* alleles studied that are represented in Figure 2.15. Of these, three result in single amino acid changes, two deletions result in the production of a premature stop codon, and two coding changes produce immediate stop codons. In $slit^{GA178}$ nucleotide 321 is changed from a cysteine to a guanine that codes for Glutamic acid rather than Glutamine in the beginning of the first Leucine repeat. Nucleotide 1052 of $slit^{GA945}$ is altered from a thymine to a guanine that results in Valine being converted into a Glycine at the beginning of the second LRR, and nucleotide 1421 of $slit^{532}$ is changed from a cytosine to a thymine changing Alanine to Valine at the end of the second LRR. A deletion of nucleotide 2508 in $slit^{GA20}$ brings a premature stop codon into frame at the third Leucine rich region in the last LRR. Two changes in the third EGF-like repeat, one change of nucleotide 3109 from a cytosine to a thymine in $slit^{1912}$ and one change of an adenine to a thymine at nucleotide 3141 of $slit^{JG107}$ both produce premature stop codons. Finally, a deletion of nucleotide 3571 in $slit^{550}$ brings a stop codon into frame at the beginning of the G-domain. Coding changes could not be detected in $slit^{3149}$ and $slit^{2990}$ although sequencing of these alleles was repeated three times. Although sequences changes may exist in the coding regions of these alleles, it is likely that mutations occurred outside of the coding domains.

Figure 2.15 Schematic showing point mutations identified in alleles of *slit*.

EMS induced point mutations were identified for each mutant allele of *slit* in relation to the regions of protein translation that each directly affected. Coding changes indicated in red script are annotated beneath respective *slit* alleles and the precise cDNA sequence is given. Protein motifs are identified as per figure legend.

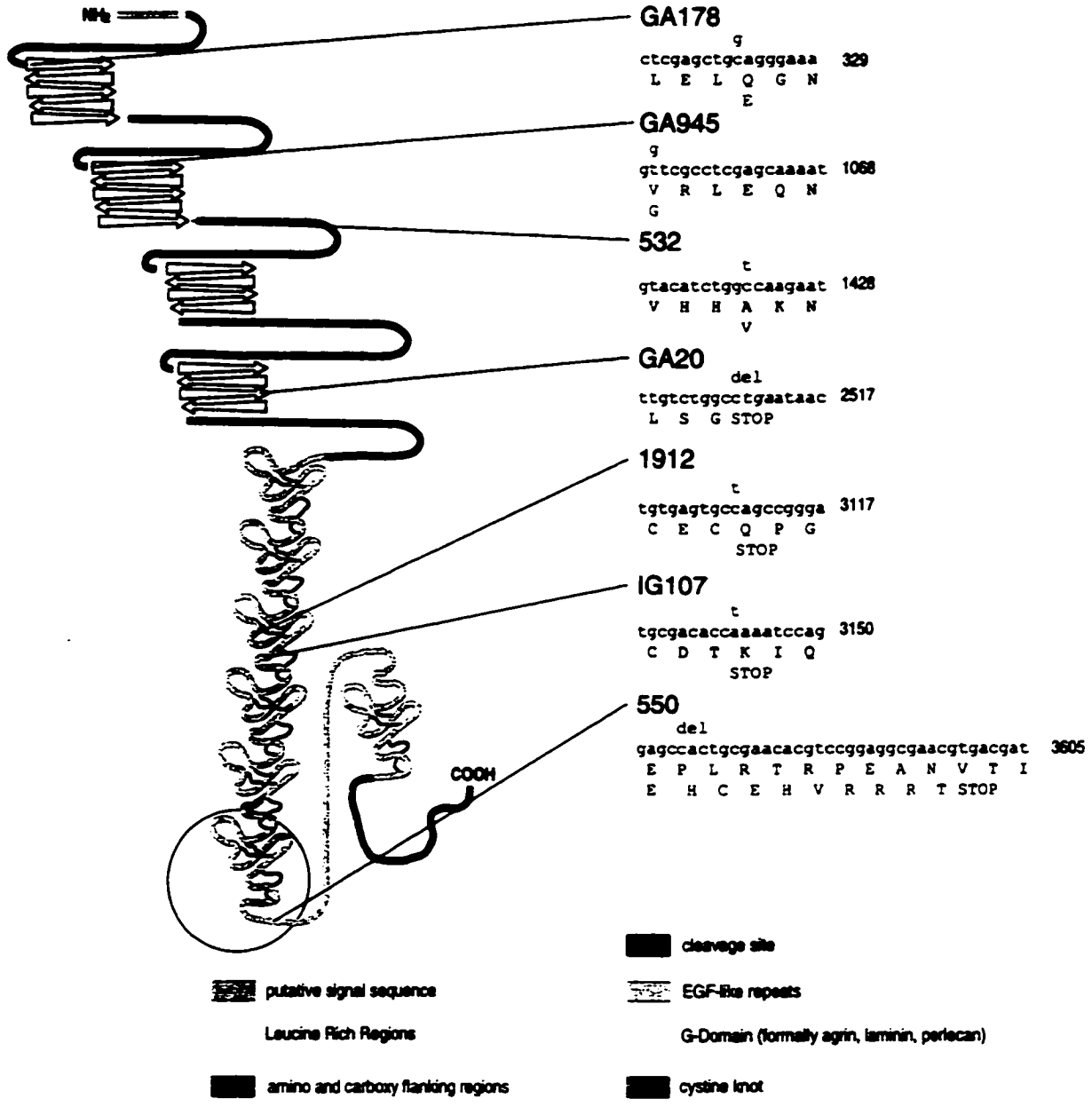
NH2
COOH
GA178
g
ctcgagctgcagggaaa 329
L E L Q G N
E
GA945
g
gttcgcctcgagcaaaat 1068
V R L E Q N
G
532
t
gtacatctggccaagaat 1428
V H H A K N
V
GA20
del
ttgtctggcctgaataac 2517
L S G STOP
1912
t
tgtgagtgccagccggga 3117
C E C Q P G
STOP
IG107
t
tgcgacaccaaaatccag 3150
C D T K I Q
STOP
550
del
gagccactgcgaacacgtccggaggcgaacgtgacgat 3605
E P L R T R P E A N V T I
E H C E H V R R R T STOP
cleavage site
putative signal sequence
EGF-like repeats
Leucine Rich Regions
G-Domain (formally agrin, laminin, perlecan)
amino and carboxy flanking regions
cystine knot

Table 2.2 Poylmorphisms found in alleles of *slit*.

Alleles	Slit cDNA Sequence (bp)

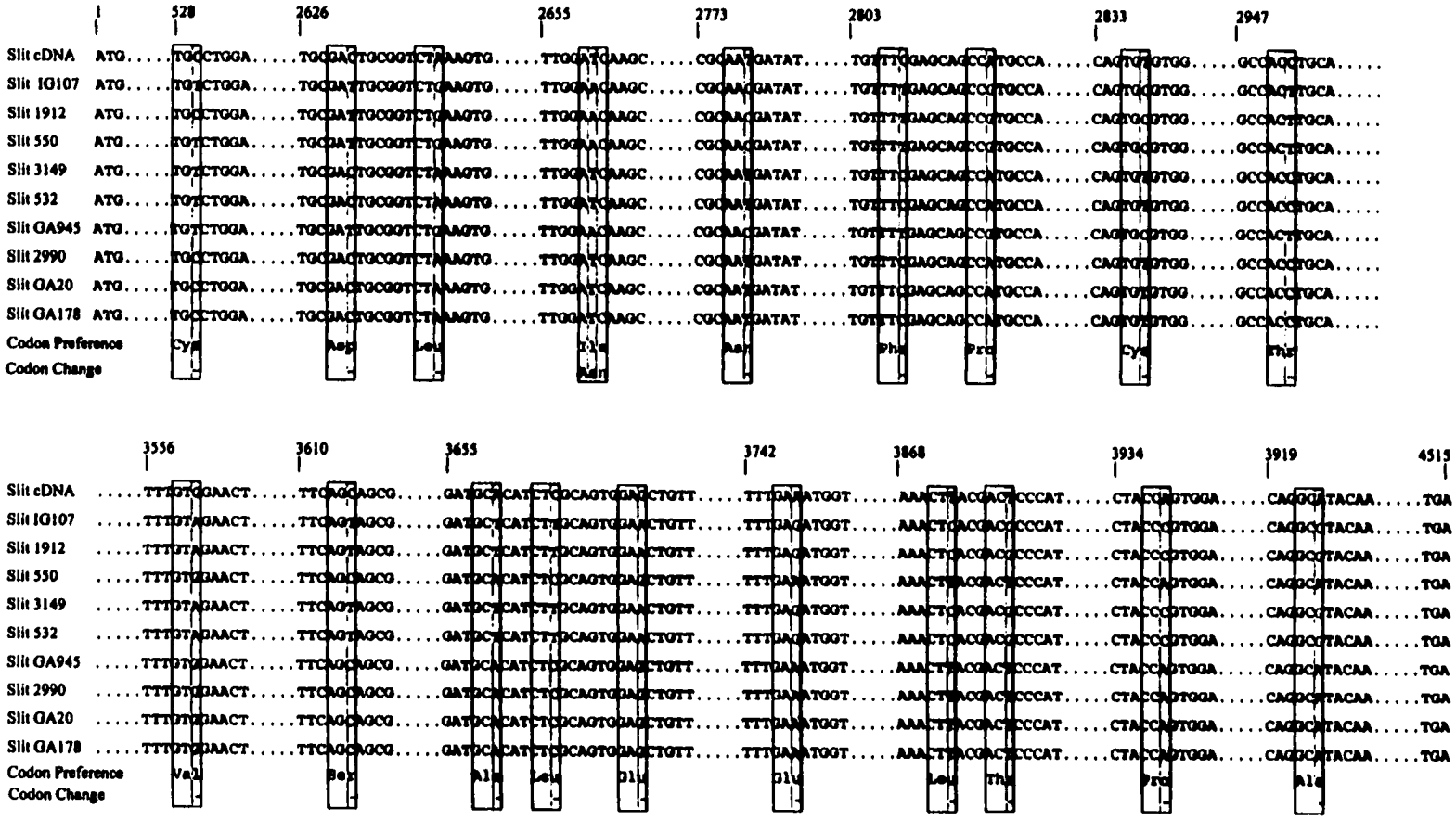

DISCUSSION 2

Mutant screens performed by Seeger (1993) and Nüsslein-Volhard (1984) have provided us with 9 EMS generated point mutations that result in varying degrees of CNS collapse when examined over a deficiency uncovering *slit*. Additionally, 3 P-element induced alleles were also examined that have a range of CNS phenotypes (Rothberg *et al*, 1990). Perturbations in Slit function in the P-element alleles are likely due to insertions of the transposons that map from 10 to 100 b.p. upstream of the transcription initiation site. Disruptions in different regions of the initiation site in each of these alleles is believed to reduce the levels of Slit expression producing a range of *slit* phenotypes (Rothberg *et al*, 1990). The severity of the CNS phenotype observed in embryos deficient for *slit* can be attributed to disruption of multiple levels of *slit* function suggested by the differing levels of Slit activity observed in different mutant alleles. We have examined the characteristics of the mutant phenotypes in the CNS, MG, muscle apodemes, and the heart for each allele of *slit* and compared them to their respective point mutations in an attempt to develop a structural and functional understanding of *slit*.

Slit in the midline

Slit is secreted by the MG and localized to the MG. Previous investigations have also shown that Slit is acquired by the growth cones of axons that traverse the MG (Rothberg *et al*, 1990). In mutations that remove Slit, the MG appear ventralized and are reduced in number, suggesting that Slit is somehow responsible for maintaining glia morphology and position at the midline (Sonnenfeld & Jacobs, 1994). Upon a more careful inspection, EM micrographs through a cross section of the anterior commissure reveal that the MG remain associated with the commissurally projecting axons that

normally traverse them, suggesting that *slit* may have a more intimate role at the midline (Sonnenfeld & Jacobs, 1994;Sonnenfeld & Jacobs, 1995;Battye *et al*, 1999).

Deficiencies that remove Slit function result in a collapse of the longitudinal and commissural axon tracts onto the MG and eliminates all intersegmental connections, replacing the normal pattern of the ladder-like axon scaffold. Examination of 13 different mutations in *slit* reveals a range of stage 16 midline guidance errors from severe, in which all midline axons fuse onto the MG boundary to mild, in which only the most medial axons erroneously project across or fuse at the midline. The development of the wild-type axon scaffold of the *Drosophila* CNS is dependent on stereotypical decisions made by the early pioneering growth cones to establish correct pathways. Early growth cones near the *Drosophila* midline make three characteristic decisions, the MP and pCC neurons make anterior and posterior projections along the longitudinal axon tracts and never cross the midline. The RP neurons project across the midline along with other interneurons and their growth cones and then turn anteriorly or posteriorly along the contralateral longitudinal axon tracts and never cross the midline again. The aCC among other neurons remain ipsilateral midline and exit the nerve cord via one of the nerve roots (Jacobs & Goodman, 1989b). As the CNS develops, thick longitudinal tracts form on each side of the ventral midline and an anterior and posterior commissure develop within each neuromere comprised of selected axons establishing contralateral connections. The early pCC axons represent the most medial fascicles, while the MP axons and other axons separate to form the lateral most fascicles (Campos-Ortega & Hartenstein, 1997;Hidalgo & Booth, 2000).

Evidence of midline guidance errors in *slit* mutants are obvious in the very early projections of the pCC and MP neurons. Severe mutations are notable for the medial displacement of both the pCC and MP cell bodies that pioneer the first longitudinal growth cones. Projections from these cells immediately fuse with contralateral axon bundles at the midline and remain trapped within each neuromere. Early projections of the MP neurons in moderate *slit* mutants initially extend distinct growth cones, despite a pronounced displacement of the MPs towards the midline. As the MP projections extend to meet the neighboring neuromere they fall short and fuse within the midline. Growth cones emanating from the pCC project inappropriately across the midline where they appear to fuse with the posterior projections from the contralateral MPs. In contrast, MP and pCC morphology is indiscernible from wild-type in mild *slit* hypomorphs. Processes from the MP neurons develop normally, making appropriate projections towards neighboring neuromeres, yet the pCC growth cones continue to make aberrant projections across the midline. Severe and moderate mutations in *slit* cause dramatic pathfinding errors in the early projections from both the MP and pCC neurons that result in a collapse of axon tracts towards the midline. Although these errors are not observed in the MP projections in mild *slit* phenotypes, the pCC neurons continue to make inappropriate projections across the midline, a point I will address later.

From the initial pioneers that form the basis of the wild-type axon scaffold, other neurons extend their growth cones along these axon tracts and either extend across the midline within the axon commissures or remain ipsilateral to the midline and extend A/P to it. The A/P projections along the midline are notably diminished in stage 16 severe *slit* mutants, suggested by the reduction in antibody labeling of intersegmental axons. Large

bundles of axons are observed knotted within each neuromere that we understand to represent the increased number of inappropriate projections across the midline observed in early stages of development. The number of intersegmental axons detectable by BP102 dramatically increases in moderate *slit* mutants. Although individual groups of longitudinal axon tracts remain fused to each other, they are observed to separate from the midline. Consequently, in areas where axons separate it is possible to detect the increased number of inappropriate axon projections across the midline. Mutations in *slit* resulting in mild CNS phenotypes suggest that the most medially longitudinal axons are most sensitive to Slit signaling. Both P-element induced mutations (that reduce levels of Slit expression), and mild EMS alleles result in pathfinding errors in only the most medial longitudinal axon fascicles, represented in part by the projections of the pCC neurons. In each category of *slit* CNS phenotypes, evidence indicates that the medial axon fascicles have a greater propensity to cross the midline. The role of Slit in establishing a midline boundary for the developing CNS does not appear to be a simple linear signaling event. More likely Slit establishes a gradient of signal, to which medial axons have a high threshold and more lateral axons respond at a lower threshold. This does not explain why even during initial pathfinding events, pCC and not MP growth cones are influenced by mutation in *slit* causing mild phenotypes. The means by which these axons respond to Slit as a signal is unclear. Perhaps multiple receptors result in neurons that are independently sensitive to Slit gradients or downstream mechanisms determine individuals cells response to the strength of Slit signal. In fact, if Robo1 is the repellent receptor for Slit, three distinct Robo receptors have been identified that are distributed differently along the three longitudinal axon fascicles (Dickson *et al*, 2000).

If each of these Robo receptors responds with a different sensitivity to Slit, this would explain varying sensitivities to a Slit ligand in different longitudinal fascicles.

Muscle insertions are dependent on Slit signaling

Previously, we have described the localization of Slit protein to the points of muscle insertion at the muscle apodemes. By identifying abnormalities in muscle pattern formation in *slit* mutant embryos associated with this localized Slit labeling, we are able to conclude that Slit signaling is important in muscle development. Furthermore, the severity of muscle abnormalities observed in different *slit* mutants correlates with the established gradient of CNS phenotypes.

Severe mutations in *slit* result in a gross distortion of both the medial and ventral muscle apodemes. Growth cones of muscles derived from the medial apodemes that normally insert underneath the lateral edge of the nerve cord, instead project directly over it and insert into the contralateral epidermis. Distortions observed in the muscle apodemes are likely a result of the inappropriate projections and insertions of the muscle growth cones. Consequently, in moderate *slit* alleles where fewer muscles insert over the midline, the abnormalities found in muscle apodemes are less severe. As in CNS phenotypes observed in mild *slit* mutants, muscle abnormalities are minor and result in only occasional pathfinding errors that do not overtly affect the muscle apodemes. The role of Slit in both CNS and muscle development appears to directly related to the function of growth cone guidance.

Both neuronal and muscle growth cones depend on cues provided in part by the extracellular matrix in order to guide them to extremely specialized sites of contact (Muller & Kypta, 1995;Tessier-Lavigne & Goodman, 1996;Mueller, 1999). Three

structural domains within Slit have been associated with signaling and protein-protein interaction in the ECM; however, the G-domain shares close homology with Agrin and Laminin (Gesemann *et al*, 1996) suggesting that it is most likely to participate in muscle growth cone guidance. Additionally, we have not been able to determine whether *Slit* is natively expressed at the sites of muscle insertion or is exported there, leaving us the question as to how Slit becomes localized within these regions. A cleaved C-terminal product of Slit including the G-domain would be small (55 kDa) and highly diffusible making it an excellent candidate for muscle growth cone guidance. Yet, prior to the generation of G-Domain specific antibodies and an ultra structural analysis of muscle morphology the role of the *slit* G-domain in muscle guidance will be difficult to determine.

Slit has a singular role in heart morphogenesis

Drosophila heart morphogenesis is marked by the orderly migration of cardioblast cells at the leading edge of the dorsal vessel where they eventually pair with their adjacent partners at the dorsal midline forming a uniform tube that is the *Drosophila* heart. Perturbed migration of the cardioblast cells was observed in all *slit* mutant alleles resulting in clusters of cardioblasts that delayed dorsal closure. Delayed dorsal closure was exacerbated by the formation of blisters where cardioblast clusters failed to pair with their contralateral counterparts causing the heart tube to form multiple breaks. Recent studies show that cell-cell adhesion is critical to normal heart development in order to facilitate exchange of short range signaling molecules (Haag *et al*, 1999). Components involved in maintaining cell adhesion during heart morphogenesis include *faint sausage, shotgun/DE-cadherin, laminin A,* and *fas*. Fas and potentially other, as yet unidentified

molecules are responsible for the adhesion and alignment of ipsilateral cardioblasts, whereas, Shotgun controls the contact between opposite cardioblasts (Haag *et al*, 1999). The mutant phenotype observed in all *slit* mutants resembles the loss of contact or communication between ipsilateral cardioblasts as they migrate dorsally. As an ECM protein with a unique combination of protein motifs, it seems reasonable to assume that the localized expression of *Slit* beginning in the cardiac precursors introduces Slit as a possible candidate to represent those other, as yet unidentified proteins alluded to by Haag *et al.* (1999).

MG depend on Slit signaling to migrate appropriately

Severe mutations in *slit* cause the MG to become ventralized and reduced in number. We know that this disruption of MG positioning does not break the close association found between the MG and commissural axons, but is this a secondary phenotype caused by perturbations in the axon scaffold or does Slit perform a separate role in establishing MG positions? Antibody staining to Wrapper indicates that even in severe alleles of Slit the MG are still capable of extending processes to ensheath local axons. Furthermore, ventralization of the MG occurs prior to appearance of the early midline axon growth cones, suggesting that Slit has a role in establishing the position of the MG at the dorsal boundary of the ventral midline very early in development. MG numbers are only reduced in severe mutations; however even in the mildest *slit* phenotypes the MGM and MGP can be found ventrally displaced. The MGA that do not migrate significantly in the wild type embryos maintain their position near the anterior commissure (Klambt *et al*, 1991). Perhaps Slit has an independent role that is involved in the migration of the MGM and MGP that maintains their association as they form the

posterior commissure. As in the formation of the heart, the close association between related cell types is essential for short distance signaling and tissue morphology. Perhaps *slit* is involved in a similar role in the MG.

Slit expression

We have identified 13 mutations in the *slit* locus that affect CNS, MG, muscle, and heart development producing a range of phenotypes described above. All *slit* mutants were found to produce a detectable *Slit* transcript in tissues where wild-type expression was observed. Protein expression was detectable in 9 of the 13 alleles with the exceptions of $slit^{IG107}$, $slit^{GA20}$, and $slit^{1912}$. $slit^{IG107}$ has been reported as a phenotypic null in previous publications (Rothberg *et al*, 1988;Rothberg *et al*, 1990). We believe however, that the absence of detectable intersegmental axons observed in embryos deficient for *slit* (*Df(2R)*WMG) differentiates them from phenotypes described in $slit^{IG107}$, $slit^{GA20}$, and $slit^{1912}$ mutant embryos. These *slit* mutant embryos all develop some intersegmental axons. The limited sensitivity of the monoclonal antibody and the detection of Slit transcript in severe mutant embryos suggests that $slit^{IG107}$, $slit^{GA20}$, and $slit^{1912}$ may not represent true phenotypic nulls, and we have chosen to refer to them as severe hypomorphs from here on in.

Mutations in *slit* affect larval viability

Screens of EMS induced mutations provided us with nine alleles of *slit* that were adult lethal, including 3 P-element induced alleles that resulted in adult lethality. We have identified roles for Slit in the embryonic CNS, MG, muscle pathfinding, and in the morphogenesis of the heart. Defects observed in the MG, muscles, and cardioblast cells in themselves are not be expected to alter embryonic viability, but would likely prove

vital for the larva (Haag *et al*, 1999;Fogerty *et al*, 1994). Perturbations described in the axon scaffold alone can be sufficient to arrest development in embryonic mutants (Klambt & Goodman, 1991a;Klambt *et al*, 1991). Severe mutations associated with *slit* rarely hatch, and those that do, die immediately thereafter. Although, a small proportion of larva of moderate *slit* alleles survive to pupariate from the moderate *slit* alleles, viable larva are diminished in size, uncoordinated and never eclose after pupariation. A much higher proportion of embryos from mild *slit* alleles survive as larva. These larva appear sluggish and uncoordinated, but under supportive conditions low numbers survive to eclose as adult *slit* mutants, suggesting that the CNS phenotype is not totally penetrant in mild *slit* alleles. The behaviour of viable larva indicates problems associated with coordinated muscle movements necessary for the contractions that larva employ to move them through their environment (Bunch *et al*, 1998). Additionally, the diminished size and lethargy noted could be associated with deformations of the heart tube or related defects. Until a more detailed analysis of post embryonic defects caused by mutations in *slit* can be addressed, we can only conclude that the range of phenotypes associated with CNS and muscle defects foreshadows the expected viability of the mutant embryo.

Point mutations in Slit correspond with observed phenotypes

The characterization of EMS induced alleles of *slit* was undertaken with the hope that observed mutant phenotypes could later be attributed to domain specific mutations in *slit* coding regions. Nine lethal EMS induced mutations which map to the *slit* locus in region 52D on the second chromosome have been selected and ranked based on the severity of their mutant phenotype. Three of four mutations that resulted in severe *slit* phenotypes occurred in the LRR and the 4th generated a premature Stop codon at the end

of the 3rd EGF-like repeat upstream of the native splice site. Two of these mutations generated single amino acid changes at the beginning of the beta-pleated-sheet of the 1st and 2nd LRR and the last produced a deletion that introduced a premature STOP codon into the reading frame of the 4th LRR. Truncated forms of Slit removed 1/3 of the complete protein but were not immunodetectable. Therefore we could not analyze their stability or pattern of distribution. Point mutations in the LRR generated conservative coding changes resulting in severe mutant phenotypes where Slit was immunodetectable. Based on the sensitivity of the *slit* phenotype to changes in the LRR, this would suggest that the LRR domains play an important role in Slit function in the CNS.

Of the three mutations associated with moderate *slit* phenotypes, two produced premature STOP codons, only one of which was detectable with an antibody to Slit. A single deletion occurring downstream of the native cleavage site produced a premature STOP early in the G-Domain of Slit. Immunodetection of Slit protein in the MG and cardioblasts verified that a form of Slit containing all the LRR and 6 EGF-like repeats was expressed and localized within the native *slit* expressing cells. Attempts to confirm Slit labeling in the muscle apodemes failed; however, inconsistencies observed in the sensitivity of the antibody indicate that we cannot rule out the presence of Slit at these sites. Moderate CNS phenotypes described in $slit^{550}$ mutant embryos exhibit clear separation of longitudinal axons and a substantial increase in the number of intersegmental axons. At least in part, the presence of Slit with intact LRR and EGF domains is sufficient to establish a semblance of the midline boundary that is removed by other mutations within the LRR domain. One other moderate *slit* allele was attributed to a single amino acid change found at the end of the 2nd LRR repeat. Similar to $slit^{550}$,

slit^{532} mutants developed a partial separation and thickening of the longitudinal axon fascicles that suggests, regions within the LRR domains are differentially sensitive to changes in amino acid sequence. Of the nine EMS alleles reviewed in this study, 7 have been associated with severe or moderate CNS phenotypes that taken in context with viability data suggests that mutations in *slit* affecting CNS development are largely embryonic lethal.

Failure to locate mutations responsible for two alleles of *slit*, one mild and one severe, was attributed to the likelihood that these point mutations occurred in regulatory regions of the gene or regions controlling splicing. As was observed in P-element induced alleles of *slit*, the reduction of *Slit* transcription was sufficient to generate a range of CNS phenotypes. The gradient of sensitivity to Slit signaling observed at the midline leads us to believe that longitudinal axon tracts have different receptors with which they respond to the Slit at the midline. Therefore, a reduction of transcribed *Slit* would reduce the availability of Slit in midline cells and cause aberrations in the axon scaffold.

Genetic screens of the 52D chromosomal region focused on isolating lethal EMS induced mutations that resulted in mutant CNS phenotypes. Mutations in *slit* specific to heart or muscle function in all likelihood are not lethal or can be corrected for during development, and therefore would not be detected in our mutant screening method. It will be necessary to focus on isolating or generating mutations that specifically affect muscle and/or heart morphology in order to further pursue Slit's function in these tissues.

Slit demonstrates repellent functions at the midline boundary

The total collapse of the axon scaffold observed in embryos deficient for *slit* is remarkable. Similar phenotypes observed with mutation in *sim*, in which MEC and their lineages fail to differentiate (Crews *et al*, 1988), and with mutation in members of the '*spitz* group' that affect midline cell survival (Klambt & Goodman, 1991b;Klambt & Goodman, 1991a) involve the development of the MG. In both these examples, the collapse of the axon scaffold is the result of the removal of glia cells that provide the necessary guidance cues required for establishing the axon pathways that form the axon scaffold (Tessier-Lavigne & Goodman, 1996). Early analysis of *slit* function led researchers to believe that *slit*, much like *sim* and the *spitz* groups genes, was involved in early differentiation and cell survival (Rothberg *et al*, 1990). Early patterns of expression, the EGF-like structure, and the midline fusion phenotype strongly pointed towards a role for *slit* in the ECM functioning as a growth factor for the developing MGs (Rothberg *et al*, 1990).

In this investigation we have shown that in the absence of Slit, MG do not lose their association with midline commissures, or their ability to protect and ensheath local axons that form them. Additionally, mutations in *slit* altering signaling to early growth cones, causes axons to either collapse onto the midline where they remain throughout development or cross the midline, inappropriately fasciculating with contralateral longitudinal axons. The characterization of a range of midline phenotypes attributed to different mutations in *slit* and reductions in Slit expression suggest that subsets of longitudinal axons differentially respond to a gradient of Slit signaling at the midline. In this light Slit appears to be required in order to establish a repulsive barrier that selectively permits commissural axons to cross the midline but repels longitudinal axons

at predetermined distances from the midline, based on their responsiveness to the repellent signaling. Furthermore, the identification of point mutations in LRR of Slit that cause partial or complete collapses of the axon scaffold suggest the LRR regions in Slit are required for establishing the proposed repulsive signaling barrier at the midline. Genetic data presented here suggests that *slit* may function as a repellent ligand in the *Drosophila* midline, a role that is dependent on intact LRR domains. In the next chapter we will focus on verifying this role by using transgenic *slit* to restore Slit to the midline of *slit* mutant embryos. In addition, we will investigate the role of Slit and truncated forms of Slit in rescuing the midline phenotype of *slit* mutant embryos and in ectopic patterns of expression.

Slit is a repulsive ligand in the *Drosophila* CNS

CHAPTER 3

In chapter three we will determine what role Slit protein performs *in vivo* and the domains of Slit that are important in *slit* function. First, we will attempt to rescue the *slit* mutant phenotype using complete and truncated *slit* transgenes. Following this, we will investigate the role of Slit *in vivo* using overexpression and ectopic expression assays in different tissues. Finally, using *slit* transgenes with internal deletions we will attempt to refine our understanding of specific structural domains by over expressing and ectopically expressing each *slit* transgene in different tissues.

MATERIALS AND METHODS 3

Fly Maintenance

Refer to Methods Section 1.

Genetic stocks

slit^{IG107} was isolated by Nüsslein-Volhard (Nüsslein-Volhard, 1984) and restored to a wild-type background prior to study. Stocks were backcrossed to a stock deficient for *slit* (Df(2R)WMG) in order to verify the lack of complementation and analyzed based on a *CyO-P{eng-lacZ}* marked balancer. Rescue experiments were conducted using: a lethal insert of *P{slit1.0-GAL4}* (Christian Klämbt) and *P{sim-GAL4}* (Nambu *et al.*, 1990) maintained in a *slit*^{IG107} background. Overexpression and ectopic expression was achieved using *P{slit1.0-GAL4}, P{sim-GAL4}, P{en-GAL4}* (Orihara *et al.*, 1999); *P{scab-GAL4}* (C. Goodman), *P{sevenles-GAL4}, P{eyeless-GAL4}, P{C321-GAL4}, P{C15J2-GAL4},* and *P{elav*^{C155}*-GAL4}* (Lin & Goodman, 1994) as described below.

Genomic clones and cDNA

Refer to Methods Section 1.

Transgenic constructs

Using the newly generated complete *slit* cDNA in pBS KSII+ we generated a restriction map of the *slit* coding region. From this map, nine transgenic constructs were created as follows (Fig. 3.1):

-*slit* complete [HindIII (-8bp) to SpeI (4461bp)]

-*slitΔL1-L4* [Bpu1102I (134) to BstEII(2539) treated with Mung Bean Nuclease (Gibco-BRL, 18019-018)] which removed a majority of the Leucine-rich repeats 1-4 including most of the sequence downstream of the start codon

-*slitΔL1.5-L4* [MluI (569) to DraII (1679,2579) treated with Mung Bean Nuclease] which removed from mid-Leucine 1 to the end of Leucine 4

-*slitΔL3-L4* [DraII (1679-2579) treated with T4 DNA Polymerase (Gibco-BRL, 18005-017)] removed a majority of the third Leucine-rich repeat to the end of the 4th

-*slitΔL1-L3* [BsmI (170,386,940,2288)] removed from slightly downstream of the start codon to very early in the 4th Leucine-rich repeat

-*slitΔE2-E6* [NsiI (2913) to MunI (3463) treated with Mung Bean Nuclease] removed the 2nd to the 6th EGF repeats

-*slitΔE2-E7* [ClaI (2913) to SfiI (4231) treated with Mung Bean Nuclease] removed from the 2nd EGF to the last EGF repeat which also removed the ALPS (Agrin, Laminin, Proline) motif and the Cysteine knot

-*slitΔG-E7* [SspBI (3733) to SfiI (4231) treated with T4 DNA polymerase] removed the ALPS motif and the cysteine knot

-*slitΔG* [MamI (3658) to SalI (4000)] removed a majority of the ALPS motif

The complete *slit* cDNA in pBS(KSII+) was digested and the cut ends were polished as indicated above. The cut plasmids were isolated by phenol 1:1 and then chloroform 1:1 extraction, precipitated with 1/10th volume of 3M NaAcetate in 2.5 volumes of 100 % chilled ethanol and then washed twice in 70% ethanol. The dried DNA was resuspended in 7µl of sddH_2O to which was added 2µl of 5X T4 DNA Ligase

Buffer (Gibco-BRL, 15224-025) and 1 µl or 5U of T4 DNA Ligase. The mixture was vortexed, briefly centrifuged and incubated at 11°C for 20+ hours. The ligation was heated to 65°C for 15 minutes to stop the reaction, briefly centrifuged, and 1µl was removed and diluted in 9 µl of sddH_2O. The DNA was placed on ice and 50 µl of DH5α Competent Cells (Gibco-BRL, 18265-0017) were carefully added to the tube, mixed and left to incubate for one hour on ice. The cells were then heat shocked at 42°C for 15 seconds, placed on ice for 2 minutes and finally incubated in 950µl of 1x LB broth while been shaken at 37°C for 60 minutes. The transformed cells were distributed evenly onto LB agar plates containing 100 µg/ml of ampicillin (Gibco-BRL, 11593-019) at various concentrations and incubated at 37°C until colonies were detectable. Positive colonies were isolated using a Qiagen miniprep kit (12123) and screened for the appropriately sized insert by restriction digest. Plasmids containing the correct sized insert were sequenced to verify appropriate reading frames around the deleted DNA.

In order to facilitate cloning of each construct into the *Drosophila* transformation vector *pUAST*(Brand & Perrimon, 1993), KpnI phosphorylated polylinkers (New England BioLabs, 1041) were added to the 3' end of the *slit* cDNA in place of the XbaI restriction site in the Multiple Cloning Region (MCR) of pBS(KSII+). Truncated constructs were digested with XbaI in 20 µl of 1x Restriction Buffer (Gibco-BRL, 15226-038) for 3 hours at 37°C. Cut ends were polished by directly adding 1 µl of 100mM dNTPs (Gibco-BRL, 10297) and 1µl of Klenow (Gibco-BRL DNA Polymerase I Large (Klenow) Fragment, 18012-021) to the digested DNA and incubated on ice for 15 min. The reaction was stopped and cleaned by phenol extraction and the dried DNA was eluted in 6 µl of sddH_2O. Polylinkers (1µl, 1µg) were added to the eluted DNA along

with 2µl of T4 5x DNA Ligase Buffer and 1 µl of T4 DNA Ligase. The ligation and transformation were completed as above and positive colonies were verified by digestion and sequencing. The transformation vector *pUAST* and each *slit* construct was digested with KpnI and cleaned by phenol extraction. The plasmid vector was dephosphorylated with 1U of shrimp Alkaline Phosphatase (Roche, 1758250) and combined with each *slit* cDNA at a ratio of 30 fmoles(vector): 90 fmoles(insert) to a total of 100 ng. The DNA was ligated and transformed as previously indicated, after which the positive colonies were again screened by restriction digest and sequenced to determine orientation and efficacy.

Plasmid DNA for transformations was prepared with Qiagen's EndoFree Maxi Kit (12362) and combined with endotoxin free helper vector DNA (pπ25.1wc,(Karess & Rubin, 1984;Rubin *et al*, 1985)) in a ratio of 5:1 respectively to a total of 3 µg. For direct transformation it is recommended that the helper vector be injected at a concentration of 50-150 µg/ml and the transformation vector to be inserted between 300 and 1000 µg/ml(Rubin & Spradling, 1982;Spradling & Rubin, 1982). The pooled DNA was precipitated with 1/10th volume of 3M NaAcetate and 2.5 volumes of 100% chilled ethanol, washed 3x with 70% ethanol, after which the dried pellet was resuspended in 50µl of injection buffer (5 mM KCl; 0.1mM PO4 [pH7.8]). Glass Capillary Filaments (FHC, 30-30-0; 1.0mm OD; 0.75 mm I.D.) were pulled in half to produce one 5mm long shank with a 200 µm O.D. and a 2 mm tip with a 10 µm O.D. using a Flaming/Brown type Micropipette/Patch puller-P97 (300-97A). Each tip was gently broken against a piece of capillary glass and backfilled with endofree DNA respective to each construct. Injection buffer with DNA was pressure injected into yw- embryo stocks aged,

divitillinized, and dehydrated for 1.5 hours. Embryos were prepared and injected on a Leica DM IL inverted tissue culture microscope as described in Roberts (Roberts, 1986).

Transgenic stocks

Larva from each injected transgenic construct were collected and pooled in pairwise tubes containing fly food and dry yeast. Individual eclosing flies were crossed to the appropriate *yw*⁻ adults and raised at 22°C followed by regularly screening of the F1 progeny. Flies exhibiting eye pigmentation were isolated and crossed again to *yw*- adult stocks after which, stocks were purified for their eye marker. Each purified stock was crossed to various marked balancers in order to map the general location of the P-element insertion and then tested for slit expression by crossing to a *P[eng-gal4]* line (Fig. 3.2) and staining for mAb Slit. From transgenic stocks with insertions on the 2nd chromosome flies were recombined with *slit²/CyO[eng-lacZ]* and verified while insertions on the X or 3rd chromosome were crossed into *slit²/Cyo[eng-LacZ]* and stabilized.

Rescue and Overexpression stocks

In order to facilitate rescue of the *slit²* phenotype, two midline glial cell drivers *P[sim-gal4]* and *P[slit1.0-gal4]* were recombined into the *slit²* genetic background and then crossed to each of the transgenic *slit* constructs already in *slit* null backgrounds. The resultant progeny were fixed and immunolabelled for mAb 1D4, BP 102, α-sim, mAb Slit, and the *P{LacZ}* balancer.

Ectopic and midline overexpression of the *slit* transgenes was driven by a variety of *P{GAL4}* lines characterized in Appendix D. Midline overexpression was attained by crossing the various *slit* transgenes with the *P[sim-gal4]* and *P[slit1.0-gal4]* stocks and

immunolabelling both the F1 and F2 embryos with mAb Slit, BP102, and mAb 1D4. The ectopic overexpression patterns were classified into two categories: segmental, whose pattern of expression was confined within each segment boundary; and general, whose pattern of expression extended across boundaries and arose in a variety of embryonic tissues. Segmental expression stocks included *P[eng-gal4]* and *P[scab-gal4]* and the general expression stocks consisted of *P[elav-gal4]*, *P[C15J2-gal4]*, *P[C321-gal4]*, *P[sev-gal4]*, *P[eyeless-gal4]*, and *P[ap-gal4]*. Each of these stocks was crossed with each of the *slit* transgenic stocks and immunolabelled with mAb Slit, BP102, and mAb 1D4.

Embryos demonstrating both mAb Slit labeling in the respective *P{GAL4}* patterns of expression were mounted whole in salicylate to be visualized under a Zeiss Axiophot microscope at 63X oil objective and documented on Kodak T-64 ecktachrome colour slide film. Constructs that deleted the epitope to mAb slit failed to stain during the screening procedure and were selected based on the axon tract phenotype that differed remarkably from control samples and their ability to rescue the *slit* mutant CNS phenotype.

Tissue *in situ* hybridization

Refer to Methods Section 1.

Immunocytochemistry

Drosophila embryos were collected on apple juice agar plates and aged from 16-30 hours at 22°C. Fixation and immunocytochemistry was adapted from Patel (1994). mAb slit (1:200), mAb 1D4 (1:4), BP102 (1:2) (N. Patel, C. Goodman, G.), and α β-gal

(Cappel, 55976) were diluted in phosphate-buffered saline (PBS) as indicated and processed as in methods section 1.

Data presentation

Refer to Methods Section 1.

RESULTS 3

slit transgenes

In order to generate a structural and functional understanding of Slit we created a number of *slit* transgenes, one that represented the entire protein and others that lacked selected protein motifs. The structure of these constructs is represented in Figure 3.1. A complete *slit* cDNA was constructed with 3 bp of 5' UTR and a hemaglutinin epitope tag that incorporated the original *slit* 3' terminus (Appendix C). Deletion constructs that removed regions of Slit protein motifs were generated from the complete *slit* transgene and then sequenced for cloning errors.

Eight different *slit* deletion constructs were generated. Four constructs removed regions of the LRR that included Leucine 1-4 (*P{UAS-slitΔL1-L4}*), Leucine 1-3 (*P{UAS-slitΔL1-L3}*), half of Leucine 1-Leucine 4 (*P{UAS-slitΔL1.5-L4}*), and Leucine 3-4 (*P{UAS-slitΔL3-L4}*). One deleted the EGF-like repeats 2-6 (*P{UAS-slitΔE2-E6}*), one the EGF-like repeats 2-7, that also removed the G-domain (*P{UAS-slitΔE2-E7}*), and two constructs that lacked the G-domain, one including EGF 7 (*P{UAS-slitΔG-E7}*), and one with just the G-domain (*P{UAS-slitΔG}*). Sequencing and *in vitro* translation of each *slit* transgene confirmed that each construct maintained the intended reading frame and generated the predicted protein (data not shown).

To study the effect of Slit and modified Slit proteins *in vivo*, *slit* transgenes were sub-cloned into a *Drosophila* transformation vector containing a mini-white reporter gene and injected with the helper plasmid pπ25.1 into early embryos from a fly stock deficient for the {w+} eye colour gene. Transgenic flies generated from each one of these constructs were purified and P-element insertions were mapped and characterized. Using

Figure 3.1 Schematic of *slit* transgene constructs.

A complete *slit* cDNA was prepared that included all the characterized protein motifs as labeled. Deletion constructs were engineered that removed regions of cDNA coding different protein motifs as indicated in purple. Deletion constructs were sub cloned into the *Drosophila* transformation vector *P{UAST}*, and used to generate transgenic flies with each *slit* transgene.

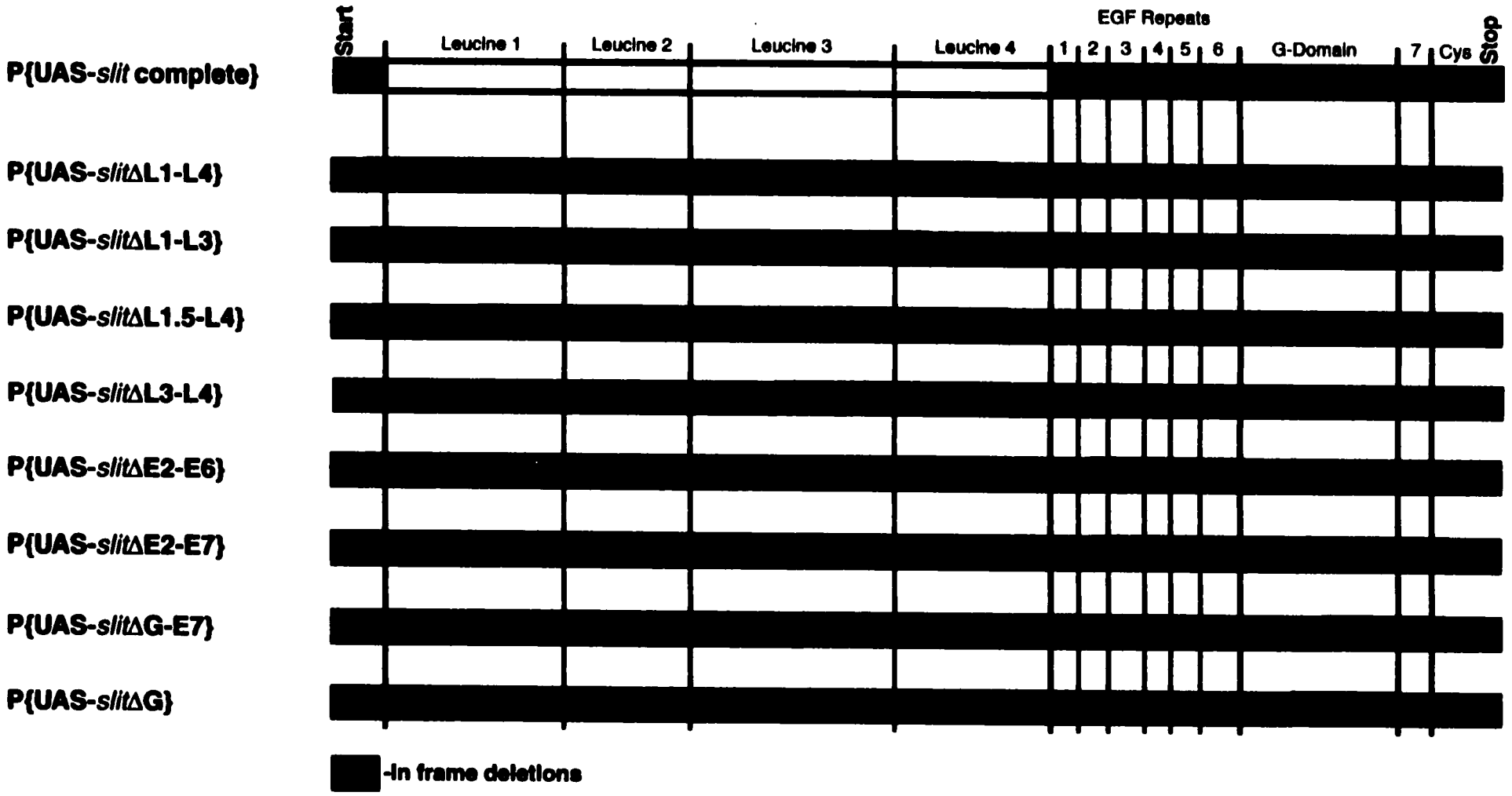
Start
Leucine 1
Leucine 2
Leucine 3
Leucine 4
EGF Repeats
1
2
3
4
5
6
G-Domain
7
Cys
Stop
P{UAS-slit complete}
P{UAS-slitΔL1-L4}
P{UAS-slitΔL1-L3}
P{UAS-slitΔL1.5-L4}
P{UAS-slitΔL3-L4}
P{UAS-slitΔE2-E6}
P{UAS-slitΔE2-E7}
P{UAS-slitΔG-E7}
P{UAS-slitΔG}
-In frame deletions

either a Slit monoclonal antibody or a *Slit in situ* probe, *slit* transgene expression driven by a *P{engGAL-4}* driver was screened for each construct (Fig. 3.2). Fly stocks that demonstrated strong transgene expression were identified and subsequently recombined into a $slit^{lG107}$ genetic background.

Transgenic Slit expression rescues *slit* mutant phenotypes

Embryos mutant for *slit* are characterized by a collapse of the ladder-like axon scaffold and the displacement of the MG. Assuming a direct role for Slit in the establishment of a normal axon scaffold, the expression of a functional transgenic Slit in $slit^{lG107}$ MG should rescue the *slit* associated midline phenotype. Furthermore, similar expression of *slit* deletion constructs should aid in the isolation of functional domains of Slit responsible for the observed midline phenotype.

Slit expression was observed in the wild type MG at the midline of the anterior and posterior commissures labeled (Fig. 3.3, A black arrow). When a complete *slit* transgene was expressed in these cells (*P{Slit1.0GAL-4}*) in a $slit^{lG107}$ background, a partial rescue of the mutant CNS phenotype was observed (B). The longitudinal intersegmental axons had separated to reveal the anterior and posterior commissures reminiscent of a mild *slit* hypomorph. *slit* deletion constructs that disrupted Leucine Rich domains (C, (*P{UAS-slitΔL1-L4}*); D, (*P{UAS-slitΔL1-L3}*); E, (*P{UAS-slitΔL1.5-L4}*); F, (*P{UAS-slitΔL3-L4}*) did not produce a noticeable midline rescue. Strong transgene expression was observed in these embryos (data not shown). Deletion of the EGF-like repeats (G, *P{UAS-slitΔE2-E6}*) enhanced the CNS rescue over that observed with the complete *slit* cDNA. Intersegmental axons appeared thicker (arrow) and the separation of the longitudinal fascicles was more pronounced. When both the G-domain and EGF-

Figure 3.2 Embryos expressing *slit* transgenes label with probes to Slit protein and RNA The expression pattern of *P{UAS-tau lacZ}* in the intersegmental boundaries generated by *P{engGAL4}* is visualized with an antibody to β-galacotosidase in sagittally mounted embryos (A, arrow). The expression of each *slit* transgene is readily detected (arrowhead) at the intersegmental boundaries in embryos B (*P{UAS-slit complete}, slit* mAb); C (*P{UAS-slitΔL1-L4}, slit* mAb); D (*P{UAS-slitΔL1-L3}, slit* mAb); E (*P{UAS-slitΔL1.5-L4}, slit* mAb); F (*P{UAS-slitΔL3-L4}, slit* mAb); G (*P{UAS-slitΔE2-E6}, slit* RNA); H (*P{UAS-slitΔE2-E7}, slit* RNA); I (*P{UAS-slitΔG-E7}, slit* mAb); J (*P{UAS-slitΔG}, slit* mAb) were *slit* is ectopically expressed (*P{engGAL4}*) and labeled as indicated.

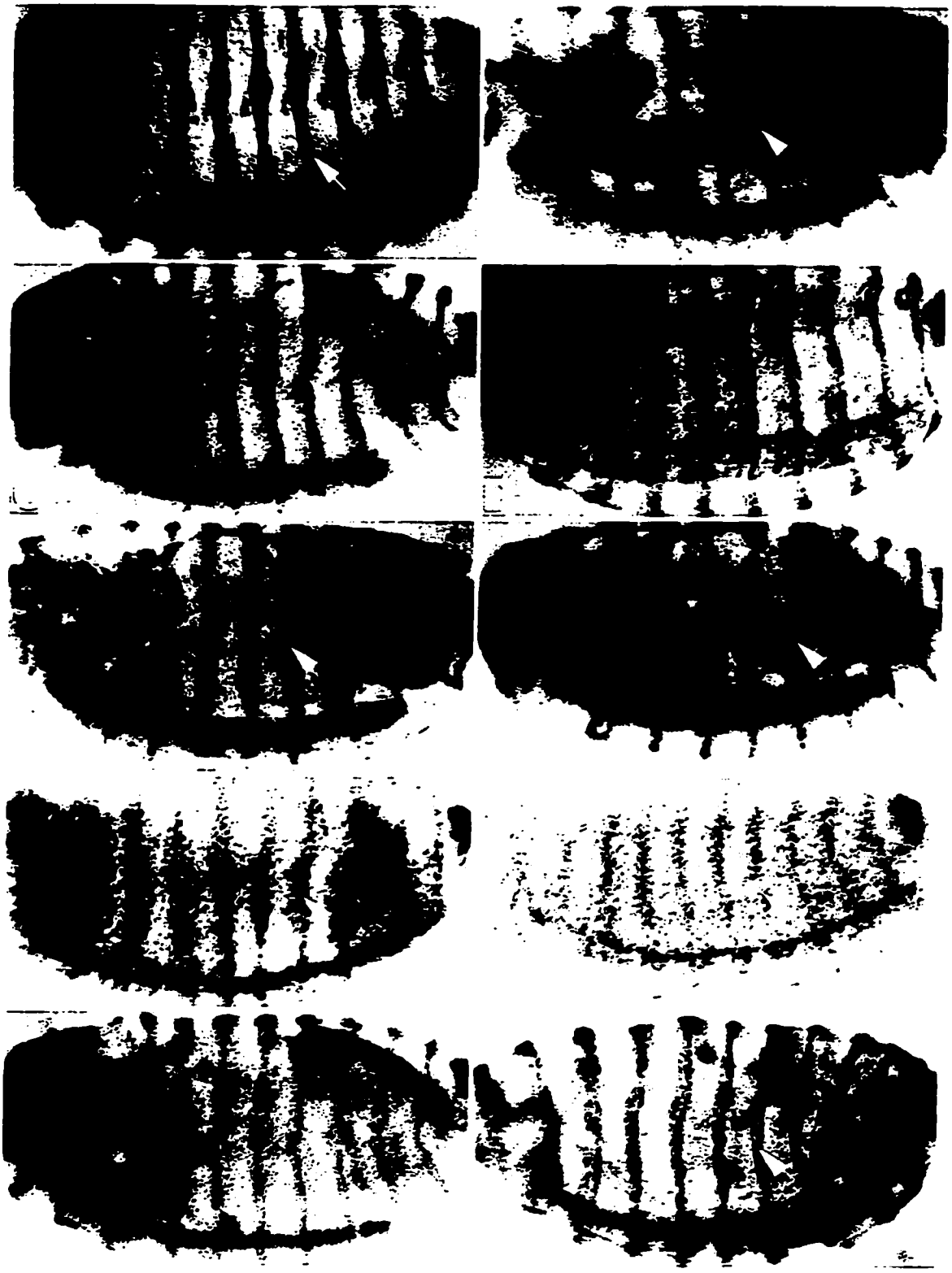

Figure 3.3 Do *slit* transgenes restore *slit* function in the ventral midline? Native Slit (black) is expressed in the MG overlying the axon commissures of a BP102 labeled (brown) wild type nerve cord (A, black arrow). Partial restoration of midline commissure architecture (B, arrowhead) and longitudinal axon fascicles (arrow) is obtained in $slit^{lG107}$ mutant embryos expressing *P{UAS-slit complete}* in the midline cells (*P{slit1.0GAL4}*, $slit^{lG107}$/*P{UAS-slit complete}*, $slit^{lG107}$ embryos). Embryos expressing *slit* transgenes that lack portions of the Leucine protein motifs in the midline cells (*P{slit1.0GAL4}*) fail to restore midline commissures [(C, *P{slit1.0GAL4}*, $slit^{lG107}$/*P{UAS-slitΔL1-L4}*, $slit^{lG107}$) , (D, *P{slit1.0GAL4}*, $slit^{lG107}$/*P{UAS-slitΔL1-L3}*, $slit^{lG107}$) , (E, P*{slit1.0GAL4}*, $slit^{lG107}$/ *P{slit1.0GAL4}*, $slit^{lG107:}$ *P{UAS-slitΔL1.5-L4}*/ *P{UAS-slitΔL1.5-L4}*) , (F, *P{slit1.0GAL4}*, $slit^{lG107}$/ *P{slit1.0GAL4}*, $slit^{lG107:}$ *P{UAS-slitΔL3-L4}*/ *P{UAS-slitΔL3-L4}*)]. The *slit* transgene in which the EGF2-6 domains are deleted (G) substantially restores the commissure architecture of embryos in which it is expressed (*P{slit1.0GAL4}*, $slit^{lG107}$/*P{UAS-slitΔE2-E6}*, $slit^{lG107}$). A similar transgene encoding a protein that also removes the G-domain and EGF7 only partially restores axon commissures in embryos (H, P*{slit1.0GAL4}*, $slit^{lG107}$/ *P{slit1.0GAL4}*, $slit^{lG107}$; *P{UAS-slitΔE2-E7}*/ *P{UAS-slitΔE2-E7}*) whereas transgenes with only the G-domain and EGF7 (I, *P{slit1.0GAL4}*, $slit^{lG107}$/*P{UAS-slitΔG-E7}*, $slit^{lG107}$) removed or solely the G-domain (J, P*{slit1.0GAL4}*, $slit^{lG107}$/ *P{slit1.0GAL4}*, $slit^{lG107:}$ *P{UAS-slitΔG}*/ *P{UAS-slitΔG}*) effectively restore Slit function.

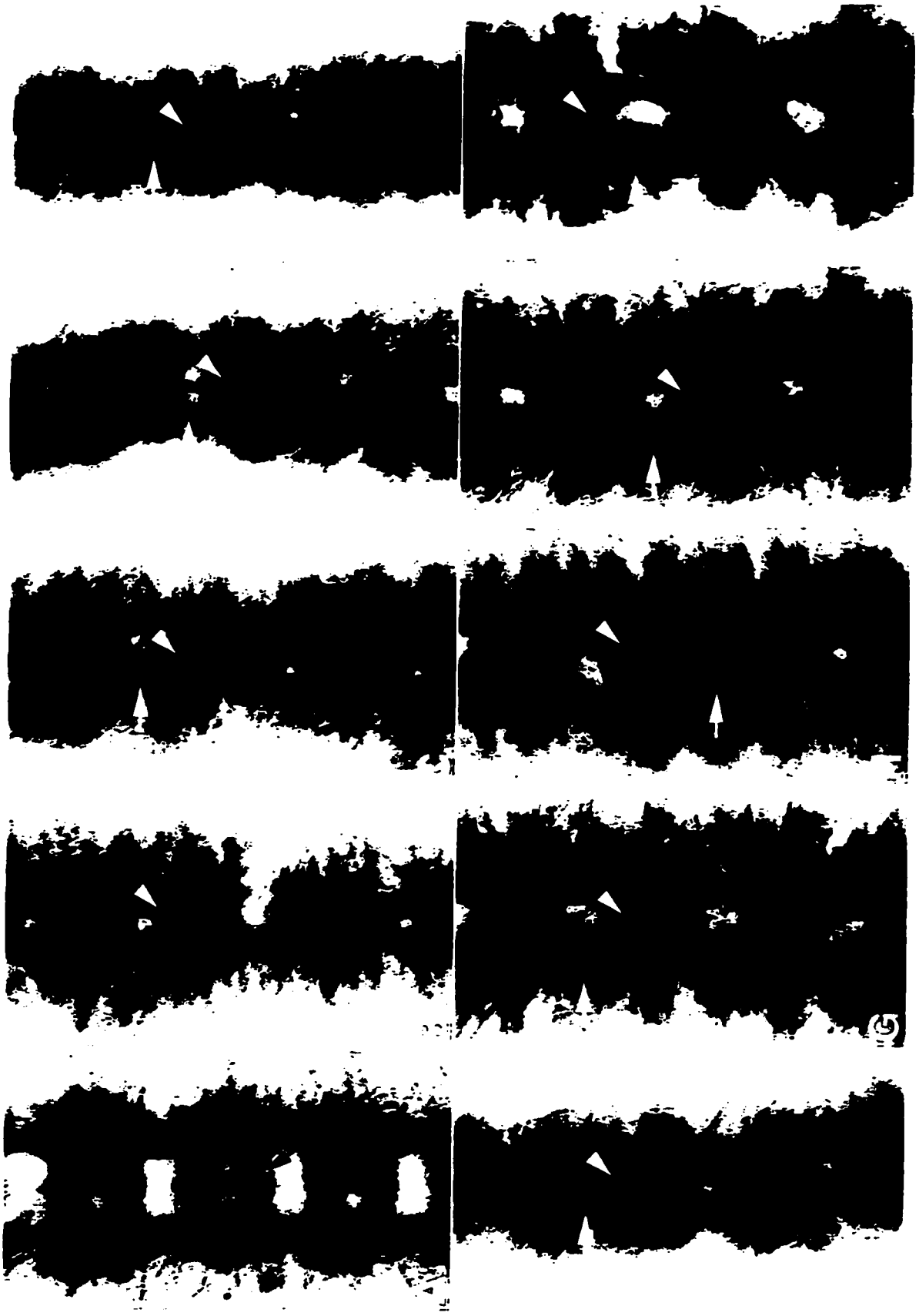

Figure 3.4 Do *slit* transgenes restore *slit* function in the midline glia?

Native Slit is expressed in the midline glia of the ventral nerve cord of wild type embryos immunolabelled for Slit (A, arrow). Complete restoration of midline glial cell position (B, arrow) is obtained in $slit^{lG107}$ mutant embryos expressing *P{UAS-slit complete}* in the midline cells (*P{slit1.0GAL4}*, $slit^{lG107}$/*P{UAS-slit complete}*, $slit^{lG107}$ assessed with an antibody to Slit). Embryos expressing *slit* transgenes that lack portions of the Leucine protein motifs in the midline cells (*P{slit1.0GAL4}*) fail to restore midline glia position [(C, *P{slit1.0GAL4}*, $slit^{lG107}$/*P{UAS-slitΔL1-L4}*, $slit^{lG107}$) , (D, *P{slit1.0GAL4}*, $slit^{lG107}$/*P{UAS-slitΔL1-L3}*, $slit^{lG107}$) , (E, P*{slit1.0GAL4}*, $slit^{lG107}$/ *P{slit1.0GAL4}*, $slit^{lG107:}$ *P{UAS-slitΔL1.5-L4}*/ *P{UAS-slitΔL1.5-L4}*) , (F, *P{slit1.0GAL4}*, $slit^{lG107}$/ *P{slit1.0GAL4}*, $slit^{lG107:}$ *P{UAS-slitΔL3-L4}*/ *P{UAS-slitΔL3-L4}*)]. The *P{slit1.0GAL4}* expression also produces secondary Slit labeling in peripheral cells (black arrowhead) in some embryos. Transgenes with only the G-domain and EGF7 (G, *P{slit1.0GAL4}*, $slit^{lG107}$/*P{UAS-slitΔG-E7}*, $slit^{lG107}$) removed or solely the G-domain (H,P*{slit1.0GAL4}*, $slit^{lG107}$/ *P{slit1.0GAL4}*, $slit^{lG107:}$ *P{UAS-slitΔG}*/ *P{UAS-slitΔG}*) effectively restore MG position at the midline.

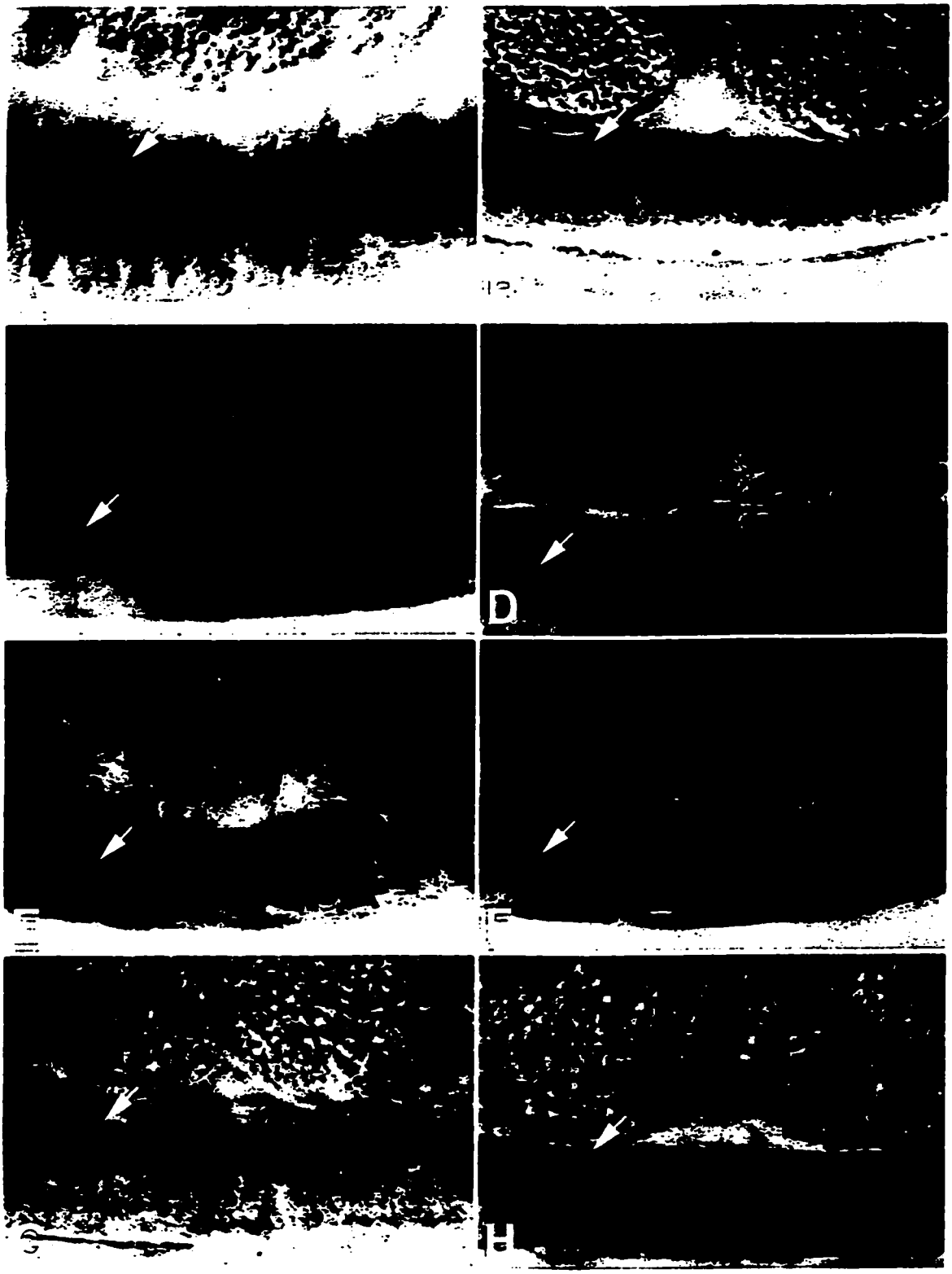
D

novel tissues, we hoped to further define the role that *slit* plays in CNS development by altering the pattern of repellent signaling. A range of *P{GAL4}* expression constructs (Appendix D) were selected that could be used to express transgenic *slit* in both native and foreign expression patterns.

Overexpression of *slit* in the MEC and MG disrupted midline axon guidance. Transgenic *slit* expression in the wild-type midline cells (Fig. 3.5 A, F black arrow) produced deviations of the developing commissural and longitudinal axons away from areas of elevated *slit* expression (B, G arrowhead). Where the intersegmental axons normally transversed each segment boundary, thinning (B, arrow) and breaks (G, arrow) in the axon tracts were observed. *slit* transgenes that lacked LRR 3 and 4 (C, D *P{UAS-slitΔL3-L4}*) did not result in disruption in CNS architecture. When over expressed in the pattern of native Slit expression (G, *P{Slit1.0-GAL4}*) no change in CNS architecture was observed from wild-type. However, overexpression with *P{sim-GAL4}* in a larger proportion of the midline cells resulted in a partial collapse or condensation of midline axons (C, arrowhead) with a general thinning of the intersegmental longitudinal axon tracts (arrow) possibly caused by a dominant negative affect. Midline overexpression of *slit* transgenes lacking the 6 EGF (D, I *P{UAS-slitΔE1-L6}*) repeats or the G-domain (E, J *P{UAS-slitΔG*) produced similar effects on midline guidance. In both these conditions repulsion of commissural and longitudinal axons away from areas of *slit* transgene expression was observed (D, E, I, J arrowhead) and breaks in the intersegmental axon tracts were present (arrow). All *slit* transgenes that retained the complete LRR disrupted midline CNS architecture when over expressed with either *P{sim-GAL4}* or *P{Slit1.0-*

Figure 3.5 Overexpression of Slit in the MG disrupts midline axon guidance. The pattern of *P{UAS tau-lacZ}* expression (black arrow, α β-gal labeled in brown) using *P{sim-GAL4}* (A) and *P{slit1.0-GAL4}* (F) is demonstrated in the MG and MEC cells of the midline overlying the commissural axons labeled with BP102 (black). Transgenic *slit* constructs were over expressed in both GAL4 patterns *P{sim-GAL4}* (B-E) and *P{slit1.0-GAL4}* (G-H). Examples of longitudinal axon morphology are indicated with a white arrow, commissure formation is denoted with an arrowhead (BP102 labeling, brown) and Slit expression is labeled in black where detectable. Overexpression of the complete *slit* transgene in the midline cells causes thinning and/or breaks in the longitudinal axon tracts (B,G) and disrupts midline commissure formation in areas of high Slit expression (arrowhead). *slit* transgenes lacking the LRR (*slitΔL3-L4)* fail to disrupt commissure formation (C,H); however, expression in the MEC's appears to inhibit longitudinal axon separation from the midline and causes partial thinning of some longitudinal axons (C, arrow). Transgenes expressing complete LRR, with either the EGF (*slitΔE2-E6,* D & I) or the G-domain (*slitΔG,* E & J) deleted severely disrupt midline architecture. Longitudinal and commissural axons are disrupted or missing showing evidence of repulsion from areas Slit overexpression.

E
C
A
F

GAL4}; however, deletion of LRR 3-4 alone was sufficient to abolish the repellent function observed by Slit.

Ectopic expression of Slit in all neurons repelled CNS axons towards the midline. Expression of the complete *slit* transgene using *P{elav-GAL4}* (Fig. 3.6 A, black arrow) and *P{C15J2-GAL4}* (F, black arrow) resulted in BP102 labeled axons collapsing around each neuromere (B, G arrowhead) diminishing (B, arrow) or displacing (G, arrow) the number of intersegmental axons that left each neuromere. When LRR 3-4 (*P{UAS-slitΔL3-L4}*) were deleted, ectopic expression of the *slit* transgene did not effect neuronal development (C, H) and the ventral nerve cord appeared to develop normally. This was not the case if the EGF motifs (D, I *P{UAS-slitΔE2-E6}*) or G-domain (E, H *P{UAS-slitΔG}*) were deleted. Here we observed a similar collapse of axons around each neuromere (D, E, I) and a disruption in the intersegmental longitudinal axons (D, E, I, H arrow). In some instances axons were observed to project away from the midline (D, I, H white arrowhead) but remained concentrated within the boundaries of the hemisegment, suggesting these neurons may be responding to conflicting signaling gradients (D, I, H black arrowhead). Ectopic Slit expression repelled CNS axons towards the midline, yet when LRR 3-4 (*P{UAS-slitΔL3-L4}*) were deleted this effect was no longer observed. Deletion of the EGF and G-domains (*P{UAS-slitΔE2-E6}, P{UAS-slitΔG}*) did not alter the repulsive signal properties observed in the complete *slit* transgene, but additional repulsive signaling in the midline suggested some other function of Slit had been disrupted.

Localized expression of transgenic Slit at the intersegmental boundaries with *P{eng-GAL4}* and *P{scab-GAL4}* (Fig. 3.7 A, F respectively) disrupted longitudinal axon

Figure 3.6 Ectopic overexpression of Slit disrupts midline axon guidance.

The pattern of *P{UAS tau-lacZ}* expression (black arrow, α β-gal labeled in brown) using *P{elav-GAL4}* (A) and *P{C15J2-GAL4}* (F) is demonstrated in neuronal tissue and cells surrounding the midline overlying the commissural axons labeled with BP102 (black). Transgenic *slit* constructs were over expressed in both GAL4 patterns *P{elav-GAL4}* (B-E) and *P{C15J2-GAL4}* (G-H). Examples of longitudinal axon morphology are indicated with a white arrow, commissure formation is denoted with an arrowhead (BP102 labeling, brown) and Slit expression is labeled in black where detectable. Ectopic overexpression of the complete *slit* transgene causes the longitudinal axon tracts (B,G) to collapse towards the midline and in cases of localized Slit overexpression (G) longitudinal axon tracts are absent. *slit* transgenes lacking the LRR (*slitΔL3-L4)* fail to disrupt longitudinal and commissural axon formation (C,H) when ectopically over expressed. Transgenes expressing complete LRR, with either the EGF (*slitΔE2-E6,* D & I) or the G-domain (*slitΔG,* E & J) deleted severely disrupt midline architecture but show evidence of axon collapse at the midline (black arrowhead). Longitudinal and commissural axons are disrupted or missing showing evidence of repulsion from areas Slit overexpression.

A
B
C
D
E
F
G
H

Figure 3.7 Ectopic overexpression of Slit at the intersegmental boundaries disrupts midline axon guidance.

The pattern of *P{UAS tau-lacZ}* expression (black arrow, α β-gal labeled in brown) using *P{eng-GAL4}* (A) and *P{scab-GAL4}* (F) is demonstrated at the intersegmental boundaries crossing the midline and overlying the commissural axons labeled with BP102 (black). Transgenic *slit* constructs were over expressed in both GAL4 patterns *P{eng-GAL4}* (B-E) and *P{scab-GAL4}* (G-H). Examples of longitudinal axon morphology are indicated with a white arrow, commissure formation is denoted with an arrowhead (BP102 labeling, brown) and Slit expression is labeled in black where detectable. Ectopic overexpression of the complete *slit* transgene causes the longitudinal axon tracts (B,G) to break (B) or collapse towards the midline (G) in areas of Slit overexpression, but leaves commissural axons intact. *slit* transgenes lacking the LRR (*slitΔL3-L4)* fail to disrupt longitudinal and commissural axon formation (C,H) when ectopically over expressed. Transgenes expressing complete LRR, with either the EGF (*slitΔE2-E6,* D & I) or the G-domain (*slitΔG,* E & J) deleted disrupts midline architecture. Longitudinal and commissural axons are disrupted or missing showing evidence of repulsion from areas Slit overexpression; however, commissural axons appear intact.

formation and repelled longitudinal axons towards the midline. Expression of the complete *slit* transgene at the intersegmental boundaries produced Slit expression overlying the region of the midline where native Slit expression was normally absent. Transgenic Slit expression using *P{eng-GAL4}* (B, arrow), resulted in breaks in the intersegmental axons; similarly, when Slit was expressed using *P{scab-GAL4}* (G, arrow) the longitudinal axons appeared thinner and were displaced towards the ventral midline region. There was no visible effect after *slit* transgenes lacking the LRR 3-4 (*P{UAS-slitΔL3-L4}*) were expressed at the intersegmental boundaries (C, H), but constructs lacking only the EGF motifs or G-domain (*P{UAS-slitΔE2-E6}, P{UAS-slitΔG}*) resulted in similar abnormalities observed with ectopic expression of the complete *slit* cDNA (D, E, I, J). The repellent properties of transgenes with deletions of the EGF motifs (D, I *P{UAS-slitΔE2-E6}*) and/or G-Domain (E, J *P{UAS-slitΔG}* and DNS) were not important in the repellent function of Slit. This was evidenced by a collapse of longitudinal axons towards the midline when these constructs were ectopically expressed using *P{eng-GAL4}* and *P{scab-GAL4}*. Furthermore, the disruption of LRR 3-4 was sufficient to negate affects observed in assays using the entire *slit* cDNA.

Expression of transgenic *slit* at the intersegmental boundaries disrupted MG development when LRR 1-3 had been deleted. Localized expression of a different *slit* transgene in which LRR 1-3 were missing (Fig. 3.8, D *P{UAS-slitΔE2-E6}*) resulted in abnormal positioning of the MG (black arrow) in stage 16 embryos. Normal MG development (A, white arrow) was not disrupted by the expression of *slit* transgenes with the complete *slit* coding sequence (B), or the LRR 1-4 (C, *P{UAS-slitΔL1-L4}*), LRR 1.5-

Figure 3.8 Ectopic expression of *slit* transgenes with deleted LRRs at the intersegmental boundary partially disrupts MG morphology

The wild type morphology of Slit labeled MG (A, arrow) shows distinct groups of midline Glia at the midline of each neuromere. Ectopic overexpression of the complete *slit* transgene using *P{eng-GAL4}* and labeled with an mAb to *slit* (arrow & arrowhead) shows that the MG maintain their uniform morphology (B). *slit* transgenes that delete large portions of the LRR's (C, *slitΔL1-L4*; D, *slitΔL1-L3*; E, *slitΔL1.5-L4*) disrupt the compact groups of midline glia (black arrow) and obscure the definition of each neuromere boundary observed in wild type embryos. Transgenes expressing complete LRR, with either the EGF (*slitΔE2-E6,* D & I) or the G-domain (*slitΔG,* E & J) deleted and a construct only deleting a small region of the LRR (*slitΔL3-L4*) fail to notably alter MG morphology.

A
B
C

4 (E, *P{UAS-slitΔL1.5-L4}*), LRR 3-4 (F, *P{UAS-slitΔL3-L4}*), G-domain and EGF-7 (G, *P{UAS-slitΔG-E7}*), and G-domain alone (H, *P{UAS-slitΔG}*) deleted.

Overexpression and ectopic expression of *slit* in the developing embryo has been shown to disrupt axon development in the midline CNS. In particular, the repellent signaling properties that we propose for Slit requires LRR 3-4 and does not require the EGF or G-domains. Despite our ability to rescue the mutant MG phenotype using transgenes with intact LRRs, overexpression of these transgenes does not result in changes in MG morphology.

DISCUSSION 3

We have proposed that Slit functions as a gradient dependent repulsive signal provided by the MG in order to establish the bilaterally symmetric axon tracts that develop on each side of the ventral midline. Our objective was to confirm this role of Slit by restoring Slit function in a *slit*$^{-}$ CNS using transgenes expressed in midline cells. Furthermore, to advance our understanding of the structure and function of Slit, we examined the native and ectopic expression of transgenes representing both complete and selectively truncated forms of Slit. Here we show that restoring Slit to the MG by expression of a *slit* transgene is sufficient to rescue the midline axon guidance phenotype observed in severe *slit* mutants. Ectopic and overexpression of complete and truncated *slit* transgenes, confirms that the LRR are required for mediating Slit repulsive signaling observed at the ventral midline. Furthermore, these overexpression experiments indicate that Slit repulsive signaling functions in a graded manner where threshold to a Slit repellent signal decreases in axons more lateral to the midline.

Restoration of Slit in MG rescues the severe *slit*$^{-}$ CNS and MG phenotypes

To determine the role of Slit in the collapse of the axon scaffold we expressed transgenic Slit in the MG of *slit*^{IG107} mutant embryos to assess possible rescue of the mutant phenotype. Using two different MG specific GAL4 expression lines (*slit*^{IG107}-*P{sim-GAL4}/slit*^{IG107}-*P{UAS-slit*^{complete}*}* & *slit*^{IG107}-*P{slit1.0-GAL4}/slit*^{IG107}-*P{UAS-slit*^{complete}*}*) we were able to partially re-establish a repulsive signaling gradient sufficient to move all longitudinal axons from the midline. Transgenic Slit expression also restored the MG to a wild type morphology. These data suggest that Slit is responsible for establishing the midline repellent signal that creates a barrier between symmetrical halves

in the *Drosophila* embryo. Furthermore, rescue of the *slit* mutant phenotype confirms that *slit* transgenes are capable of generating a functional Slit protein.

Slit acts as a repulsive signal

If Slit acts in a gradient dependent manner to provide repulsive signaling in the midline, then overexpression and ectopic expression of complete *slit* transgenes during development should misdirect axon growth. Indeed overexpression of transgenic Slit in the MG and MEC reduces the number of commissural axons and extends the midline boundary of repellent signal causing longitudinal fascicles to increase in density and at times project further away from the midline (Battye *et al*, 1999). Additionally, pan neural expression and ectopic expression of Slit at intersegmental boundaries results in an imbalance of repulsive signal that repels growth cones from the areas of elevated Slit expression. In competition with native expression of Slit at the midline boundary, more lateral axon tracts are repelled medially and away from intersegmental boundaries in response to increased levels of ectopic Slit, whereas, medial axons remain separate from the midline. Simply increasing ectopic levels of Slit expression was not sufficient to repel all axons onto the midline. Clearly, medial and lateral longitudinal axon tracts respond differentially to a graded Slit signal provided by the MG. When levels of *slit* expression are increased in the MG all axons are repelled away from the midline. However, when Slit is ectopically expressed outside of the midline some axons collapse towards the midline but most do not enter it. It appears that altering or moving the gradient of Slit repellent signaling differentially affects CNS axons, some of which (lateral) are more sensitive to changes in Slit, and others (medial) that are less sensitive.

That withstanding, all axons that respond to transgenic *slit* are repelled from regions of transgenic expression, supporting the hypothesis that Slit is a repellent ligand.

Leucine Rich Repeats are required for repellent signaling in the midline

In order to examine the role of specific Slit protein domains in Slit repellent signaling we employed the use of selectively truncated *slit* transgenes in attempts to rescue the mutant CNS and MG phenotype. Furthermore, in order to validate rescue phenotypes we also evaluated the effects of ectopic transgene expression of the truncated constructs. Deletion of all or part of the LRRs was sufficient to abolish phenotypic rescue of either the CNS or MG morphology. However, transgenes lacking all domains with the exception of the LRR were capable of partially restoring repellent and migratory function to the MG. Similarly, axon guidance errors generated by ectopic and overexpression of complete *slit*, were not observed when transgenic Slit lacked domains in the LRRs, but were observed when all LRRs were intact. Together with phenotypic data showing that mutations involving the LRR result in a reduction in function coinciding with severe CNS mutant phenotypes, these data indicate that the LRR are required for Slit repellent function. Attempts to remove individual LRR domains in the first 2 repeats were not successful, therefore at this time we must assume that all LRR are vital for Slit repellent function. Future studies in which LRR 1 and 2 can be selectively deleted, may provide a more detailed insight into the role of LRR in repellent signaling. Ectopic expression of LRR in the MG did not alter MG morphology despite the rescue of mutant MG phenotype using transgenes containing only the LRR. The function of Slit LRRs in MG morphology obviously does not involve repellent activity; however, overexpression of the LRR in the MG does appear to alter MG morphology. Perhaps

expression of these domains have a dominant negative effect, suppressing native Slit function in the MG. What this function may be has yet to be identified.

To date, these are the first indications for a specific role for LRR in repellent signaling. Other proteins containing LRRs including Decorin, Biglycan, Fibromodulin, Lumican, and Keratocan (reviewed by (Hocking *et al*, 1998)) have been noted for their roles as modulators of matrix assembly, regulating cell growth, adhesion, and migration. Invertebrate nervous systems contains a number of LRR containing proteins such as Connectin (Nose *et al*, 1992;Nose *et al*, 1994), Chaoptin (Van, Jr. *et al*, 1988), and Toll (Halfon *et al*, 1995;Halfon & Keshishian, 1998) that are known to play significant roles in target recognition, axon pathfinding and cell differentiation during nervous system development. The LRR in Toll has been shown to regulate its signaling activity by mediating receptor/ligand interactions at the cell surface (Winans & Hashimoto, 1995). Therefore, if Slit acting as a repellent ligand lost its ability to interact with a Slit receptor through mutations or deletions of the LRR, we would expect to see a loss of repellent signaling in the ventral midline. Further investigations currently underway in the Goodman Lab (Bland, K) into LRR specific functions in Slit will be required to better understand the role of LRR in repellent signaling.

Do EGF domains localize Slit?

We have shown that repellent signaling does not require an intact EGF, G, or Cysteine rich domain. These domains in other proteins, have specific functions in the ECM that would suggest they contribute to or act independently of Slit repellent function in the midline. EGF-like domains play a critical role in extracellular events which include cell adhesion and receptor ligand interactions (Campbell & Bork, 1993). Internal

deletions of the EGF domains of Slit do not perturb rescues of the *slit* mutant phenotype. Furthermore, ectopic and overexpression effects observed using EGF truncated transgenes are more pronounced and global than observed with either the complete or isolated LRR transgenes. In particular, overexpression in the MG and ectopic expression at the intersegmental boundaries results in an increase in observed errors in axon guidance. Taken together these results suggest a reduction of signal localization. Increased guidance errors observed in EGF deficient *slit* transgenes, could represent reduced affinity of Slit with the ECM, thereby increasing the native diffusion gradient established at the midline.

Vertebrate Slits are proteolytically cleaved at the start of the 6^{th} EGF repeat (Brose *et al*, 1999) and recent data from our lab and personal communications with the Goodman lab indicate that a similar processing event occurs in *Drosophila*. Cleavage of Slit generates two potentially functional proteins. We have shown that the Slit LRRs mediate repulsive signaling at the midline and that EGF may play a role in localizing that signal to the ECM. Therefore, a cleavage product containing only the LRR and 5 EGF repeats could represent a cleaved repulsive signal intended to be localized to the immediate ECM or cell surface.

A function for the cleavage product representing the G-Domain flanked by two EGF domains and a C-terminal cysteine rich region has yet to be determined. Ectopic and overexpression of C-terminal EGF and G-domains produced no notable CNS guidance errors; however, cursory analysis of MG morphology suggests that C-terminal Slit may be involved in MG development. MG appear to be displaced within the nerve cord when carboxy terminal *slit* transgenes lacking all of the LRR and most of the EGF-

like repeats are expressed at the intersegmental boarders. It will be necessary to repeat these experiments using MG markers such as AA142 to monitor these cells specifically.

What of the G-Domain?

One of the more intriguing protein motifs in Slit, the G-Domain shares homology with Agrins, Perlecans, and α-Laminin G-domains and has been attributed with functions involving cell adhesion (Sasaki *et al*, 1988;Brown *et al*, 1997), spreading, migration (Sasaki *et al*, 1998), and neurite outgrowth (Sephel *et al*, 1989). Deleting the G-domain in Slit produced overexpression phenotypes similar to those observed with the removal of just the EGF-like repeats. However, when both G and EGF domains are removed, observed guidance errors were reduced in comparison to assays that removed each domain independently. It is possible that the EGF and G domains play complementary roles in the function of complete Slit or represent binding of different Slit receptors responsible for transducing Slit signaling at the midline. Insight into function of the C-terminal protein domains awaits further analysis.

Slit is a repellent ligand and more

Slit is a large glycoprotein containing three prominent ECM domains known to function in protein-protein interactions. The first, a tandem array of LRR has been shown to function in providing a repulsive signal gradient in the MG of the *Drosophila* ventral midline. The second, a series of 6 EGF-like repeats appears necessary to localize either the complete Slit or a cleaved LRR N-terminal protein to the ECM. Additionally, limited data indicates that the EGF and G domains (third ECM domain) when present in the complete Slit may function to regulate MG development. A third prominent ECM domain represented by G-domain, remains to be functionally characterized, but may act

in a complementary role with the EGF domain or both may have an independent role in Slit signaling to different axon growth cones. The C-terminal Cysteine rich regions may be responsible for stabilizing protein interactions as is typical in other proteins (Noonan *et al*, 1988;Patthy, 1992).

Slit binding to Robo1 requires the LRR's

CHAPTER 4

To conclude our experiments we will investigate the proposed interaction of *slit* with *robo1* using both genetic and molecular approaches to dissect *slit* function. Using the range of *slit* alleles characterized in Chapter 2, we will investigate the penetrance of the *slit/robo1* interaction in the CNS, MG, and cardioblasts. Additionally, utilizing transgenes established in Chapter 3 we will determine the *in vitro* binding capability of each of these constructs with Robo1.

MATERIALS AND METHODS 4

Fly Maintenance

Refer to Methods Section 1.

Genetic stocks

Most *slit* and *robo*^{1} alleles were isolated on a background deficient for Fasciclin III and Fasciclin I as reported in Seeger (Seeger *et al.*, 1993). *slit*^{JG107} was isolated by Nüsslein-Volhard (Nüsslein-Volhard, 1984), *slit*^{E158} by Bellen *et al.* (1989), *slit*^{F81}, and *slit*^{F119} by Bier *et al.* (1989). All alleles and fly stocks were restored to a wild-type background prior to study and analyzed based on a *CyO-P{eng-lacZ}* marked balancer. Alleles used for viability testing and mutant sequencing were transferred to a *CyO-P{y*$^{+}$*)* balancer and all *slit* stocks were backcrossed to a stock deficient for *slit* (Df(2R)WMG) in order to verify the lack of complementation.

Immunocytochemistry

Drosophila embryos were collected on apple juice agar plates and aged from 16-30 hours at 22°C. Fixation and immunocytochemistry was adapted from Patel (1994). mAb Slit (1:200), mAb 1D4 (1:4), BP102 (1:2) (N. Patel, C. Goodman, G.), mAb Robo (Fessler), and α β-gal (Cappel, 55976) were diluted in phosphate-buffered saline (PBS) as indicated an processed as in methods section 1.

Genetic slit and robo interactions

Mutant *slit* and *robo* alleles maintained in the same genetic backgrounds were crossed to test for genetic interactions between these two genes (*slit/CyOP[eng-lacZ] X robo*^{1}*/CyO[eng-lacZ]*). Eggs from these crosses were collected, aged and then fixed for

staining with mAb 1D4. Embryos carrying single mutations for both *robo*^{1} and *slit* (*robo*^{1}/slit) were distinguished by α β-gal staining of the lac-Z balancer. Nerve cords were dissected out and then mounted for visualization by light microscopy. A sample pool of nerve cords for each heteroallelic combination was analyzed for the total number of segments and the number of segments with misrouted axon projections. The percent of misrouted axon projection for each combination were calculated and subjected to a Tukey Test for significant difference between sample means.

Midline axon tract structure

Refer to Methods Section 2.

Mesectodermal cell position

Refer to Methods Section 2.

Heart morphology

Refer to Methods Section 2.

Genomic clones and cDNA

Refer to Methods Section 1.

Transgenic constructs

Refer to Methods Section 3.

Transgenic stocks

Refer to Methods Section 3.

***In Vitro* expression**

Using the T3 promoter within pBS(KSII+) each *slit* construct was *in vitro* transcribed using T3 Cap Scribe (Roche, 1581058) creating an RNA template for later translation. Constructs were digested with XbaI and phenol/chloroform purified. Clean

linearized DNA was eluted in 19µl of 1x Cap Scribe Buffer, mixed with 10U of T3 RNA polymerase and incubated at 37°C for 3 hours synthesizing RNA capped with P^1-5'-(7-methyl)-guanosine-P^3-5'-guanosine-triphosphate. Capped RNA (10µl) was transferred to one of two translation reactions.

Initially, all constructs were translated using a Biotin *In Vitro* translation kit (Roche, 1559451) to determine product size and efficacy of each construct. Synthesized RNA was added to a reticulocyte lysate that translated capped RNA into biotin-labeled proteins using a charged lysine-tRNA labeled with biotin. Translated proteins were run on a 4% SDS-PAGE alongside wide range colour markers (Sigma, C3437) and blotted (Bio-Rad, 170-3935) onto PVDF Western Blotting Membranes (Roche, 1722034) soaked in methanol and preabsorbed in transfer buffer. The membranes were washed 5*10 minutes with 1x TTE and then blocked in 1x TTE containing 10% Blocking Reagent (Roche, 1096176) for 60 minutes. A premixed solution of Avidin-Biotinylated HRP (Vector Laboratories, PK-6100) was exchanged for the blocking solution and left to incubate for another 60 minutes. The membranes were washed 5*15 minutes in 1xTTE and then reacted with 2mls of ECL (Amersham Pharmacia Biotech, RPN 2106) chemiluminescence for detection of biotin labeled proteins on Kodak X-OMAT AR (XAR) Film.

After constructs were confirmed each was translated along with capped *robo* mRNA (donated cDNA in pcDNA3 with a T7 promoter from Goodman) using Reticulocyte, Type II (Roche Translation Kit, 1103032). Unlabelled proteins were run on a 4% SDS-PAGE and blotted for detection by mAb Slit or mAb Robo. Blocked membranes were washed 5*15 minutes and incubated for 2 hours with a 1:10000 dilution

of purified primary antibody in blocking solution. Following primary labeling the membranes were washed 4*30 minutes, blocked a further 60 minutes and then incubated in GαM conjugated to HRP (Cappel, 55572) for 1 hour. Finally, the membranes were washed 5*15 minutes in 1xTE and then reacted with 2mls of ECL (Amersham Pharmacia Biotech, RPN 2106) chemiluminescence for detection of HRP bound primary antibody on Kodak X-OMAT AR (XAR) Film.

***In Vitro* binding**

In order to determine requirements of Slit binding to Robo *in vitro*, 20 µl of biotin-translated protein from each of the *slit* constructs was incubated with 20 µl of unlabeled *robo* while being rotated at 4°C for 2 hours in 500 µl 0.1M PB. Following Slit/Robo incubation, 25 µl of Avidin Agarose (Roche, 1745441) was added to each tube and incubated a further 15-20 hours rotating at 4°C. The Avidin Agarose was washed 5x with 0.1 M PB. Biotin bound to the Avidin complex was eluted by rotating the agarose with 50µl of elution buffer (2mM D-Biotin-B-Hydroxysuccinimidester (Roche, 732494), 0.1 M PB, 0.15M NaCl [pH 7.2]) for 1 hour after which 10 µl of 5X sample buffer was added and each mixture was heated to 80°C for 5 minutes. For each construct 12 µl of supernatant was loaded onto each of three 4% gels for SDS-PAGE alongside a wide range M.W. colour maker and then blotted onto a PVDF membrane. Each membrane was washed and blocked before being separated for incubation with mAb Slit, mAb Robo, or ABC kit. After washing, the Slit and Robo antibody incubated membranes were incubated with GαM HRP and then all membranes were washed 5*15 minutes in 1xTTE and then reacted with 2mls of ECL (Amersham Pharmacia Biotech, RPN 2106)

chemiluminescence for detection of HRP bound primary antibody or biotinylated proteins on Kodak X-OMAT AR (XAR) Film.

Data presentation

Refer to Methods Section 1.

RESULTS 4

Embryos that are mutant for *robo* are not able to properly respond to axon guidance cues at the ventral midline so that the longitudinal axons make repeated inappropriate projections back and forth across the midline (Kidd *et al*, 1998a). The 'roundabout' pattern observed in FasII labeled axons (Fig. 4.1 B, arrow) is strikingly similar to the mild CNS phenotypes that were observed in FasII labeled *slit* hypomorphs such as $slit^{2990}$ (see Chapter 2). Embryos that are heterozygous for $robo^{1}$ (C) or $slit^{IG107}$ (Appendix B) develop normal FasII labeled longitudinal axon tracts that are comparable to wild-type (A). By generating heterozygous combinations of *slit* mutant alleles with $robo^{1}$ we were able to study a genetic interaction between these two genes.

robo and *slit* interact genetically to establish ventral midline guidance cues

Longitudinal axon tracts of embryos that are heterozygous for both *slit* and *robo* made inappropriate projections across the ventral midline that were not observed in embryos heterozygous for either *slit* or *robo*. The observed genetic interaction was either restricted to the most medial longitudinal axon fascicle or involved all the FasII labeled axons. Embryos mutant for a single copy of $slit^{IG107}$ (Fig. 4.1, D), $slit^{3149}$ (H), or $slit^{550}$ (J) and $robo^{1}$ developed misprojections in only the most medial axons. The actual number of inappropriate projections that crossed the midline did not differ notably between *slit/robo* phenotypes that involved all longitudinal fascicles and those such as $slit^{IG107}$, $slit^{3149}$, and $slit^{550}$ than only involved the medial fascicles. However, interactions involving inappropriate projections of all fascicles suggest that mutations in these alleles perturb Slit signaling to additional receptors on the other longitudinal tracts. Point mutations in $slit^{3149}$ were not identified, but mutations in $slit^{IG107}$ and $slit^{550}$ were both

Figure 4.1 ***slit*** **and** ***robo*** **interact genetically to maintain midline guidance in the ventral nerve cord.**

The longitudinal axon fascicles of a wild type ventral nerve cord form a pair of three well defined axon tracts that are separated by the ventral midline and label with an antibody to Fasciclin II (A). In embryos mutant for $robo^{1}$, misguided axon fascicles repeatedly project across the midline generating loops around the midline (B, arrow), however embryos heterozygous for a mutation in $robo^{1}$ show normal axon development (C). Embryos that are heterozygous for both $robo^{1}$ and each of the *slit* alleles develop longitudinal axon fascicles axons that deviate across the midline (D-O, arrows). The percentage of crossovers from a survey of nerve cord segments show that the proportion of crossovers generally decreases with the severity of phenotypes associated with embryos homozygous for each respective allele of *slit*. *slit* alleles interacting with $robo^{1}$ ($slit/robo^{1}$) are as follows: D, $slit^{JG107}$; E, $slit^{GA20}$; F, $slit^{GA178}$; G, $slit^{GA945}$; H, $slit^{3149}$; I, $slit^{1912}$; J, $slit^{550}$; K, $slit^{532}$; L, $slit^{2990}$; M, $slit^{F81}$; N, $slit^{F119}$; & O, $slit^{E158}$.

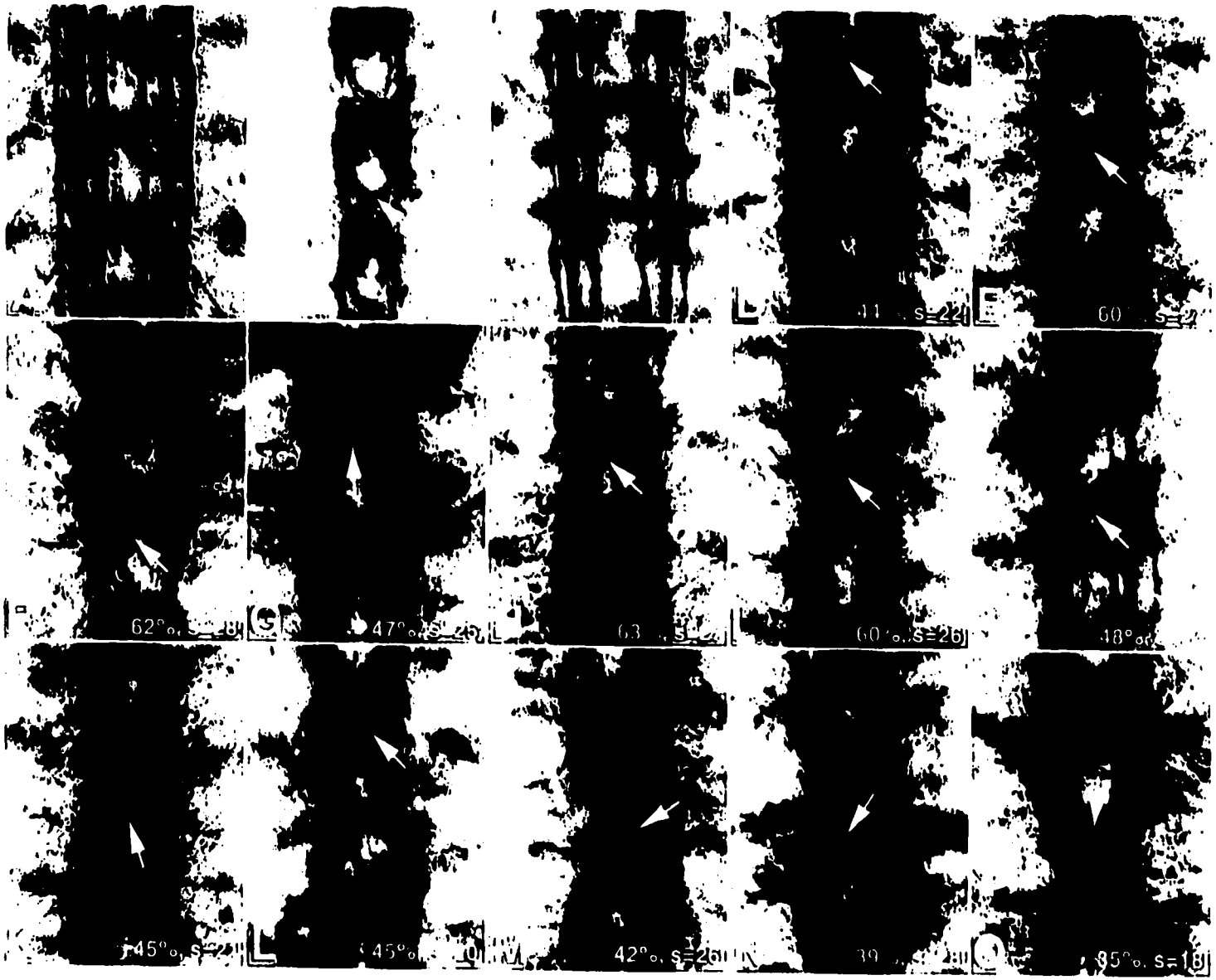

detected in the 3' terminus of the protein. With the exception of *slit*^{1912}, all remaining mutations were located in the 5' LRR, and were associated with *slit/robo* phenotypes that involved all FasII labeled axons. The severe *slit/robo* phenotypes that included *slit*^{GA20} (E), *slit*^{GA945} (F), *slit*^{GA178} (G), *slit*^{1912} (I), *slit*^{532} (K), *slit*^{2990} (L), *slit*^{F81} (M), *slit*^{F119} (N), and *slit*^{E158} (O), with *robo*^{1} had fused longitudinal axon tracts that appeared to collapse towards the midline while making inappropriate projections across adjacent axon fascicles and across the midline. Although significant differences in the number of actual projections across the midline were not observed between different *slit/robo* interactions, generally fewer axon crossovers were recorded in *robo* interactions with mild *slit* hypomorphs (L-O) as compared to severe *slit* hypomorphs (E-I).

robo is not required for MG development

Severe, moderate and mild alleles of *slit* were observed to differentially affect MG number and position (Fig.4.2 A, C, E, G, I) in *slit* mutant embryos. Genetic interactions that were observed in CNS pathfinding between *slit* alleles with *robo*^{1} were not also observed in respect to MG morphology and number (B, D, F, H, J). In embryos mutant for *robo*^{1} (B, arrow) MG develop normally by stage 16 and are indistinguishable from wild type embryos (A). Consequently, heterozygous combinations of *slit*^{JG107} (D), *slit*^{1912} (E), *slit*^{532} (G), and *slit*^{2990} (H) with *robo*^{1} do not result in changes in mutant embryos that affect MG morphology or number. Therefore, it is not likely that the genetic interaction between *robo* and *slit* has anything to do with *slit's* role in MG development.

Figure 4.2 Genetic interaction between alleles of *slit* and *robo*^{1} affecting axon guidance do not alter MG position and number.

MG at the anterior and posterior commissure in a sagittal plane are labeled for β-galacotosidase expression from the enhancer-trap line AA142 in wild type embryos (A, arrow). At stage 16 the midline glia have been reduced in number to an average of 3.28 ±0.46 cells per segment (n=32) in wild type embryos and are further reduced in number (2.41 ±0.76) in severe mutations in *slit* (*slit*^{JG107}, C). The MG are ventrally displaced in embryos mutant for *slit*^{JG107} (C), *slit*^{1912} (E), *slit*^{532} (G), and *slit*^{2990} (I), but are normal in embryos heterozygous for these *slit* alleles and *robo*^{1} (*slit/robo*^{1}) respectively (D, F, H, J). No changes in MG number were observed in any *slit/robo*^{1} heteroallelic combinations.

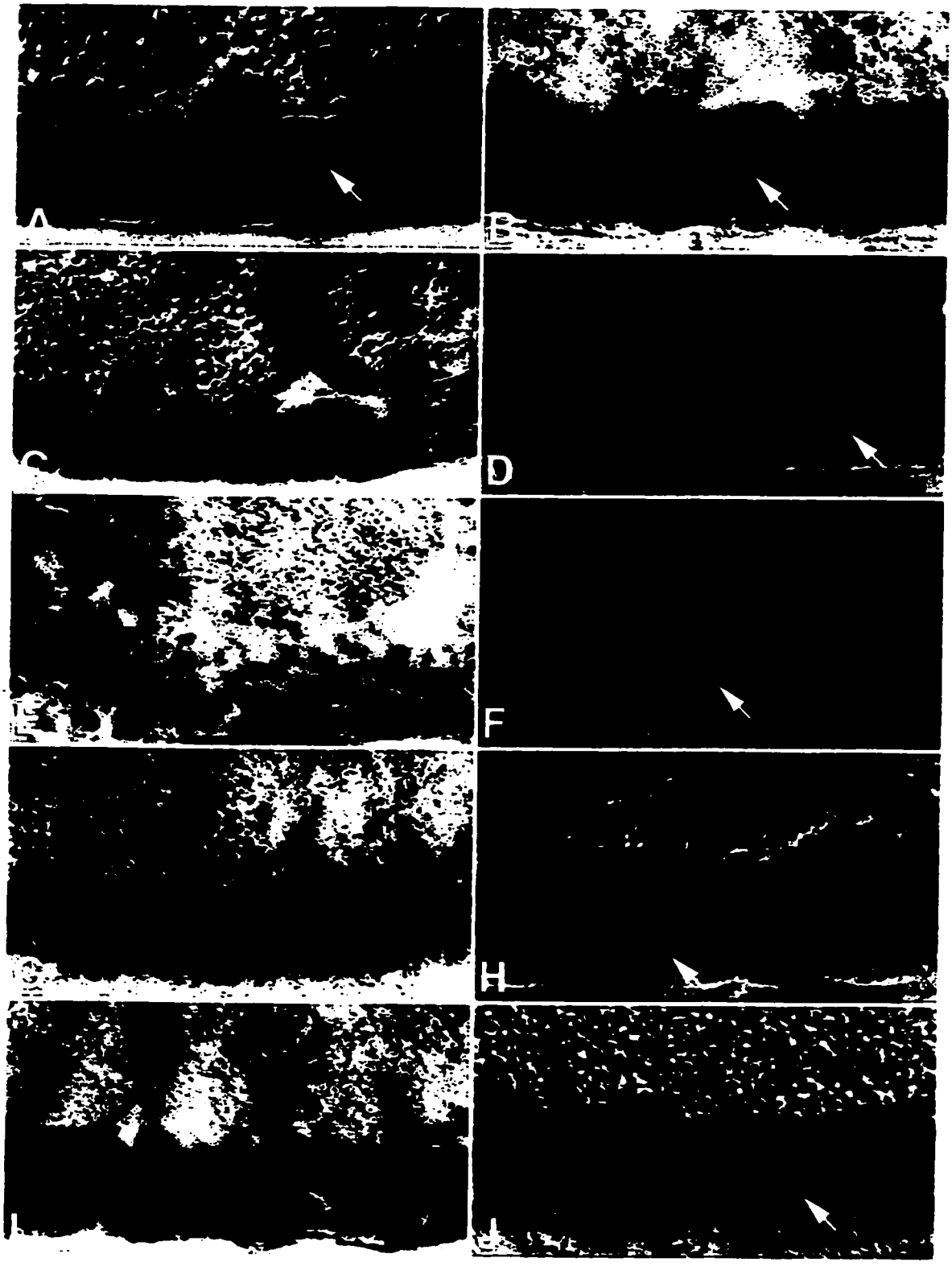
A
B
C
D
F
H
I
J

robo is not active in heart development

Mutations in *slit* have been shown to affect development of the embryonic heart. *slit's* role in guiding the migration of cardioblast cells towards the dorsal midline and maintaining the pairwise grouping of these cells during formation of the dorsal vessel is still unclear. In order to examine whether the genetic interaction observed between $robo^{1}$ and *slit* in the development of the midline CNS is duplicated in the development of the heart, we studied heart development in transheterozygous $robo^{1}/slit$ embryos. Embryos that are mutant for $robo^{1}$ have no difficulty in forming a dorsal tube (Fig. 4.3, B) that is comparable to that of a wild type embryo (A). In embryos heterozygous for $slit^{IG107}$, the cardioblast cells form small blisters due to inappropriate pairing of cells at the dorsal midline (C, arrow). These blisters are not observed in embryos heterozygous for $robo^{1}$ (D). After dorsal closure the cardioblast cells of $slit^{IG107}$ mutant embryos remain unpaired and the heart structure appears distorted (E, arrow) whereas, embryos heterozygous for both $slit^{IG107}$ and $robo^{1}$ (F) do not appear different from embryos heterozygous for $slit^{IG107}$ alone. These results suggest that Robo has no role in heart development either directly or indirectly through Slit.

Slit and Robo expression is localized to ventral midline and muscle apodemes

Analysis of genetic interactions between $robo^{1}$ and *slit* suggest that these two genes act in a related pathway to establish guidance cues in the ventral midline. Slit has been described as an ECM protein with signaling properties (Rothberg *et al*, 1990), and Robo1 is a dosage-sensitive axon guidance receptor that is expressed on the growth cones of midline axons (Kidd *et al*, 1998c). By examining the expression pattern of both Slit and Robo1, we intend to show that the co-localized expression of both these proteins

Figure 4.3 A genetic interaction between *slit*^{JG107} and *robo*^{1} affecting midline axon guidance does not alter heart morphology in Slit expressing cardioblast cells.
The cardioblast cells of the dorsal vessel proper have been labeled for β-galacotosidase expression from the enhancer trap stock B2-3-20 showing the pairwise array of cardioblast cells at the dorsal midline (A, black arrowhead). The pairwise grouping of cardioblasts breaks down in embryos mutant for a single allele of *slit*^{JG107}/+ (C, arrow) and homozygous *slit*^{JG107} embryos (E, arrow). Heart morphology is comparable to wild type in embryos mutant for *robo*^{1} (B) and heterozygous for *robo*^{1}/+ (D). A heteroallelic combination of *slit*^{JG107}/*robo*^{1} (F) does not result in phenotypic changes differing from an embryo heterozygous for *slit*^{JG107} (arrow).

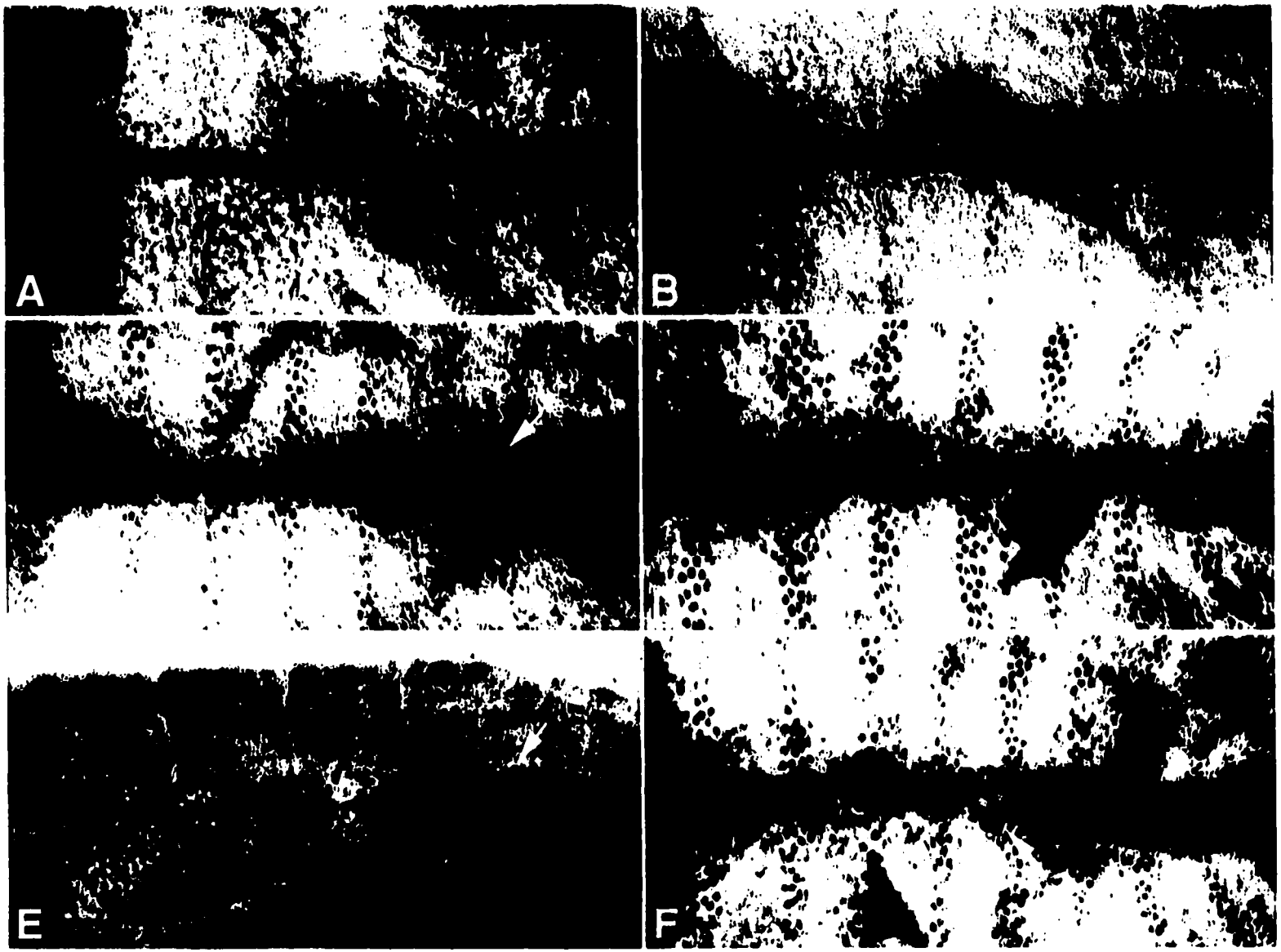
A
B
E
F

makes them excellent candidates for the role of ligand and receptor in midline axon repulsion.

Robo expression is observed on the longitudinal axon tracts of the nerve cord (Fig. 4.4 A, white arrow) and appears to a lesser degree on the commissures that cross the ventral midline (*). When *slit*^{JG107} mutant embryos are labeled with an antibody to Robo, it is clear that the Robo expressing axons converge onto the midline in *slit* mutants. Additionally, expression of Slit in MG of *robo*^{1} mutant embryos (Fig. 4.4 F, black arrow) coincides with the unregulated midline crossovers observed in *robo1* mutant embryos. Lateral to the midline, Robo is detected at the muscle apodemes (Fig. 4.4 B, white arrowhead) similar to where Slit has been shown to localize (C, white arrowhead). Localized expression of Robo at the points of muscle insertion (G, white arrowhead) directly coincides with the earlier detection of Slit at these same muscle inserts (Fig. 1.5 G, white arrowhead). It was observed that in *slit* mutant embryos, the ventral oblique muscles make inappropriate projections across the midline and based on personal communication with Kimberly Bland (Goodman Lab). *robo*^{1} mutant embryos also exhibit aberrant muscle phenotypes. It is probable that *slit* and *robo*^{1} interact genetically in muscle development. The expression of Slit in the MG (E) and cardioblast cells (H) of *robo*^{1} mutant embryos indicates that these tissues are normal in *robo*^{1} mutants. Previous results showing no genetic interactions between *slit* and *robo*^{1} in the development of these tissues suggests that Slit function is likely independent of Robo1 in MG and heart development.

Figure 4.4 Robo expression coincides with Slit expression at the midline and the intersegmental muscles.

Robo expression in wild type embryos is found on the longitudinal axon fascicles of the nerve cord (A, white arrow) and is detectable on commissural axons (*) using a mAb to *robo*. Robo antibody labeling is detected on muscle apodemes (B, white arrowhead) and coincides with Slit antibody labeling at the muscle apodemes (C, white arrowhead), points of muscle insertion at the intersegmental boundary (G, white arrowhead) and the commissures (*) of the midline (C, black arrow). Embryos that are mutant for $robo^{1}$ develop longitudinal fascicles that cross and recross the midline resulting in commissures that are thick and fuzzy with thinner longitudinal tracts (D, BP102 black arrowhead). The pattern of Slit expression in the MG of $robo^{1}$ mutants appears normal from a sagittal (E, black arrow) and ventral (F) perspective, however Robo labeling in the midline of $slit^{IG107}$ mutant embryos (I) show that Robo expressing fascicles collapse on the midline when Slit is absent. Robo expression was not detected in the cardioblast cells of the dorsal vessel and *slit* labeling of embryos mutant for $robo^{1}$ (H, black arrow) show that the dorsal vessel proper appears normal.

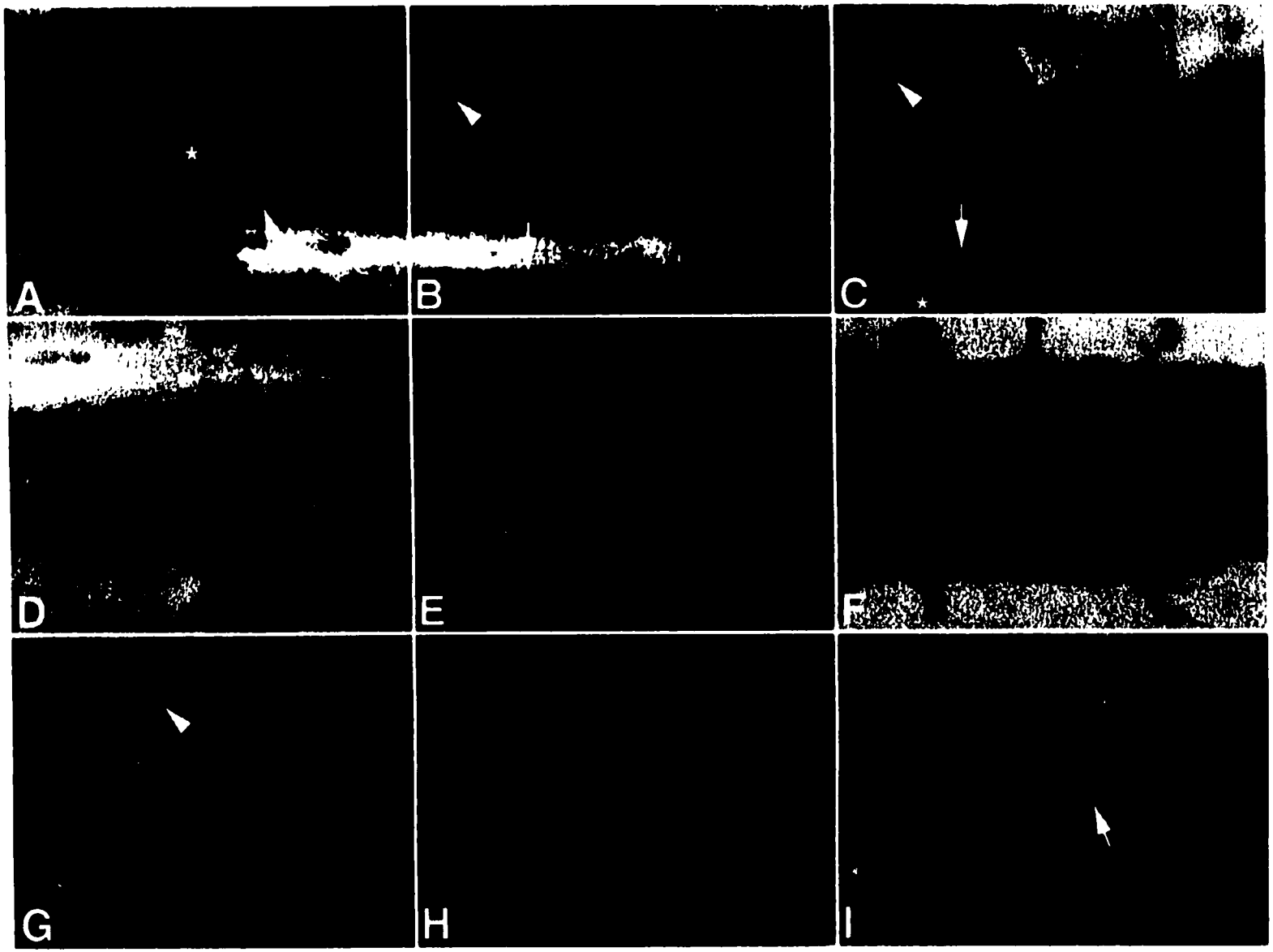
A
B
C
D
E
F
G
H
I

LRRs in Slit are required to bind Robo1

Genetic interaction and protein co-localization of *slit* and *robo* would suggest that these two genes function together in the development of the embryonic CNS and musculature. Robo has been identified as a receptor on the growth cone of pioneering axons and Slit is a large secreted glycoprotein with a signaling domain expressed in the MG. The LRR of Slit have been shown to mediate the repulsive role of Slit in the ventral midline. If Slit and Robo do interact to maintain repulsive cues in the ventral midline, it is likely that Slit and Robo will interact through the LRRs. By using the deleted *slit* transgene constructs to make *in vitro* proteins we were able to determine that the LRR of Slit are required to bind Robo.

In vitro translated *slit* transgenes with incorporated biotin were incubated with *in vitro* translated *robo* and bound to an Avidin-agarose column. After careful rinsing, Avidin bound proteins were eluted from the column and equal portions from each reaction were run on three 4% polyacrylamide gels. The resulting gels were immunoblotted with Avidin-HRP, mAb Slit, and mAb Robo. Protein complexes were eluted from each column (Fig. 4.5 Avidin-HRP) representing different *slit* transgenes. The mAb for Slit was able to detect all *in vitro* constructs that retained the EGF-6 motif in their open reading frame (α-Slit) and Avidin labeled all Slit proteins. mAb Robo labeling (α-Robo) indicates that only Slit protein with intact LRRs were able to bind Robo protein. One exception was the deletion transgene *slitΔE2-E7* that included all LRRs, but failed to label with the antibody to Robo. Deletion of the smallest LRR, *slitΔL3-L4* disrupted binding of the Robo protein. This suggests that LRR 3-4 perform an important role in Robo binding as well as repulsive signaling in the ventral midline.

Figure 4.5 ***In vitro*** **binding of truncated Slit to Robo**

slit transgenes both complete and containing internal deletions were ***in vitro*** translated incorporating Biotin labeled lysine and then bound to Avidin agarose columns. A non-labeled ***in vitro*** translated ***robo*** construct was incubated overnight with each Slit column, washed, and then eluted with an n-Biotin buffer. 30% of the extraction from each column was run on one of three 4.0% polyacrylamide gels and immunoblotted as indicated. Avidin-HRP visualized with chemiluminescence shows that each of the Slit constructs bound and was eluted from the Avidin columns. The Slit antibody detects all constructs except those that delete the EGF2-EGF6 region, to which the antibody binds. The immunoblot for Robo indicates that Slit complete, SlitΔE2-E6, and SlitΔG are capable of binding Robo; however, Slit protein with internal deletions of any or all the LRR fail to demonstrate any detectable Robo antigen. SlitΔE2-E7 fails to label for Robo despite the combined overlap with SlitΔE3-E6 and SlitΔG constructs.

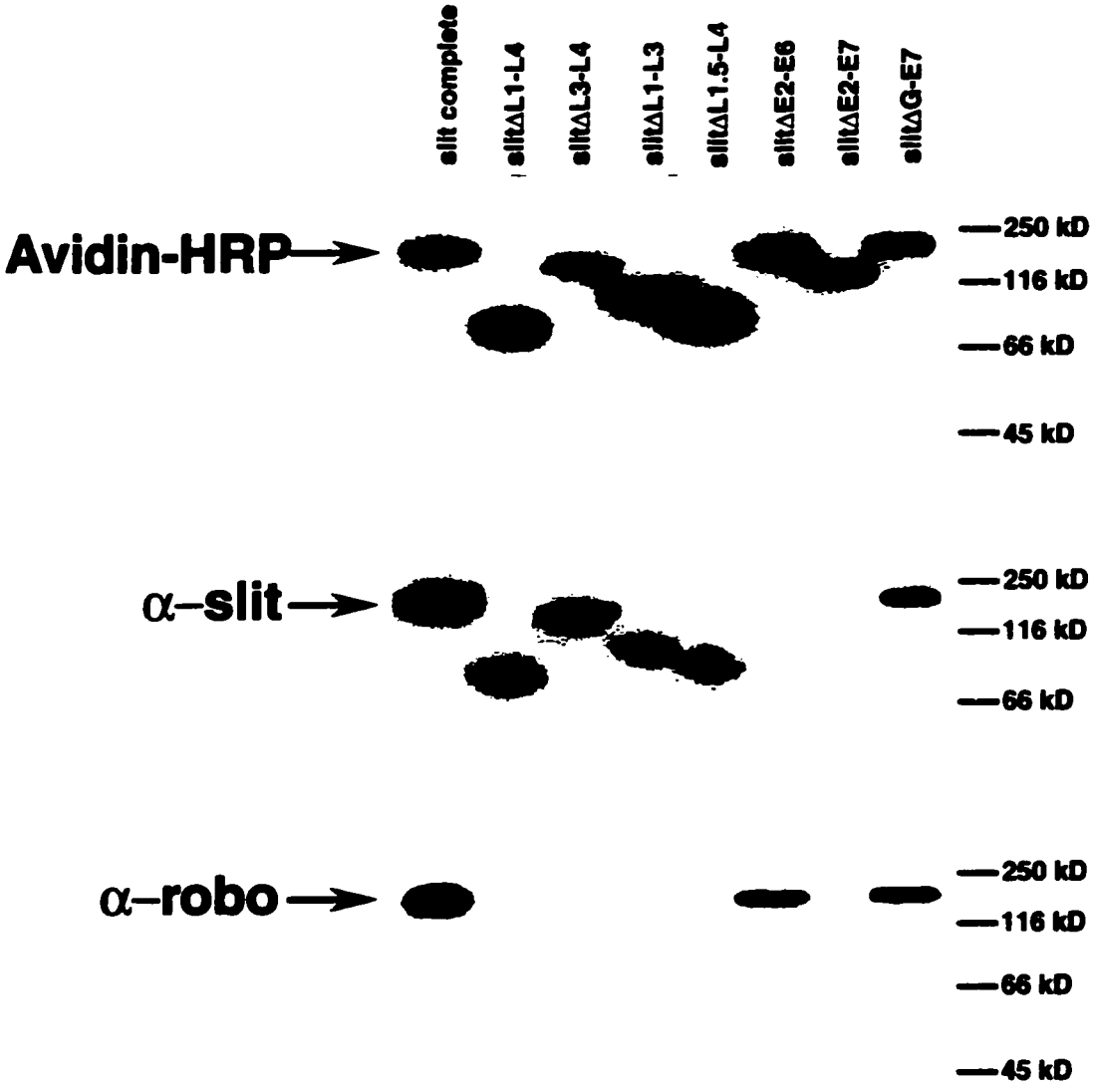
slit complete
slitΔL1-L4
slitΔL3-L4
slitΔL1-L3
slitΔL1.5-L4
slitΔE2-E6
slitΔE2-E7
slitΔG-E7
Avidin-HRP
α–slit
α–robo
250 kD
116 kD
66 kD
45 kD

DISCUSSION 4

Of all *Drosophila* CNS interneurons, about 10% extend axons ipsilaterally. The remaining 90% project once across the midline, make longitudinal projections close to the midline and then never cross again. In embryos mutant for *commissureless* (*comm.*) all axons remain ipsilateral to the midline (Tear *et al*, 1996), while conversely in embryos mutant for *roundabout* (*robo*) growth cones that normally remain ipsilateral to the midline instead cross and recross the midline, and growth cones that normally cross the midline once instead now cross multiple times (Kidd *et al*, 1998c). In axons that never cross the midline, Robo is expressed at high levels on their growth cones from the onset of Neurogenesis. For the 90% of axons that make commissural projections, Robo is expressed at high levels on their growth cones only after they cross the midline, preventing them from ever crossing again (Kidd *et al*, 1998a). In *robo;comm* double-mutants, the mutant phenotype is identical to *robo* (Seeger *et al*, 1993), additionally overexpression of Comm. results in a nearly identical *robo* loss of function phenotype (Kidd *et al*, 1998a) suggesting that Comm. regulates Robo function. It has now been shown that Comm. is transferred to Robo expressing growth cones that contact the midline, where it directly or indirectly down regulates the presence of the Robo receptor allowing these growth cones to cross the midline (Tear *et al*, 1996;Seeger & Beattie, 1999). These observations have led to the model that Robo is a repulsive guidance receptor to a midline repellent, and that Comm. down regulates the Robo receptor levels on commissural growth cones so that axons may cross the midline (Kidd *et al*, 1998a;Kidd *et al*, 1998c). Some yet unknown process reintroduces the Robo receptors back onto the commissural growth cones as they cross the midline increasing levels of

Robo expression. Robo expressed on longitudinal axons that have crossed the midline no longer appears sensitive to antagonistic affects of midline Comm.

Recently, observations by the Goodman Lab (personal communications) have shed new light onto the midline ligand for Robo. To better understand the role of Comm. in Robo function, in light of ongoing characterization of additional Robo receptors, they increased the copy number of *comm.* transgenes, in a gain-of-function (GOF) paradigm, resulting in a *slit* loss-of-function phenotype. In severe *slit* mutant embryos, all growth cones enter the midline but never leave it, but continue expressing high levels of Robo. Mutations in *comm.*, result in all growth cones failing to cross the midline, yet Robo expressing growth cones continue to explore its boundary (Tear *et al*, 1996). When Comm. is over expressed, all axons no longer respond to the midline repulsive signal and fuse at the midline. This suggests that high enough levels of Comm. are sufficient to remove all Robo receptors from CNS axons, subsequently eliminating the growth cone responsiveness to the midline repellent which all evidence indicates is Slit. We have observed that the sensitivity of CNS axons to a gradient of *slit* signaling suggests that multiple *slit* receptors exist. Multiple Slit receptors with different sensitivities can create a gradient response to Slit, a proposal that has now been confirmed (Dickson *et al*, 2000). Recent findings, suggest the presence of multiple Robo receptors at least one of which binds Slit (Brose *et al*, 1999;Kidd *et al*, 1999;Dickson *et al*, 2000). We show here that *slit* and *robo* display a dosage sensitive interaction (Battye *et al*, 1999;Kidd *et al*, 1999) that regulates repellent signaling at the midline and is likely mediated by the binding of Robo to the LRR of Slit.

slit* function interacts with *robo1

We have established a phenotypic gradient of CNS perturbations in *slit* alleles that ranges from severe, involving a complete collapse of the axon scaffold to mild in which only the most medial fascicles make guidance errors. Mild *slit* phenotypes are reminiscent of the *robo1* loss of function phenotype and severe *slit* phenotypes are similar to extreme GOFs in *comm.*, as described above. Embryos that are doubly heterozygous for both *robo1* and *slit* produce guidance errors that are not observed in embryos singly heterozygous for either *robo1* or *slit*, suggesting that these two genes interact. Considering the range of CNS phenotypes observed in *slit* mutants and that only mild *slit* hypomorphs resemble the *robo1* loss of function phenotype we would expect genetic interaction of the *slit* alleles with *robo1* would not uncover Slits function with the other Robo receptors. Indeed this is the case. A phenotypic gradient representing the genetic interaction in embryos doubly heterozygous for *robo1* and the range of *slit* alleles failed to correlate with the axon pattern of CNS phenotypes observed in homozygous *slit* mutant embryos. The frequency of midline axon crossovers did not differ dramatically between severe, and moderate or mild *slit/robo1* phenotypes. Furthermore, guidance errors involving all longitudinal fascicles occurred in interactions with severe *slit* alleles resulting from mutation in the LRR. However, this was not universally held, as $slit^{1912}$/*robo1* heterozygous embryos developed pathfinding errors in all longitudinal fascicles despite $slit^{1912}$ being associated with mutations truncating the protein in the 3rd EGF repeat. One possibility is that not all Slit mediated midline guidance functions require Robo1 as has been previously proposed. Likewise, mutations modifying forms of Slit may interfere with Slit/Robo binding or nullify Slit signaling once bound to Robo.

It is therefore possible that mutations in *slit* alleles causing CNS phenotypes, perturb *slit* and *robo1* interactions along with *slits* interaction with other receptors. These other receptors are likely Robo2 and Robo3, two additional Robo homologues that are expressed exclusively on longitudinal axons (Dickson *et al*, 2000). Robo 2 and 3 are localized in discrete domains in the longitudinal tracts. Whereas Robo1 is present on the entire width of the longitudinal tracts, Robo3 is present only on the lateral 2/3 and Robo2 only the most lateral 1/3 of the longitudinal tracts. *robo2* mutants have only mild projection defects; whereas, *robo1robo2* double mutants have a *slit* like phenotype (Dickson, *et al.*, 2000). Although direct binding of Slit to Robo2 or Robo3 has not been shown, assessment of the *robo1robo2* double mutant embryos strongly suggests that Robo2 may be a second repellent receptor for Slit.

Does Robo1 interact with Slit in other Slit expressing tissues?

Slit expression in the MG has been associated with a non-repellent function of Slit responsible for the migration or maintenance of close midline cell contacts regulating MG development. Robo expression, found on the longitudinal axons and dramatically down regulated on commissural axons is not found localized to the MG. MG morphology in *robo1* mutant embryos appears wild type, and embryos transheterozygous for both *robo1* and a range of *slit* alleles display no change in MG number or morphology. It is possible that *slit* interacts genetically with other *robo* receptors, but more likely Slit functions through other receptors or the ECM as suggested by data resulting from the overexpression of C-terminal Slit previously discussed in chapter 3. The role of Slit in MG development is then independent of *robo*.

As in the MG, Slit expression observed in the cardioblast cells was proposed to mediate cell-cell contact between ipsilateral cardioblast partners as they migrate dorsally along the epidermis (Chapter 2). No Robo1 expression has been localized to the cardioblast cells. Furthermore, the lack of any mutant heart phenotype in *robo1* mutant embryos led us to believe that Slit again functions independently of Robo in the cardioblasts. Analysis of doubly heterozygous *robo1* and *slit* alleles representing each range of *slit* mutant phenotypes did not uncover evidence of any genetic interaction of *slit* and *robo1* in heart development. Therefore, we believe that *slit's* role in heart development and development of the MG is independent of its repellent function in CNS development. Further investigations in these roles are pending.

Guidance errors observed in the development of muscles in *slit* mutant embryos are believed to be associated with a reduction of Slit repellent signaling at the ventral midline (Battye *et al*, 1999;Kidd *et al*, 1999). Expression of transgenic Slit at the midline is sufficient to rescue a *slit* mutant phenotype and pan-neural overexpression of complete Slit creates guidance errors in a subset of the ventral muscles (Goodman, personal communication). We have observed Robo1 antibody labeling resembling the deposition of Slit found at the muscle apodemes. *robo1* mutant embryos produce only minor guidance errors in the ventral muscles; however, a larger subset of muscles are observed anchoring closer to the midline than in wild type embryos (Kidd *et al*, 1999). These findings indicate that although Robo1 might not be the primary Slit receptor on muscle growth cones, Slit does function in a repellent manner to these growth cones. Analysis of *robo2* and *robo3* may provide the answers to Slits function in the muscle growth cones.

Leucine Rich Repeats in Slit are required to bind Robo1

In co-operation with the Goodman Lab we have restricted our *in vitro* investigation of Slit/Robo protein interactions to the localization of Robo binding to Slit motifs. In this task we have identified a requirement for the LRR repeats in binding of *in vitro* translated Robo1. *In vitro* translated Slit lacking any or all of the LRR failed to bind Robo1, whereas deletion of the EGF or G-domains alone did not alter Robo1 binding. Interestingly, Slit with the combined deletion of EGF and G-domains failed to bind Robo1. This could represent the introduction of instability into the translation of Slit; however, *in vivo* expression of this transgene was sufficient to partially rescue the *slit* mutant phenotype (Chapter 3). Perhaps *in vivo* mechanisms regulating the processing of Slit and Robo are not being represented here. Clearly, this warrants a more detailed analysis of Robo1 binding. Additional transgenes representing more selective deletions in the LRR will help us refine this analysis. As corroboration of our structural functional analysis of *slit* mutants, these findings confirm recent mammalian data that Slit binds Robo (Brose *et al*, 1999), and more specifically binds via the LRR.

***robo1* encodes one of the repellent receptor for Slit**

Taken together these results strongly suggest that Slit is a multifunctional molecule. In the midline CNS and muscles, Slit functions as a repellent ligand to the Robo1 receptor and likely two other members of the *robo* family, Robo2 and Robo3. In this role *slit* mediates production and control of the midline boundary. Repellent signaling through Robo1 appears to occur through the LRR regions of Slit, but Slit binding to Robo2 and Robo3 remains to be shown. Slit expression in the MG and cardioblast is believed to regulate mechanisms of cell adhesion and communication, yet

these mechanisms are not understood. Slit is now one of a growing family of signaling molecules shown to perform multiple functions and bind multiple receptors during development. As our understanding of the mechanisms that regulate the development of complex systems grows, the number of players appears to diminish while revealing diversified function.

Conclusions & Prospects

The data reported here supports a model of midline repellent signaling by *slit.* Slit is the midline ligand for Robo1. By binding Robo1, Slit communicates a repellent signaling gradient from the *Drosophila* midline that prevents CNS axons from inappropriately entering the midline. Comm. expression in the MG at each segmental commissure down regulates Robo1 on pioneering growth cones and removes their sensitivity to Slit in the midline. Roboless growth cones are then allowed to cross at the commissures, insensitive to local Slit. Upon crossing, Robo1 is permanently up regulated along with the introduction of other signaling mechanisms such as RTPKs and Ephrins onto the axon growth cone. Axons modified while crossing the commissures are then restricted from crossing the midline again. Guidance signaling by Robo, Comm., and Slit establishes repellent signaling in the midline responsible for establishing the bilateral halves of the *Drosophila* CNS.

Data presented in this investigation has established that the Slit LRR repeats are required for Slit repellent signaling in the midline. Transgenic rescues of *slit* mutant CNS phenotypes and overexpression assays along with *in vitro* binding data all indicate that Robo1 mediated repellent signaling at the midline requires the Slit LRR domains and that Slit binds Robo1 via the LRR. The role of LRR domains in other proteins such as

Trk, Decorin, and Fibromodulin also mediate protein-protein interactions, which would suggest that the LRR domains in Slit are likely responsible for binding Slit to the Robo receptor expressed on axon growth cones. Whether protein interactions between LRR in Slit and Robo1 directly mediate repulsive mechanisms within the growth cone or simply localize other active Slit domains is unclear. Overexpression phenotypes observed using isolated LRR domains suggest that Slit-LRR/Robo1 interactions directly mediate repulsive mechanisms, however, genetic interaction data using *robo1* mutants show that these interactions do not completely uncover the *slit* mutant phenotype. The identification of Robo2 and Robo3 mutations in *Drosophila* that when functionally removed with Robo1 reveal a *slit*-like phenotype suggest that Slit also interacts with other Robo receptors to maintain repulsive signaling in the midline. Whether Slit repellent signaling through Robo2 and Robo3 requires the LRR in Slit has yet to be determined. If this is the case as one may expect considering the isolated LRR *slit* transgene rescues, then Slit's role in the midline repulsion is largely mediated through Slit's LRR domains. Repulsive mechanisms in the midline appear therefore appear to be mediated by a single protein, Slit, that acts through a group of different Robo receptors to establish a gradient of repulsive signaling at the midline. Midline crossing regulated in part by Comm. regulation of Robo1 expression is sufficient for axon growth cones to reach the midline checkpoint where they are directed to continue across the midline and modified such that they can not cross again. This model emphasizes the fact that a single protein acting through a number of receptors can define such a complex process establishing the border that defines the bilaterally symmetric halves of an embryo.

The structural complexity and pattern of Slit expression suggested that Slit functions extend beyond those identified in the CNS midline and indeed this appears to be the case. Perhaps directly related to Slits role as a guidance molecule, we found that *slit* performed an important role in muscle development during insertion of the muscles at the lateral border of the *Drosophila* ventral midline. However, we have also identified potential roles for Slit in MG and heart development that seem independent of guidance functions. Hence, Slit not only mediates variable means of axon guidance through different repulsive receptors, but also performs yet unidentified roles in MG and heart development that are independent of its function in CNS development. Future work elaborating Slits role in Robo mediated repulsion and characterizing Slits function in the MG and cardioblast cells will expand our understanding of multifunctional proteins that appear to have independent functions in different systems.

OVERVIEW

Slit and Robo have complementary patterns of expression in the *Drosophila* midline. The Slit ligand expressed in the midline glia is bound by the repulsive receptor Robo that is expressed on axon growth cones developing on each side of the midline. The midline therefore represents a repulsive barrier to Robo expressing axons. Similarly, complementary patterns of Slit and Robo expression have been identified in a number of different tissues, one for example being the developing vertebrate forebrain (Nguyen Ba-Charvet, Brose, et al. 1999). Within regions of the brain, (Hu 1999) Slit2 expression has been specifically localized to the Septum with little or no expression described in the surrounding lateral of medial ganglionic eminence (Li, Chen, et al. 1999). The Septum is known to provide repulsive and other signaling cues to the olfactory bulb axons while

they project to their cortical targets forming the lateral olfactory tract (Keynes, Tannahill, et al. 1997). Robo is expressed in the olfactory bulb and neocortex in a pattern complementary to Slit where it is ideally located to act as a receptor to Slit (Li, Chen, et al. 1999).

In the mouse visual system Slit and Robo are expressed at the appropriate time and place to regulate retinal ganglion cell out growth (Erskine, Williams, et al. 2000). Slit expression in the CD44 neurons that define the inhibitory zone of the posterior optic chiasm, the diencephalon region (Erskine, Williams, et al. 2000)(Wu, Wong, et al. 1999), the hypothalamus, and the epithalamus (Ringstedt, Braisted, et al. 2000) define the pathway that the Robo2 expressing RGC follow from the eye to the midbrain. The gradient of Slit 1 and 2 within the retinal RGC layers exhibits a high ventral to low dorsal pattern of expression that is reminiscent of the EphAB/EphrinAB graded expression described in the same tissues (Hornberger, Dutting, et al. 1999).

Another cortical pathway that is heavily dependent on axon guidance during development is the hippocampus (Amaral & Witter 1989)(Chedotal, Del Rio, et al. 1998). Projections of the perforant pathway connect the entorhinal cortex through the amygdala to the granule cells in the dentate gyrus and CA3 neurons (Chedotal, Del Rio, et al. 1998). Slit2 expression in the entorhinal cortex, the gentate gyrus and on the CA3 neurons defines a boundary that is somewhat complementary to the patterns of Robo1 and Robo2 expression in the hippocampus. The repulsive nature ascribed to these Slit expressing tissues has been previously attributed to the secreted Semaphorins that are expressed in the same tissues. It appears that wiring of these tissues requires multiple overlapping cues.

Further examples of Slit/Robo expression patterns have been defined in the floorplate and adjacent axon growth cones (Brose, Bland, et al. 1999) where Slit and Robo act as guidance molecules. Slit also has been found to promote collateral branching of sensory neurons entering the spinal cord from the dorsal root ganglion (Wang, Brose, et al. 1999). In this capacity Slit would appear to have a bifunctional role as a positive regulator of axon branching and a repulsive midline guidance cue. Slit and Robo expression in the Murine kidney also suggests that these molecules function in morphogenesis (Piper, Georgas, et al. 2000). Cleary, a careful investigation of Slit and Robo expression and function need to be conducted.

Although only limited evidence has been uncovered as to the function of Slit and Robo in these tissues, the pattern and location of Slit and Robo expression in the CNS suggests that these proteins affect guidance decisions. Furthermore, extensive characterization of other guidance molecules such as Eph/Ephrin (O'Leary & Wilkinson 1999), Semaphorin/Neuropilin (Raper 2000), and Netrin/DCC (Hiramoto, Hiromi, et al. 2000) that function in similar complementary gradients overlapping those of Slit and Robo lend support to a general role for Slit/Robo molecules in axon guidance.

In the *Drosophila* midline, Slit causes the collapse of filopodia on Robo expressing growth cones that have extended onto the midline. Once medial projections are pruned in this manner, growth cones reorient along the longitudinal axon tracts (Kidd, Russell, et al. 1998)(Murray & Whitington 1999). Conversely, sensory neurons extending into the spinal cord from the dorsal root ganglion in vertebrates sprout collateral branches in response to Slit (Wang, Brose, et al. 1999). These seemingly disparate roles both involve fundamental changes in growth cone function in response to

Slit. In an inspired experiment by Bashaw and Goodman (1999) in which the cytoplasmic domains of the Robo repulsive receptor and the Frazzled attractive receptor where exchanged, they revealed that the nature of the guidance response was determined by the intracellular protein structure of the receptor. This insight further supports the notion that guidance molecules may function as both attractive and repulsive signals dependent on the receptor complex they interact with (Terman & Kolodkin 1999)(Yu & Kolodkin 1999). More importantly, these investigations identify the cytoplasmic domains of guidance receptors as the mediators of axon guidance responses. So, how do extracellular signals induce changes in growth cone behaviour through receptor cytoplasmic domains?

One example of a receptor mediated change in axon growth cone motility was revealed with the identification of the *Drosophila* guidance receptor typrosine phospatase (RPTP) Dlar (Wills, Marr, et al. 1999)(Wills, Bateman, et al. 1999 805). Dlar is an orphan membrane receptor whose cytoplasmic domain associates with the Enabled/VASP family of proteins and Abelson (Abl). The Enabled/VASP family members control the cytoskeletal motility apparatus by binding the actin regulatory protein Profilin (Hu & Reichardt 1999). Enabled is phosphorylated and binds Profilin. Profilin then catalyzes the exchange of ADP for ATP in globular Actin, favouring further Actin polymerization.

The regulation of Actin dynamics determines the motility of growth cone guidance by controlling the extension and retraction of lamellipodia and filopodia along the extracellular matrix (Suter & Forscher 2000) (for a complete review see the special issue of the Journal of Neurobiology, 2000, (44)). Abl kinase antagonizes Dlar function

by binding both the cytoplasmic domain of Dlar and its substrate Enabled. The interaction between Abl, Dlar, and Enabled may either directly or indirectly affect the phosphorylation of Enabled such that Profilin activity is reduced (Wills, Bateman, et al. 1999). The regulation of Enabled phosphorylation generates a state-dependent switch that controls growth cone behaviour via the actin cytoskeleton. This illustrates one guidance pathway in which surface receptors control growth cone motility.

Other pathways that regulate cellular actin structures include the small Rho family GTPases (Hu & Reichardt 1999) and have been linked to the molecular basis of Semaphorin-mediated axon guidance (Nakamura, Kalb, et al. 2000) and its receptors Neuropilin and the Plexins (Raper 2000). The discovery of Abl and Enabled binding domains in the cytoplasmic region of the Robo receptor indicates that Robo guidance likely functions through the Enable/VASP family pathway (Bashaw, Kidd, et al. 2000). Other outputs that control axonal pathfinding and cytoskeletal organization include KETTE, a transmembrane protein that interacts with the vertebrate SH2-SH3 adapter protein NCK (Hummel, Leifker, et al. 2000) and Dock which is the invertebrate homologue of NCK (Clemens, Ursuliak, et al. 1996). These proteins function through the small GTPase RAC1 similar to the Semaphorin pathway described above (Ruan, Pang, et al. 1999).

Genetic interactions between *robo*, *abl*, and *ena* resulting in thicker axon commissures and defects in longitudinal axon tracts suggest that Robo cytoplasmic signaling in part functions through the Enabled family of molecules (Bashaw, Kidd, et al. 2000). Mutations in the Robo cytoplasmic domain that interfere with Enabled binding

cause a mild Robo phenotype, while mutations in domains phosphorylated by Abl generate a hyperactive Robo receptor.

Further evidence suggesting the importance of Robo phosphorylation was provided while studying the CNS specific receptor protein tyrosine phosphatases 10D and 69D (Sun, Bahri, et al. 2000). Double mutations removing both of these genes resulted in substantial ectopic midline crossing and demonstrated dosage sensitive interaction with both *slit* and *robo* in invertebrates (Sun, Bahri, et al. 2000). The established guidance roles of receptor Tyrosine Phosphatases such as CRYP in the developing visual system (Muller & Brandli 1999), LAR in the CNS (Baker & Macagno 2000), and PTP-δ in the vertebrate brain (Wang & Bixby 1999)(Wang & Bixby 1999) further emphasizes the importance of Phosphotases in growth and guidance functions. As Robo function depends in part on the phosphorylation states of both Abl and Enabled, and *robo* demonstrates interaction with the RPTPs 10D and 69D, these proteins may all interact to mediate growth motility at the growth cones leading edge. By varying the number and combination of molecules involved in cytoplasmic signaling events it is possible to imagine a multitude of molecular events that may be involved in regulating Actin assembly and disassembly.

In terms of Slit's function in midline guidance, Robo appears to down-regulate Actin polymerization causing growth cones to withdraw from the midline. In the presence of Comm, growth cones continue to extend into and across the midline indicating that Robo function is antagonized. Comm's role in antagonizing Robo function is clear however the mechanism by which this is accomplished is not. Data indicate that Comm is transferred from the midline glia to the growth cone of Robo

expressing axons. We now can suggest a number of mechanisms by which down-regulation of Robo may occur. Once Comm is acquired by axon growth cones it may endocytose Robo (Tear, Harris, et al. 1996)(Wolf, Seeger, et al. 1998), indirectly block Robo phosphorylation and Actin polymerization, or directly block interactions with the Robo cytoplasmic domain. These possibilities emphasize the importance of the Robo cytoplasmic domain in repulsive signaling to Slit.

Slit has also been demonstrated to have an inductive role in collateral branching of dorsal root ganglion sensory neurons (Wang, Brose, et al. 1999). These alternate roles for Slit may easily be arrived at by small changes in Robo cytoplasmic function or alternately through different receptors. To date, 3 different Robo receptors with different cytoplasmic domains and patterns of expression have been identified.(Dickson *et al*, 2000) Overall, it is becoming readily apparent that the diversity and complexity in guidance functions required during nervous system development is mediated by a few families of receptors that have more diverse functions. Recent data presented by Bashaw and Goodman (1999) and Terman and Kolodkin (1999) demonstrating that receptor complexes and cytoplasmic signaling events are the key to receptor function emphasizes the need to more clearly define the role of these cytoplasmic events in axon guidance. This also creates a new perspective from which to investigate Slits function in non-guidance roles in other tissues.

References

(1997) Unified nomenclature for Eph family receptors and their ligands, the ephrins. Eph Nomenclature Committee [letter]. *Cell*, **90**, 403-404.

Ackerman,S.L. & Knowles,B.B. (1998) Cloning and mapping of the UNC5C gene to human chromosome 4q21-q23. *Genomics*, **52**, 205-208.

Ackerman,S.L., Kozak,L.P., Przyborski,S.A., Rund,L.A., Boyer,B.B., & Knowles,B.B. (1997) The mouse rostral cerebellar malformation gene encodes an UNC-5-like protein. *Nature*, **386** , 838-842.

Andac,Z., Sasaki,T., Mann,K., Brancaccio,A., Deutzmann,R., & Timpl,R. (1999) Analysis of heparin, alpha-dystroglycan and sulfatide binding to the G domain of the laminin alpha1 chain by site-directed mutagenesis. *J.Mol.Biol.*, **287**, 253-264.

Arendt,D. & Nubler-Jung,K. (1999) Comparison of early nerve cord development in insects and vertebrates. *Development*, **126**, 2309-2325.

Ashburner,M. (1989) *Drosophila,* Cold Spring Harbor Laboratory, Cold Spring Harbor, NY.

Auld,V. (1999) Glia as mediators of growth cone guidance: studies from insect nervous systems. *Cell Mol.Life Sci.*, **55**, 1377-1385.

Badenhorst,P., Harrison,S., & Travers,A. (1996) End of the line? Tramtrack and cell fate determination in Drosophila. *Genes Cells*, **1**, 707-716.

Bagnard,D., Thomasset,N., Lohrum,M., Puschel,A.W., & Bolz,J. (2000) Spatial distributions of guidance molecules regulate chemorepulsion and chemoattraction of growth cones. *J.Neurosci.*, **20**, 1030-1035.

Bashaw,G.J. & Goodman,C.S. (1999) Chimeric axon guidance receptors: the cytoplasmic domains of slit and netrin receptors specify attraction versus repulsion [see comments]. *Cell*, **97**, 917-926.

Battye,R., Stevens,A., & Jacobs,J.R. (1999) Axon repulsion from the midline of the Drosophila CNS requires slit function. *Development*, **126**, 2475-2481.

Bergemann,A.D., Zhang,L., Chiang,M.K., Brambilla,R., Klein,R., & Flanagan,J.G. (1998) Ephrin-B3, a ligand for the receptor EphB3, expressed at the midline of the developing neural tube. *Oncogene*, **16**, 471-480.

Bhat,K.M., van Beers,E.H., & Bhat,P. (2000) Sloppy paired acts as the downstream target of wingless in the Drosophila CNS and interaction between sloppy paired and gooseberry inhibits sloppy paired during neurogenesis. *Development*, **127**, 655-665.

Booth,G.E., Kinrade,E.F., & Hidalgo,A. (2000) Glia maintain follower neuron survival during Drosophila CNS development. *Development*, **127**, 237-244.

Brand,A.H. & Perrimon,N. (1993) Targeted gene expression as a means of altering cell fates and generating dominant phenotypes. *Development*, **118**, 401-415.

Brose,K., Bland,K.S., Wang,K.H., Arnott,D., Henzel,W., Goodman,C.S., Tessier-Lavigne,M., & Kidd,T. (1999) Slit proteins bind Robo receptors and have an evolutionarily conserved role in repulsive axon guidance. *Cell*, **96**, 795-806.

Brown,J.C., Sasaki,T., Gohring,W., Yamada,Y., & Timpl,R. (1997) The C-terminal domain V of perlecan promotes beta1 integrin-mediated cell adhesion, binds heparin, nidogen and fibulin-2 and can be modified by glycosaminoglycans. *Eur.J.Biochem.*, **250**, 39-46.

Bunch,T.A., Graner,M.W., Fessler,L.I., Fessler,J.H., Schneider,K.D., Kerschen,A., Choy,L.P., Burgess,B.W., & Brower,D.L. (1998) The PS2 integrin ligand tiggrin is required for proper muscle function in Drosophila. *Development*, **125**, 1679-1689.

Campbell,I.D. & Bork,P. (1993) Epidermal growth factor-like modules. *Curr.Opin.Struct.Biol.*, **3**, 385-392.

Campos-Ortega,J.A. (1997) Asymmetic division: dynastic intricacies of neuroblast division. *Curr.Biol.*, **7**, R726-R728.

Campos-Ortega,J.A. & Hartenstein,V. (1997) *The embryonic development of Drosophila melanogaster*, 2nd ed. edn, Springer, Berlin.

Chan,S.S., Zheng,H., Su,M.W., Wilk,R., Killeen,M.T., Hedgecock,E.M., & Culotti,J.G. (1996) UNC-40, a C. elegans homolog of DCC (Deleted in Colorectal Cancer), is required in motile cells responding to UNC-6 netrin cues. *Cell*, **87**, 187-195.

Chen,H., Chedotal,A., He,Z., Goodman,C.S., & Tessier-Lavigne,M. (1997) Neuropilin-2, a novel member of the neuropilin family, is a high affinity receptor for the semaphorins Sema E and Sema IV but not Sema III [published erratum appears in Neuron 1997 Sep;19(3):559]. *Neuron*, **19**, 547-559.

Chiba,A., Hing,H., Cash,S., & Keshishian,H. (1993) Growth cone choices of Drosophila motoneurons in response to muscle fiber mismatch. *J.Neurosci.*, **13**, 714-732.

Chien,C.B. (1998) Why does the growth cone cross the road? *Neuron*, **20**, 3-6.

Ciossek,T., Monschau,B., Kremoser,C., Loschinger,J., Lang,S., Muller,B.K., Bonhoeffer,F., & Drescher,U. (1998) Eph receptor-ligand interactions are necessary for guidance of retinal ganglion cell axons in vitro. *Eur.J.Neurosci.*, **10**, 1574-1580.

Colamarino,S.A. & Tessier-Lavigne,M. (1995) The role of the floor plate in axon guidance. *Annu.Rev.Neurosci.*, **18**, 497-529.

Colavita,A. & Culotti,J.G. (1998) Suppressors of ectopic UNC-5 growth cone steering identify eight genes involved in axon guidance in Caenorhabditis elegans. *Dev.Biol.*, **194**, 72-85.

Cook,G., Tannahill,D., & Keynes,R. (1998) Axon guidance to and from choice points. *Curr.Opin.Neurobiol.*, **8**, 64-72.

Crair,M.C. (1999) Neuronal activity during development: permissive or instructive? *Curr.Opin.Neurobiol.*, **9**, 88-93.

Crews,S.T. (1998) Control of cell lineage-specific development and transcription by bHLH- PAS proteins. *Genes Dev.*, **12**, 607-620.

Crews,S.T. & Fan,C.M. (1999) Remembrance of things PAS: regulation of development by bHLH-PAS proteins. *Curr.Opin.Genet.Dev.* , **9**, 580-587.

Crews,S.T., Thomas,J.B., & Goodman,C.S. (1988) The Drosophila single-minded gene encodes a nuclear protein with sequence similarity to the per gene product. *Cell*, **52**, 143-151.

Dickson,B.J., Rajagopalan,S., Nicolas,E., & Vivancos,V. (2000) Multiple Robo receptors control midline crossing and lateral positioning of CNS axons. (Abstract).*41st Annual Drosophila Research Conference*, **41**, 98.

Doe,C.Q. (1996) Asymmetric cell division and neurogenesis. *Curr.Opin.Genet.Dev.*, **6**, 562-566.

Doherty,P. & Walsh,F.S. (1994) Signal transduction events underlying neurite outgrowth stimulated by cell adhesion molecules. *Curr.Opin.Neurobiol.*. **4**, 49-55.

Drescher,U., Kremoser,C., Handwerker,C., Loschinger,J., Noda,M., & Bonhoeffer,F. (1995) In vitro guidance of retinal ganglion cell axons by RAGS, a 25 kDa tectal protein related to ligands for Eph receptor tyrosine kinases. *Cell*, **82**, 359-370.

Elkins,T., Hortsch,M., Bieber,A.J., Snow,P.M., & Goodman,C.S. (1990) Drosophila fasciclin I is a novel homophilic adhesion molecule that along with fasciclin III can mediate cell sorting. *J.Cell Biol.*, **110**, 1825-1832.

Fambrough,D. & Goodman,C.S. (1996) The Drosophila beaten path gene encodes a novel secreted protein that regulates defasciculation at motor axon choice points. *Cell*, **87**, 1049-1058.

Fleming,J.E. & Kwak,E.L. (1986) In vitro translation products of Drosophila mitochondria are contaminated with newly synthesized bacterial proteins. *Biochem.Biophys.Res.Commun.*, **136**, 797-801.

Fogerty,F.J., Fessler,L.I., Bunch,T.A., Yaron,Y., Parker,C.G., Nelson,R.E., Brower,D.L., Gullberg,D., & Fessler,J.H. (1994) Tiggrin, a novel Drosophila extracellular matrix protein that functions as a ligand for Drosophila alpha PS2 beta PS integrins. *Development*, **120**, 1747-1758.

Gabay,L., Scholz,H., Golembo,M., Klaes,A., Shilo,B.Z., & Klambt,C. (1996) EGF receptor signaling induces pointed P1 transcription and inactivates Yan protein in the Drosophila embryonic ventral ectoderm. *Development*, **122**, 3355-3362.

Gad,J.M., Keeling,S.L., Shu,T., Richards,L.J., & Cooper,H.M. (2000) The spatial and temporal expression patterns of netrin receptors, DCC and neogenin, in the developing mouse retina. *Exp.Eye Res.*, **70**, 711-722.

Gad,J.M., Keeling,S.L., Wilks,A.F., Tan,S.S., & Cooper,H.M. (1997) The expression patterns of guidance receptors, DCC and Neogenin, are spatially and temporally distinct throughout mouse embryogenesis. *Dev.Biol.*, **192**, 258-273.

Gesemann,M., Brancaccio,A., Schumacher,B., & Ruegg,M.A. (1998) Agrin is a high-affinity binding protein of dystroglycan in non-muscle tissue. *J.Biol.Chem.*, **273**, 600-605.

Gesemann,M., Cavalli,V., Denzer,A.J., Brancaccio,A., Schumacher,B., & Ruegg,M.A. (1996) Alternative splicing of agrin alters its binding to heparin, dystroglycan, and the putative agrin receptor. *Neuron*, **16**, 755-767.

Gesemann,M., Denzer,A.J., & Ruegg,M.A. (1995) Acetylcholine receptor-aggregating activity of agrin isoforms and mapping of the active site. *J.Cell Biol.*, **128**, 625-636.

Giesen,K., Hummel,T., Stollewerk,A., Harrison,S., Travers,A., & Klambt,C. (1997) Glial development in the Drosophila CNS requires concomitant activation of glial and repression of neuronal differentiation genes. *Development*, **124**, 2307-2316.

Gilbert,S.F., Opitz,J.M., & Raff,R.A. (1996) Resynthesizing evolutionary and developmental biology [see comments]. *Dev.Biol.* , **173**, 357-372.

Glass,D.J., Apel,E.D., Shah,S., Bowen,D.C., DeChiara,T.M., Stitt,T.N., Sanes,J.R., & Yancopoulos,G.D. (1997) Kinase domain of the muscle-specific receptor tyrosine kinase (MuSK) is sufficient for phosphorylation but not clustering of acetylcholine receptors: required role for the MuSK ectodomain? *Proc.Natl.Acad.Sci.U.S.A*, **94**, 8848-8853.

Glass,D.J., DeChiara,T.M., Stitt,T.N., DiStefano,P.S., Valenzuela,D.M., & Yancopoulos,G.D. (1996) The receptor tyrosine kinase MuSK is required for neuromuscular junction formation and is a functional receptor for agrin. *Cold Spring Harb.Symp.Quant.Biol.*, **61**, 435-444.

Goodman,C.S. (1994) The likeness of being: phylogenetically conserved molecular mechanisms of growth cone guidance. *Cell*, **78**, 353-356.

Goodman,C.S. (1996) Mechanisms and molecules that control growth cone guidance. *Annu.Rev.Neurosci.*, **19**, 341-377.

Goodman,C.S., Bastiani,M.J., Doe,C.Q., & Dulac,S. (1986) Growth cone guidance and cell recognition in insect embryos. *Dev.Biol.(N.Y.1985.)*, **3**, 283-300.

Gotwals,P.J., Fessler,L.I., Wehrli,M., & Hynes,R.O. (1994) Drosophila PS1 integrin is a laminin receptor and differs in ligand specificity from PS2. *Proc.Natl.Acad.Sci.U.S.A*, **91**, 11447-11451.

Grenningloh,G., Rehm,E.J., & Goodman,C.S. (1991) Genetic analysis of growth cone guidance in Drosophila: fasciclin II functions as a neuronal recognition molecule. *Cell*, **67**, 45-57.

Guthrie,S. (1997) Axon guidance: netrin receptors are revealed. *Curr.Biol.*, **7**, R6-R9.

Haag,T.A., Haag,N.P., Lekven,A.C., & Hartenstein,V. (1999) The role of cell adhesion molecules in Drosophila heart morphogenesis: faint sausage, shotgun/DE-cadherin, and laminin A are required for discrete stages in heart development. *Dev.Biol.*, **208**, 56-69.

Halfon,M.S., Hashimoto,C., & Keshishian,H. (1995) The Drosophila toll gene functions zygotically and is necessary for proper motoneuron and muscle development. *Dev.Biol.*, **169**, 151-167.

Halfon,M.S. & Keshishian,H. (1998) The Toll pathway is required in the epidermis for muscle development in the Drosophila embryo. *Dev.Biol.*, **199**, 164-174.

Hallbook,F. (1999) Evolution of the vertebrate neurotrophin and Trk receptor gene families. *Curr.Opin.Neurobiol.*, **9**, 616-621.

Hedgecock,E.M., Culotti,J.G., & Hall,D.H. (1990) The unc-5, unc-6, and unc-40 genes guide circumferential migrations of pioneer axons and mesodermal cells on the epidermis in C. elegans. *Neuron*, **4**, 61-85.

Hidalgo,A. & Booth,G.E. (2000) Glia dictate pioneer axon trajectories in the Drosophila embryonic CNS. *Development*, **127**, 393-402.

Hiramoto,M., Hiromi,Y., Giniger,E., & Hotta,Y. (2000) A Drosophila Netrin receptor, Fazzled, guides axons by controlling the distribution of Netrin. *Nature*, (in press).

Hocking,A.M., Shinomura,T., & McQuillan,D.J. (1998) Leucine-rich repeat glycoproteins of the extracellular matrix. *Matrix Biol.*, **17**, 1-19.

Holland,L.Z. & Holland,N.D. (1999) Chordate origins of the vertebrate central nervous system. *Curr.Opin.Neurobiol.*, **9**, 596-602.

Hong,K., Hinck,L., Nishiyama,M., Poo,M.M., Tessier-Lavigne,M., & Stein,E. (1999) A ligand-gated association between cytoplasmic domains of UNC5 and DCC family receptors converts netrin-induced growth cone attraction to repulsion [see comments]. *Cell*, **97**, 927-941.

Hosoya,T., Takizawa,K., Nitta,K., & Hotta,Y. (1995) glial cells missing: a binary switch between neuronal and glial determination in Drosophila. *Cell*, **82**, 1025-1036.

Hummel,T., Menne,T., Scholz,H., Granderath,S., Giesen,K., & Klambt,C. (1997) CNS midline development in Drosophila. *Perspect.Dev.Neurobiol.*, **4**, 357-368.

Hummel,T., Schimmelpfeng,K., & Klambt,C. (1999b) Commissure formation in the embryonic CNS of Drosophila. *Dev.Biol.*, **209**, 381-398.

Hummel,T., Schimmelpfeng,K., & Klambt,C. (1999a) Commissure formation in the embryonic CNS of Drosophila. *Development*, **126**, 771-779.

Imondi,R., Wideman,C., & Kaprielian,Z. (2000) Complementary expression of transmembrane ephrins and their receptors in the mouse spinal cord: a possible role in constraining the orientation of longitudinally projecting axons. *Development*, **127**, 1397-1410.

Jacobs,J.R. (1993) Perturbed glial scaffold formation precedes axon tract malformation in Drosophila mutants. *J.Neurobiol.*, **24**, 611-626.

Jacobs,J.R. (2000) The Midline Glia of Drosophila: a molecular genetic model for the developmental functions of Glia. *Prog.Neurobiol.*, **62**, 475-508.

Jacobs,J.R. & Goodman,C.S. (1989a) Embryonic development of axon pathways in the Drosophila CNS. I. A glial scaffold appears before the first growth cones. *J.Neurosci.*, **9**, 2402-2411.

Jacobs,J.R. & Goodman,C.S. (1989b) Embryonic development of axon pathways in the Drosophila CNS. II. Behavior of pioneer growth cones. *J.Neurosci.*, **9**, 2412-2422.

Jacobs,J.R., Hiromi,Y., Patel,N.H., & Goodman,C.S. (1989) Lineage, migration, and morphogenesis of longitudinal glia in the Drosophila CNS as revealed by a molecular lineage marker. *Neuron*, **2**, 1625-1631.

Jessell,T.M. & Dodd,J. (1990) Floor plate-derived signals and the control of neural cell pattern in vertebrates. *Harvey Lect.*, **86**, 87-128.

Jones,B.W., Fetter,R.D., Tear,G., & Goodman,C.S. (1995) glial cells missing: a genetic switch that controls glial versus neuronal fate. *Cell*, **82**, 1013-1023.

Karess,R.E. & Rubin,G.M. (1984) Analysis of P transposable element functions in Drosophila. *Cell*, **38**, 135-146.

Keeling,S.L., Gad,J.M., & Cooper,H.M. (1997) Mouse Neogenin, a DCC-like molecule, has four splice variants and is expressed widely in the adult mouse and during embryogenesis. *Oncogene*, **15**, 691-700.

Keino-Masu,K., Masu,M., Hinck,L., Leonardo,E.D., Chan,S.S., Culotti,J.G., & Tessier-Lavigne,M. (1996) Deleted in Colorectal Cancer (DCC) encodes a netrin receptor. *Cell*, **87**, 175-185.

Keshishian,H., Broadie,K., Chiba,A., & Bate,M. (1996) The drosophila neuromuscular junction: a model system for studying synaptic development and function. *Annu.Rev.Neurosci.*, **19** , 545-575.

Kidd,T., Bland,K.S., & Goodman,C.S. (1999) Slit is the midline repellent for the robo receptor in Drosophila. *Cell*, **96**, 785-794.

Kidd,T., Brose,K., Mitchell,K.J., Fetter,R.D., Tessier-Lavigne,M., Goodman,C.S., & Tear,G. (1998a) Roundabout controls axon crossing of the CNS midline and defines a novel subfamily of evolutionarily conserved guidance receptors. *Cell*, **92**, 205-215.

Kidd,T., Brose,K., Mitchell,K.J., Fetter,R.D., Tessier-Lavigne,M., Goodman,C.S., & Tear,G. (1998b) Roundabout controls axon crossing of the CNS midline and defines a novel subfamily of evolutionarily conserved guidance receptors. *Cell*, **92**, 205-215.

Kidd,T., Russell,C., Goodman,C.S., & Tear,G. (1998c) Dosage-sensitive and complementary functions of roundabout and commissureless control axon crossing of the CNS midline. *Neuron*, **20**, 25-33.

Klaes,A., Menne,T., Stollewerk,A., Scholz,H., & Klambt,C. (1994) The Ets transcription factors encoded by the Drosophila gene pointed direct glial cell differentiation in the embryonic CNS. *Cell*, **78**, 149-160.

Klambt,C. (1993) The Drosophila gene pointed encodes two ETS-like proteins which are involved in the development of the midline glial cells. *Development*, **117**, 163-176.

Klambt,C. & Goodman,C.S. (1991a) Role of the midline glia and neurons in the formation of the axon commissures in the central nervous system of the Drosophila embryo. *Ann.N.Y.Acad.Sci.*, **633**, 142-159.

Klambt,C. & Goodman,C.S. (1991b) The diversity and pattern of glia during axon pathway formation in the Drosophila embryo. *Glia*, **4**, 205-213.

Klambt,C., Jacobs,J.R., & Goodman,C.S. (1991) The midline of the Drosophila central nervous system: a model for the genetic analysis of cell fate, cell migration, and growth cone guidance. *Cell*, **64**, 801-815.

Klambt,C., Schimmelpfeng,K., & Hummel,T. (1999) Glia development in the embryonic CNS of Drosophila. *Adv.Exp.Med.Biol.*, **468**, 23-32.

Knobel,K.M., Jorgensen,E.M., & Bastiani,M.J. (1999) Growth cones stall and collapse during axon outgrowth in Caenorhabditis elegans. *Development*, **126**, 4489-4498.

Kolodkin,A.L., Matthes,D.J., & Goodman,C.S. (1993) The semaphorin genes encode a family of transmembrane and secreted growth cone guidance molecules. *Cell*, **75**, 1389-1399.

Kolodziej,P.A., Timpe,L.C., Mitchell,K.J., Fried,S.R., Goodman,C.S., Jan,L.Y., & Jan,Y.N. (1996) frazzled encodes a Drosophila member of the DCC immunoglobulin subfamily and is required for CNS and motor axon guidance. *Cell*, **87**, 197-204.

Krishnan,P., Hocking,A.M., Scholtz,J.M., Pace,C.N., Holik,K.K., & McQuillan,D.J. (1999) Distinct secondary structures of the leucine-rich repeat proteoglycans decorin and biglycan. Glycosylation-dependent conformational stability. *J.Biol.Chem.*, **274**, 10945-10950.

Kunisch,M., Haenlin,M., & Campos-Ortega,J.A. (1994) Lateral inhibition mediated by the Drosophila neurogenic gene delta is enhanced by proneural proteins. *Proc.Natl.Acad.Sci.U.S.A*, **91**, 10139-10143.

Kwiatkowska,D. & Kwiatkowska-Korczak,J. (1999) [Adhesive glycoproteins of the extracellular matrix]. *Postepy Hig.Med.Dosw.*, **53**, 55-74.

Lanoue,B.R., Gordon,M.D., Battye,R., & Jacobs,J.R. (2000) Genetic analysis of vein function in the Drosophila embryonic nervous system [In Process Citation]. *Genome*, **43**, 564-573.

Lanoue,B.R. & Jacobs,J.R. (1999) Rhomboid function in the midline of the Drosophila CNS. *Dev.Genet.*, **25**, 321-330.

Le Douarin,N.M. & Halpern,M.E. (2000) Discussion point. Origin and specification of the neural tube floor plate: insights from the chick and zebrafish [see comments]. *Curr.Opin.Neurobiol.*, **10**, 23-30.

Lee,C.M., Yu,D.S., Crews,S.T., & Kim,S.H. (1999) The CNS midline cells and spitz class genes are required for proper patterning of Drosophila ventral neuroectoderm. *Int.J.Dev.Biol.*, **43**, 305-315.

Leptin,M. (1991) twist and snail as positive and negative regulators during Drosophila mesoderm development. *Genes Dev.*, **5**, 1568-1576.

Leptin,M. (1995) Drosophila gastrulation: from pattern formation to morphogenesis. *Annu.Rev.Cell Dev.Biol.*, **11**, 189-212.

Leptin,M. (1999) Gastrulation in Drosophila: the logic and the cellular mechanisms. *EMBO J.*, **18**, 3187-3192.

Li,H.S., Chen,J.H., Wu,W., Fagaly,T., Zhou,L., Yuan,W., Dupuis,S., Jiang,Z.H., Nash,W., Gick,C., Ornitz,D.M., Wu,J.Y., & Rao,Y. (1999) Vertebrate slit, a secreted ligand for the transmembrane protein roundabout, is a repellent for olfactory bulb axons. *Cell*, **96**, 807-818.

Lin,D.M., Fetter,R.D., Kopczynski,C., Grenningloh,G., & Goodman,C.S. (1994) Genetic analysis of Fasciclin II in Drosophila: defasciculation, refasciculation, and altered fasciculation. *Neuron*, **13**, 1055-1069.

Ma,Y., Certel,K., Gao,Y., Niemitz,E., Mosher,J., Mukherjee,A., Mutsuddi,M., Huseinovic,N., Crews,S.T., Johnson,W.A., & Nambu,J.R. (2000) Functional interactions between Drosophila bHLH/PAS, Sox, and POU transcription factors regulate CNS midline expression of the slit gene. *J.Neurosci.*, **20**, 4596-4605.

Marlin,S.G., Douglas,R.M., & Cynader,M.S. (1991) Position-specific adaptation in simple cell receptive fields of the cat striate cortex. *J.Neurophysiol.*, **66**, 1769-1784.

Martinez,A.A. (1994) Pathways of cell communication during development: signalling and epistases. *Trends Genet.*, **10**, 219-222.

Martinez,A.A. (1998) Interactions between Wingless and Notch during the assignment of cell fates in Drosophila. *Int.J.Dev.Biol.*, **42**, 325-333.

Matise,M.P., Lustig,M., Sakurai,T., Grumet,M., & Joyner,A.L. (1999) Ventral midline cells are required for the local control of commissural axon guidance in the mouse spinal cord. *Development*, **126**, 3649-3659.

Menne,T.V. & Klambt,C. (1994) The formation of commissures in the Drosophila CNS depends on the midline cells and on the Notch gene. *Development*, **120**, 123-133.

Menne,T.V., Luer,K., Technau,G.M., & Klambt,C. (1997) CNS midline cells in Drosophila induce the differentiation of lateral neural cells. *Development*, **124**, 4949-4958.

Menon,K.P. & Zinn,K. (1998) Tyrosine kinase inhibition produces specific alterations in axon guidance in the grasshopper embryo. *Development*, **125**, 4121-4131.

Meyerhardt,J.A., Look,A.T., Bigner,S.H., & Fearon,E.R. (1997) Identification and characterization of neogenin, a DCC-related gene. *Oncogene*, **14**, 1129-1136.

Mitchell,K.J., Doyle,J.L., Serafini,T., Kennedy,T.E., Tessier-Lavigne,M., Goodman,C.S., & Dickson,B.J. (1996) Genetic analysis of Netrin genes in Drosophila: Netrins guide CNS commissural axons and peripheral motor axons. *Neuron*, **17**, 203-215.

Mueller,B.K. (1999) Growth cone guidance: first steps towards a deeper understanding. *Annu.Rev.Neurosci.*, **22**, 351-388.

Muller,B.K., Bonhoeffer,F., & Drescher,U. (1996) Novel gene families involved in neural pathfinding. *Curr.Opin.Genet.Dev.*, **6**, 469-474.

Muller,U. & Kypta,R. (1995) Molecular genetics of neuronal adhesion. *Curr.Opin.Neurobiol.*, **5**, 36-41.

Nakayama,M., Nakajima,D., Nagase,T., Nomura,N., Seki,N., & Ohara,O. (1998) Identification of high-molecular-weight proteins with multiple EGF-like motifs by motif-trap screening. *Genomics*, **51**, 27-34.

Nambu,J.R., Franks,R.G., Hu,S., & Crews,S.T. (1990) The single-minded gene of Drosophila is required for the expression of genes important for the development of CNS midline cells. *Cell*, **63**, 63-75.

Nambu,J.R., Lewis,J.O., & Crews,S.T. (1993) The development and function of the Drosophila CNS midline cells. *Comp Biochem.Physiol Comp Physiol*, **104**, 399-409.

Nambu,J.R., Lewis,J.O., Wharton,K.A., Jr., & Crews,S.T. (1991) The Drosophila single-minded gene encodes a helix-loop-helix protein that acts as a master regulator of CNS midline development. *Cell*, **67**, 1157-1167.

Noonan,D.M., Fulle,A., Valente,P., Cai,S., Horigan,E., Sasaki,M., Yamada,Y., & Hassell,J.R. (1991) The complete sequence of perlecan, a basement membrane heparan sulfate proteoglycan, reveals extensive similarity with laminin A chain, low density lipoprotein-receptor, and the neural cell adhesion molecule. *J.Biol.Chem.*, **266**, 22939-22947.

Noonan,D.M., Horigan,E.A., Ledbetter,S.R., Vogeli,G., Sasaki,M., Yamada,Y., & Hassell,J.R. (1988) Identification of cDNA clones encoding different domains of the basement membrane heparan sulfate proteoglycan. *J.Biol.Chem.*, **263**, 16379-16387.

Nose,A., Mahajan,V.B., & Goodman,C.S. (1992) Connectin: a homophilic cell adhesion molecule expressed on a subset of muscles and the motoneurons that innervate them in Drosophila. *Cell*, **70**, 553-567.

Nose,A., Takeichi,M., & Goodman,C.S. (1994) Ectopic expression of connectin reveals a repulsive function during growth cone guidance and synapse formation. *Neuron*, **13**, 525-539.

Nusslein-Volhard,C., Kluding,H., & Jurgens,G. (1985) Genes affecting the segmental subdivision of the Drosophila embryo. *Cold Spring Harb.Symp.Quant.Biol.*, **50**, 145-154.

Nusslein-Volhard,C. & Wieschaus,E. (1980) Mutations affecting segment number and polarity in Drosophila. *Nature*, **287**, 795-801.

Nusslein-Volhard,C.W.E.a.K.H. Mutations affecting the pattern of the larval cuticle in Drosophila melanogaster I. Zygotic loci on the second chromosome. Roux's Arch.Dev.Biol. 193, 267-282. 1984.
Ref Type: Generic

O'Leary,D.D. & Wilkinson,D.G. (1999) Eph receptors and ephrins in neural development. *Curr.Opin.Neurobiol.*, **9**, 65-73.

Ohyama,K. (1999) [Guidance of commissural axons in the neural tube--related to the induction and differentiation of ventral neurons]. *Kaibogaku Zasshi*, **74**, 453-463.

Pasquale,E.B. (1997) The Eph family of receptors. *Curr.Opin.Cell Biol.*, **9**, 608-615.

Patel,N.H., Kornberg,T.B., & Goodman,C.S. (1989a) Expression of engrailed during segmentation in grasshopper and crayfish. *Development*, **107**, 201-212.

Patel,N.H., Schafer,B., Goodman,C.S., & Holmgren,R. (1989b) The role of segment polarity genes during Drosophila neurogenesis. *Genes Dev.*, **3**, 890-904.

Patthy,L. (1992) A family of laminin-related proteins controlling ectodermal differentiation in Drosophila. *FEBS Lett.*, **298**, 182-184.

Pawson,T. & Nash,P. (2000) Protein-protein interactions define specificity in signal transduction. *Genes Dev.*, **14**, 1027-1047.

Placzek,M., Dodd,J., & Jessell,T.M. (2000) Discussion point. The case for floor plate induction by the notochord [comment]. *Curr.Opin.Neurobiol.*, **10**, 15-22.

Przyborski,S.A., Knowles,B.B., & Ackerman,S.L. (1998) Embryonic phenotype of Unc5h3 mutant mice suggests chemorepulsion during the formation of the rostral cerebellar boundary. *Development*, **125**, 41-50.

Richter,S., Hartmann,B., & Reichert,H. (1998) The wingless gene is required for embryonic brain development in Drosophila. *Dev.Genes Evol.*, **208**, 37-45.

Roberts,D.B. (1986) *Drosophila : a practical approach*, IRL, Oxford.

Roth,S., Stein,D., & Nusslein-Volhard,C. (1989) A gradient of nuclear localization of the dorsal protein determines dorsoventral pattern in the Drosophila embryo. *Cell*, **59**, 1189-1202.

Rothberg,J.M. & Artavanis-Tsakonas,S. (1992) Modularity of the slit protein. Characterization of a conserved carboxy- terminal sequence in secreted proteins and a motif implicated in extracellular protein interactions. *J.Mol.Biol.*, **227**, 367-370.

Rothberg,J.M., Hartley,D.A., Walther,Z., & Artavanis-Tsakonas,S. (1988) slit: an EGF-homologous locus of D. melanogaster involved in the development of the embryonic central nervous system. *Cell*, **55**, 1047-1059.

Rothberg,J.M., Jacobs,J.R., Goodman,C.S., & Artavanis-Tsakonas,S. (1990) slit: an extracellular protein necessary for development of midline glia and commissural axon pathways contains both EGF and LRR domains. *Genes Dev.*, **4**, 2169-2187.

Rubin,G.M., Hazelrigg,T., Karess,R.E., Laski,F.A., Laverty,T., Levis,R., Rio,D.C., Spencer,F.A., & Zuker,C.S. (1985) Germ line specificity of P-element transposition and some novel patterns of

expression of transduced copies of the white gene. *Cold Spring Harb.Symp.Quant.Biol.*, **50**, 329-335.

Rubin,G.M. & Spradling,A.C. (1982) Genetic transformation of Drosophila with transposable element vectors. *Science*, **218**, 348-353.

Sambrook,J., Fritsch,E.F., & Maniatis,T. (1989) *Molecular cloning :a laboratory manual*, 2nd ed. edn, Cold Spring Harbor Laboratory Press, Cold Spring Harbor, N.Y.

Sasaki,M., Kleinman,H.K., Huber,H., Deutzmann,R., & Yamada,Y. (1988) Laminin, a multidomain protein. The A chain has a unique globular domain and homology with the basement membrane proteoglycan and the laminin B chains. *J.Biol.Chem.*, **263**, 16536-16544.

Sasaki,T., Forsberg,E., Bloch,W., Addicks,K., Fassler,R., & Timpl,R. (1998) Deficiency of beta 1 integrins in teratoma interferes with basement membrane assembly and laminin-1 expression. *Exp.Cell Res.*, **238**, 70-81.

Schmid,A., Chiba,A., & Doe,C.Q. (1999) Clonal analysis of Drosophila embryonic neuroblasts: neural cell types, axon projections and muscle targets. *Development*, **126**, 4653-4689.

Scholz,H., Deatrick,J., Klaes,A., & Klambt,C. (1993) Genetic dissection of pointed, a Drosophila gene encoding two ETS- related proteins. *Genetics*, **135**, 455-468.

Seeger,M., Tear,G., Ferres-Marco,D., & Goodman,C.S. (1993) Mutations affecting growth cone guidance in Drosophila: genes necessary for guidance toward or away from the midline. *Neuron*, **10**, 409-426.

Seeger,M.A. & Beattie,C.E. (1999) Attraction versus repulsion: modular receptors make the difference in axon guidance [comment]. *Cell*, **97**, 821-824.

Sephel,G.C., Tashiro,K.I., Sasaki,M., Greatorex,D., Martin,G.R., Yamada,Y., & Kleinman,H.K. (1989) Laminin A chain synthetic peptide which supports neurite outgrowth. *Biochem.Biophys.Res.Commun.*, **162**, 821-829.

Serafini,T., Colamarino,S.A., Leonardo,E.D., Wang,H., Beddington,R., Skarnes,W.C., & Tessier-Lavigne,M. (1996) Netrin-1 is required for commissural axon guidance in the developing vertebrate nervous system. *Cell*, **87**, 1001-1014.

Shu,T., Valentino,K.M., Seaman,C., Cooper,H.M., & Richards,L.J. (2000) Expression of the netrin-1 receptor, deleted in colorectal cancer (DCC), is largely confined to projecting neurons in the developing forebrain. *J.Comp Neurol.*, **416**, 201-212.

Song,H.J. & Poo,M.M. (1999) Signal transduction underlying growth cone guidance by diffusible factors. *Curr.Opin.Neurobiol.*, **9**, 355-363.

Sonnenfeld,M.J. & Jacobs,J.R. (1994) Mesectodermal cell fate analysis in Drosophila midline mutants. *Mech.Dev.*, **46**, 3-13.

Sonnenfeld,M.J. & Jacobs,J.R. (1995) Apoptosis of the midline glia during Drosophila embryogenesis: a correlation with axon contact. *Development*, **121**, 569-578.

Spradling,A.C. & Rubin,G.M. (1982) Transposition of cloned P elements into Drosophila germ line chromosomes. *Science*, **218**, 341-347.

Stemerdink,C. & Jacobs,J.R. (1997) Argos and Spitz group genes function to regulate midline glial cell number in Drosophila embryos. *Development*, **124**, 3787-3796.

Stoeckli,E.T. & Landmesser,L.T. (1998) Axon guidance at choice points. *Curr.Opin.Neurobiol.*, **8**, 73-79.

Streuli,C.H. & Edwards,G.M. (1998) Control of normal mammary epithelial phenotype by integrins. *J.Mammary.Gland.Biol.Neoplasia.*, **3**, 151-163.

Sullivan,W., Ashburner,M., & Hawley,R.S. (2000) *Δροσοπηιλα Προτοχολσ*; Χολδ Σπρινγ Ηαρβορ Λαβορατορψ Πρεσσ, Χολδ Σπρινγ Ηαρβορ.

Sun,Q., Bahri,S., Schmid,A., Chia,W., & Zinn,K. (2000) Receptor tyrosine phosphatases regulate axon guidance across the midline of the Drosophila embryo. (Abstract).*Development*, **127**, 801-812.

Takahashi,T., Fournier,A., Nakamura,F., Wang,L.H., Murakami,Y., Kalb,R.G., Fujisawa,H., & Strittmatter,S.M. (1999a) Plexin-neuropilin-1 complexes form functional semaphorin-3A receptors. *Cell*, **99**, 59-69.

Takahashi,T., Fournier,A., Nakamura,F., Wang,L.H., Murakami,Y., Kalb,R.G., Fujisawa,H., & Strittmatter,S.M. (1999b) Plexin-neuropilin-1 complexes form functional semaphorin-3A receptors. *Cell*, **99**, 59-69.

Takke,C. & Campos-Ortega,J.A. (1999) her1, a zebrafish pair-rule like gene, acts downstream of notch signalling to control somite development. *Development*, **126**, 3005-3014.

Takke,C., Dornseifer,P., Weizsacker,E., & Campos-Ortega,J.A. (1999) her4, a zebrafish homologue of the Drosophila neurogenic gene E(spl), is a target of NOTCH signalling. *Development*, **126**, 1811-1821.

Tear,G. (1998) Molecular cues that guide the development of neural connectivity. *Essays Biochem.*, **33**, 1-13.

Tear,G., Harris,R., Sutaria,S., Kilomanski,K., Goodman,C.S., & Seeger,M.A. (1996) commissureless controls growth cone guidance across the CNS midline in Drosophila and encodes a novel membrane protein. *Neuron*, **16**, 501-514.

Tessier-Lavigne,M. (1995) Eph receptor tyrosine kinases, axon repulsion, and the development of topographic maps. *Cell*, **82**, 345-348.

Tessier-Lavigne,M. & Goodman,C.S. (1996) The molecular biology of axon guidance. *Science*, **274**, 1123-1133.

Van Vactor,D., O'Reilly,A.M., & Neel,B.G. (1998) Genetic analysis of protein tyrosine phosphatases. *Curr.Opin.Genet.Dev.*, **8**, 112-126.

Van,V.D., Jr., Krantz,D.E., Reinke,R., & Zipursky,S.L. (1988) Analysis of mutants in chaoptin, a photoreceptor cell-specific glycoprotein in Drosophila, reveals its role in cellular morphogenesis. *Cell*, **52**, 281-290.

von Dassow,G., Meir,E., Munro,E.M., & Odell,G.M. (2000) The segment polarity network is a robust developmental module [In Process Citation]. *Nature*, **406**, 188-192.

Walsh,F.S., Skaper,S.D., & Doherty,P. (1994) Cell adhesion molecule (NCAM and N-cadherin)-dependent neurite outgrowth is modulated by gangliosides. *Prog.Brain Res.*, **101**, 113-118.

Warren,J.T., Jr., Chandrasekhar,A., Kanki,J.P., Rangarajan,R., Furley,A.J., & Kuwada,J.Y. (1999) Molecular cloning and developmental expression of a zebrafish axonal glycoprotein similar to TAG-1. *Mech.Dev.*, **80**, 197-201.

Winans,K.A. & Hashimoto,C. (1995) Ventralization of the Drosophila embryo by deletion of extracellular leucine-rich repeats in the Toll protein. *Mol.Biol.Cell*, **6**, 587-596.

Winberg,M.L., Mitchell,K.J., & Goodman,C.S. (1998a) Genetic analysis of the mechanisms controlling target selection: complementary and combinatorial functions of netrins, semaphorins, and IgCAMs. *Cell*, **93**, 581-591.

Winberg,M.L., Noordermeer,J.N., Tamagnone,L., Comoglio.P.M., Spriggs,M.K., Tessier-Lavigne,M., & Goodman,C.S. (1998b) Plexin A is a neuronal semaphorin receptor that controls axon guidance. *Cell*, **95**, 903-916.

Windisch,J.M., Marksteiner,R., & Schneider,R. (1995) Nerve growth factor binding site on TrkA mapped to a single 24-amino acid leucine-rich motif. *J.Biol.Chem.*, **270**, 28133-28138.

Wu,W., Wong,K., Chen,J., Jiang,Z., Dupuis,S., Wu,J.Y., & Rao,Y. (1999) Directional guidance of neuronal migration in the olfactory system by the protein Slit [see comments]. *Nature*, **400**, 331-336.

Yin,X., Watanabe,M., & Rutishauser,U. (1995) Effect of polysialic acid on the behavior of retinal ganglion cell axons during growth into the optic tract and tectum. *Development*, **121**, 3439-3446.

Zallen,J.A., Kirch,S.A., & Bargmann,C.I. (1999) Genes required for axon pathfinding and extension in the C. elegans nerve ring. *Development*, **126**, 3679-3692.

Zallen,J.A., Yi,B.A., & Bargmann,C.I. (1998) The conserved immunoglobulin superfamily member SAX-3/Robo directs multiple aspects of axon guidance in C. elegans. *Cell*, **92**, 217-227.

Zhou,L., Xiao,H., & Nambu,J.R. (1997) CNS midline to mesoderm signaling in Drosophila. *Mech.Dev.*, **67**, 59-68.

Appendix A. Sequence of PCR primers

The name and sequence of all primers used in this thesis are presented.

Oligonucleotides

Orientation 5'	3'	Enzymes in bold
Name		
DV1bf1	CTTCAGAGCTCTGCCACAATGGCC	
DV1br1	GGATACAGCTGAGAGCTGCCGAAT	
DV1br2	CCCTTGAAGACGCGTCTACCCACG	
DV1bf2	CATA**AAGCTT**CCACAATGGCCGCGCC	-HindIII
DV1bf3	CATAAAT**GGGCCC**CAATGGCCGCGCC	-ApaI
SfiIf	AGCAC**GGCCAGCGCGGCC**GCTACT	-SfiI
SpeIr	TTCTT**ACTAGT**TCCGCACTTGCGC	-SpeI
pBH	GGAAGCTTGGGTACCTCCGCGGAG	
HAKf	CATAAA**GGTACC**ACAATGGCCGCG	KpnI
HABr	TCAGTAGCA**GTGCAC**GGTGCATCC	Bbr-PI
HAM1r	GCGCGTCGTTTCGCTGCACGGTAA	
HAM2f	CGGAGAACCACTTTAGACCGCAGT	
Slitant1a	CAGGAATTCGGAGCAGAATGGAATTCTCATGTA	
Slitant1b	GGGCTTAAGCAAAGTCGACCAGCTTATGATTGAT	
Slitant2a	CAGCATTAGCTTCGTCCACA	
Slitant2b	CTTCATGCAGCCCTTAAAGC	
Slitcos1a	AAAACGCCTCGAACTCGATA	
Slitcos1b	CGATCGTGTGGATCTGATTG	
Slitcos2a	ACTCGAGCGACTGGACATCT	
Slitcos2b	GTCGTCGAAAGCTGGAGAAC	
Slitcos3a	GTTCTCCAGCTTTCGACGAC	
Slitcos3b	TCGTTGTCGTTGAGCAAAG	
Slitcos4a	CTTTTGCTCAACGACAACGA	
Slitcos4b	TGCGTTCGTAGTGAATCTGC	
Slitcos5a	GCAGATTCACTACGAACGCA	
Slitcos5b	GGTGTGGACAGGATCAGCTT	
Slitcos6a	ACCTCAAGTCGTTGACCCAC	
Slitcos6b	TGTTCTGGCACTTGATCTCG	
Slitcos7a	CGAGATCAAGTGCCAGAACA	
Slitcos7b	TGTGGACGAAGCTAATGCTG	
Slitcos8a	CAGCATTAGCTTCGTCCACA	
Slitcos8b	CTTCATGCAGCCCTTAAAGC	
Slitcos9a	GCACAGCAGGCATACAAGAA	
Slitcos9b	AGCAATTGGGTAGTCGCATC	
genomic1	GAAATCTCAGCGGACGTGGAGCG	
genomic2	GAATCAGCATCAATTACACTCCCA	
genomic2b	TGAATCAGCATCAATTACACTCCC	
genomic2rev	CGCCCTACGGTAGCTGCAGCTCCT	

genomic3	CCGCCGGCCGCCTTGGTGCTTTTC
genomic3rev	CCGGTCCTCCCAGACTTCTCCTCG
genomic3revb	GTGCAACTCTAACCAGCCGCTGG
genomic4	CCCTACCTCCCTCATACAAATGTT
genomic5rev	CGACGTAGGGGAAAACAGGGCGGT
genomic6	GCGGGGCGGAGAACAGCTGTCCGC
genomic6rev	GCTGAAACCGTTATGCCGCAGGAC
genomic7	GCTTCTTCCAATTAGAACTGCTGC
genomic7rev	CCCCTCCACCCACTTTCACTGGCC
genomic8rev	CCAACCGTTGGGACACCCCTAAC
genomic9	GGGCGAGAACAAGATCAAGGAGAT
genomic10rev	CCACCGTACTGTTTCGTCTTAACG
genomic11	CCCGCCGAAACATCGGAGCTGTAT
mutx1f	CGGGGGCCACTTTCAATTAGGCAC
mutx1rb	CGCTAACTTCTCGAACTTACCCGG
mutx1r	GGCCCATTCAAGCTCTTCAATCGC
mutx1ir	TCACTCGCTCCACGTCCGCTGAGA
mutx23f	GCATCCACACCGCAGCGACTTG
mutx23R	CTCCATAATCTGACGCTACTCA
mutx4f	CTCCAAAGTAGTAGCCGATAGT
mutx4r	GGCACGCAGCTCCATTGATTGG
mutx45f	CGGATGCTCGTTTTCCCAGCTACC
mutx45r	GGCAACAACACCTCCACCACCGGG
mutx5f	GGCCGGATCATCTGCTCCACTC
mutx5r	CCCGCAATGCTTTGTTTTCCTC
mutx67f	CCGGAGCTCGAACCGGAGCAAG
mutx67r	GCGGGAGCAGCCGGAGGGCAGC
mutx7af	ACAGCATCTGGCCAAGAATCCTTT
mutx7ar	GTGCAGTCCCAGGAACATCTTGTT
mutx8f	CGAGCTTTGTTAACATTCGTCG
mutx8fb	CCCTTTATCAACGCCGTTATCGTA
mutx8r	CCACTCGAGTGCTTGGTGGGCG
mutx8rb	GTCATTAGGCCTAGTTGGACTTAC
mutx8rc	CATTCTGGTTGATCCGGATTACTG
mutx9ar	GGCAATCGTCGATATTCGTCTCGC
mutx9afi	GTGACTGTGTGCTAGCCTAATGCA
mutx9ari	CGCTCTGCTTATAGCTGCTAACGG
mutx9bfi	GCGAGACGAATATCGACGATTGCC
mutx9bri	CCGGCTACCTTTCATGGTACGGC
mutx9br	ACGGCATGGTACTTTCCATCGGCC
mutx9cfi	GGCCGATGGAAAGTACCATGCCGT
mutx9cri	CCATGAGTTTTGAGTGTGGGCCCC
mutx9cr	CCCCGGGTGTGAGTTTTGAGTACC
mutx910f	GCCGCATAACCGTTTCAGCCAT
mutx910r	GGAGCAGGATGCAGGGACATGG

mutx10fi	CGCACACGCATATTCATGACATTC
mutx10ri	CGCTGATGGGTTAACGAGCTTGCC
mutx10r	CCGTTCGAGCAATTGGGTAGTCGC
mutx1112f	CCATGTCCCTGCATCCTGCTCC
mutx1112r	GCAGAGAATCTGGGATTCCGGCC
mutx1314r	GCAGAGAATCTGGGATTCCGGC
mutx1516ar	GGCAATCGTCGATATTCGTCTCGC
mutx16br	GTACTCGCACCACTTTCCAGTGTA
mutx16cr	TGTGATCTTTTGCTGGCGCTGGGC
mutx1617dr	GTGTACACCCGGGTGTGAGTTGTG
ALPSf	TACACTGGAAAGTGGTGCGAGTAC
ALPSr	GTTCTCCAGGCAAGGATCCACCGG

Appendix B. Longitudinal axon fascicles are abnormal in early and late embryos heterozygous for both *slit* and an allele deficient for slit (Df(2R)WMG)

Embryos that were heterozygous for Df(2R)WMG developed abnormal FasII labeled axons that appeared thin and collapsed towards the ventral midline in both early (A, stage 12) and late (C, stage 16) embryos. The observed CNS architecture deteriorated further in embryos homozygous for this deficiency (B, D). Stage 12 embryos that were heterozygous for $slit^{IG107}$ (E) or $slit^{550}$ (I) exhibited a normal pattern of axon development that was disrupted when each of these alleles was heterozygous over Df(2R)WMG (F, J); however, embryos heterozygous for $slit^{550}$/DF(2R)WMG were less severely affected. Similarly, abnormalities observed in stage 16 embryos heterozygous for $slit^{IG107}$ (G) or $slit^{550}$ (K) were augmented when embryos were heterozygous for both *slit* and Df(2R)WMG, but again less so for $slit^{550}$/DF(2R)WMG.

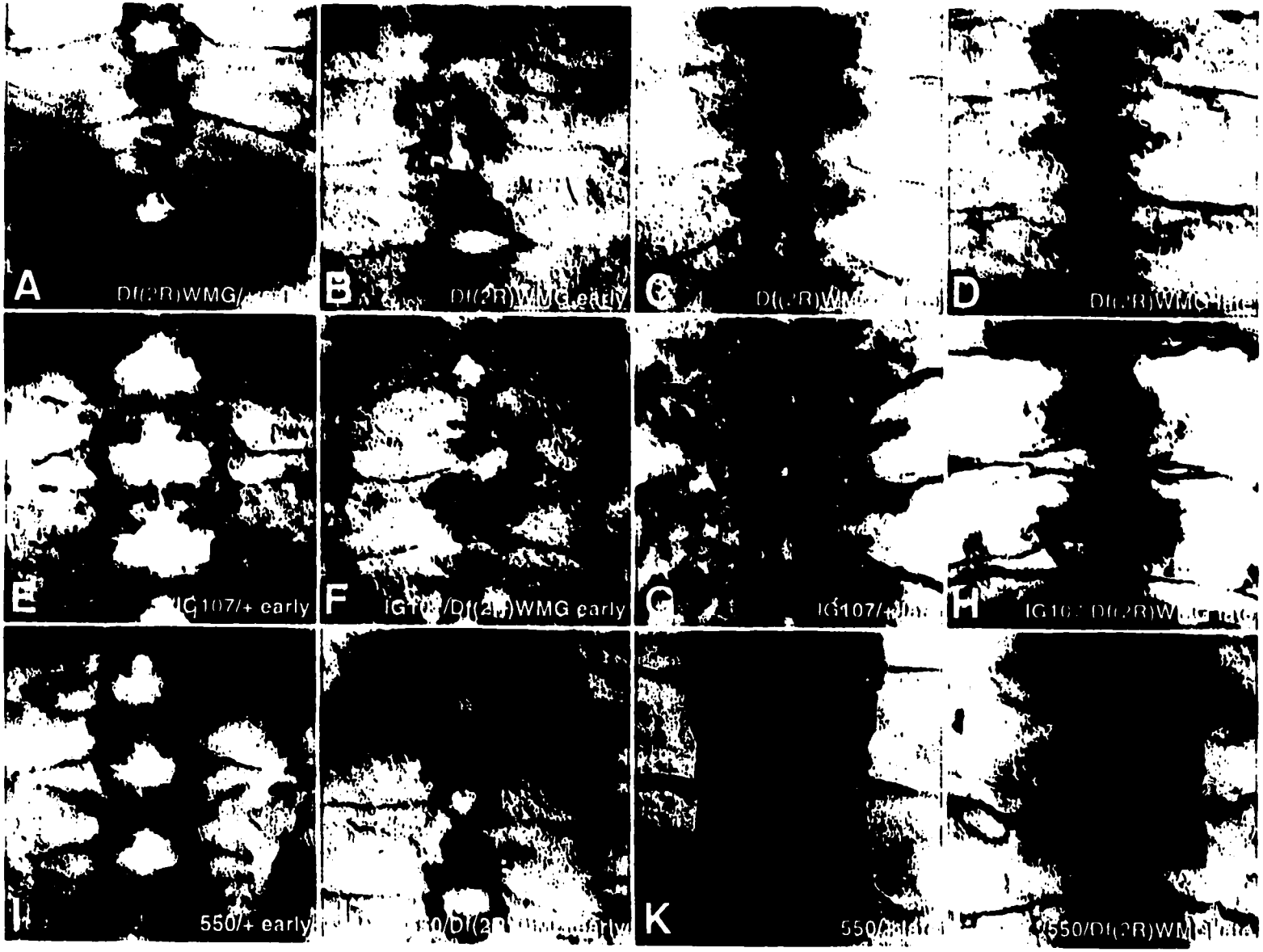
A
B
C
D
E
IG107/+ early
F
G
H
I
550/+ early
K

Appendix C. Outline of *slit* transgene construction with HA tag.

A 3' hemaglutanin sequence was synthesized and then sub cloned into a plasmid vector prior to insertion of the complete *slit* cDNA.

pBS slit HA

pBS KSII+ Bluescript with an engineered HA tag assigning the native slit stop codon.

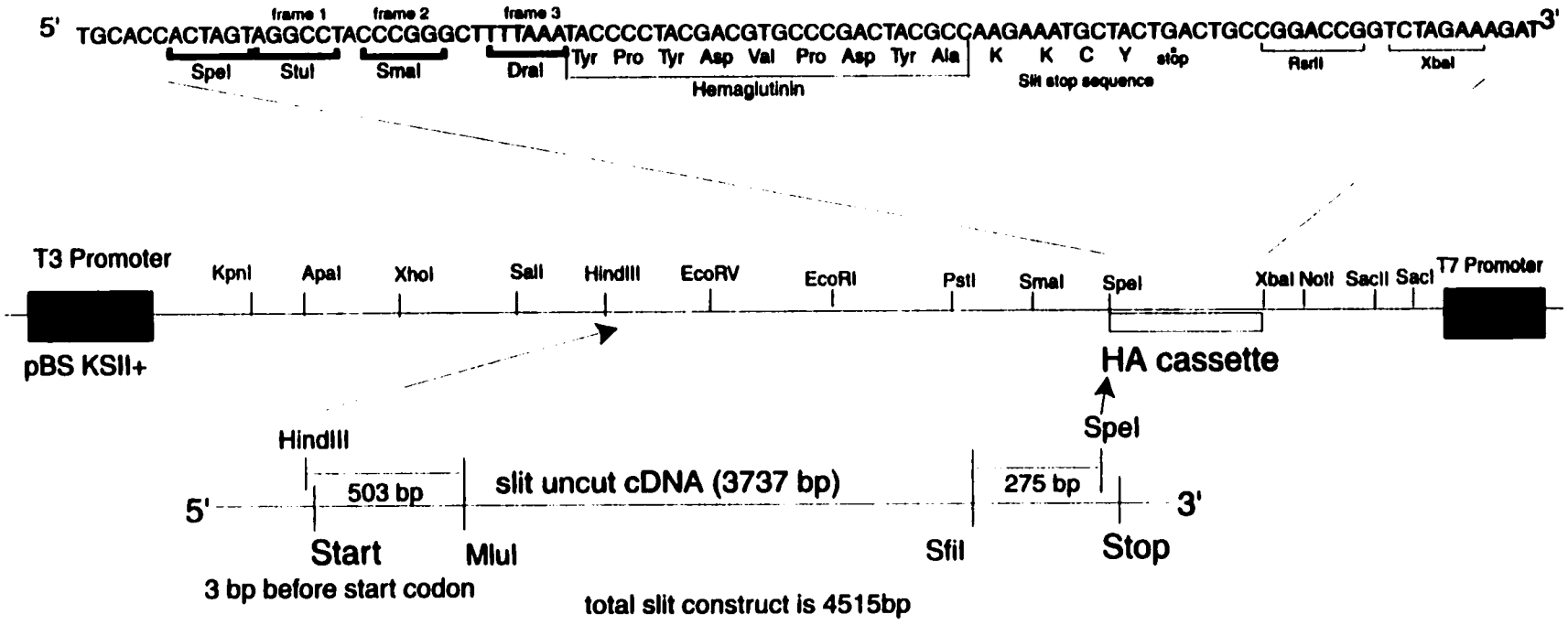

This PCR engineered construct has been cloned into our HA pBSKSII+ construct which has the native slit stop codon incorporated into the HA tag.

Appendix D. GAL4 patterns of expression and control labeling of midline axons. Each of the acquired *P{GAL4}* lines was crossed to *P{UAS-tau lacZ}* and immunolabelled with anti-β-galactosidase (arrow) expression and BP102 CNS labeling (arrowhead). Midline glia GAL4 lines were *P{slit1.0-GAL4}* (A) and *P{sim-GAL4}*. Ectopic expression at the intersegmental boundaries was achieved with *P{eng-GAL4}* (D), *P{scab-GAL4}*, *P{ap-GAL4}* (F), and *P{eyeless-GAL4}*. Ectopic overexpression was driven by *P{elav-GAL4}* (C), *P{sevenless-GAL4}* (H), *P{C321-GAL4}* (I), and P*{C15J2-GAL4}* (J). No aberrant pattern of BP102 labeling was noted with the expression of the Tau gene fused to the Lac-Z promoter in these tissues.

B
H